



**UNIVERSIDADE ESTADUAL PAULISTA
“JÚLIO DE MESQUITA FILHO”
FACULDADE DE MEDICINA**

Guilherme Ribeiro Romualdo

**Cafeína, Trigonelina e Ácido Clorogênico:
Modulação da expressão de miRNAs na
Hepatocarcinogênese associada à Fibrose**

Tese apresentada à Faculdade de Medicina, Universidade Estadual Paulista “Júlio de Mesquita Filho”, Câmpus de Botucatu, para obtenção do título de Doutor em Patologia.

Orientador: Prof. Dr. Luís Fernando Barbisan
Coorientador: Prof. Dr. Bruno Cogliati

**Botucatu
2020**

Guilherme Ribeiro Romualdo

Cafeína, Trigonelina e Ácido Clorogênico:
Modulação da expressão de miRNAs na
Hepatocarcinogênese associada à Fibrose

Tese apresentada à Faculdade de Medicina, Universidade Estadual Paulista “Júlio de Mesquita Filho”, Câmpus de Botucatu, para obtenção do título de Doutor em Patologia.

Orientador: Prof. Dr. Luís Fernando Barbisan
Coorientador: Prof. Dr. Bruno Cogliati

Botucatu
2020

FICHA CATALOGRÁFICA ELABORADA PELA SEÇÃO TÉC. AQUIS. TRATAMENTO DA INFORM.
DIVISÃO TÉCNICA DE BIBLIOTECA E DOCUMENTAÇÃO - CÂMPUS DE BOTUCATU - UNESP
BIBLIOTECÁRIA RESPONSÁVEL: ROSEMEIRE APARECIDA VICENTE-CRB 8/5651

Ribeiro Romualdo, Guilherme.

Cafeína, Trigonelina e Ácido clorogênico : modulação da expressão de miRNAs na hepatocarcinogênese associada à fibrose / Guilherme Ribeiro Romualdo. - Botucatu, 2020

Tese (doutorado) - Universidade Estadual Paulista "Júlio de Mesquita Filho", Faculdade de Medicina de Botucatu

Orientador: Luís Fernando Barbisan

Coorientador: Bruno Cogliati

Capes: 40105008

1. Fígado - Câncer. 2. Fígado - Cirrose. 3. Ácido fenólico. 4. Cafeína. 5. MicroRNAs.

Palavras-chave: Ácido clorogênico; Cafeína; Hepatocarcinogênese; MicroRNAs; Trigonelina.

Resumo

A expressão alterada de microRNAs contribui para o desenvolvimento do carcinoma hepatocelular (CHC). Em contraste, o consumo de café reduz em ~40% o risco de desenvolvimento de fibrose/cirrose hepática e CHC, enquanto o café descafeinado não. Esses efeitos são atribuídos à cafeína (CAF) ou à sua combinação com outros compostos comuns e altamente biodisponíveis no café, como a trigonelina (TRI) e o ácido clorogênico (ACG)? Assim, avaliou-se se a CAF individualmente ou combinada à TRI e/ou ao ACG atenuam a hepatocarcinogênese associada à fibrose, investigando a potencial modulação da expressão global de microRNAs. Camundongos C3H/HeJ foram submetidos a um modelo de hepatocarcinogênese associada à fibrose induzido por dietilnitrosamina/tetracloro de carbono e tratados com CAF (50 mg/kg peso corpóreo (p.c.) 5x/semana, gavagem), CAF+TRI (50 e 25 mg/kg p.c.), CAF+ACG (50 e 25 mg/kg p.c.) ou CAF+TRI+ACG (50, 25 e 25 mg/kg p.c.) por 10 semanas. Somente o tratamento com CAF+TRI+CGA atenuou o desenvolvimento de focos pré-neoplásicos hepáticos. Somente a combinação de todos os compostos reduziu a proliferação celular (Ki-67) em focos pré-neoplásicos e aumentou a apoptose (caspase-3 clivada) em tecido adjacente. CAF+TRI+CGA reduziu o estresse oxidativo hepático, aumentando a atividade ou os níveis proteicos de membros do eixo antioxidante Nrf2/GSH-Px/SOD. O tratamento com CAF+TRI+CGA também atenuou o eixo pró-inflamatório IL-17/ NFκB, reduzindo a quantidade de macrófagos CD68+, a ativação de células estreladas (α -SMA) e a deposição de colágeno. Por fim, o tratamento com CAF+TRI+ACG aumentou a expressão hepática de miR-144-3p e miR-15b-5p, considerados supressores de tumor ou antifibróticos, reduzindo os níveis proteicos de EGFR (alvo de miR-144-3p) e de membros da família antiapoptótica Bcl-2 (Bcl-2, Mcl-1 e Bcl2l2, alvos de miR-15b-5p). Portanto, a combinação de compostos de café, ao invés de CAF isoladamente, atenuou a hepatocarcinogênese associada à fibrose, em parte, pela modulação da expressão de miRNAs.

Abstract

Aberrant microRNA expression implicates on hepatocellular carcinoma (HCC) development. Conversely, daily coffee consumption reduces by ~40% the risk for fibrosis/cirrhosis and HCC, while decaffeinated coffee does not. It is currently unknown whether these protective effects are solely related to caffeine (CAF), or to its combination with other common and/or highly bioavailable coffee compounds, such as trigonelline (TRI) and chlorogenic acid (CGA). We evaluated whether CAF individually or combined with TRI and/or CGA alleviates fibrosis-associated hepatocarcinogenesis, examining the involvement of miRNA profile modulation. Male C3H/HeJ mice were submitted to a diethylnitrosamine/carbon tetrachloride-induced model. Animals received CAF (50 mg/kg), CAF+TRI (50 and 25 mg/kg), CAF+CGA (50 and 25 mg/kg) or CAF+TRI+CGA (50, 25 and 25 mg/kg), intragastrically, 5x/week, for 10 weeks. Only CAF+TRI+CGA combination reduced the incidence, number and proliferation (Ki-67) of hepatocellular preneoplastic foci while enhanced apoptosis (cleaved caspase-3) in adjacent tissue. CAF+TRI+CGA treatment also decreased hepatic oxidative stress by enhancing the antioxidant Nrf2 axis. CAF+TRI+CGA had the most pronounced effects on decreasing hepatic pro-inflammatory IL-17/NFκB signaling, contributing to reduce CD68-positive macrophage number, stellate cell activation, and collagen deposition. The miRNAomic profile revealed that CAF+TRI+CGA upregulated tumor suppressors miR-144-3p and antifibrotic miR-15b-5p, frequently altered in human HCC. CAF+TRI+CGA reduced protein levels of pro-proliferative EGFR (miR-144-3p target) and antiapoptotic Bcl-2 family members (miR-15b-5p targets). Our results suggest that the combination of most common and highly bioavailable coffee compounds, rather than CAF individually, attenuates early fibrosis-associated hepatocarcinogenesis by modulating miRNA expression profile.

Sumário

Capítulo 1 – Revisão de Literatura.....	1
1.1 Hepatocellular carcinoma: of murine and men.....	1
1.2 miRNAs: small molecules with great responsibilities.....	19
Referências.....	30
1.3 Artigo de revisão publicado.....	38
Capítulo 2 – Artigo científico.....	61
Certificate of submission.....	61
Abstract.....	63
1. Background.....	64
2. Materials and methods.....	65
3. Results.....	72
4. Discussion.....	79
5. Conflicts of interest.....	83
6. Acknowledgements.....	83
7. Funding information.....	84
8. References.....	85
9. Figures.....	90
10. Tables.....	99
11. Supplementary material.....	103
Conclusões.....	126
Apêndice.....	127



Capítulo 1

Revisão de literatura

Observação: O capítulo 1 compreende as subsecções 1.1, 1.2 e 1.3. A subsecção 1.3, referente as evidências epidemiológicas e experimentais do café e seus compostos isolados sobre a carcinogênese do trato gastrointestinal e fígado, foi publicada na revista *“Food Research International”* (fator de impacto 3,579; JCR 2018).

1.1 Hepatocellular carcinoma: of murine and men

According to the World Health Organization (WHO), liver primary malignant neoplasias, mainly represented by Hepatocellular Carcinoma (HCC), are the sixth most incident while the fourth deadliest cancers worldwide, comprising around 800,000 new cases and deaths/year (WHO, 2018) (Figure 1). In addition, HCC-related incidence and mortality crude numbers are expected to increase by 60% from 2018 to 2040 (WHO, 2018) (Figure 2). Moreover, HCC is considered a poor prognosis disease, with a median survival time of 11 months after diagnosis, and 3-year survival rates ranging from 19 to 30% (Greten et al., 2005; op den Winkel et al., 2012). These epidemiological data evoke the importance of HCC as a global health problem and elicit the need for novel preventive and therapeutic strategies. Moreover, populational data on HCC display two important features: gender and geographical disparities (Figures 3 and 4). Standardized incidence rates (cases or deaths *per* 100,000 people) in Asian and African continents together are almost 2-fold higher than in Europe and North America (Figure 3). Noteworthy, HCC is not part of the top ten most incident and deadliest cancers in Brazil (INCA, 2018). Geographical disparity is clearly linked to the occurrence of the main risk factors for this malignancy. In addition, 70% of HCC cases and -related deaths occur in men (Figure 4). The mechanisms concerning gender disparity, involving the promoting activity of testosterone and protective effect of estrogens, were only elucidated with the use of preclinical rodent models, and will be further discussed.

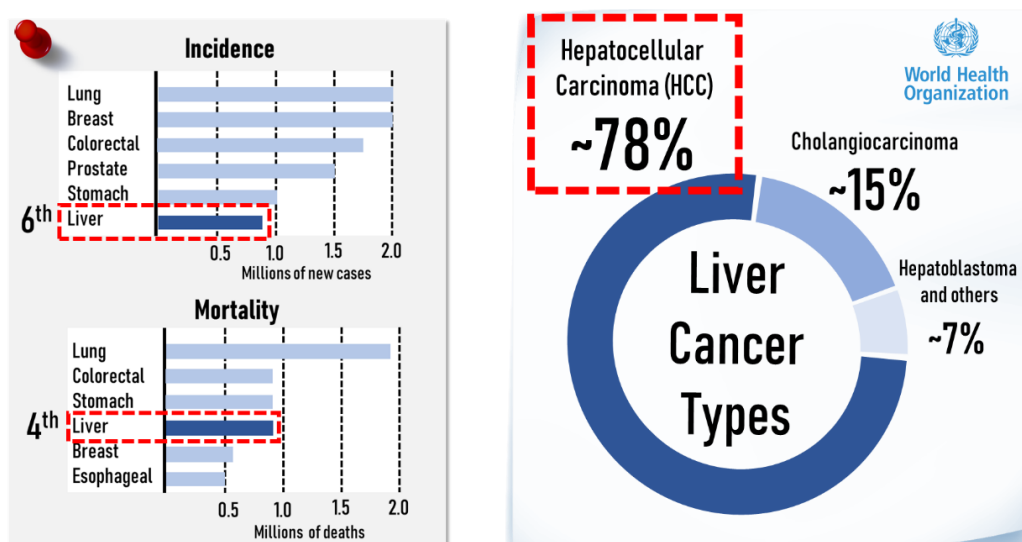


Figure 1. Infographics on HCC epidemiological global data in 2018. Primary liver cancers, mostly represented by HCC (responsible for 78% cases/deaths), are part of the top 10 ranked cancers in both incidence and mortality crude numbers (WHO, 2018).

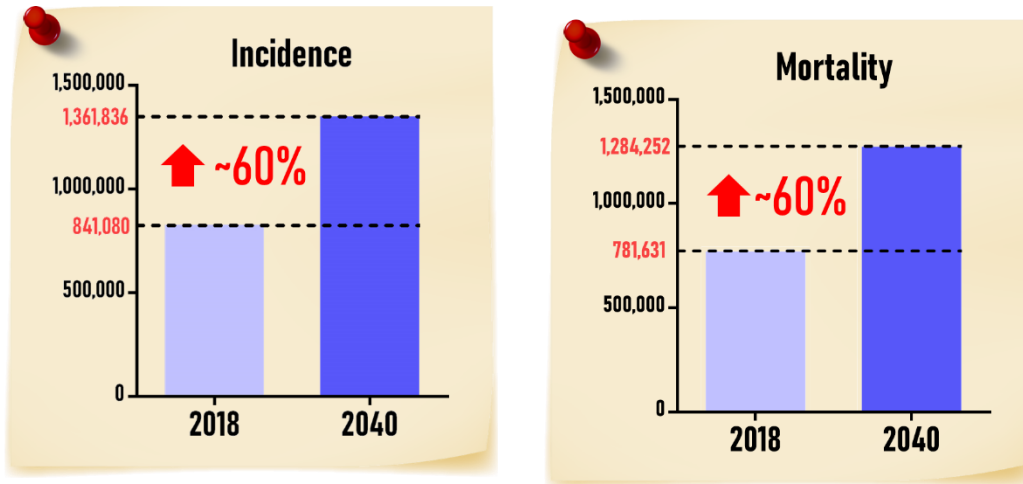


Figure 2. Estimated increase in both incidence and mortality crude numbers for HCC, considering 2018 to 2040 projection (WHO, 2018).

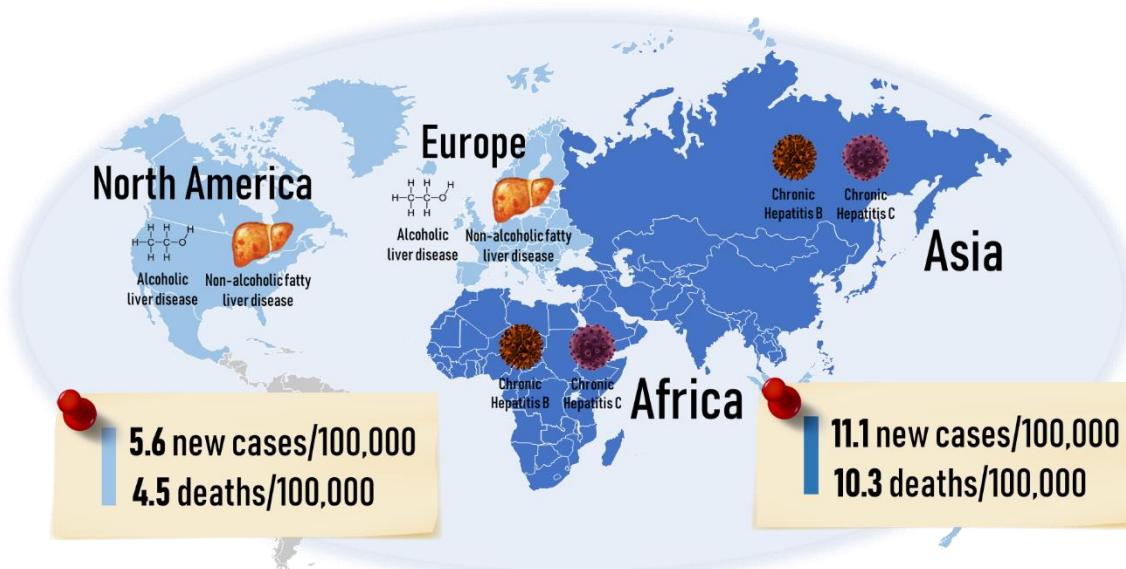


Figure 3. Geographical disparity feature of HCC-related standardized incidence and mortality rates between Africa/Asia and North America/Europe (WHO, 2018). The main risk factors are also presented according to the continent (Baecker et al., 2018)

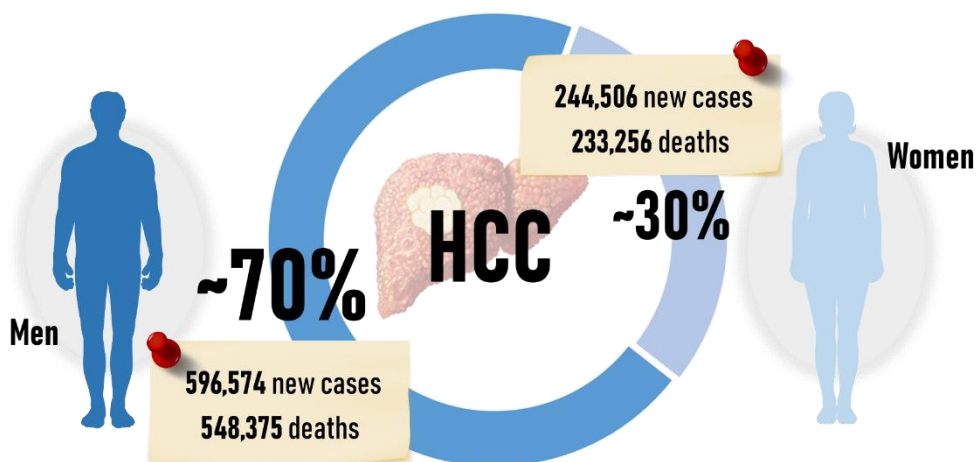
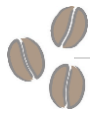


Figure 4. Gender disparity feature of HCC-related incidence and mortality crude number between men and women (WHO, 2018).



Around 70 - 90% of HCC cases develop in the background of liver fibrosis/cirrhosis caused by chronic hepatitis B (HBV) and C (HCV) virus infection, non-alcoholic fatty liver disease (NAFLD) and/or alcoholic liver disease (ALD) (Yang et al., 2011; Baecker et al., 2018). Globally, 44% and 21% of all cases are attributed to HBV and HCV chronic infections, respectively, whereas 26% and 16% are linked to ALD and NAFLD-related metabolic syndromes (mostly obesity and diabetes) (Baecker et al., 2018). Concerning Central Asia and Central Sub-Saharan Africa, HBV and HCV are indeed the most prominent risk factors, responsible for 57%-60% and 41%-50% of all cases, respectively (Baecker et al., 2018). On the other hand, in Central Europe and North America, ALD and NAFLD-related metabolic syndromes are the most protruding ones, linked to 30%-32% and 20%-24% of all cases, correspondingly (Makarova-Rusher et al. 2016; Baecker et al., 2018). Since some authors consider the chronic viral infections as the most important risk factors for HCC development, HBV/HCV-related HCC attributable fraction may in part explain geographical disparity among the cited continents (Figure 3). Nonetheless, recent studies have reported on the increasing prevalence of ALD and, specially, NAFLD in high income European countries and USA (Makarova-Rusher et al. 2016; Baecker et al., 2018). It is worthy of note that non-alcoholic steatohepatitis (NASH), the advanced stage of NAFLD, is the second leading etiology of HCC-related liver transplant in the USA (Wong et al., 2014; 2015). In general, HCC is considered a complex and multifactorial disease concerning its risk conditions since their co-existence of is often observed, as HBV and HCV co-infections and co-occurrence of ALD and NAFLD (Baecker et al., 2018).

The risk factors are proposed act through multiple different molecular mechanisms that predispose to chronic liver disease and culminate on the emergence of hepatocellular preneoplastic and neoplastic lesions. Overall, HCV and HBV chronic infections have both direct and indirect mechanisms (Levrero & Zucman-Rossi, 2016; Vescovo et al., 2016) (Figure 5). The direct ones are related to components of the viral particle (Figure 5). In order to induce viral replication, HBV genome integrates the host hepatocyte genome in a feature known as insertional mutagenesis (Minami et al., 2005). This integration may establish genomic instability and predispose to DNA damage and more severe genomic alterations, as mutations and chromosomal rearrangements in oncogenes or tumor suppressor genes (Minami et al., 2005). Moreover, the HBx protein, also responsible for orchestrating viral replication, is accounted for translational repression (as it promotes DNA methylation) or activation (as it promotes DNA acetylation) (Cougot et al., 2007; Zheng et al. 2009) (Figure 5). Regarding HCV, the core protein of the viral particle directly interacts with mitochondrial proteins, predisposing to mitochondrial stress and dysfunction (Kim et al., 2013) (Figure 5). Core is implicated on post-translational modifications in important tumor suppressor proteins, as p53 protein, the “guardian of the genome” (Kao et al., 2004). The role of other



HCV proteins [nonstructural proteins (NS) NS3, N4B and NS5B] on intracellular signaling is also speculated, yet not fully understood. During chronic viral infections, HBV and HCV are able to evade the viral particle clearance mediated by both innate and adaptive immune systems through viral replication and mutations (Levrero & Zucman-Rossi, 2016; Vescovo et al., 2016). As long as viral particles are adapted to inflammatory microenvironment, the persistent inflammation may cause long-term hepatocyte damage and death, creating a necro inflammatory context that eventually progress to liver fibrosis and cirrhosis (Levrero & Zucman-Rossi, 2016; Vescovo et al., 2016). In this process, pro-inflammatory cytokine release, oxidative stress and cell death signals are the stimuli for hepatic stellate cell (HSC) activation (Tsuchida & Friedman, 2017) (Figure 6). Inactivated under physiological conditions, these cells progressively turn into proliferative, contractile and fibrogenic myofibroblast through epithelial-mesenchymal transition (EMT), being established as the central drivers of liver fibrosis and cirrhosis (Tsuchida & Friedman, 2017) (Figure 6). Chronic cycles of hepatocyte death and extracellular matrix (ECM) synthesis and accumulation, mainly collagen type I and III, lead to the progressive substitution of liver parenchyma by fibrous septa, characterizing fibrosis (Tsuchida & Friedman, 2017). The evolution of this condition, featuring profound liver architecture modification and functional and regenerative capacity loss, culminates on liver nodulation (“islands” of hepatocytes surrounded by ECM, Figure 6), is called cirrhosis (Tsuchida & Friedman, 2017). The interplay between macrophages and activated HSC through paracrine signaling mediated by growth factors [transforming growth factor- β (TGF β), platelet-derived growth factor (PDGF), vascular endothelial growth factor (VEGF) and connective tissue growth factor (CTGF)] and cytokines (as interleukin 17) is also a key event on fibrosis establishment and progression to cirrhosis (Meng et al., 2012; Tsuchida & Friedman, 2017).

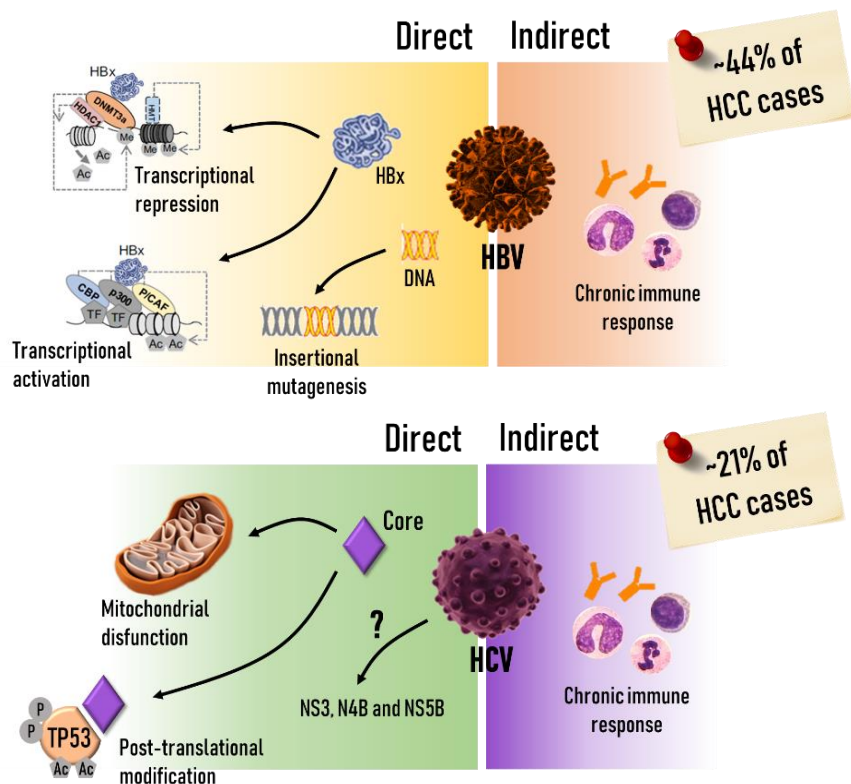


Figure 5. Molecular mechanism involved in HBV and HCV-related HCC, attributed to 44% and 21% HCC cases globally. Direct and indirect mechanisms are proposed (Kao et al., 2004; Cougot et al., 2007; Zheng et al. 2009; Kim et al., 2013; Levrero & Zucman-Rossi, 2016; Vescovo et al., 2016; Baecker et al., 2018).

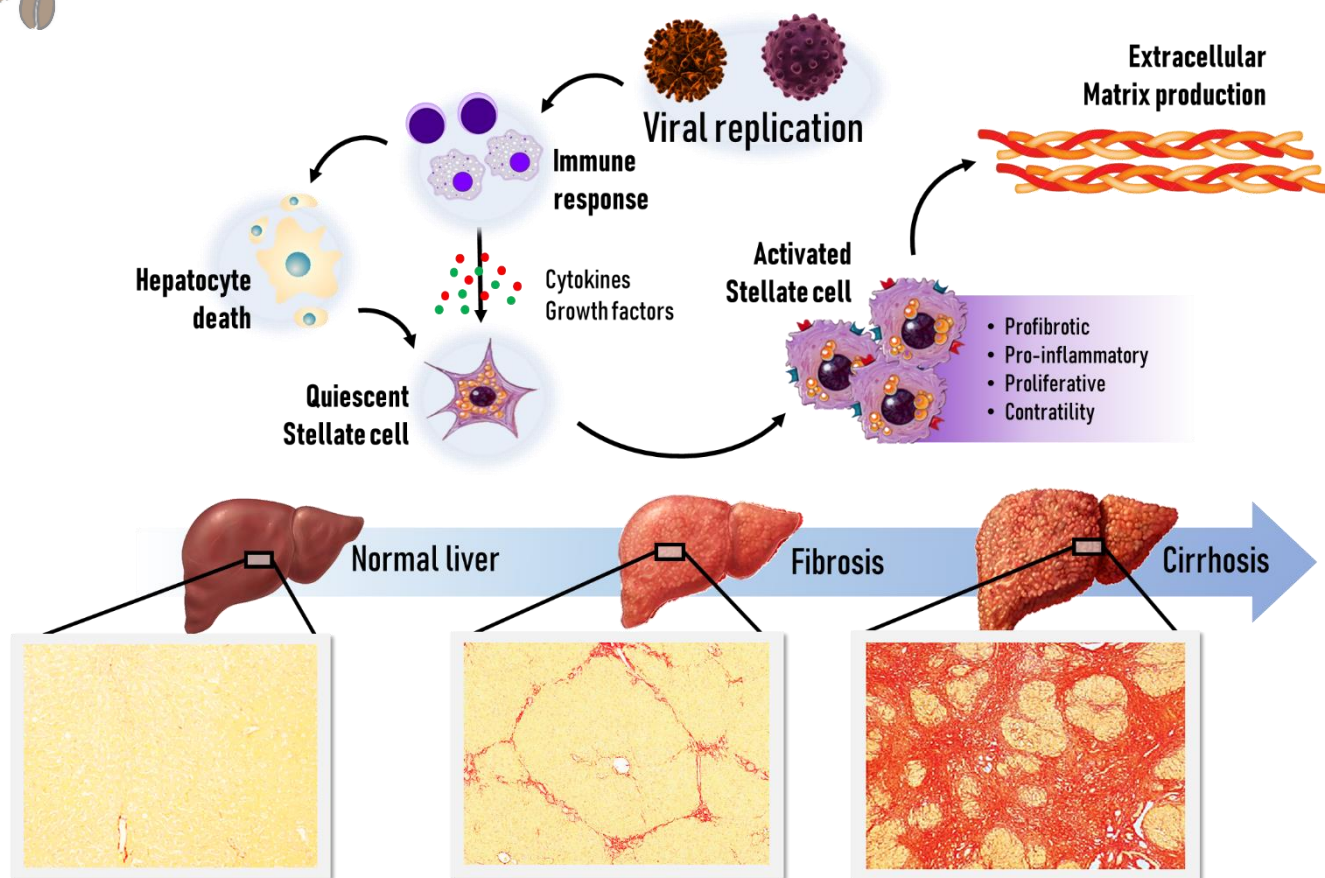
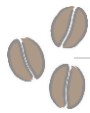


Figure 6. The main outcomes of HBV/HCV-related chronic liver disease. Chronic immune response and hepatocyte death are the stimuli for hepatic stellate cell activation, a key event on hepatic fibrogenesis. The progressive accumulation of collagen, as well as liver nodulation, are depicted in photomicrographs of Sirius red-stained sections of human liver. Adapted from Tsuchida & Friedman, 2017.

WHO estimates that ethanol ($\text{CH}_3\text{CH}_2\text{OH}$), the main component of alcoholic beverages, is linked to 12.6% of cancer-related deaths globally (WHO, 2018). Concerning excessive and chronic ethanol consumption, attributed to ~26% of HCC cases globally, epidemiological data point out to a linear positive correlation between alcohol intake and increased risk for HCC development (Chuang et al., 2015). It is estimated that a drink *per day*, corresponding to ~12 g of ethanol (half a pint of beer or one glass of wine), leads to 8% risk increase for HCC risk. Two (~24 g of ethanol) and four drinks (~48 g of ethanol) are associated with 19% and 54% risk increases, respectively (Chuang et al., 2015). Although some authors consider excessive and chronic ethanol intake as an independent risk factor for HCC, strong synergism is observed in the co-occurrence with viral infections and metabolic disorders (Yuan et al., 2004). After consumption (Figure 7), ethanol undergoes hepatic metabolism into acetaldehyde (CH_3CHO) by alcohol dehydrogenase (ADH), cytochrome P450 2E1 (CYP2E1) and/or, to a lesser extent, catalase (Cederbaum, 2012). Subsequently, acetaldehyde is oxidized into acetate (CH_3COOH) by aldehyde dehydrogenase (ALDH) (Cederbaum, 2012) (Figure 7). Acetaldehyde and acetate are highly reactive and prone to bind to biomolecules, specially DNA, forming stable DNA adducts (Figure 7). Ethanol metabolism



also leads to reactive oxygen species (ROS) release (Cederbaum, 2012). Both ROS and ethanol metabolites are accounted for genomic instability, a key hallmark for neoplastic transformation and progression. Oxidative damage may also cause hepatocellular death, activating immune response (Cederbaum, 2012). Oxidative stress, cell death and immune response are the stimuli for HSC activation and fibrosis, as previously highlighted (Tsuchida & Friedman, 2017). In addition, ethanol alters energy metabolism in the liver. ADH- and ALDH-mediated reactions lead to the accumulation of reduced nicotinamide adenine dinucleotide (NADH) (You & Arteel, 2019) (Figure 7). This high concentration of NADH inhibits fatty acid (FA) oxidation and promote FA synthesis. Progressively, triacylglycerols accumulate in the hepatocytes, leading to a condition known as “fatty liver”. The context of lipotoxicity in fatty liver also contributes to cell death and immune response that lead to HSC activation (You & Arteel, 2019). In addition to these mechanisms, ethanol causes enteric dysbiosis and subsequent intestinal barrier disruption (Stärkel et al., 2018) (Figure 7). Gut permeability enables the translocation of lipopolysaccharide (LPS), a bacterial endotoxin that reaches the liver *via* circulation and activates immune response, ultimately contributing to HSC activation and fibrosis (Tsuchida & Friedman, 2017; Stärkel et al., 2018).

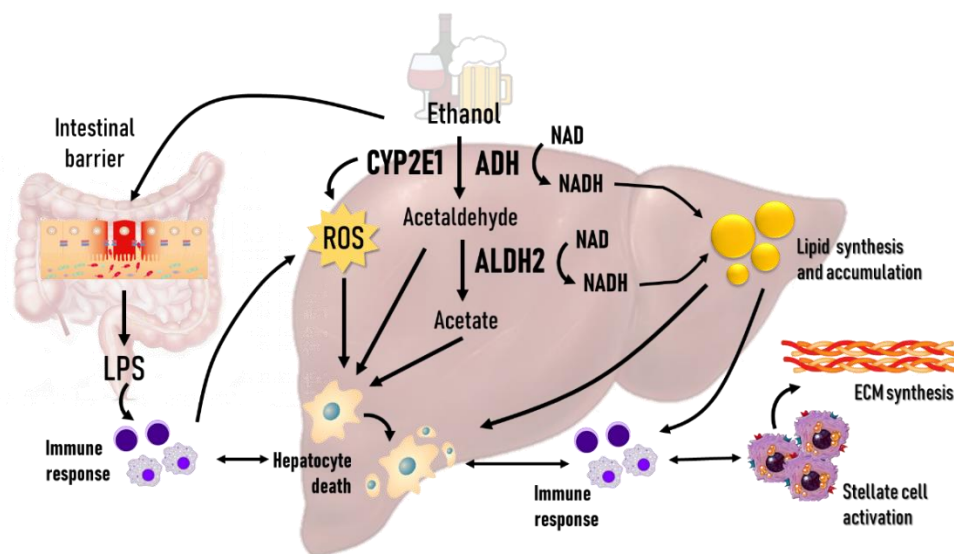
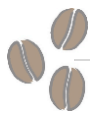


Figure 7. The main ethanol-related mechanisms on the induction on alcoholic liver disease (ALD), a growing risk condition for HCC in high income countries (Cederbaum, 2012; Tsuchida & Friedman, 2017; Stärkel et al., 2018; You & Arteel, 2019).

Lastly, the mechanisms involved in NAFLD-related HCC are intrinsically related to the frequency of metabolic disorders, including type 2 diabetes mellitus (T2DM) and especially obesity, an imminent public health problem in high income countries (Makarova-Rusher et al., 2016). According to the Center of Disease Control (CDC) of the USA, the prevalence of obesity was 39.8% and affected about 93.3 million adults in 2015-2016 (CDC, 2018). Interestingly, ~34% of USA population presents NAFLD, indicating a potential causal relationship between obesity and this HCC risk condition



(Kim et al., 2013). The western fast food culture, established in 60's and globally widespread nowadays, contributes to the enhanced consumption of saturated fats and refined sugars (Fraser et al., 2010). A saturated fat-rich diet increases serum free fatty acids (FFA) levels, as well as FFA delivering to the organs, including the liver (Kutlu et al., 2018) (Figure 8). Increased FFA uptake drastically alters hepatic lipid metabolism, stimulating *de novo* lipogenesis while decreasing triglyceride disposal by fatty acid oxidation and by the secretion of triglyceride-rich lipoproteins (Kutlu et al., 2018). Some authors rely on the “two-hit” theory to explain NAFLD molecular pathogenesis (Kutlu et al., 2018). The first hit involves the triglyceride accumulation in more 5% of hepatocytes, characterizing simple steatosis (Kutlu et al., 2018). The progressive fat accumulation may establish a lipotoxic context that leads to hepatocyte death and triggers inflammatory response, which is considered the “second hit” (Kutlu et al., 2018) (Figure 8). Subsequently, chronic inflammation leads to HSC activation, fibrosis, and the coexistence of all these conditions is denominated NASH, which is the most advanced stage of NAFLD development (Kutlu et al., 2018). The consumption of high-sugar drinks, containing high fructose and glucose levels, also contribute to NAFLD (Jensen et al., 2018). Briefly, fructose and glucose metabolism increase acetyl-CoA bioavailability, stimulating *de novo* lipogenesis and triglyceride accumulation (Jensen et al., 2018) (Figure 8). A fat-rich diet consumption is also responsible for visceral body fat accumulation and gut permeability (Vonghia & Francque, 2015; Federico et al., 2016). Pro-inflammatory adipokines produced by increased visceral fat, as well as enhanced endotoxemia caused by gut leakiness also promote the “second-hit” events (Vonghia & Francque, 2015; Federico et al., 2016) (Figure 8). The chronic pro-inflammatory context in NASH contributes to the acquisition of “tumor-promoting inflammation” cancer hallmark.

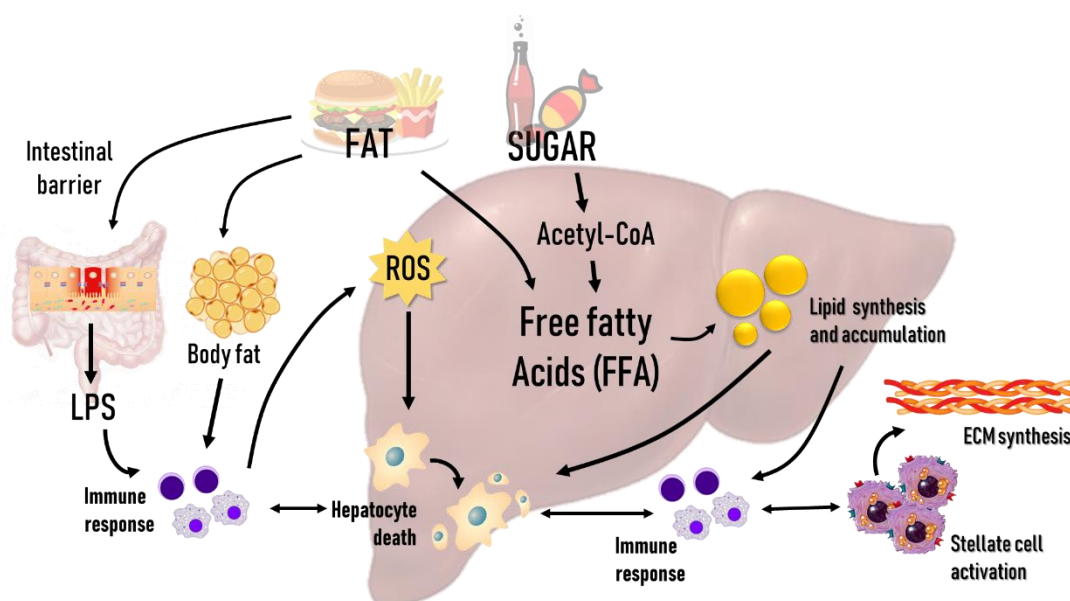
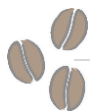


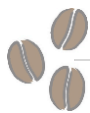
Figure 8. The main western diet-related mechanisms on the induction on alcoholic liver disease (NAFLD), another rising risk condition for HCC in high income countries. ROS = reactive oxygen species; LPS = lipopolysaccharide (Vonghia & Francque, 2015; Federico et al., 2016; Jensen et al., 2018; Kutlu et al., 2018).



The emergence of HCC, which is a complex and stepwise process, so called hepatocarcinogenesis, involves the progressive accumulation of molecular and morphological alterations under the mechanisms of the above cited risk factors. The cirrhotic background (up to 90% of HCC cases) and the metabolic alterations (as observed in ALD and NAFLD), confer “tumor-promoting inflammation” and “deregulated energetics” features to hepatic microenvironment, predisposing to molecular changes. The multistep sequence of (epi)genetic alterations disrupts core cellular functions, favoring the acquisition of sustained cell proliferation, immortality, genomic instability and mutation, migration and invasion, angiogenesis traits, known as hallmarks of cancer (Figure 9). Gradually, these features favor the development of benign hepatocellular lesions, as dysplastic nodules, HCC and metastatic tumors (Figure 9).

In humans, altered hepatocyte foci (AHF), microscopic alterations composed of 20-30 hepatocytes, are frequently observed in cirrhotic livers (around 68% of patients) (Su & Bannasch, 2003). These lesions display different phenotypes: small cell change (presenting decreased nuclear and cytoplasm ratio) or glycogen-storing foci (GSF) (Su & Bannasch, 2003; Libbrecht et al., 2007). Although similar alterations are frequently observed in experimental HCC mouse models, the relevance of AHF as early alterations in human hepatocarcinogenesis, as well as the importance of their screening, is yet to be elucidated (Su & Bannasch., 2003; Libbrecht et al., 2007). Generally, the earliest hepatocellular lesion with real clinical importance for human hepatocarcinogenesis develops in cirrhotic livers as macroscopic dysplastic nodules (DN). Further classified into low or high-grade DN, some of these lesions harbor Telomerase reverse-transcriptase (*TERT*) promoter mutations (~25%) (Nault et al., 2013). *TERT* gene encodes telomerase enzyme, responsible for telomere length maintenance. This activating mutation enables unlimited telomere stability, conferring the immortalization feature to DN (Nault et al., 2013; 2014). *TERT* mutations are also observed in HCC (comprising 44% of cases, considered the most common genetic alteration), whereas other DN-related mutations are not so frequent in this malignancy (Nault et al., 2014; Cancer Genome Atlas Research Network, 2017). For this reason, DN are considered premalignant conditions and *TERT* mutations are predictive biomarkers of liver neoplastic transformation (Nault et al., 2014). Interestingly, HCC features not only mutations, but also *TERT* amplification is observed in 10% of HCC cases (Cancer Genome Atlas Research Network, 2017).

Among other important genetic alterations in HCC, there are inactivating mutations in tumor suppressor genes tumor protein (*TP53*) (31%), axin 1 (*AXIN1*) (8%), and RB transcriptional corepressor 1 (*RB1*) (4%) (Cancer Genome Atlas Research Network, 2017). Activating mutations on catenin beta 1 (*CTNNB1*) (27%) oncogene are also recurrent (Cancer



Genome Atlas Research Network, 2017). The widely-known *TP53* gene, that translates the most extensively studied protein in the solid tumors, has crucial roles on inducing cell cycle arrest (Cdkn1a and Gadd45a), DNA repair (Gadd45a) and apoptosis (BH3 domain-only proteins Puma, Noxa, Bad, Bax, and Bak)-related proteins (Chen, 2016). Thus, mutations on *TP53* may impair these cellular processes, contributing to the acquisition of “evasion of growth suppressors”, “genomic instability and mutation” and “resistance to cell death” hallmarks, correspondingly. Besides *TP53* mutations, the hypermethylation of O6-methylguanine-DNA methyltransferase (*MGMT*) promoter (39% of cases) is also proposed to hinder DNA repair and predispose to genomic instability (Zhang et al., 2003; Cancer Genome Atlas Research Network, 2017).

AXIN1 and *APC* are negative regulators of the pro-proliferative Wnt/ β -catenin pathway (Zhan et al., 2017). In the off-state of this pathway, β -catenin, which a transcriptional co-regulator, is phosphorylated, ubiquitinated and led to degradation by APC/Axin/GSK-3 β -complex. In the presence of Wnt ligand (on-state), GSK-3 β is displaced from APC/Axin complex, leading to β -catenin accumulation and translocation to the nucleus, where it binds to LEF/TCF transcription factors (Zhan et al., 2017). LEF/TCF/ β -catenin promotes the expression pro-proliferative genes, including *Myc* and Cyclin D1 (*CCND1*) (Zhan et al., 2017). Deactivating *AXIN1* and activating *CTNNB1* mutations result on intrinsic activation of Wnt/ β -catenin pathway in HCC, conferring “sustained cell proliferation” hallmark to this malignancy (Zhan et al., 2017). Aberrant methylation profile is also related to Wnt/ β -catenin pathway, since increased hypermethylation of *APC* promoter is observed in 63.1% of HCC cases (Csepregi et al., 2008; Zhang et al., 2016). Despite of being quite heterogeneous, epidermal growth factor receptor (EGFR) overexpression is observed 32–66% of HCC tissues (Buckley et al., 2008; Panvichian et al., 2015). In addition, *EGFR* extra copy numbers are present in 45% of cases (Buckley et al., 2008). EGFR is transmembrane tyrosine kinase receptor activated by epidermal growth factor (EGF) and transforming growth factor α (TGF- α) ligands (Wee & Wang, 2017). Bindings results in EGFR dimerization and activation of downstream signaling pathways, including Ras-Raf-MAPK and phosphatidylinositol 3-kinase (P13K)/protein-serine/threonine kinase Akt, involved in cell growth, proliferation and survival (Wee & Wang, 2017). In HCC, increased EGFR signaling is proposed to contribute to “sustained cell proliferation hallmark”, as well as Wnt/ β -catenin pathway.

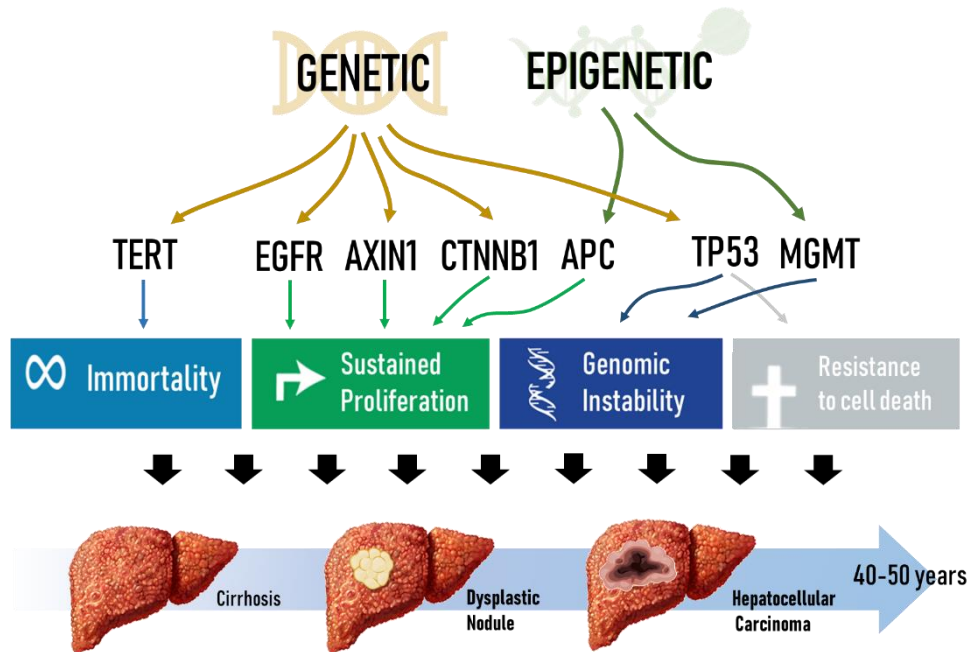
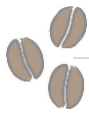
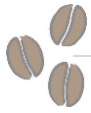


Figure 9. The main (epi)genetic alterations observed during human hepatocarcinogenesis. The multistep sequence of molecular alterations disrupts core cellular functions, favoring the acquisition of the hallmarks of cancer. Gradually, these traits favor the development of benign hepatocellular lesions and HCC (Zhang et al., 2003; Buckley et al., 2008; Nault et al., 2013; 2014; Panvichian et al., 2015; Cancer Genome Atlas Research Network, 2017).

In order to elucidate the molecular and morphological events involved in complex stepwise hepatocarcinogenesis, and to investigate preventive and therapeutic alternatives to HCC, a myriad of *in vitro* and *in vivo* models is applied in literature (as revised by Bakiri et al., 2013 and Hirschfield et al., 2018). The *in vitro* study of the multistage hepatocarcinogenesis process involves both primary cultures of hepatocytes and well-established HCC cell lines (Arellanes-Robledo et al., 2017; Hirschfield et al., 2018). By using primary hepatocyte cultures of human or animal origin, it is possible to understand the cellular and molecular events involved in malignant transformation, as genomic instability, cell proliferation and apoptosis (Arellanes-Robledo et al., 2017). On the other hand, a great number of human HCC cell lines have been established for the study of HCC progression stage (Arellanes-Robledo et al., 2017; Hirschfield et al., 2018). These cell lines have proved to be a useful tool in biomedical research, enabling the development of pharmacological therapies and screening of toxic compounds (Arellanes-Robledo et al., 2017; Hirschfield et al., 2018). Nonetheless, monolayer homotypical cell culture using HCC cell lines (Figure 10) lacks molecular and microenvironmental heterogeneity as observed in the corresponding human disease. Among all cell lines used, HepG2 (ATCC® HB-8065™),



which is derived from a 15-year-old American boy, has been the most used HCC *in vitro* model from 2000 to 2016, followed by Huh7, taken from a 57-year-old Japanese male (Arellanes-Robledo et al., 2017).

However, cell line heterogeneity is a limitation, since some of them harbor punctual resemblances with human HCC, while lacking many other molecular characteristics. The *CTNNB1* mutation, frequently observed in human HCC, was only observed in SNU-398 and C3A (Figure 10) cell lines (Hirschfield et al., 2018). SNU-398, Huh7 and HepG2 displayed *TERT* promoter mutations (Hirschfield et al., 2018). In addition, Huh7 also showed *TP53* mutation, while SNU-398, C3A and HepG2 did not. SNU-449 features *AXIN1* and *TP53* mutations while lacks *TERT* mutation (Hirschfield et al., 2018). Moreover, both SNU-398 and -449 present part of HBV genome, indicating insertional mutagenesis, which is not featured in Huh7, C3A and HepG2 (Hirschfield et al., 2018). Some cell lines, as HepG2 and its clonal derivative C3A, display HCC clinical characteristics such as increased serum α -fetoprotein (AFP) levels in the medium (Hirschfield et al., 2018). In order to mimic tumoral complexity and microenvironment, 3D heterotypical cultures using the above cited cell lines have been established (Figure 10) (Abu-Absi et al., 2004). Hepatocytes cultured on moderately adhesive surfaces or in suspension aggregate to form spheroids. In order to mimic a functional liver, tumoral cells are usually co-cultivated fibroblast-like cells, including the activated HSC (as human LX-2 and rat HSC-T6) and fibroblasts (as mouse NIH/3T3) (Abu-Absi et al., 2004; He et al., 2018; Khawar et al., 2018). Mixed cell 3D cultures systems sometimes contain three different cell types, as hepatocytes, HSC and macrophages (Prestigiaco et al., 2017). In comparison to homotypical spheroids, mixed-cell spheroids display enhanced expression of collagen I and pro-fibrotic factors such as, TGF- β 1 and CTGF (Khawar et al., 2018). In order to add microenvironmental complexity to spheroid model, some protocols are based on the co-activation of the fibroblast-like cells by treating the spheroids with pro-inflammatory LPS, IL-6, PDGF or TGF β (Prestigiaco et al., 2017; Ouchi et al., 2019; Pingitore et al., 2019). These examples of heterotypical 3D culture models, also called heterospheroids, are well-accepted models for the study of inflammation/fibrosis-associated-HCC (Figure 10). Recently, *in vitro* models of NASH-associated HCC have been established, using 3D heterotypical spheroid backbone, by adding FFA in the medium (Ouchi et al., 2019; Pingitore et al., 2019) (Figure 10). In comparison to non-exposed spheroids, FFA-treated ones accumulate of fat and exacerbate collagen synthesis (Ouchi et al., 2019; Pingitore et al., 2019).

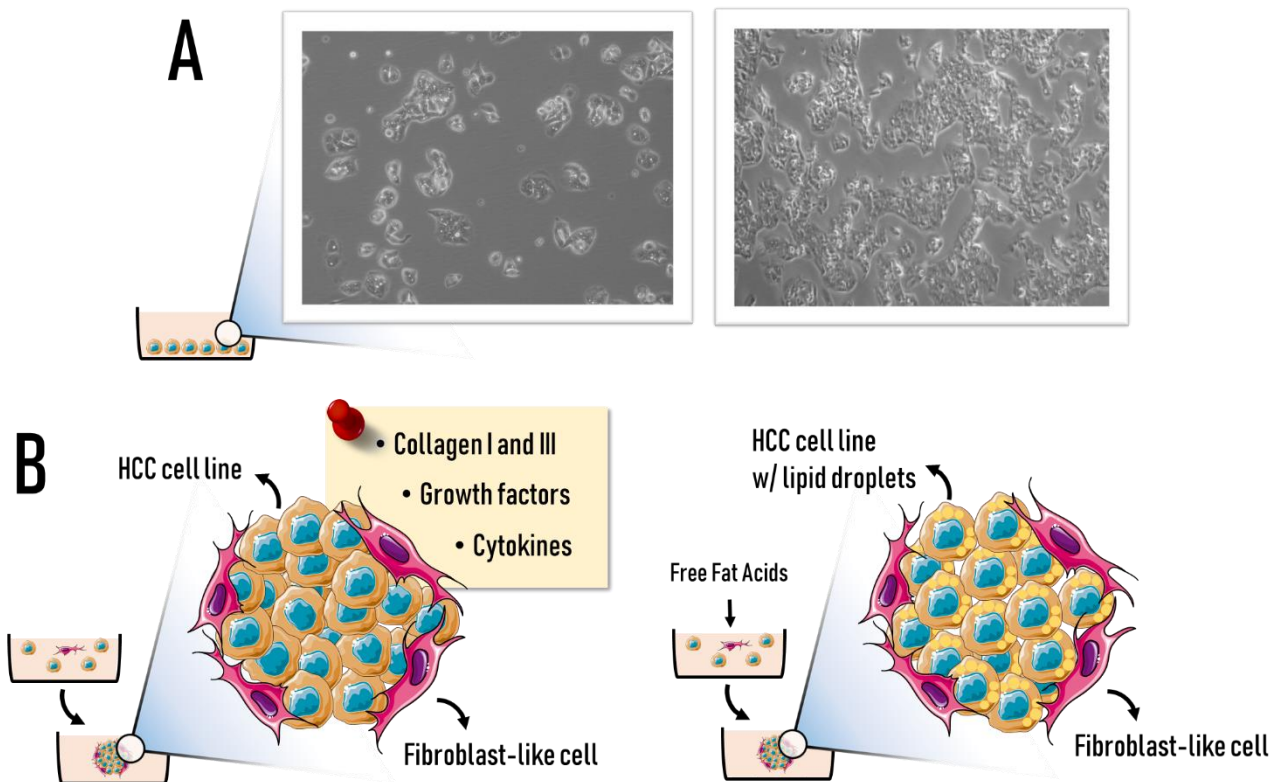
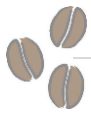
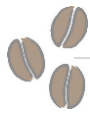


Figure 10. (A) Example of homotypical monolayer cell culture in low and high densities of C3A cell line (ATCC® CRL-10741™), a clonal derivative of HepG2, the most applied HCC cell line in research (Arellanes-Robledo et al., 2017). (B) Graphical examples of heterotypical 3D cell culture systems with HCC and fibroblast-like cells, applied as fibrosis-associated or NASH-associated HCC models (Khawar et al., 2018; Pingitore et al., 2019)

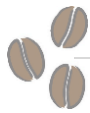
In addition to the *in vitro* bioassays, a relatively large number of rodent models to study hepatocarcinogenesis are presently available and can be organized as follows: (1) chemically-induced, (2) xenograft, (3) viral, and (4) genetically engineered mouse (GEM) models (Bakiri et al., 2013). Chemically-induced bioassays rely on the administration of genotoxic and non-genotoxic compounds that lead to the development of hepatocellular preneoplastic and malignant neoplastic lesions in mice (*Mus musculus*) and rats (*Rattus norvegicus*) (Heindryckx et al., 2009; Bakiri et al., 2013). Some of these preclinical bioassays present striking morphological and molecular similarity to the corresponding human disease, presenting potential translational application (Petrelli et al., 2014; Romualdo et al., 2017). Nevertheless, the greatest disadvantages on choosing these bioassays are the methodological inconsistency (e.g. different chemical compounds,



doses, frequencies of administration, etc.) and mouse inter-strain variability (less or more susceptible) (Heindryckx et al., 2009; Bakiri et al., 2013). Due to these reasons, literature lacks standard chemically-induced preclinical rodent models.

Among the most used chemicals in these models, diethylnitrosamine (DEN), also called N-nitrosodiethylamine (NDEA), is a N-nitrosamine naturally found in tobacco and cured meat (Scanlan, 1983) (Figure 11). The daily human ingestion of N-nitrosamines is around 0.5 to 1.0 μg (Scanlan, 1983). DEN holds the “Group 2A: probably carcinogenic to humans” classification according to the International Agency for Research on Cancer (IARC, 2019). DEN hepatocarcinogenic properties were first described in the 60’s, when administered to rats and golden hamsters in drinking water (Dontenwill & Mhor, 1961; Thomas, 1961). In more recent protocols, DEN is usually administered intraperitoneally to rats or mice, in single or multiple doses (Romualdo et al., 2017; 2018). After DEN injection, its biotransformation happens in the liver by cytochrome P450 (CYP) 2E1, generating ROS and carbonium ions (Verna et al., 1996; Jin et al., 2007) (Figure 11). These highly reactive metabolites bind to biomolecules, including the DNA. DEN-induced DNA alkylation or oxidation predispose to DNA damage, genomic instability and mutation (Verna et al., 1996). Although the exact molecular alteration caused by DEN in hepatocytes is not known, DEN is considered a complete carcinogen that leads to the development of preneoplastic and malignant hepatocellular lesions (Verna et al., 1996) (Figure 12). DEN is frequently given to rodents in their neonatal (mice) or adult phases (rats and mice) (Vesselinovitch et al., 1984; Romualdo et al., 2017; 2018). The main advantage of using neonatal protocol in mice is the hepatic postnatal (PND) development context (Vesselinovitch & Mihailovich, 1983; Septer et al., 2011). Compared to adult liver, proliferation rates are increased in the liver of neonatal mice (Septer et al., 2011). When given to neonatal mice at the 15-20 PND, the pro-proliferative hepatic context promotes the clonal expansion of DEN-initiated hepatocytes, ultimately favoring hepatocellular (pre)neoplastic lesion development and shortening the time for HCC development (Vesselinovitch & Mihailovich, 1983).

Furthermore, inter-strain mouse susceptibility also interferes with the outcomes of chemically-induced hepatocarcinogenesis. In both adult or neonatal mice models, C3H/HeJ mice presents increased susceptibility to DEN-induced regimens compared to other commonly applied strains, as C3B6F1 (intermediate susceptibility), C57BL/6J and BALB/c (decreased susceptibility) (Lee et al., 1989; Weghorst et al., 1989). Although the molecular basis for liver tumor susceptibility have not been fully investigated, several loci that influence susceptibility and resistance have been mapped (Maronpot., 2009). The greater susceptibility of the C3H/HeJ strain is mostly attributed to hepatocarcinogenicity sensitivity 7 (*Hcs7*) locus, which promotes hepatocyte growth and proliferation, especially in preneoplastic lesions (Bilger et al., 2004; Maronpot, 2009). Indeed, due to this genetic feature, C3H/HeJ mice spontaneously develop HCC in the absence of



carcinogen in a long latency time (up to 76 weeks) (Connor et al., 2018). Nonetheless, even in neonatal mouse models using susceptible strains, a long latency time is necessary for these lesions to achieve high incidence and multiplicity (up to ~40 weeks, in a strain-, protocol-dependent manner) (Bakiri et al., 2013). Therefore, in order to reduce the experimental time, DEN is applied as genotoxic “initiator” and usually combined with another drug or surgical process (as 2/3 partial hepatectomy) as a “promoter” (Bakiri et al., 2013) (Figure 12). The promoter’s main goal is to establish a context that favors the clonal expansion of DEN-initiated hepatocytes (Bakiri et al., 2013) (Figure 12).

One of the most applied promoters is carbon tetrachloride (CCl_4) (Uehara et al., 2013; Chappell et al., 2014; Romualdo et al., 2018) (Figure 11). Although DEN intraperitoneal administrations lead to the development of hepatocellular (pre)neoplastic lesions, these models lack the fibrosis/cirrhosis scenario observed in up to 90% HCC cases (Yang et al., 2011). Thus, the use combined DEN + CCl_4 regimen is suitable for the study of fibrosis- or cirrhosis-associated hepatocarcinogenesis process (Uehara et al., 2013; Chappell et al., 2014; Romualdo et al., 2018). When intraperitoneally administered to rats and mice, this haloalkane is majorly metabolized by CYP2E1 (CYP2B1, CYP2B2 and CYP3A also play minor roles) to form the highly reactive trichloromethyl ($^*\text{CCl}_3$) and trichloromethyl peroxy ($^*\text{OCCl}_3$) radicals (Weber et al., 2003) (Figure 11). This radical, as well as ROS generated by increased CYP2E1, can bind and damage to biomolecules, as lipids, proteins and nucleic acids (Weber et al., 2003). Lipid peroxidation reactions, initially mediated by $^*\text{OCCl}_3$, damage and increase the permeability of mitochondrial, endoplasmic reticulum, and plasma membranes (Weber et al., 2003). Protein oxidation impairs enzyme activity, while RNA damage may reduce protein synthesis (Weber et al., 2003). This context predisposes to hepatocyte death, triggering inflammatory response (Weber et al., 2003). Oxidative stress, cell death and inflammatory mediators are the stimuli for HSC activation and, ultimately, liver fibrosis (Weber et al., 2003) (Figure 11). Multiple intraperitoneal CCl_4 administrations, in unique or increasing doses, mimic cycles of viral replication and liver damage in the corresponding human disease (Uehara et al., 2013; Chappell et al., 2014; Romualdo et al., 2018). The establishment of a pro-inflammatory and pro-fibrotic background is thought to promote DEN-initiated hepatocytes (Uehara et al., 2013; Chappell et al., 2014; Romualdo et al., 2018). Growth factors and cytokines produced by immune cells during chronic inflammatory response may have paracrine mitogenic effects on (pre)neoplastic hepatocytes, inducing focal lesion growth (Uehara et al., 2013). Indeed, the combination of DEN initiation (single dose in neonatal mice) and CCl_4 promotion (twice a week for 14 weeks, starting at 8 weeks of age) regimens increased by 50% the incidence of HCC compared to DEN-initiated mice, suggesting an acceleration of HCC development (Uehara et al.,

2013). Even though CCl_4 is applied as a promoter, adduct formation between $^*\text{CCl}_3$ and DNA may also function as initiator, leading to HCC development in a protocol-dependent manner (Weber et al., 2003; Uehara et al., 2013; Chen et al., 2015)

Other chemical promoters are recurrently used in models, as the non-fibrogenic phenobarbital (PB) and the fibrogenic thioacetamide (TAA). The mechanism regarding PB promotion is not fully elucidated, but its administration in low doses in drinking water or diet positively selects hepatocytes harboring the activating mutations of the *Cttnb1* gene, which lead to activated β -catenin signaling (Aydinlik et al., 2001). For this reason, some authors denominate PB as a “tumor selector” rather than a promoter (Braeuning & Schwarz, 2016), since *Cttnb1* mutations are not frequent in protocols using only DEN (Connor et al., 2018). Similar to CCl_4 , TAA undergoes metabolic activation by CYP2E1, generating S-oxide (TASO) and S,S-dioxide (TASO(2)) compounds that sequentially exert biomolecule damage, cell death, inflammatory response, HSC activation, ECM synthesis and fibrosis/cirrhosis in a protocol-dependent manner (Hajovsky et al., 2012; Crespo et al., 2016; Romualdo et al., 2017). The use of fibrogenic promoters in chemically-induced models result on remarkable molecular and resemblances with human fibrosis/cirrhosis-associated HCC (Romualdo et al., 2017), usually caused by chronic viral infections. For ALD- and NAFLD- associated HCC bioassays, DEN initiation protocols are commonly combined with dietary interventions. For ALD models, Lieber-DeCarli (~5% of ethanol) liquid diet is usually given to rodents after DEN initiation, promoting β -catenin nuclear translocation and mRNA upregulation of its downstream targets (Mercer et al., 2014). Concerning NASH, recent models using “western diet” approach promote HCC in a context of progressive lipid accumulation, lipotoxicity, HSC activation and fibrosis (Kishida et al., 2016; Tsuchida et al., 2018). Mouse models frequently use high fat diet formulations (20-60% of fat) and fructose/glucose mix (55/45%) in drinking water (Kishida et al., 2016; Tsuchida et al., 2018). The combination of CCl_4 repeated applications and western diet was also applied for this purpose in order to establish a NASH context experimentally (Tsuchida et al., 2018)

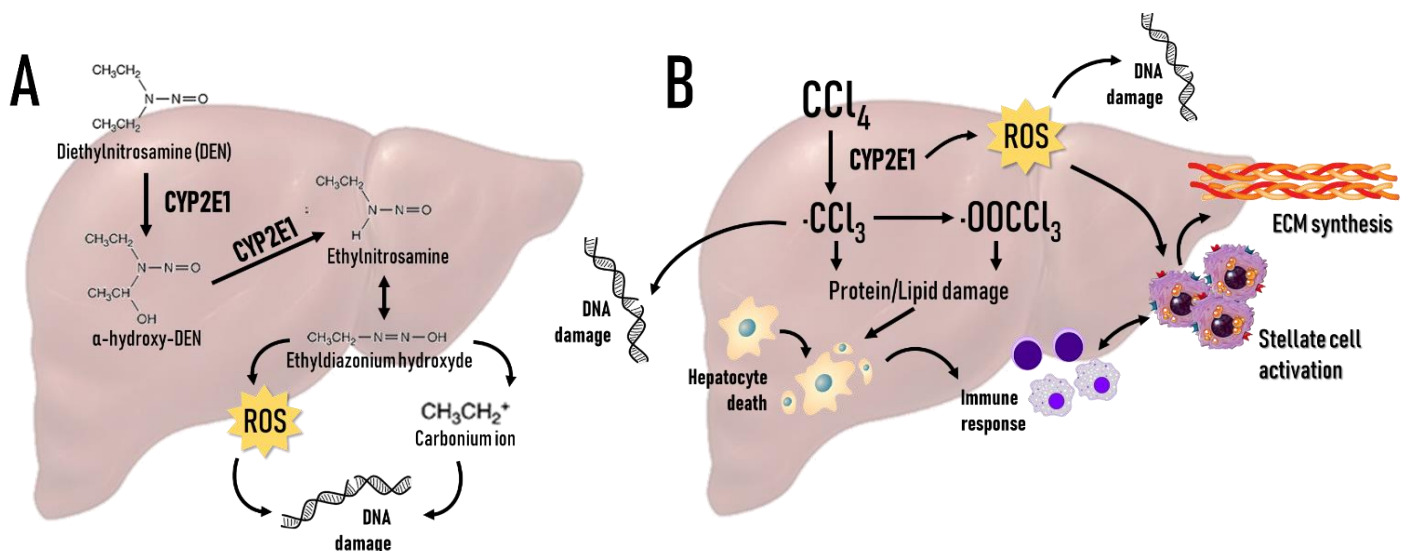
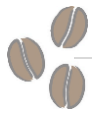
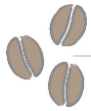


Figure 11. (A) Diethylnitrosamine (DEN) and **(B)** carbon tetrachloride (CCl_4) liver metabolism and their cellular outcomes (Verna et al., 1996; Weber et al., 2003). $^*\text{CCl}_3$ = trichloromethyl radical; $^*\text{OCCl}_3$ = trichloromethyl peroxy radical; ROS = reactive oxygen species.



The first and smallest morphologically recognizable lesion in chemically-induced models of hepatocarcinogenesis in mouse are AHF (up to ~20 weeks, in a strain- and protocol-dependent manner). The gold standard for AHF identification is the microscopic screening in Hematoxylin and Eosin (HE)-stained sections (Thoolen et al., 2010). Foci present clear phenotypical variations and are usually classified as basophilic, eosinophilic or clear cell foci according to the tinctorial characteristic of most hepatocytes (Thoolen et al., 2010) (Figure 13). Basophilic cell foci are composed of smaller cells than normal hepatocytes, and cytoplasm exhibits distinct basophilia due to free ribosomes or rough endoplasmic reticulum (Thoolen et al., 2010). Both clear and eosinophilic cell foci are composed of enlarged cells due to glycogen storage in excess (Thoolen et al., 2010). Strong eosinophilia may result from enhanced smooth endoplasmic reticulum, peroxisome, or mitochondria (Thoolen et al., 2010). These phenotypes seem not occur at random considering that these lesions are theorized to undergo a “metabolic turnover” (Figure 13). At first, DEN increases insulin growth factor II (IGF-II) levels, and IGF-II downstream signaling decreases glucose-6-phosphatase (G6Pase) activity, promoting the emergence of glycogen storage phenotypes (Lahm et al., 2002; Bannasch et al., 2003). IGF signaling also promotes ras-, raf-, mitogen activated signaling cascade, enhancing cell proliferation (Bannasch et al., 2003). Progressively, foci shift from anabolic to catabolic glucose metabolism in order to provide energy for the increasing cell proliferation, giving rise to basophilic phenotype (Bannasch et al., 2003) (Figure 13). Along with the “deregulated energetics” hallmark, some of AHF display *Hras* (15% of G6Pase-negative foci) and *Braf* (97.3% of basophilic foci) oncogene mutation (Buchmann et al., 1989; Yamamoto et al., 2017). These mutations may provide a proliferative and growth advantage to these lesions (Buchmann et al., 1989; Yamamoto et al., 2017). Although these molecular alterations are not common in human HCC, and considering that the importance of similar AHF in human hepatocarcinogenesis is not elucidated, mouse AHF are considered putative preneoplastic lesions in chemically-induced models and predisposed to neoplastic progression under adequate promoting stimuli (Figure 12) (Buchmann et al., 1989; Bannasch et al., 2003; Yamamoto et al., 2017). The screening of these lesions enables carcinogenicity testing during the early stages of hepatocarcinogenesis, avoiding the use of long latency chemically-induced protocols (Klaunig & Kamendulis, 1999; Bannasch et al., 2003, Ogawa, 2009). Indeed, AHF have been extensively used in research for the investigation of the early molecular events of hepatocarcinogenesis, as well as for the screening of preventive/promoting agents (Romualdo et al., 2016; 2017; Cast et al., 2018; Pedersen et al., 2019).

The subsequent molecular events that explain the malignant transformation of AHF are yet to be fully unraveled, but the initiation→ promotion→ progression stepwise theory is widely accepted in literature (Figure 12) (Klaunig & Kamendulis, 1999; Bannasch et al., 2003, Ogawa, 2009). Indeed, recent findings indicate that some hepatocytes of DEN-



induced AHF presenting oncogenic dephosphorylation of CCAAT/enhancer binding protein α (C/EBP α) acquire a “stemness” feature, being classified as potential tumor-initiating hepatocyte (PTIH) (Cast et al., 2018). Similar events were also described in early and late stages of aggressive human HCC, suggesting that the preneoplastic foci with PTIHs are the origin of mouse HCC (Cast et al., 2018). Other findings indicated that over 80% DEN-induced HCC displayed activating hotspot mutations in either *Hras* or *Braf* oncogenic drivers, what could also support that HCC may emerge from AHF (Connor et al., 2018). Activating *Egfr* oncogene mutations (~20%) were also observed, leading to Ras-Raf-MAPK pathway activation, similarly to the corresponding human disease (Connor et al. 2018). Truncating *Apc* mutations occurred in 21% of HCC, supporting a role for deregulation of Wnt/ β -catenin signaling DEN-induced hepatocarcinogenesis, as also observed in human HCC (Connor et al., 2018). Chemically-induced models also reflect some of the epigenetic changes observed in humans. In a DEN-induced and CCl₄-promoted fibrosis-associated hepatocarcinogenesis model, the repair-related *Mgmt* gene was also hypermethylated in ~70% of HCC, leading to decreased expression of this repair-related gene (Chappell et al., 2014).

Finally, the establishment of reliable chemically-induced models enabled the translation investigation of the potential mechanisms involved in sexual disparity, since mice models reflect this feature of the corresponding human disease (Romualdo et al., 2018). Using neonatal DEN-induced mouse models, it was observed that androgen receptor (AR) knockout reduced the incidence and the number of tumors in male mice, suggesting the promoting effect of AR on hepatocarcinogenesis (Ma et al., 2008). AR activation may hinder p53-mediated DNA damage sensing/repair system and cell apoptosis, increasing cellular oxidative stress and DNA damage (Ma et al., 2008). In contrast, these models also provided a mechanism for a protective role of estrogen in female (Naugler et al., 2007). Estrogen may attenuate malignant transformation *via* downregulation of IL-6 release from Kupffer cells (Naugler et al., 2007). Other mechanisms are recently proposed, since the effects of sex hormones on lipid metabolism may interfere with HCC development (Greten, 2019).

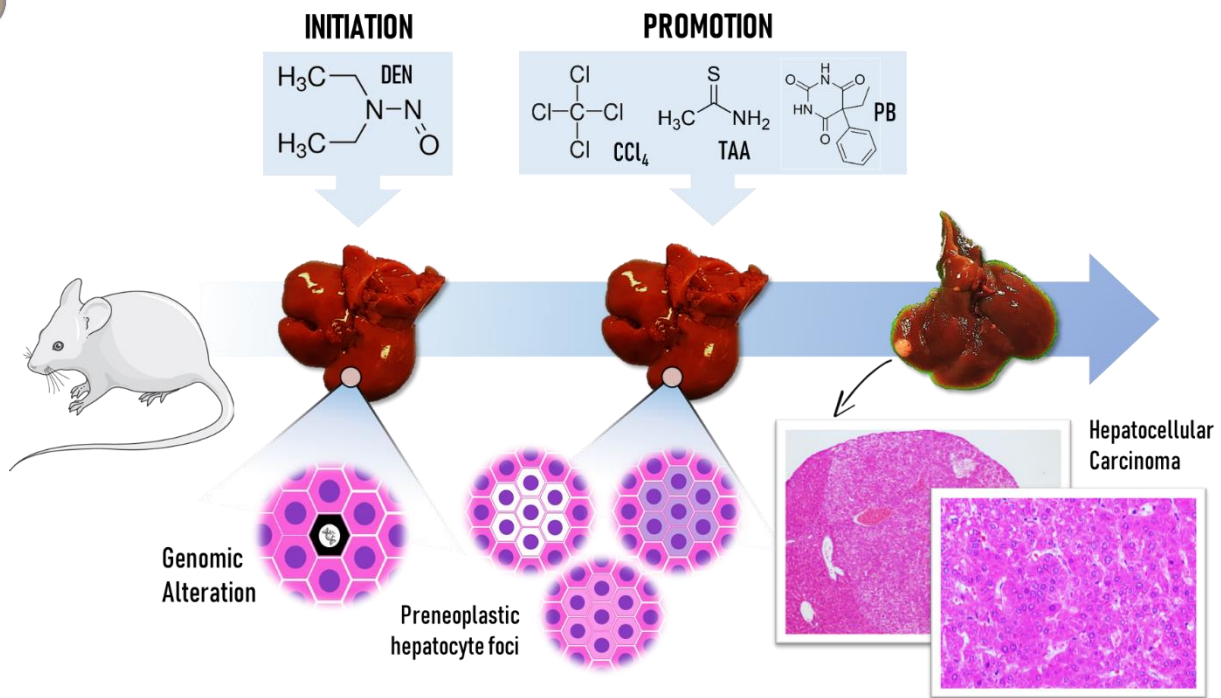
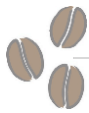


Figure 12. Multistep chemically-induced hepatocarcinogenesis in mice (Klaunig & Kamendulis, 1999; Bannasch et al., 2003, Ogawa, 2009). DEN = diethylnitrosamine; CCl₄ = carbon tetrachloride; TAA = thioacetamide; PB = phenobarbital.

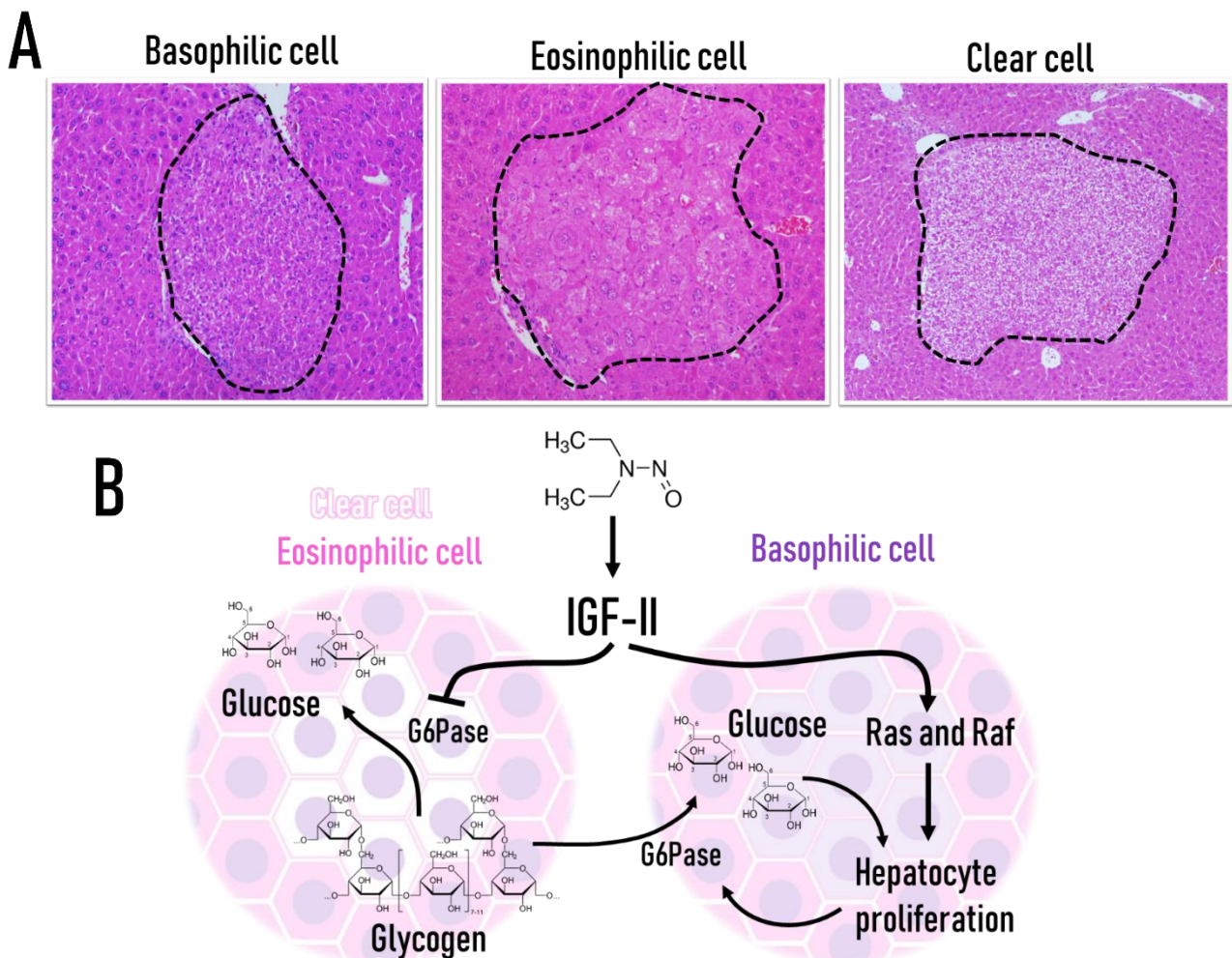
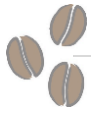


Figure 13. (A) Representative photomicrographs of HE-stained sections showing basophilic, eosinophilic and clear cell preneoplastic altered hepatocyte foci phenotypes found in DEN-treated mice. (B) Gradual metabolic shift from anabolic (clear cell and eosinophilic phenotypes) to catabolic (basophilic phenotype) glucose metabolism during DEN-induced hepatocarcinogenesis (Lahm et al., 2002; Bannasch et al., 2003). DEN = diethylnitrosamine; IGF-II = insulin growth factor II; G6Pase = glucose-6-phosphatase.



1.2 miRNAs: small molecules with great responsibilities

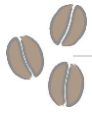
MicroRNAs (miRNAs) were first described in 1993 in *Caenorhabditis elegans* as small non-coding RNAs that display an average of 22 nucleotides in length (Lee et al., 1993). At the time of its discovery, lin-4, the first miRNA described, presented antisense complementarity to lin-14 gene, indicating that lin-4 would control lin-14 translation via an antisense RNA-RNA interaction (Lee et al., 1993). Three decades later, thousand of miRNAs have been identified (computationally and/or experimentally) in eukaryotes and even in viruses, and there is accumulating evidence on the post-transcriptional gene expression control by these small molecules, demonstrating strong interspecies sequence conservation (Li et al., 2010; De Rie et al., 2017). miRNA synthesis is classified into canonical and non-canonical pathways (O'Brien et al., 2018).

In the first step of canonical miRNA biogenesis (Figure 14), these non-coding RNAs are first transcribed by RNA polymerase II and III (Pol II) as 7-methylguanosine(m⁷G)-capped structures with polyadenylated tails, so called primary miRNAs transcripts (pri-miRNAs) (Lee et al., 2004; Borchert et al., 2006). After transcription, pri-miRNAs fold into a double stranded molecule with an apical loop and basal stem, in a duplex hairpin-like structure (Figure 14). Most miRNAs are intragenic and processed within intronic regions of protein-coding genes, whereas others are intergenic, regulated by their own promoter (Kim & Kim, 2007) (Figure 14). Sometimes miRNAs are transcribed together as long polycistronic transcripts called clusters, which are further processed to the individual mature miRNAs (Tanzer & Stadler, 2004) (Figure 14). The clustered miRNAs transcripts harbor complex functional interactions, and around 25% of human and 31% of mouse miRNAs are transcribed from polycistronic precursors (Olive et al., 2015). The mature sequence of the functional miRNA is embedded in a hairpin-like sequence found on the pri-miRNA (Figure 14). Sequentially, still in the nucleus, pri-miRNAs are processed to single hairpin precursor (pre-miRNA) by protein complex called microprocessor (Denli et al., 2004). This protein complex mostly comprises DiGeorge Syndrome Critical Region 8 (DGCR8), which is a double-stranded RNA binding protein, and Drosha, a RNase III enzyme. DGCR8 is responsible for recognizing the pri-miRNA, while Drosha cleaves the lower stem of the duplex hairpin structure, leaving a hydroxyl group (OH) at 3' end, and overhangs of 2 nucleotides and one phosphate (P) at 5' end (Denli et al., 2004; Alarcón et al., 2015) (Figure 14). Of note, 1917, 1.234 and 496 pre-miRNA hairpin sequences are currently annotated in miRBase V22 for human, mouse and rat genomes, respectively (Kozomara et al., 2019).

Then, pre-miRNAs are exported from the nucleus to the cytoplasm by protein complex mainly formed by exportin 5, that interacts with the 2 nucleotide 3' overhang through hydrogen bonds and ionic interactions (Okada et al. 2009)

(Figure 14). Then, pre-miRNAs are processed by RNase III endonuclease Dicer (Denli et al., 2004), that removes the terminal loop of the hair pin-like structure, resulting in a mature miRNA duplex (Denli et al., 2004) (Figure 4). In this doubled stranded (ds) RNA, the direction of the strand determines the name of the mature form: 5p strand comes from the 5' end, while the 3p strand originates from the 3' end. According to miRbase V22, 2654, 2013 and 769 mature sequence entries are found for human, mouse and rat genomes, respectively (Kozomara et al., 2019). Next, one of the strands is loaded on the RNA-induced silencing complex (RISC), which is key process in small RNA-mediated gene expression control (Khvorova et al., 2003). Both strands derived from the mature ds-miRNA can be loaded into the Argonaute (AGO) family of proteins (AGO1-4 in humans), which are core part of RISC (Khvorova et al., 2003). AGO interacts with the miRNA strand through three specific domains: the Piwi–Argonaute–Zwille (PAZ), the middle (MID) and the P-element induced wimpy testes (PIWI) (Nakanishi et al., 2012). The MID and PIWI hold the 5' end, while the PAZ domain binds to 3' end (Nakanishi et al., 2012). Although the process of strand selection by RISC is not fully understood, the proportion of AGO-loaded 5p or 3p strand fluctuates, greatly depending on the cell type or environment (Meijer et al., 2014). Some findings rely on a “strand bias” regarding AGO loading based on thermodynamic stability: the strand with lower 5' end stability or 5' uracil is preferentially loaded into AGO and is denominated the “guide” strand (Khvorova et al., 2003). However, many other structural preferences are proposed (Yoda et al., 2010). Upon AGO selection, the unloaded strand, which is called the “passenger” strand, will be unwound from the guide strand (Khvorova et al., 2003). In general, mature miRNAs are thought to be stable molecules that maintain long half-lives in the organs, including the liver (Gatfield et al., 2009).

The non-canonical miRNA biogenesis encompasses different pathways (Figure 15), majorly divided into Drosha/DGCR8-independent and Dicer-independent pathways (O'Brien et al., 2018). Of note, some of proteins involved in canonical synthesis are also participants of the non-canonical biogenesis. In Drosha/DGCR8-independent pathway, shorter pre-miRNA hairpins are generated from the same long primary transcript than mRNA *via* splicing machinery, that is proposed to substitute Drosha/DGCR8-mediated processing (Ruby et al., 2007) (Figure 15). Next, this pre-miRNA follows the canonical pathway, being exported to the cytoplasm by Exportin 5, cleaved by Dicer complex and loaded in RISC (Ruby et al., 2007). Another example of Drosha/DGCR8-independent biogenesis is the transcription of 7-methylguanosine (m7G)-capped pre-miRNA (Xie et al., 2013) (Figure 15). Since the transcript is already a pre-miRNA, it bypasses nuclear cleavage and is exported to cytoplasm by Exportin 1 (Xie et al., 2013) (Figure 15). After dicing, the 3' strand of the duplex has an advantage on AGO loading due to capped end of 5' strand (Xie et al., 2013). The miR-451 is an example of Dicer-independent biogenesis (Cheloufi et al., 2010). The Drosha processing of this miRNA generates a



short pre-miRNA hairpin that is not recognized by Dicer machinery (Cheloufi et al., 2010). Thus, the hairpin is directly loaded into AGO2 and 5p strand is cleaved by AGO2 catalytic region to generate an intermediate 3', while 3p strand is sliced (Cheloufi et al., 2010) (Figure 15).

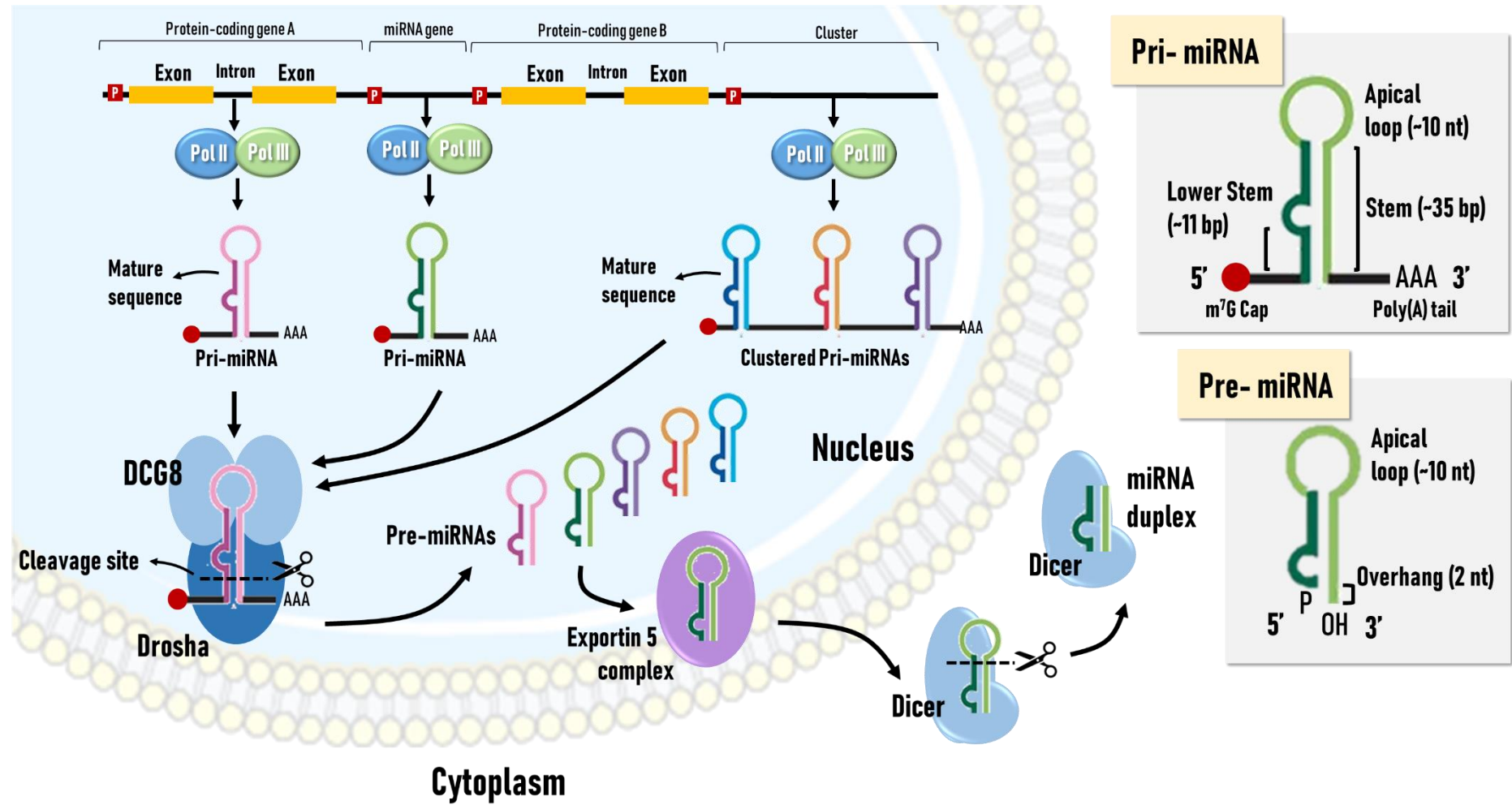
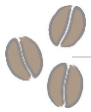


Figure 14. Canonical miRNA biogenesis (Denli et al., 2004; Lee et al., 2004; Borchert et al., 2006; Kim & Kim, 2007; Okada et al. 2009; Alarcón et al., 2015; Olive et al., 2015).

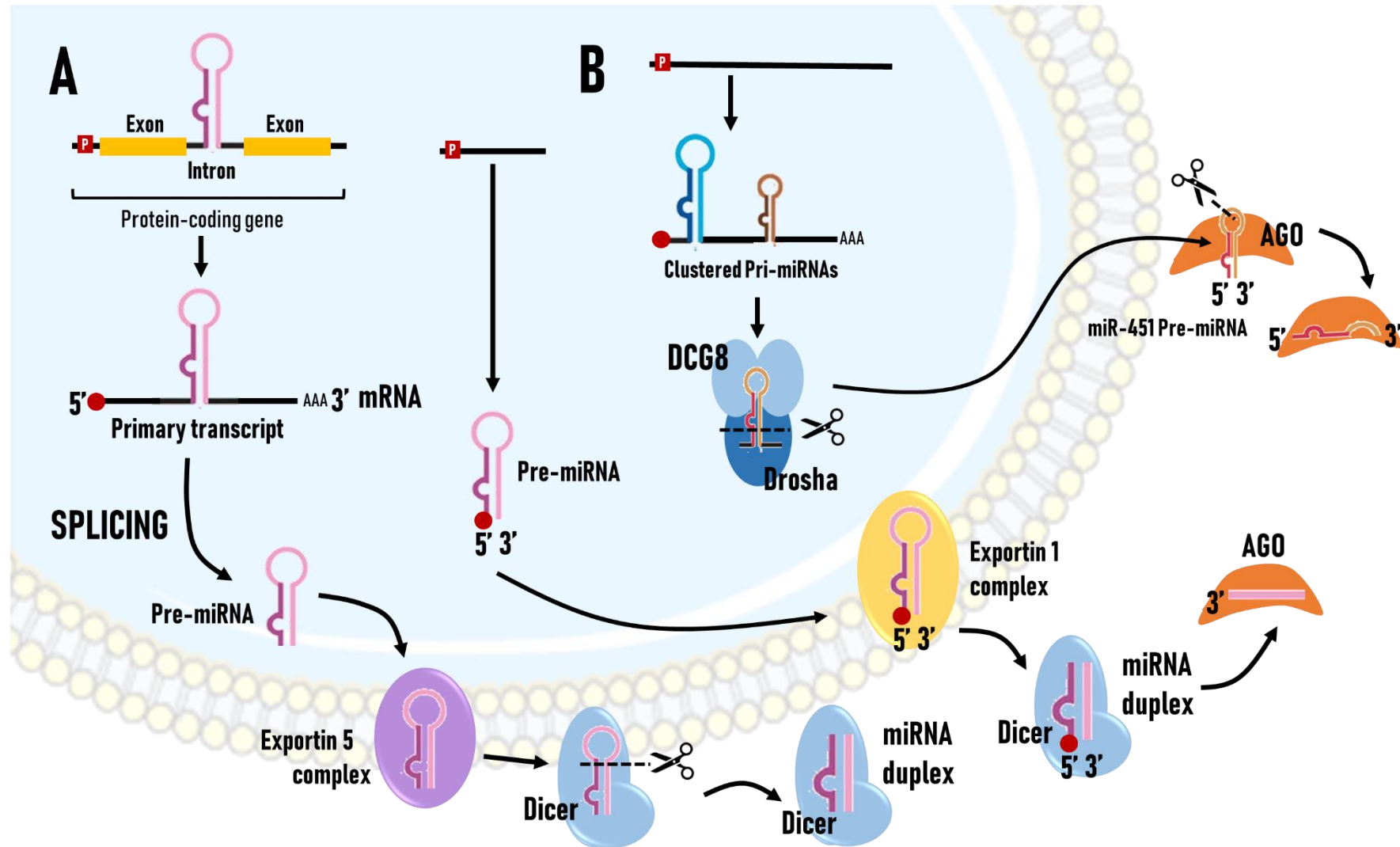
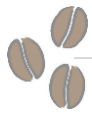


Figure 15. Non-canonical (A) Drosha/DCG8-independent and (B) Dicer-independent miRNA biogenesis (Ruby et al., 2007; Cheloufi et al., 2010; Xie et al., 2013)



Once loaded in the RISC complex, then denominated miRISC, the mature guide strand is proposed to interact with mRNAs, binding to specific sequences at the 3' untranslated region (UTR) of their target mRNAs (Figure 16). In bioinformatics, this interaction is the main criteria for target-site prediction algorithms. The nucleotides 2–8 from the 5' end of the miRNA are known as the seed, which is crucial for target mRNA recognition and matching (Bartel, 2009) (Figure 16). Once mRNA strand presents the complementarity for this nucleotide sequence (seed matching), it is predicted to be canonical target of the referred miRNA (Bartel, 2009). mRNA complementarity to 2–7 nt or 3–8 nt miRNA seed are much weaker but still considered canonical (Agarwal et al., 2015). This interaction is also supplemented with AGO binding (MID domain) with first nucleotide (nt1) of the target mRNA, preferentially an adenine (Schirle et al., 2015) (Figure 16). Other factors may influence a strong seed binding. These include additional base pairs towards the 3' end of the mature miRNA sequence, as ~13–16 of the miRNA, also called the “supplemental region” (Grimson et al., 2007) (Figure 16). It is predicted that more than 60% of all human protein-coding genes display at least one conserved miRNA-binding site (Friedman et al. 2009). To date, 3' UTR are the most accepted miRNAs seeds, but 5' UTR, coding sequence, and promoter regions are also proposed as potential interaction sites (Xu et al., 2014).

miRNAs encompass complex widespread networks of interactions with mRNA, as briefly depicted in Figure 16. One miRNA may interact with different mRNAs, and individually control entire cellular pathways (Selbach et al., 2008). miRNA clusters are also proposed to control the same cellular pathway (Mestdagh et al., 2010). Moreover, the same mRNA can be co-regulated by different miRNAs (Uhlmann et al., 2010). Some findings indicate cooperative repression of the same target by many miRNAs, what could explain the use of non-canonical interaction sites depending on the vacancy of the canonical ones (Flamand et al., 2017). The current model for post-transcriptional gene suppression occurs through (1) mRNA decay/cleavage and (2) translation repression (Figure 16). Upon seeding, miRISC recruits the glycine-tryptophan protein of 182 kDa (GW182) family of proteins [called trinucleotide repeat-containing gene 6 A/B/C (TNRC6A/B/C)] in humans, such as the poly(A)-deadenylase complex subunits 2 and 3 (PAN2 and PAN3) and carbon catabolite repressor protein 4 (CCR4-NOT), that promote the deadenylation the target mRNA (Behm-Ansmant et al., 2006). This process is initiated by PAN2/3 and completed by the CCR4-NOT complex (Behm-Ansmant et al., 2006). Subsequently, deadenylation stimulates the decapping by the mRNA-decapping enzyme subunit 1 (DCP1)–DCP2 complex (Behm-Ansmant et al., 2006). Next, an interaction between DCP1 and 5'–3' exoribonuclease 1 (XRN1) leads the mRNA to rapid 5'→3' degradation (Braun et al., 2012). In addition, miRISC inhibits the initial steps of translation by releasing initiation factor 4 A-I (eIF4A-I) and eIF4A-II hence inhibiting ribosome scanning and assembly, in a GW182-independent mechanism (Fukao et al., 2014). The mRNA

decay is generally responsible for most of miRNA:mRNA regulatory interactions (~84%), considered the predominant reason for gene silencing and hence reduced protein output (Guo et al., 2010). Some findings indicate that miRNA may exert a “fine tune” effect on gene expression, and the outcomes on reducing protein expression levels are about 20% (Baek et al., 2008). Nonetheless, the exact miRNA-mediated effect on protein levels are difficult to predict since miRNA function is increased on certain physiological and pathological contexts (Mendell & Olson, 2012).

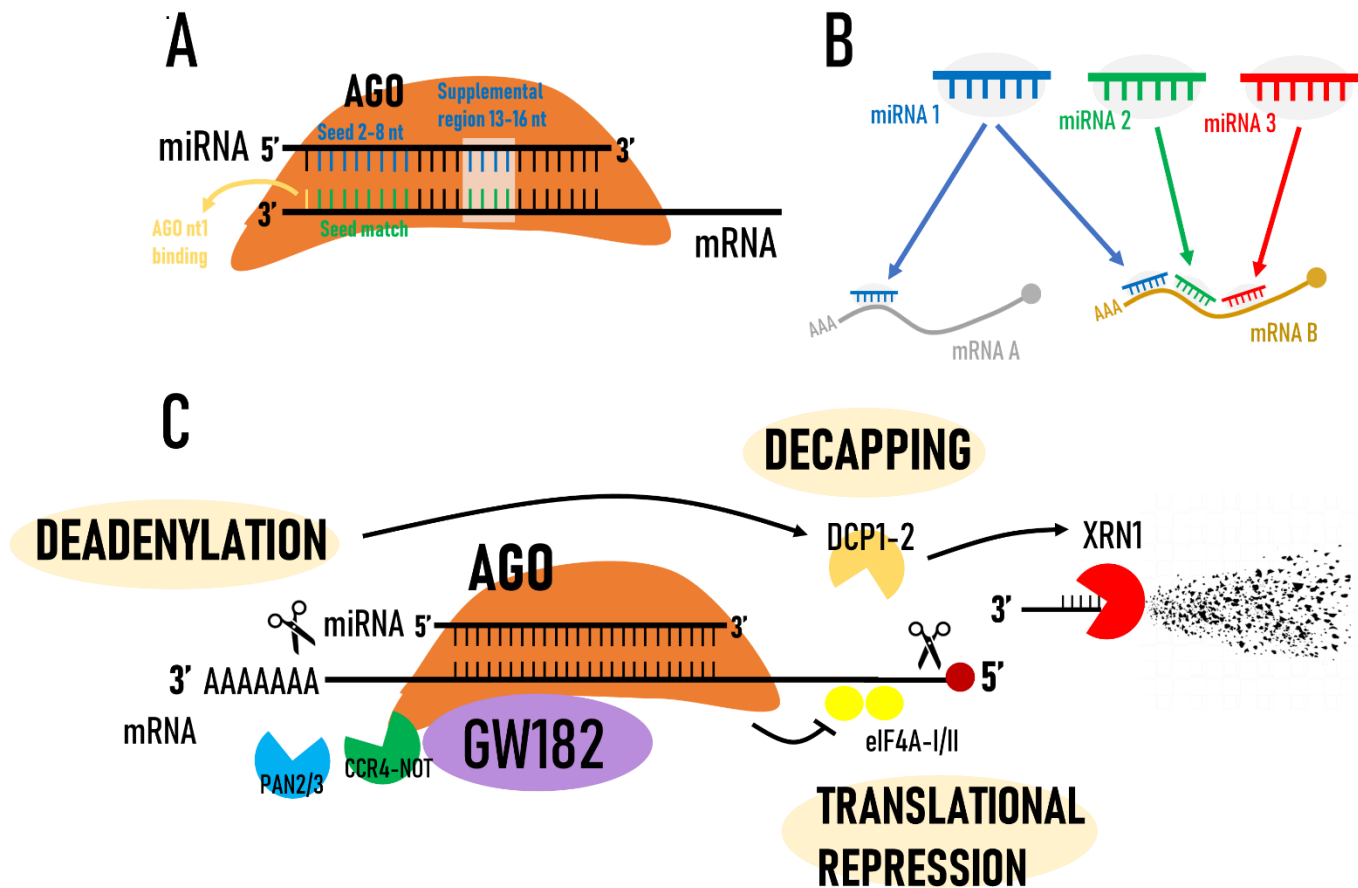


Figure 16. (A) miRNA and mRNA canonical interactions (Grimson et al., 2007; Bartel, 2009; Agarwal et al., 2015; Schirle et al., 2015); (B) Potential networks between miRNAs and mRNA (Selbach et al., 2008; Uhlmann et al., 2010); (C) miRNA-mediated mechanisms of posttranscriptional mRNA silencing (Behm-Ansmant et al., 2006; Braun et al., 2012; Fukao et al., 2014).

Due to miRNA-mediated gene silencing and outcome on protein expression, these small non-coding RNAs are proposed to participate on many key cellular pathways, contributing to a variety of physiological events (Bartel et al., 2009). On the other hand, deregulation of miRNA expression is associated with numerous diseases, particularly cancer (Xu et al., 2018). In this context, miRNAs can be considered oncogenes (called oncomirs) or tumor suppressors miRNAs, although

overall downregulation of miRNA expression is a hallmark of cancer (Xu et al., 2018). miRNAs may not only participate on tumoral biology, but also contribute with the molecular pathogenesis of preceding risk conditions, as liver fibrosis/cirrhosis (He et al., 2012). In this background, these non-coding RNAs are classified as antifibrotic or pro-fibrotic miRNAs (He et al., 2012) (Figure 17). The screening of deregulated miRNAs, as well as their molecular targets, have been encouraged in the last decades for their potential utility as biomarkers or novel therapeutic targets.

Both up or downregulation of some miRNAs may directly influence many key cellular events during liver fibrosis, mainly including HSC activation, and collagen synthesis and accumulation (He et al., 2012). The miR-29 family members (including miR-29a, miR-29b and miR-29c), so called 'master fibromiRNAs', are the most extensively studied in this HCC risk condition. All members of this family are found to be downregulated in human fibrotic livers and serum samples, being inversely correlated with fibrosis staging (Roderburg et al., 2012). Reduced levels of this miRNA family were also translationally confirmed by using both surgical (bile duct ligation) and chemically-induced (CCl₄-induced) mouse models of fibrosis (Roderburg et al., 2012). Cell isolation revealed miR-29 family is downregulated predominantly in HSC (Roderburg et al., 2012). miR-29 family targets collagen-related genes (*Col1a1*, *Col1a2*, *Col4a5*, and *Col5a3*), and its downregulation leads to collagen synthesis and accumulation, promoting liver fibrosis (Roderburg et al., 2012) (Figure 17). In contrast, the transfection of a miR-29b mimic, increasing miR-29b levels in a HSC cell line, led to decreased expression of these collagen-related genes, evidencing a potential antifibrotic role for miR-29 family upregulation in humans (Roderburg et al., 2012). Further roles of miR-29b on HSC activation were unveiled both *in vivo* (CCl₄-induced model in mice) and *in vitro* (human LX-1 and rat HSC-T6 cell lines), since the upregulation of this miRNA by ultrasound-mediated transfer or transfection decreased phosphoinositide-3-kinase regulatory subunit 1 (*PIK3R1*) and protein kinase B (*AKT3*) targets, responsible for signaling onset of HSCs activation (Wang et al., 2014) (Figure 17). With concern to collagen synthesis, miR-122 appears to negatively regulate this process *via* targeting prolyl4-hydroxylase subunit alpha-1 (*P4HA1*), a gene that encodes a component of prolyl 4-hydroxylase enzyme, responsible for collagen post-translational maturation (Li et al., 2013) (Figure 17). Indeed, miR-122 and *P4HA1* expressions are inversely correlated in human HSC LX-2 cell line and in the liver of CCl₄-treated mice (Li et al., 2013).

Recently, miR-34a-5p was also found to be downregulated in human liver fibrotic samples, human HSC cell lines, as well as in CCl₄-induced liver fibrosis in mice (Feili et al., 2018). This miRNA targets Smad4 mRNA in humans, which is a positive co-regulator of pro-inflammatory TGF- β /Smad2-3 pathway (Feili et al., 2018). In fact, when miR-34a-5p was upregulated by mimic transfection, it reduced the protein levels of Smad4 and, as a result, TGF- β /Smad2-3 (Feili et al.,

2018). Regarding TGF- β pathway, miR-17-5p targets the negative regulator Smad7, contributing to the activation of HSCs (Figure 17). miR-17-5p levels are increased in rat HSCs, human cirrhotic liver and serum samples, as well as in CCl₄-treated rat liver fibrotic tissues (Yu et al., 2015). In contrast, the use of a miR-17-5p inhibitor in rat HSC-T6 and in human serum restored Smad7 protein levels, increasing both mRNA and protein expression of α -SMA and collagen I in HSC-T6 cells (Yu et al., 2015). Another important upregulated miRNA in human HSC LX-2 cell line, human liver samples and liver samples from CCl₄-treated rats and mice is miR-214-3p (Ma et al., 2018). The increased miR-214 inhibits the expression of suppressor-of-fused homolog (Sufu), a negative regulator of the Hedgehog pathway, hence contributing to HSC activation and fibrosis (Ma et al., 2018) (Figure 17). In contrast, the use of an AntagomiR increases Sufu protein levels, ameliorating fibrosis *in vivo* (Ma et al., 2018). Altogether, these and other miRNAs are proposed orchestrate fibrosis-related cellular events thereby contributing to the establishment of a proinflammatory context that promote HCC development (He et al., 2012).

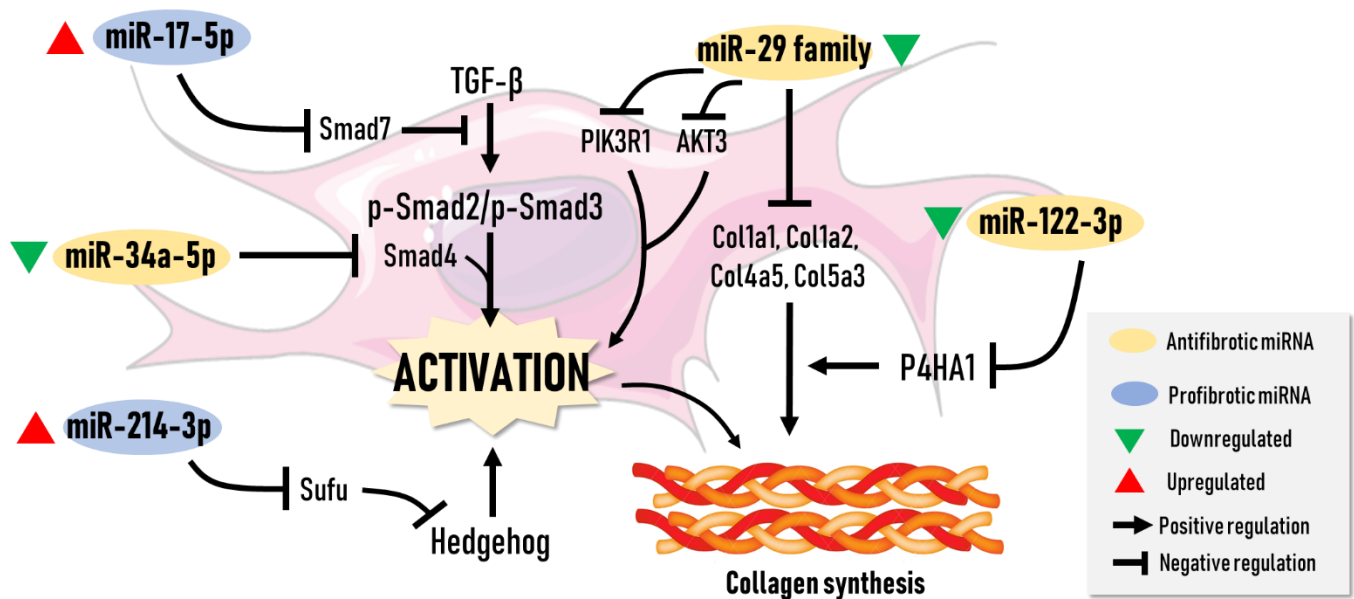


Figure 17. Some of the main miRNAs involved in liver fibrosis and their proposed targets and implications on fibrosis-related outcomes, focusing on hepatic stellate cell activation and collagen synthesis (Roderburg et al., 2012; Li et al., 2013; Wang et al., 2014; Yu et al., 2015; Feili et al., 2018; Ma et al., 2018).

Deregulated miRNA expression is also a common feature of HCC that contributes to the acquisition of key cancer hallmarks, as proliferation, apoptosis, invasion, metastasis and angiogenesis hallmarks (Xu et al., 2018). Some of these miRNAs and their biological properties are depicted in Figure 18. miR-144-3p is among the tumor-suppressor miRNAs with growing number of publications in the last years (Cao et al., 2014; Yu et al., 2016; Bao et al., 2017; Liang et al., 2017; Gu

et al., 2019). The downregulation of this miRNA is widely reported in many human HCC cell lines (HepG2, Huh7 and Hep3B) and samples, being inversely correlated with tumor staging (Cao et al., 2014; Yu et al., 2016; Bao et al., 2017; Liang et al., 2017; Gu et al., 2019). miR-144-3p is proposed to negatively control cell proliferation, migration and invasion hallmarks by directly targeting 3'UTR regions of Cyclin B1 (*CCNB1*) (Gu et al., 2019), *SMAD4* (Yu et al., 2016), E2F transcription factor 3 (*E2F3*) (Cao et al., 2014) and Zinc finger X-chromosomal protein (ZFX) (Bao et al., 2017) in humans (Figure 18). In general, the transfection of miR-144-3p mimics *in vitro* reduced the mRNA and protein of the targets, contributing to reduced cell proliferation, migration and invasion, as well as delaying tumor formation in xenograft models (Gu et al., 2019). The key role of miR-144-3p was also recently described in chemically-induced mouse models of HCC (He et al., 2017). In a neonatal DEN-induced model using susceptible C3H mouse strain, miR-144-3p levels were also decreased in HCC tissue. Intravenous administration of a miR-144-3p mimic decreased protein and gene expression of EGFR, a direct target of this miRNA in the liver, and its downstream Src/AKT signaling, resulting in decreased HCC size (He et al., 2017). Thus, upregulating miR-144 may be a therapeutic strategy to suppress tumor growth in HCC.

Other two key tumor suppressor miRNAs in HCC are miR-195-5p and miR-206 (Wu et al., 2017; Yu et al., 2017) (Figure 18). Both were downregulated in human HCC tissue, and miR-195-5p levels were inversely correlated to metastasis (Wu et al., 2017; Yu et al., 2017). Of note, miR-206 levels were also decreased in human HCC cell lines (HepG2, Hep3B and Huh7) and HCC from both cMyc and V-Akt murine thymoma viral oncogene homolog 1/neuroblastoma RAS viral oncogene homolog (AKT/Ras) transgenic mouse models (Wu et al., 2017). The yes-associated protein 1 (YAP) gene expression is controlled by miR-195-5p, while cMET and cyclin-dependent kinase (CDK6) oncogenes are direct targets of miR-206 (Wu et al., 2017; Yu et al., 2017). *In vitro* treatments with miR-195-5p reduced migration and invasion of HCC cells by suppressing YAP (Yu et al., 2017), and *in vivo* miR-206 overexpression prevented HCC growth in cMyc mice by reducing *cMet* and *Cdk6* (Wu et al., 2017).

Although most of deregulated miRNAs in HCC are downregulated, some may function as oncogenes as they are upregulated in tumoral tissue (Xu et al., 2018). The oncomiR miR-155-5p and its direct target tumor suppressor PTEN were found to be upregulated and downregulated, respectively, in DEN-induced HCC rat tissue, human HCC tissue and cell line (Hep3B) (Fu et al., 2017). Besides, miR-155-5p upregulation and PTEN downregulation were significantly associated with HCC staging (Fu et al., 2017). Conversely, miR-155-5p inhibitors increased promoted proliferation, invasion and migration by decreasing PTEN and increasing PI3K/Akt pathway in xenograft models and Hep3B and HepG2 tumor cells (Fu et al., 2017). Similar findings were observed concerning oncomiR miR-454-3p (Yu et al., 2015), whose expression was increased

in human HCC cell lines (HepG2 and Huh7) and samples, displaying even higher expression in HCC-derived metastatic tumors (Yu et al., 2015). The expression of chromodomain–helicase–DNA–binding-5 (CHD5), a direct target of miR-454-3p, was inversely correlated with the expression of miR-454-3p in HCC tissues as well (Yu et al., 2015). In contrast, a miR-454-3p inhibitor decreased CHD5 mRNA and protein levels, reducing migration and proliferation *in vitro*, while decreasing tumor growth in a xenograft mouse model (Yu et al., 2015). Therefore, these studies have shed light on miRNAs as important biomarkers for cancer diagnosis, survival and treatment prediction, as well as novel strategies for cancer therapy. However, the number of mature miRNAs discovered in human and rodents keeps increasing, and their roles on both health and disease are yet to be unveiled.

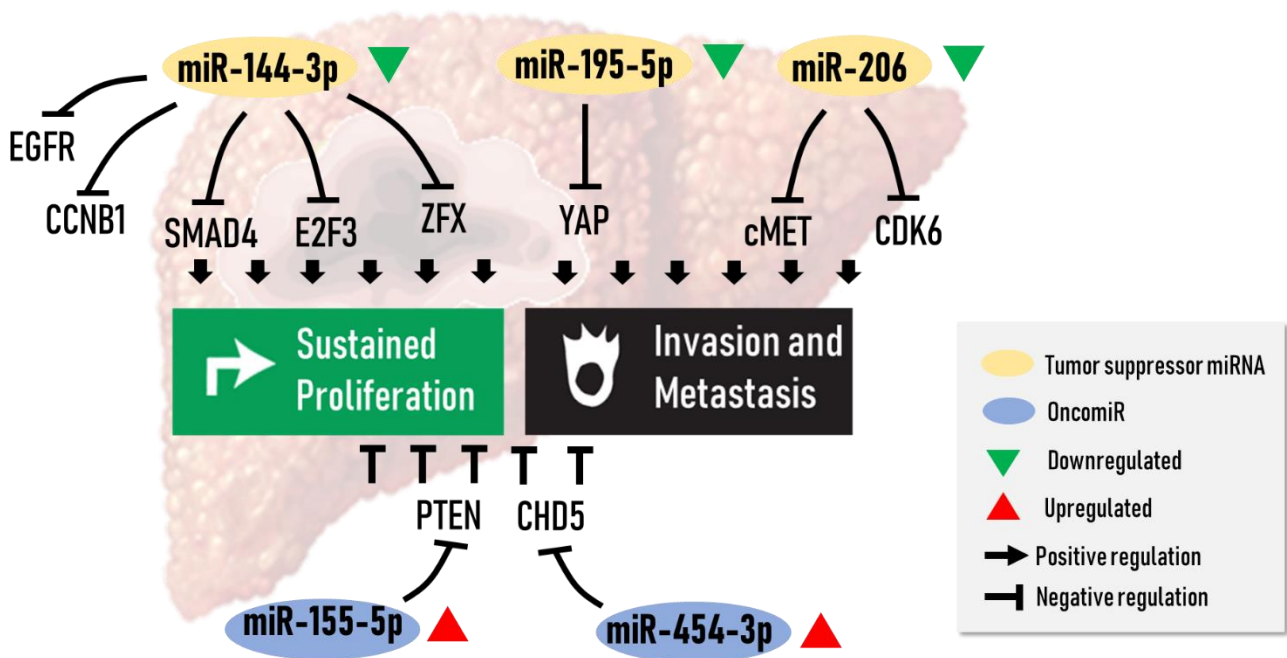
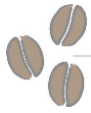
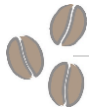


Figure 18. Some of the main miRNAs involved in HCC progression, focusing on sustained proliferation and invasion a migration features (Gu et al., 2019, Cao et al., 2014, Yu et al., 2015; Yu et al., 2016, Bao et al., 2017, Fu et al., 2017; He et al., 2017; Wu et al., 2017; Yu et al., 2017 Xu et al., 2018).

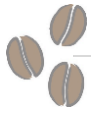


References

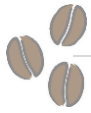
- Abu-Absi SF, Hansen LK, Hu WS. Three-dimensional co-culture of hepatocytes and stellate cells. *Cytotechnology*. 2004;45(3):125–40.
- Agarwal V, Bell GW, Nam JW, Bartel DP. Predicting effective microRNA target sites in mammalian mRNAs. *Elife*. 2015;4(AUGUST2015):1–38.
- Alarcón CR, Lee H, Goodarzi H, Halberg N, Tavazoie SF. N6-methyladenosine marks primary microRNAs for processing. *Nature*. 2015;519(7544):482–5.
- Arellanes-Robledo J, Hernández C, Camacho J, Pérez-Carreón JI. *In vitro* models of HCC. *Liver Pathophysiol Ther Antioxidants*. 2017;563–79.
- Aydinlik H, Nguyen TD, Moennikes O, Buchmann A, Schwarz M. Selective pressure during tumor promotion by phenobarbital leads to clonal outgrowth of beta-catenin-mutated mouse liver tumors. *Oncogene* [Internet]. 2001 Nov 22;20(53):7812–6.
- Baecker A, Liu X, La Vecchia C, Zhang ZF. Worldwide incidence of hepatocellular carcinoma cases attributable to major risk factors. *Eur J Cancer Prev*. 2018;27(3):205–12.
- Baek D, Villén J, Shin C, Camargo FD, Gygi SP, Bartel DP. The impact of microRNAs on protein output. *Nature*. 2008;455(7209):64–71.
- Bakiri L, Wagner EF. Mouse models for liver cancer. *Mol Oncol* [Internet]. 2013;7(2):206–23.
- Bannasch P, Haertel T, Qin S. Significance of hepatic preneoplasia in risk identification and early detection of neoplasia. *Toxicol Pathol*. 2003;31(1):134–9.
- Bao H, Li X, Li H, Xing H, Xu B, Zhang X, et al. MicroRNA-144 inhibits hepatocellular carcinoma cell proliferation, invasion and migration by targeting ZFX. *J Biosci*. 2017;42(1):103–11.
- Bartel DP. MicroRNAs: target recognition and regulatory functions. *Cell*. 2009;136:215–33.
- Behm-Ansmant I, Rehwinkel J, Doerks T, Stark A, Bork P, Izaurralde E. mRNA degradation by miRNAs and GW182 requires both CCR4:NOT deadenylase and DCP1:DCP2 decapping complexes. *Genes Dev*. 2006;20(14):1885–98.
- Bilger A, Bennett LM, Carabeo RA., Chiaverotti TA., Dvorak C, Liss KM, et al. A potent modifier of liver cancer risk on distal mouse chromosome 1: Linkage analysis and characterization of congenic lines. *Genetics*. 2004;167(2):859–66.
- Borchert GM, Lanier W, Davidson BL. RNA polymerase III transcribes human microRNAs. *Nat Struct Mol Biol*. 2006;13(12):1097–101.
- Braeuning A, Schwarz M. Is the question of phenobarbital as potential liver cancer risk factor for humans really resolved? *Arch Toxicol*. 2016;90(6):1525–6.
- Braun JE, Truffault V, Boland A, Huntzinger E, Chang C Te, Haas G, et al. A direct interaction between DCP1 and XRN1 couples mRNA decapping to 5' exonucleolytic degradation. *Nat Struct Mol Biol* [Internet]. 2012;19(12):1324–31.
- Buchmann A, Mahr J, Bauer-Hofmann R, Schwarz M. Mutations at codon 61 of the Ha-ras proto-oncogene in precancerous liver lesions of the B6C3F1 mouse. *Mol Carcinog*. 1989;2(3):121–5.
- Buckley AF, Burgart LJ, Sahai V, Kakar S. Epidermal growth factor receptor expression and gene copy number in conventional hepatocellular carcinoma. *Am J Clin Pathol*. 2008;129(2):245–51.
- Cao T, Li H, Hu Y, Ma D, Cai X. miR-144 suppresses the proliferation and metastasis of hepatocellular carcinoma by targeting E2F3. *Tumor Biol*. 2014;35(11):10759–64.
- Cast A, Valanejad L, Wright M, Nguyen P, Gupta A, Zhu L, et al. C/EBP α -dependent preneoplastic tumor foci are the origin of hepatocellular carcinoma and aggressive pediatric liver cancer. *Hepatology*. 2018;67(5):1857–71.
- Cederbaum AI. Alcohol Metabolism. *Clin Liver Dis* [Internet]. 2012;16(4):667–85.



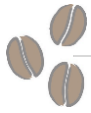
- Center of Disease Control (CDC), 2018. Adult Obesity Facts. [Online]. Available from: <https://www.cdc.gov/obesity/data/adult.html> [Accessed 22 October 2019].
- Chappell G, Kutanzi K, Uehara T, Tryndyak V, Hong HH, Hoenerhoff M, et al. Genetic and epigenetic changes in fibrosis-associated hepatocarcinogenesis in mice. *Int J Cancer*. 2014;134(12):2778–88.
- Cheloufi S, Dos Santos CO, Chong MMW, Hannon GJ. A dicer-independent miRNA biogenesis pathway that requires Ago catalysis. *Nature*. 2010;465(7298):584–9.
- Chen J. The cell-cycle arrest and apoptotic and progression. *Cold Spring Harb Perspect Biol*. 2016;1–16.
- Chen X, Yamamoto M, Fujii K, Nagahama Y, Ooshio T, Xin B, et al. Differential reactivation of fetal/neonatal genes in mouse liver tumors induced in cirrhotic and non-cirrhotic conditions. *Cancer Sci*. 2015;106(8):972–81.
- Chuang SC, Lee YCA, Wu GJ, Straif K, Hashibe M. Alcohol consumption and liver cancer risk: a meta-analysis. *Cancer Causes Control*. 2015;26(9):1205–31.
- Connor F, Rayner TF, Aitken SJ, Feig C, Lukk M, Santoyo-Lopez J, et al. Mutational landscape of a chemically-induced mouse model of liver cancer. *J Hepatol* [Internet]. 2018;69(4):840–50.
- Cougot D, Wu Y, Cairo S, Caramel J, Le L, Buendia MA, et al. The hepatitis B virus X protein functionally interacts with CREB-binding protein/p300 in the regulation of CREB-mediated transcription. *J Biol Chem* [Internet] 2007;282(7):4277–87.
- Crespo Yanguas S, Cogliati B, Willebrords J, Maes M, Colle I, van den Bossche B, et al. Experimental models of liver fibrosis. *Arch Toxicol* [Internet]. 2016;90(5):1025–48.
- Csepregi A, Röcken C, Hoffmann J, Gu P, Saliger S, Müller O, et al. APC promoter methylation and protein expression in hepatocellular carcinoma. *J Cancer Res Clin Oncol*. 2008;134(5):579–89.
- De Rie D, Abugessaisa I, Alam T, Arner E, Arner P, Ashoor H, et al. An integrated expression atlas of miRNAs and their promoters in human and mouse. *Nat Biotechnol*. 2017;35(9):872–8.
- Denli AM, Tops BBJ, Plasterk RHA, Ketting RF, Hannon GJ. Processing of primary microRNAs by the Microprocessor complex. *Nature*. 2004;432(7014):231–5.
- Dontenwill W, Mohr U. Carcinoma of the respiratory tract following treatment of the golden hamster with diethylnitrosamine. *Z Krebsforsch*. 1961;64:305–12.
- Federico A, Dallio M, Godos J, Loguercio C, Salomone F. Targeting gut-liver axis for the treatment of nonalcoholic steatohepatitis: Translational and clinical evidence. *Transl Res* [Internet]. 2016;167(1):116–24.
- Feili X, Wu S, Ye W, Tu J, Lou L. MicroRNA-34a-5p inhibits liver fibrosis by regulating TGF- β 1/Smad3 pathway in hepatic stellate cells. *Cell Biol Int*. 2018;42(10):1370–6.
- Flamand MN, Gan HH, Mayya VK, Gunsalus KC, Duchaine TF. A non-canonical site reveals the cooperative mechanisms of microRNA-mediated silencing. *Nucleic Acids Res*. 2017;45(12):7212–25.
- Fraser LK, Edwards KL, Cade J, Clarke GP. The geography of fast food outlets: A review. *Int J Environ Res Public Health*. 2010;7(5):2290–308.
- Friedman RC, Farh KKH, Burge CB, Bartel DP. Most mammalian mRNAs are conserved targets of microRNAs. *Genome Res*. 2009;19(1):92–105.



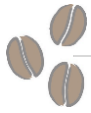
- Fu X, Wen H, Jing L, Yang Y, Wang W, Liang X, et al. MicroRNA-155-5p promotes hepatocellular carcinoma progression by suppressing PTEN through the PI3K/Akt pathway. *Cancer Sci*. 2017;108(4):620–31.
- Fukao A, Mishima Y, Takizawa N, Oka S, Imataka H, Pelletier J, et al. MicroRNAs trigger dissociation of eIF4A1 and eIF4AII from target mRNAs in humans. *Mol Cell* [Internet]. 2014;56(1):79–89.
- Gatfield D, Le Martelot G, Vejnar CE, Gerlach D, Schaad O, Fleury-Olela F, et al. Integration of microRNA miR-122 in hepatic circadian gene expression. *Genes Dev*. 2009;23(11):1313–26.
- Greten TF, Papendorf F, Bleck JS, Kirchhoff T, Wohlberedt T, Kubicka S, et al. Survival rate in patients with hepatocellular carcinoma: a retrospective analysis of 389 patients. *Br J Cancer* [Internet]. 2005;92(10):1862–8.
- Greten TF. Gender disparity in HCC: Is it the fat and not the sex? *J Exp Med*. 2019;216(5):1014–5.
- Grimson A, Farh KKH, Johnston WK, Garrett-Engle P, Lim LP, Bartel DP. MicroRNA targeting specificity in mammals: determinants beyond seed pairing. *Mol Cell*. 2007;27(1):91–105.
- Gu J, Liu X, Li J, He Y. MicroRNA-144 inhibits cell proliferation, migration and invasion in human hepatocellular carcinoma by targeting CCNB1. *Cancer Cell Int* [Internet]. 2019;19(1):1–10.
- Guo H, Ingolia NT, Weissman JS, Bartel DP. Mammalian microRNAs predominantly act to decrease target mRNA levels. *Nature* [Internet]. 2010;466(7308):835–40.
- Hajovsky H, Hu G, Koen Y, Sarma D, Cui W, Moore DS, et al. Metabolism and toxicity of thioacetamide and thioacetamide S-Oxide in rat hepatocytes. *Chem Res Toxicol*. 2012;25(9):1955–63.
- He Q, Okajima T, Onoe H, Subagyo A, Sueoka K, Kuribayashi-Shigetomi K. Origami-based self-folding of co-cultured NIH/3T3 and HepG2 cells into 3D microstructures. *Sci Rep*. 2018;8(1):2–8.
- He Q, Wang F, Honda T, Lindquist DM, Dillman JR, Timchenko NA, et al. Intravenous miR-144 inhibits tumor growth in diethylnitrosamine-induced hepatocellular carcinoma in mice. *Tumor Biol*. 2017;39(10):1–8.
- He Y, Huang C, Zhang S, Sun X, Long X, Li J. The potential of microRNAs in liver fibrosis. *Cell Signal* [Internet]. 2012;24(12):2268–72.
- Heindryckx F, Colle I, Van Vlierberghe H. Experimental mouse models for hepatocellular carcinoma research. *Int J Exp Pathol* [Internet]. 2009;90(4):367–86.
- Hirschfield H, Bian CB, Higashi T, Nakagawa S, Zeleke TZ, Nair VD, et al. *In vitro* modeling of hepatocellular carcinoma molecular subtypes for anti-cancer drug assessment. *Exp Mol Med*. 2018;50(1): e419.
- INCA, 2018. Incidência de Câncer no Brasil. [Online]. Available from: <http://www1.inca.gov.br/estimativa/2018/index.asp> [Accessed 22 October 2019].
- International Agency for Research on Cancer, 2019. Agents Classified by the IARC Monographs, Volumes 1–124. [Online]. Available from: <https://monographs.iarc.fr/agents-classified-by-the-iarc/> [Accessed 22 October 2019].
- Jensen T, Abdelmalek MF, Sullivan S, Nadeau KJ, Green M, Roncal C, et al. Fructose and sugar: A major mediator of non-alcoholic fatty liver disease. *J Hepatol* [Internet]. 2018;68(5):1063–75.
- Jin SK, Wanibuchi H, Morimura K, Gonzalez FJ, Fukushima S. Role of CYP2E1 in diethylnitrosamine-induced hepatocarcinogenesis *in vivo*. *Cancer Res*. 2007;67(23):11141–6.
- Kao C, Chen S, Chen J, Lee YW. Modulation of p53 transcription regulatory activity and post-translational modification by hepatitis C virus core protein. *Oncogene* [Internet] 2004;53:2472–83.



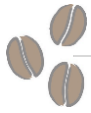
- Khawar IA, Park JK, Jung ES, Lee MA, Chang S, Kuh HJ. Three dimensional mixed-cell spheroids mimic stroma-mediated chemoresistance and invasive migration in hepatocellular carcinoma. *Neoplasia (United States)* [Internet]. 2018;20(8):800–12.
- Khvorova A, Reynolds A, Jayasena SD. Functional siRNAs and miRNAs exhibit strand bias. *Cell*. 2003;115(2):209–16.
- Kim D, Kim WR, Kim HJ, Therneau TM. association between noninvasive fibrosis markers and mortality among adults with nonalcoholic fatty liver disease in the United States. *Hepatology*. 2013;57(4):1357-65.
- Kim S, Syed GH, Siddiqui A. Hepatitis C Virus Induces the Mitochondrial Translocation of Parkin and Subsequent Mitophagy. *PLoS Pathog* [Internet] 2013 Mar;9(3):e1003285.
- Kim YK, Kim VN. Processing of intronic microRNAs. *EMBO J*. 2007;26(3):775–83.
- Kishida N, Matsuda S, Itano O, Shinoda M, Kitago M, Yagi H, et al. Development of a novel mouse model of hepatocellular carcinoma with nonalcoholic steatohepatitis using a high-fat, choline-deficient diet and intraperitoneal injection of diethylnitrosamine. *BMC Gastroenterol* [Internet]. 2016;16(1):1–13.
- Klaunig JE, Kamendulis LM. Mechanisms of cancer chemoprevention in hepatic carcinogenesis: modulation of focal lesion growth in mice. *Toxicol Sci* [Internet]. 1999;52(2 Suppl):101–6.
- Kozomara A, Birgaoanu M, Griffiths-Jones S. MiRBase: From microRNA sequences to function. *Nucleic Acids Res*. 2019;47(D1):D155–62.
- Kutlu O, Kaleli HN, Ozer E. Molecular pathogenesis of nonalcoholic steatohepatitis- (NASH-) related hepatocellular carcinoma. *Can J Gastroenterol Hepatol*. 2018;2018.
- Lahm H, Gittner K, Krebs O, Sprague L, Deml E, Oesterle D, et al. Diethylnitrosamine induces long-lasting re-expression of insulin-like growth factor II during early stages of liver carcinogenesis in mice. *Growth Horm IGF Res*. 2002;12(1):69–79.
- Lee GH, Nomura K, Kitagawa T. Comparative study of diethylnitrosamine-initiated two-stage hepatocarcinogenesis in C3H, C57BL and BALB mice promoted by various hepatopromoters. *Carcinogenesis*. 1989;10(12):2227–30.
- Lee RC, Feinbaum RL, Ambros V. The *C. elegans* heterochronic gene *lin-4* encodes small RNAs with antisense complementarity to *lin-14*. *Cell* [Internet]. 1993;75(5):843-54.
- Lee Y, Kim M, Han J, Yeom KH, Lee S, Baek SH, et al. MicroRNA genes are transcribed by RNA polymerase II. *EMBO J*. 2004;23(20):4051–60.
- Levrero M, Zucman-rossi J. Review Mechanisms of HBV-induced hepatocellular carcinoma Review. *J Hepatol* [Internet]. 2016;64(1):S84–101.
- Li J, Ghazwani M, Zhang Y, Lu J, Li J, Fan J, et al. MiR-122 regulates collagen production via targeting hepatic stellate cells and suppressing P4HA1 expression. *J Hepatol* [Internet]. 2013;58(3):522–8.
- Li SC, Chan WC, Hu LY, Lai CH, Hsu CN, Lin W chang. Identification of homologous microRNAs in 56 animal genomes. *Genomics*. 2010;96(1):1–9.
- Liang HW, Ye ZH, Yin SY, Mo WJ, Wang HL, Zhao JC, et al. A comprehensive insight into the clinicopathologic significance of miR-144-3p in hepatocellular carcinoma. *Onco Targets Ther*. 2017;10:3405–19.
- Libbrecht L, Desmet V, Roskams T. Preneoplastic lesions in human hepatocarcinogenesis. *Liver Int*. 2005;25(1):16–27.
- Ma CL, Hsu CL, Wu MH, Wu C Te, Wu CC, Lai JJ, et al. Androgen receptor is a new potential therapeutic target for the treatment of hepatocellular carcinoma. *Gastroenterology*. 2008;135(3):947–55.



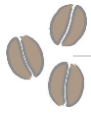
- Ma L, Yang X, Wei R, Ye T, Zhou JK, Wen M, et al. MicroRNA-214 promotes hepatic stellate cell activation and liver fibrosis by suppressing Sufu expression article. *Cell Death Dis* [Internet]. 2018;9(7):1–13.
- Makarova-Rusher O V., Altekruze SF, McNeel TS, Ulahannan S, Duffy AG, Graubard BI, et al. Population attributable fractions of risk factors for hepatocellular carcinoma in the United States. *Cancer* [Internet]. 2016;122(11):1757–65.
- Maronpot RR. Biological basis of differential susceptibility to hepatocarcinogenesis among mouse strains. *J Toxicol Pathol.* 2009;22(1):11–33.
- Meijer HA, Smith EM, Bushell M. Regulation of miRNA strand selection: Follow the leader? *Biochem Soc Trans.* 2014;42(4):1135–40.
- Mendell JT, Olson EN. MicroRNAs in stress signaling and human disease. *Cell* [Internet]. 2012;148(6):1172–87.
- Meng F, Wang K, Aoyama T, Grivennikov SI, Paik Y, Scholten D, et al. Interleukin-17 signaling in inflammatory, Kupffer cells, and hepatic stellate cells exacerbates liver fibrosis in mice. *Gastroenterology* [Internet]. 2012;143(3):765–776.e3.
- Mercer KE, Hennings L, Sharma N, Lai K, Cleves MA, Wynne RA, et al. Alcohol consumption promotes diethylnitrosamine-induced hepatocarcinogenesis in male mice through activation of the Wnt/ β -catenin signaling pathway. *Cancer Prev Res.* 2014;7(7):675–85.
- Mestdagh P, Boström AK, Impens F, Fredlund E, Van Peer G, De Antonellis P, et al. The miR-17-92 MicroRNA cluster regulates multiple components of the TGF- β pathway in neuroblastoma. *Mol Cell.* 2010;40(5):762–73.
- Minami M, Daimon Y, Mori K, Takashima H, Nakajima T, Itoh Y, et al. Hepatitis B virus-related insertional mutagenesis in chronic hepatitis B patients as an early drastic genetic change leading to hepatocarcinogenesis. *Oncogene* [Internet] 2005; 24:4340–8.
- Nakanishi K, Weinberg DE, Bartel DP, Patel DJ. Structure of yeast Argonaute with guide RNA. *Nature.* 2012;486(7403):368–74.
- Naugler WE, Sakurai T, Kim S, Maeda S, Kim K, Elsharkawy AM, et al. Gender disparity in liver cancer due to sex differences in MyD88-dependent IL-6 production. *Science* [Internet]. 2007;317(5834):121–4.
- Nault JC, Calderaro J, Tommaso L Di, Balabaud C, Zafrani ES, Bioulac-sage P. Telomerase reverse transcriptase promoter mutation is an early somatic genetic alteration in the transformation of premalignant nodules in hepatocellular carcinoma on cirrhosis. *Hepatology* 2014; 60(Dec):1983-92.
- Nault JC, Mallet M, Pilati C, Calderaro J, Bioulac-Sage P, Laurent C, et al. High frequency of telomerase reverse-transcriptase promoter somatic mutations in hepatocellular carcinoma and preneoplastic lesions. *Nat Commun* [Internet]. 2013;4(May):1–6.
- O'Brien J, Hayder H, Zayed Y, Peng C. Overview of microRNA biogenesis, mechanisms of actions, and circulation. *Front Endocrinol (Lausanne).* 2018;9(AUG):1–12.
- Ogawa K. Molecular pathology of early stage chemically induced hepatocarcinogenesis. *Pathol Int* [Internet]. 2009;59(9):605–22.
- Okada C, Yamashita E, Lee SJ, Shibata S, Katahira J, Nakagawa A, et al. A high-Resolution structure of the pre-microRNA nuclear export machinery. *Science* 2009;326(5957):1275–9.
- Olive V, Minella AC, He L. Outside the coding genome, mammalian microRNAs confer structural and functional complexity. *Sci Signal.* 2015;8(368):re2.
- op den Winkel M, Nagel D, Sappl J, op den Winkel P, Lamerz R, Zech CJ, et al. Prognosis of patients with hepatocellular carcinoma. validation and ranking of established staging-systems in a large western hcc-cohort. *PLoS One* [Internet]. 2012;7(10):e45066.
- Ouchi R, Togo S, Kimura M, Shinozawa T, Koido M, Koike H, et al. Modeling steatohepatitis in humans with pluripotent stem cell-derived organoids. *Cell Metab* [Internet]. 2019;30(2):374–384.e6.



- Panvichian R, Tantiwetruengdet A, Sornmayura P, Leelaudomlipi S. Missense mutations in exons 18-24 of EGFR in hepatocellular carcinoma tissues. *Biomed Res Int.* 2015;2015: :171845.
- Petrelli A, Perra A, Cora D, Sulas P, Menegon S, Manca C, et al. MicroRNA/gene profiling unveils early molecular changes and nuclear factor erythroid related factor 2 (NRF2) activation in a rat model recapitulating human hepatocellular carcinoma (HCC). *Hepatology.* 2014;59(1):228–41.
- Pingitore P, Sasidharan K, Ekstrand M, Prill S, Lindén D, Romeo S. Human multilineage 3D spheroids as a model of liver steatosis and fibrosis. *Int J Mol Sci.* 2019;20(7):1–16.
- Prestigiacomo V, Weston A, Messner S, Lampart F, Suter-Dick L. Pro-fibrotic compounds induce stellate cell activation, ECM-remodelling and Nrf2 activation in a human 3D-multicellular model of liver fibrosis. *PLoS One.* 2017;12(6):1–17.
- Roderburg C, Urban G-W, Bettermann K, Vucur M, Zimmermann H, Schmidt S, et al. Micro-RNA profiling reveals a role for miR-29 in human and murine liver fibrosis. *Hepatology.* 2011;53(1):209–18.
- Romualdo GR, Grassi TF, Goto RL, Tablas MB, Bidinotto LT, Fernandes AAH, et al. An integrative analysis of chemically-induced cirrhosis-associated hepatocarcinogenesis: Histological, biochemical and molecular features. *Toxicol Lett [Internet].* 2017;281(August):84–94.
- Romualdo GR, Prata GB, da Silva TC, Fernandes AAH, Moreno FS, Cogliati B, et al. Fibrosis-associated hepatocarcinogenesis revisited: Establishing standard medium-term chemically-induced male and female models. *PLoS One.* 2018;13(9):1–26.
- Ruby JG, Jan CH, Bartel DP. Intronic microRNA precursors that bypass Drosha processing. *Nature.* 2007;448(7149):83–6.
- Scanlan RA. Formation and occurrence of nitrosamines in food. *Cancer Res.* 1983 May;43(5 Suppl):2435s-2440s.
- Schirle NT, Sheu-Gruttadauria J, Chandradoss SD, Joo C, MacRae IJ. Water-mediated recognition of t1-adenosine anchors Argonaute2 to microRNA targets. *Elife.* 2015;4(September):1–16.
- Selbach M, Schwanhäusser B, Thierfelder N, Fang Z, Khanin R, Rajewsky N. Widespread changes in protein synthesis induced by microRNAs. *Nature.* 2008;455(7209):58–63.
- Septer S, Edwards G, Gunewardena S, Wolfe A, Li H, Daniel J, et al. Yes-associated protein is involved in proliferation and differentiation during postnatal liver development. *Am J Physiol - Gastrointest Liver Physiol.* 2012;302(5):G493–G503.
- Stärkel P, Leclercq S, de Timary P, Schnabl B. Intestinal dysbiosis and permeability: The yin and yang in alcohol dependence and alcoholic liver disease. *Clin Sci.* 2018;132(2):199–212.
- Su Q, Bannasch P. Relevance of hepatic preneoplasia for human hepatocarcinogenesis. *Toxicol Pathol.* 2003;31(1):126–33.
- Tanzer A, Stadler PF. Molecular evolution of a microRNA cluster. *J Mol Biol.* 2004;339(2):327–35.
- The Cancer Genome Atlas Research Network. Comprehensive and integrative genomic characterization of Hepatocellular Carcinoma. *Cell* 2017;169:1327–1341.e23
- Thomas C. On the morphology of diethylnitrosamine induced liver changes and tumors in rats. *Z Krebsforsch.* 1961;64:224-33.
- Thoolen B, Maronpot RR, Harada T, Nyska A, Rousseaux C, Nolte T, et al. Proliferative and nonproliferative lesions of the rat and mouse hepatobiliary system. *Toxicol Pathol.* 2010;38(7 Suppl):5S–81S.
- Tsuchida T, Friedman SL. Mechanisms of hepatic stellate cell activation. *Nat Rev Gastroenterol Hepatol [Internet].* 2017;14(7):397–411.
- Tsuchida T, Lee YA, Fujiwara N, Ybanez M, Allen B, Martins S, et al. A simple diet- and chemical-induced murine NASH model with rapid progression of steatohepatitis, fibrosis and liver cancer. *J Hepatol [Internet].* 2018;69(2):385–95.



- Uehara T, Ainslie GR, Kutanzi K, Pogribny IP, Muskhelishvili L, Izawa T, et al. Molecular mechanisms of fibrosis-associated promotion of liver carcinogenesis. *Toxicol Sci.* 2013;132(1):53–63.
- Verna L, Whysner J, Williams GM. N-Nitrosodiethylamine mechanistic data and risk assessment: Bioactivation, DNA-adduct formation, mutagenicity, and tumor initiation. *Pharmacol Ther.* 1996;71(1–2):57–81.
- Vescovo T, Refolo G, Vitagliano G, Fimia GM, Piacentini M. Molecular mechanisms of hepatitis C virus e induced hepatocellular carcinoma. *Clin Microbiol Infect [Internet].* 2016;22(10):853–61.
- Vesselinovitch SD, Koka M, Mihailovich N, Rao K V. Carcinogenicity of diethylnitrosamine in newborn, infant, and adult mice. *J Cancer Res Clin Oncol [Internet].* 1984;108(1):60–5.
- Vesselinovitch SD, Mihailovich N. Kinetics of diethylnitrosamine hepatocarcinogenesis in the infant mouse. *Cancer Res.* 1983;43(9):4253–9.
- Vonghia L, Francque S. Cross talk of the immune system in the adipose tissue and the liver in non-alcoholic steatohepatitis: Pathology and beyond. *World J Hepatol.* 2015;7(15):1905–12.
- Wang J, Chu ESH, Chen HY, Man K, Go MYY, Huang XR, et al. microRNA-29b prevents liver fibrosis by attenuating hepatic stellate cell activation and inducing apoptosis through targeting PI3K/AKT pathway. *Oncotarget.* 2015;6(9):7325–38.
- Weber LWD, Boll M, Stampfl A. Hepatotoxicity and mechanism of action of haloalkanes: carbon tetrachloride as a toxicological model. *Crit Rev Toxicol [Internet].* 2003;33(2):105–36.
- Wee P, Wang Z. Epidermal growth factor receptor cell proliferation signaling pathways. *Cancers (Basel).* 2017;9(5):1–45.
- Weghorst CM, Pereira MA, Klaunig E. Strain differences in hepatic tumor promotion by phenobarbital in diethylnitrosamine- and dimethylnitrosamine-initiated infant male mice. *Carcinogenesis.* 1989;10(8):1409–12.
- Wong RJ, Aguilar M, Cheung R, Perumpail RB, Harrison SA, Younossi ZM, et al. Nonalcoholic steatohepatitis is the second leading etiology of liver disease among adults awaiting liver transplantation in the United States. *Gastroenterology [Internet].* 2015;148(3):547–55.
- Wong RJ, Cheung R, Ahmed A. Nonalcoholic steatohepatitis is the most rapidly growing indication for liver transplantation in patients with hepatocellular carcinoma in the U.S. *Hepatology.* 2014;59(6):2188–95.
- World Health Organization (WHO), 2018. Global Cancer Observatory. [Online]. Available from: <https://gco.iarc.fr/> [Accessed 22 October 2019].
- Wu H, Tao J, Li X, Zhang T, Zhao L, Wang Y, et al. MicroRNA-206 prevents the pathogenesis of hepatocellular carcinoma by modulating expression of met proto-oncogene and cyclin-dependent kinase 6 in mice. *Hepatology.* 2017;66(6):1952–67.
- Xie M, Li M, Vilborg A, Lee N, Shu M Di, Yartseva V, et al. Mammalian 5'-capped microRNA precursors that generate a single microRNA. *Cell.* 2013;155(7):1568–80.
- Xu W, Lucas AS, Wang Z, Liu Y. Identifying microRNA targets in different gene regions. *BMC Bioinformatics.* 2014;15(Suppl 7):6–8.
- Yamamoto M, Tanaka H, Xin B, Nishikawa Y, Yamazaki K, Shimizu K, et al. Role of the BraFV637E mutation in hepatocarcinogenesis induced by treatment with diethylnitrosamine in neonatal B6C3F1 mice. *Mol Carcinog.* 2017;56(2):478–88.
- Yang JD, Kim WR, Coelho R, Mettler T a., Benson JT, Sanderson SO, et al. Cirrhosis is present in most patients with hepatitis b and hepatocellular carcinoma. *Clin Gastroenterol Hepatol [Internet].* 2011;9(1):64–70.
- Yoda M, Kawamata T, Paroo Z, Ye X, Iwasaki S, Liu Q, et al. ATP-dependent human RISC assembly pathways. *Nat Struct Mol Biol.* 2010;17(1):17–24.



- You M, Arteel GE. Effect of ethanol on lipid metabolism. *J Hepatol* [Internet]. 2019;70(2):237–48.
- Yu F, Guo Y, Chen B, Dong P, Zheng J. MicroRNA-17-5p activates hepatic stellate cells through targeting of Smad7. *Lab Investig*. 2015;95(7):781–9.
- Yu L, Gong X, Sun L, Yao H, Lu B, Zhu L. miR-454 functions as an oncogene by inhibiting CHD5 in hepatocellular carcinoma. *Oncotarget*. 2015;6(36):39225–34.
- Yu M, Lin Y, Zhou Y, Jin H, Hou B, Wu Z, et al. MiR-144 suppresses cell proliferation, migration, and invasion in hepatocellular carcinoma by targeting SMAD4. *Onco Targets Ther*. 2016;9:4705–14.
- Yu S, Jing L, Yin XR, Wang MC, Chen YM, Guo Y, et al. MiR-195 suppresses the metastasis and epithelial-mesenchymal transition of hepatocellular carcinoma by inhibiting YAP. *Oncotarget*. 2017;8(59):99757–71.
- Yuan JM, Govindarajan S, Arakawa K, Yu MC. Synergism of alcohol, diabetes, and viral hepatitis on the risk of hepatocellular carcinoma in blacks and whites in the U.S. *Cancer*. 2004;101(5):1009–17.
- Zhan T, Rindtorff N, Boutros M. Wnt signaling in cancer. *Oncogene*. 2017;36(11):1461–73.
- Zhang C, Li J, Huang T, Duan S, Dai D, Jiang D, et al. Meta-analysis of DNA methylation biomarkers in hepatocellular carcinoma. *Oncotarget*. 2016;7(49):81255–67.
- Zhang YJ, Chen Y, Ahsan H, Lunn RM, Lee PH, Chen CJ, et al. Inactivation of the DNA repair gene O6-methylguanine-DNA methyltransferase by promoter hypermethylation and its relationship to aflatoxin B1-DNA adducts and p53 mutation in hepatocellular carcinoma. *Int J Cancer*. 2003;103(4):440–4.
- Zheng D, Zhang L, Cheng N, Xu X, Deng Q, Teng X, et al. Epigenetic modification induced by hepatitis B virus X protein via interaction with de novo DNA methyltransferase DNMT3A q. *J Hepatol* [Internet]. 2009;50(2):377–87.



Review

Drinking for protection? Epidemiological and experimental evidence on the beneficial effects of coffee or major coffee compounds against gastrointestinal and liver carcinogenesis



Guilherme Ribeiro Romualdo^a, Ariane Bartolomeu Rocha^a, Mathieu Vinken^b, Bruno Cogliati^c, Fernando Salvador Moreno^d, María Angel García Chaves^e, Luis Fernando Barbisan^{f,*}

^a Department Pathology, Medical School, São Paulo State University (UNESP), Botucatu, Brazil

^b Department of In Vitro Toxicology and Dermato-Cosmetology, Faculty of Medicine and Pharmacy, Vrije Universiteit Brussel, Brussels, Belgium

^c Department of Pathology, School of Veterinary Medicine and Animal Science, University of São Paulo (USP), São Paulo, Brazil

^d Department of Food and Experimental Nutrition, Faculty of Pharmaceutical Sciences, University of São Paulo (USP), São Paulo, Brazil

^e Department of Oncology, Biosanitary Research Institute of Granada (ibs.GRANADA), University Hospitals of Granada-University of Granada, Granada, Spain

^f Department of Morphology, Biosciences Institute, São Paulo State University (UNESP), Botucatu, Brazil

ARTICLE INFO

Keywords:

Espresso and common coffee
Caffeine
Trigonelline
Chlorogenic acid
Gastrointestinal cancer
Liver cancer

ABSTRACT

Recent meta-analyses indicate that coffee consumption reduces the risk for digestive tract (oral, esophageal, gastric and colorectal) and, especially, liver cancer. Coffee bean-derived beverages, as the widely-consumed espresso and “common” filtered brews, present remarkable historical, cultural and economic importance globally. These drinks have rich and variable chemical composition, depending on factors that vary from “seeding to serving”. The alkaloids caffeine and trigonelline, as well as the polyphenol chlorogenic acid, are some of the most important bioactive organic compounds of these beverages, displaying high levels in both espresso and common brews and/or increased bioavailability after consumption. Thus, we performed a comprehensive literature overview of current knowledge on the effects of coffee beverages and their highly bioavailable compounds, describing: 1) recent epidemiological and experimental findings highlighting the beneficial effects against gastrointestinal/liver carcinogenesis, and 2) the main molecular mechanisms in these *in vitro* and *in vivo* bioassays. Findings predominantly address the protective effects of coffee beverages and their most common/bioavailable compounds individually on gastrointestinal and liver cancer development. Caffeine, trigonelline and chlorogenic acid modulate common molecular targets directly implicated in key cancer hallmarks, what could stimulate novel translational or population-based mechanistic investigations.

Abbreviations: 4-NQO, 4-Nitroquinoline-1-oxide; AC, Adenocarcinoma; ACF, Aberrant crypt foci; Ad-PTEN, Adenovirus-mediated transfer of phosphatase and tensin homolog; AHR, Aryl hydrocarbon receptor; Akt, Protein kinase B; AOM, Azoxymethane; ARE/XRE, Antioxidant/xenobiotic response elements; BSA, Body surface area; CCl₄, Carbon tetrachloride; COX-2, Cyclooxygenase 2; CQA, Caffeoylquinic acid; CRC, Colorectal cancer; CTGF, Connective tissue growth factor; CYP, Cytochrome P450; DEN, Diethylnitrosamine; DMBA, 7,12-Dimethylbenz[*a*]anthracene; DMH, 1,2-Dimethylhydrazine hydrochloride; DSS, Dextran sulphate sodium; EFSA, European Food Safety Authority; EGR1/mPGES-1, Early growth response protein-1/microsomal Prostaglandin E Synthase-1; EMT, Epithelial-mesenchymal transition; ERK, Extracellular signal-regulated kinase; G6Pase, Glucose 6-phosphatase; GCLC, Glutamate-cysteine ligase catalytic subunit; GR, Glutathione reductase; GSH, Reduced glutathione levels; GSH-Px, Glutathione peroxidase; GST-P, Placental glutathione-S-transferase; HCV/HBV, Hepatitis B/C virus; HCC, Hepatocellular carcinoma; HED, Human equivalent dose; HFD, High fat diet; HIF-1 α , Hypoxia-inducible factor-1 α ; HSCs, Hepatic stellate cells; HWM, High molecular weight; IARC, International Agency for Research on Cancer; IBD, Inflammatory bowel disease; IFN γ , Interferon- γ ; IRE1- α , Inositol-requiring enzyme 1 alpha; IL, Interleukin; MAM, Methylazoxymethanol; miRs, microRNAs; MDA, Malondialdehyde; MEK1, Mitogen-activated protein kinase 1; MMP, Matrix metalloproteinase; MNNG, N-Methyl-N'-nitro-N-nitrosoguanidine; MNU, N-Methyl-N-nitrosourea; NAFLD, Non-alcoholic fatty liver disease; NF- κ B, Nuclear factor κ B; NMBA, N-Nitrosomethylbenzylamine; NQO1, NAD(P)H quinone dehydrogenase 1; Nrf2, Nuclear factor erythroid-related factor 2; OR, Odds ratio; PA, Palmitic acid; PCNA, Proliferating cell nuclear antigen; PGE₂, Prostaglandin E₂; PhIP, 2-Amino-1-methyl-6-phenylimidazo[4,5-*b*]pyridine; PKC α , Protein kinase C α ; PNL, Preneoplastic lesions; PPAR γ , Peroxisome proliferator-activated receptor gamma; ROS, Reactive oxygen species; RR, Relative risk; SCC, Squamous cell carcinoma; SREBP1, Sterol regulatory element-binding protein 1; TAA, Thioacetamide; t-BOOH, Tert-butylhydroperoxide; TGF- β , Transforming growth factor β ; TIMP, Tissue inhibitor of metalloproteinase; TNF- α , Tumor necrosis factor α ; TOPK, T-LAK Cell-originated protein; UGT, UDP Glucuronosyltransferases; VEGF, Vascular endothelial growth factor.

* Corresponding author.

E-mail address: luis.barbisan@unesp.br (L.F. Barbisan).

<https://doi.org/10.1016/j.foodres.2019.05.029>

Received 22 April 2019; Received in revised form 15 May 2019; Accepted 20 May 2019

Available online 22 May 2019

0963-9969/ © 2019 Elsevier Ltd. All rights reserved.

1. Introduction

It is estimated that upper, lower digestive tract (oropharyngeal, esophageal, gastric and colorectal) and liver malignant neoplasms accounted for 24% of new cases (~4.3 million) and 31% cancer-related deaths (~3 million) in 2018. Altogether, these cancers would reach the first position in terms of incidence and mortality globally, overcoming top-ranked prostate, breast and lung cancers (Bray et al., 2018). Nutritional habits and interventions, such as the high consumption of fruits, vegetables, and coffee, have been proposed to play important roles in reducing cancer risk (Wiseman, 2018). Indeed, recent studies showed that coffee consumption, a widespread habit usually incorporated into healthy eating patterns, may promote beneficial effects on a plethora of diseases, including a 13% reduction in overall cancer risk for regular consumers (Poole et al., 2017; Yu, Bao, Zou, & Dong, 2011).

In this paper, we provide a comprehensive literature overview of recent epidemiological and experimental findings highlighting the beneficial effects of coffee or bioactive coffee compounds consumption against digestive tract and liver carcinogenesis. Considering that caffeine, chlorogenic acid, and trigonelline are some of the most abundant bioactive compounds in popularly consumed coffee beverages (“common” brewed and espresso) and/or display high bioavailability after consumption, we focused on the effects and common molecular mechanisms linked to these compounds. This review should provide insights of clinical and translational significance for further mechanistic investigation.

2. Coffee origins and chemical composition

According to Ethiopia’s popular legend, the discovery of coffee trees is attributed to a goatherd, Kaldi, who lived in the Kaffa highlands, a place which later named the plant. After eating coffee berries, his goats could not sleep. Kaldi reported his findings to a monk, who made a drink out of the berries (Tadesse, 2017). Despite this mythical origin, the production and consumption of coffee bean-derived beverages probably dated back from the 15th century, emerging in Africa and Asia, and rapidly spreading to Europe, along with the colonial voyages during the 17th century. Considered the “favorite drink of the civilized world”, coffee beverages finally reached the “New World” in the 18th century, gaining popularity due to widespread production favored by the tropical climate in Latin America (Pendergrast, 2010). Brought from the French Guianas by Francisco de Melo Palheta and frequently portrayed in Candido Portinari’s paintings, coffee production exponentially grew in Brazilian southeastern states, making this country by far the world’s largest producer (~3.1 billion Kg/year, accounting for 34% of the worldwide production) and exporter (~1.8 billion Kg/year, representing 27% of all exports), and the sixth biggest consumer of coffee beans (6.25 Kg per capita) (Fig. 1) (International Coffee Organization, 2018). In terms of production, Brazil is followed by Central and South American, Asiatic and African countries that are part of an equatorial/tropical-climate privileged region called “bean belt” (Fig. 1) (International Coffee Organization, 2018).

Nowadays, because of the extensive production of *Coffea arabica* and *Coffea canephora* species, coffee beans, and their derived beverages are considered commodities of great economic importance (International Coffee Organization, 2018). Especially the “common” brewed and espresso brews are the most consumed drinks worldwide after water, estimated to reach around 2 billion cups consumed every day. When a cup of common (also known as “conventional” or “filtered”) or espresso brew coffee is served, its composition reveals a multitude of substances, belonging to different chemical classes and thus, with many potential pharmacological properties (Caprioli et al., 2013; Caprioli et al., 2014; Derossi, Ricci, Caporizzi, Fiore, & Severini, 2018). There is an inherent fluctuation in the presence and levels of these compounds, depending on many factors that vary from “seeding

to serving”, such as plant species, growing conditions, time of harvesting, the roasting of the beans, types of preparations (common or espresso brews), among others. (Campa, Doubeau, Dussert, Hamon, & Noiro, 2005; Caporaso, Genovese, Canela, Civitella, & Sacchi, 2014; Caprioli et al., 2013; Caprioli et al., 2014; Derossi et al., 2018; Fuller & Rao, 2017; Tolessa, D’heer, Duchateau, & Boeckx, 2017). The main bioactive compound present in coffee beverages is the caffeine (1,3,7-trimethylxanthine), a xanthine alkaloid derived from guanine (Fig. 2). This purine, which is also present in tea (*Camelia sinensis*) (Lin, Wu, & Lin, 2003) and cocoa (*Theobroma cacao*, L) (Risner, 2008), is the main compound responsible for the psychoactive activity of coffee beverages. Caffeine antagonizes adenosine receptors in the neuron cells in the brain, decreasing fatigue, increasing mental acuity and improving cognitive function (Kaster et al., 2015). Being the most prominent source of daily caffeine, “common” and espresso brews display varying concentrations of this compound: In common coffee, caffeine concentrations range from 0.55 to 1.55 mg/mL while in espresso, from 2.45 to 5.83 mg/mL (Fig. 2) (Caporaso et al., 2014; Caprioli et al., 2014; McCusker, Goldberger, & Cone, 2003). Decaffeinated coffee beverages are suggested in some caffeine-avoidance medical conditions, as treatments with bronchodilators and anti-anxiety drugs (European Food Safety Authority, 2015). Decaffeinated brews are compositionally similar to caffeinated beverages apart from having little (0.10 to 0.52 mg/mL in espresso and 0.02 mg/mL in common brew) or none caffeine (McCusker, Fuehrlein, Goldberger, Gold, & Cone, 2006). Although theobromine is less abundant than caffeine, this other common methylxanthine is present in coffee drinks as well (0.027 and 0.017 mg/mL in espresso and common brews, respectively) (Bispo et al., 2002; Gennaro & Abrigo, 1992).

In terms of abundance, caffeine is followed by a family of conjugated hydroxycinnamates collectively referred to as chlorogenic acids (Fig. 2), which are polyphenols that naturally occur in a wide variety of fruits and vegetables besides coffee beans (Ludwig et al., 2014; Upadhyay & Mohan Rao, 2013). These phenolic compounds are thermolabile and, hence prone to deterioration according to the roasting process of the beans (Ludwig et al., 2014). However, coffee beverages contain substantial amounts of total chlorogenic acid, ranging from 0.24 to 0.67 mg/mL in common coffee and from 1.52 to 3.37 mg/mL in espresso coffee (Fig. 2) (Caprioli et al., 2014; Crozier, Stalmach, Lean, & Crozier, 2012; Tfouni et al., 2014). In coffee beverages, the most common chlorogenic acid isomers are 5-caffeoylquinic acid (5-CQA), 3-CQA and 4-CQA (Caprioli et al., 2014; Crozier et al., 2012; Tfouni et al., 2014). Presenting similar concentration to chlorogenic acids, trigonelline (1-methylpyridinium-3-carboxylate) is another common alkaloid in coffee beverages. This pyrimidine is commonly found in fenugreek seeds (*Trigonella foenum-graecum*) and pumpkin (Cucurbitaceae family) (Panda, Biswas, & Kar, 2013; Yoshinari, Sato, & Igarashi, 2009), and displays 0.35–0.51 mg/mL and 1.69–2.70 mg/mL range variations in common and espresso brews, respectively (Fig. 2) (Caprioli et al., 2014; Furtado, Polletini, Dias, Rodrigues, & Barbisan, 2014; Kuhn, Lang, Bezold, Minceva, & Briesen, 2017; López-Galilea, De Peña, & Cid, 2007). Due to the roasting process, part of trigonelline is demethylated to nicotinic acid, which is mainly available in espresso (0.35 mg/mL) (Caprioli et al., 2014). Moreover, common and espresso brews contain lipids, mainly represented by cafestol and kahweol (Fig. 2). These diterpene alcohols remain abundant in unfiltered coffee preparations (as Turkish) but are almost completely removed when coffee is brewed with a paper filter (Gross, Jaccaud, & Huggett, 1997). Coffee is also a source of non-digestible fiber (6.5 and 4.7 mg/mL in espresso and common brews, respectively), mainly represented by mannose and galactose polysaccharide chains (Díaz-Rubio & Saura-Calixto, 2007).

The roasting process of beans contributes to the synthesis of another class of compounds named melanoidins (espresso: 1.75–3.65 mg/mL; common: 1.79 mg/mL) (Fogliano & Morales, 2011; Lopes et al., 2016). These heterogeneous, complex, and dark-colored molecules are end-products of Maillard reactions and have high molecular weights

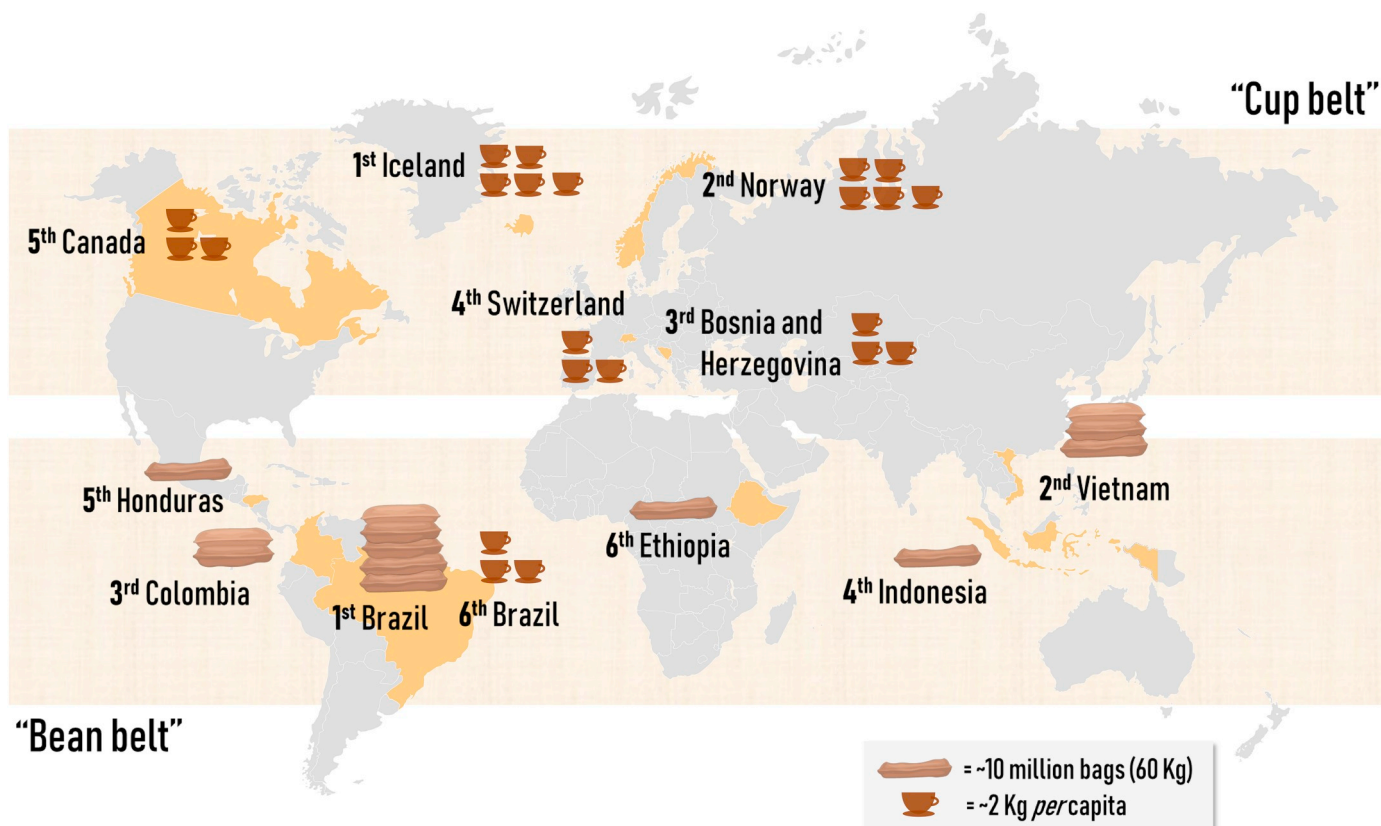


Fig. 1. The top 6 coffee consumers and producers globally. Reference: [International Coffee Organization, 2018](#).

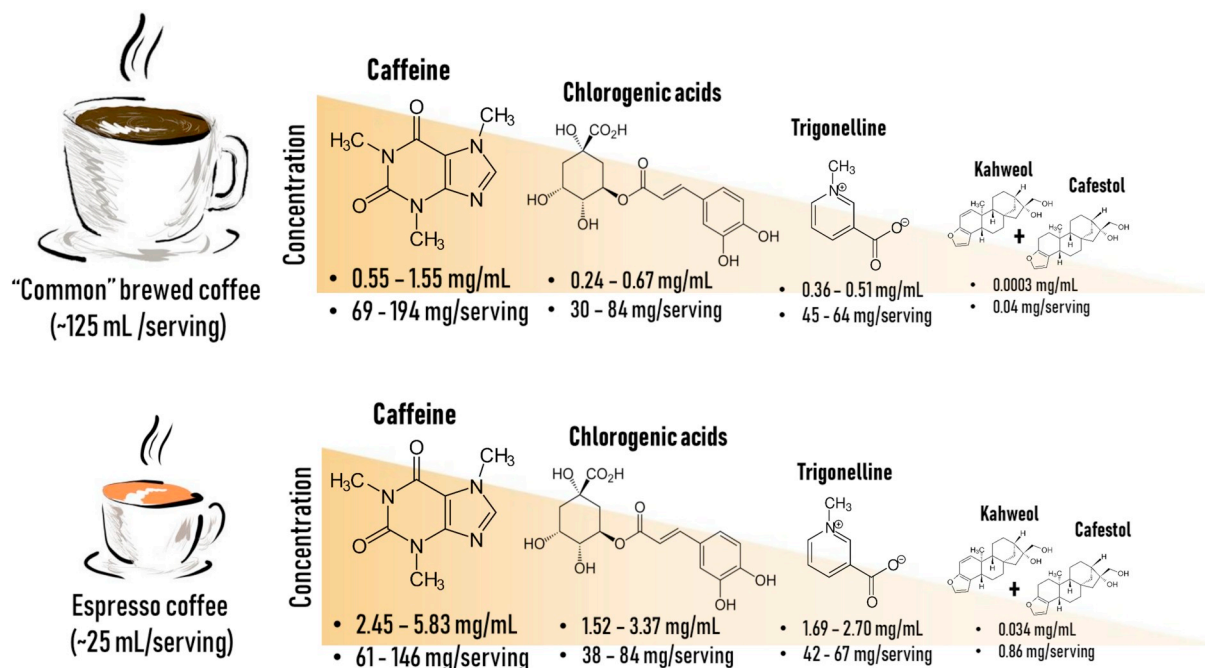


Fig. 2. Main compounds observed in common and espresso coffee brews according to their concentration and the total amount in usually applied servings.

(HMW). Coffee amino acids, polysaccharides, and phenolic compounds, especially the chlorogenic acids, contribute to the formation of coffee melanoidins (Perrone, Farah, & Donangelo, 2012). However, these HMW molecules may only reach high concentrations in over-extraction procedures during coffee beverage preparation (Bartel, Mesias, & Morales, 2015). In addition to the spectra of organic compounds, the

mineral characterization of coffee beverages revealed great amounts of potassium in both espresso and common brews (3 and ~0.8 mg/mL, respectively) and phosphorus in espresso coffee (0.6 mg/mL) (Gillies & Birkbeck, 1983; Oliveira, Ramos, Delerue-Matos, & Morais, 2015).

With respect to the contribution of these molecules to the complex sensorial characteristics of coffee, the alkaloids (astringency) and

chlorogenic acids (acidity) are major compositional drivers of flavor, while chlorogenic acids and melanoidins are responsible for the brownish color (Sunarharum, Williams, & Smyth, 2014). Interestingly, high trigonelline and caffeine contents are positively associated with higher coffee cup quality (Farah, Monteiro, Calado, Franca, & Trugo, 2006). Therefore, based on the fluctuations on compound level data, it is clear that “a cup of coffee” measurement is not reliable and reproducible for epidemiological studies, yet commonly applied. Nonetheless, based on the same concentration data, caffeine, trigonelline, and chlorogenic acid seem to be some of the most important bioactive organic compounds of espresso and regular coffee beverages (Fig. 2).

3. Coffee consumption and metabolism

Considering the “coffee cup” term ambiguity, the most reliable coffee consumption data come from annual *per capita* consumption of ground coffee (in Kg). Thus, most countries presenting the higher consumption rates (6.29–9.12 Kg *per capita*) are in a “cup belt” in the north hemisphere, mainly in Europe (Fig. 1). It is worthy of note that many European Union countries (4.90 Kg *per capita*), as well as the US (4.84 Kg *per capita*), are also considered high coffee consumers (International Coffee Organization, 2018). On the other hand, Asian and African countries, such as China, Japan, South Korea, and Ethiopia, present mild to low coffee consumption (3.5 to 0.8 Kg *per capita*) (International Coffee Organization, 2016).

Epidemiological studies in Europe and the US indicate that coffee beverages are the predominant source of caffeine, contributing from 40% to 94% to total caffeine daily intake. In these regions, coffee/caffeine consumption increases in puberty and culminates in adult and elderly ages (European Food Safety Authority, 2015; Martyn, Lau, Richardson, & Roberts, 2018; Mitchell, Knight, Hockenberry, Teplansky, & Hartman, 2014). Findings from the European Food Safety Authority (European Food Safety Authority, 2015), including data from 22 different countries comprising high coffee consumers, showed that caffeine intake derived from coffee beverages reached maximum mean values of 280.7–382.6 mg/day in adults in some countries. In the US, 3 studies showed average consumption of 105.4–136.4 mg/day (all ages) and mean values of 109.4–271 mg/day in adults (Frery, Johnson, & Wang, 2005; Knight et al., 2004; Mitchell et al., 2014). In Asia, a recent Korean study that considered all sources of caffeine (cocoa, coffee, tea, and derivatives) showed average consumptions of 67.7 mg/day (all ages) and mean values of 81.9 mg/day in adults (Lim, Hwang, Choi, & Kim, 2015). In general, these findings are in keeping with *per capita* ground coffee consumption. Although the continents or countries present clear disparity in terms of coffee consumption, it is important to point that all the presented estimates are in accordance to European Food Safety Authority (2015) daily safe limit for caffeine intake for adults (400 mg/day).

Upon coffee beverage intake, caffeine is rapidly and almost completely absorbed (99%) in the gastrointestinal tract within 45 min, 20% in the stomach and the largest part in the small intestine, being hydrophilic and sufficiently lipophilic to cross the biological membranes (Liguori, Hughes, & Grass, 1997; Nehlig, 2018). Upon the consumption of 160 mg of caffeine, corresponding to approximately 1–2 cups of common coffee (Fig. 2), this xanthine is readily bioavailable, reaching a plasma peak of $\sim 18 \mu\text{M}$ within 60–80 min (White Jr. et al., 2016). A higher coffee consumption, equivalent to 3 cups of common coffee (350 mL, Fig. 2), leads to a caffeine plasma peak of $\sim 33 \mu\text{M}$ after 60 min and presents a half-life of $\sim 5 \text{ h}$ (Lang et al., 2013). In the liver, caffeine suffers demethylation by cytochrome P450 (CYP) subunit 1A2, which virtually accounts for total caffeine metabolism (Gu, Gonzalez, Kalow, & Tang, 1992). Caffeine biotransformation originates paraxanthine, dimethylxanthine, and theobromine (Gu et al., 1992; Lang et al., 2013). It is noteworthy that caffeine metabolism is relatively comparable in humans, rats, and mice, which facilitates the establishment of translational approaches (Walton, Dorne, & Renwick, 2001).

After the consumption of 350 mL of common coffee brew (~ 3 cups, Fig. 2), trigonelline is also mainly absorbed in the small intestine and presents a plasma peak of $5.6 \mu\text{M}$ within 3 h (Lang et al., 2013; Yuyama, 1999). In the liver, trigonelline is methylated to *N*-methylnicotinamide by nicotinamide *N*-methyltransferase and subsequently oxidized to *N*-methyl-2-pyridone-5-carboxamide and *N*-methyl-4-pyridone-5-carboxamide (Lang et al., 2013). Similar to caffeine, trigonelline has a long half-life of approximately $\sim 5 \text{ h}$ (Lang et al., 2013). Despite the few experiments available on trigonelline pharmacodynamics in rodents, findings indicate that a greater part of trigonelline is also absorbed in the small intestine (Yuyama, 1999). Around 30% of chlorogenic acid is absorbed in the small intestine after consumption, and most part reaches the colon (Olthof, Hollman, & Katan, 2001). After drinking 200 mL of common coffee containing a total of 96 mg of chlorogenic acid ($\sim 0.48 \text{ mg/mL}$, in keeping with Fig. 2), this polyphenol is almost undetectable in serum after 1 h (Nardini, Cirillo, Natella, & Scaccini, 2002). Higher common coffee consumption (350 mL) leads to a $0.035 \mu\text{M}$ plasma peak of chlorogenic acid in 45 min. In contrast, the concentration of (di)hydroxycinnamic acids, their sulfates, and glucuronides, that are well-known chlorogenic acid derivatives, appears to gradually increase in serum after coffee consumption (Lang et al., 2013; Nardini et al., 2002). In particular, catechol sulfate, one of the major metabolites, displays a $2.5 \mu\text{M}$ peak within 45 min (Lang et al., 2013). This is attributed to the fact that chlorogenic acid is heavily metabolized by colonic microbiota before absorption, considering that ileostomy-submitted patients present a 3-fold decrease in the excretion of some of these metabolites compared to healthy ones (Stalmach, Steiling, Williamson, & Crozier, 2010). Although part of chlorogenic acid is also metabolized by the gut microbiota in rats, about 16% of intact chlorogenic acid is absorbed in the stomach (Lafay et al., 2006).

Collectively, these data suggest that the pharmacokinetic profiling of coffee consumption indicates that caffeine, trigonelline and the metabolites of chlorogenic acid display high bioavailability in humans (Lang et al., 2013). Particularly caffeine and trigonelline accumulate in the plasma due to their long half-life times during habitual consumption of many cups of coffee distributed over the day (Lang et al., 2013). Indeed, both caffeine and trigonelline as well as some metabolites of chlorogenic acid, have been proposed as plasma/urinary biomarkers for coffee brew consumption in humans (Midttun, Ulvik, Nygård, & Ueland, 2018; Stalmach et al., 2009). The high levels and/or bioavailability of these compounds have direct implications on the epidemiological effects and, especially, on the experimental findings regarding coffee and gastrointestinal and liver carcinogenesis.

4. Epidemiological evidence

In the last decade, many meta-analyses of prospective, case-control and cohort studies have shed light onto the beneficial effects of coffee consumption on the digestive tract and liver cancers in different populations (Tables 1–3). As discussed, most of these studies usually apply the “cup of coffee” measurement, thus not considering the variations on the serving volume and type of beverage (Fig. 1). Moreover, depending on the population observed, high and low limits of consumption are variable. In general, the relative risk (RR) or odds ratio (OR) in these meta-analyses are usually calculated based on none or low consumption (≤ 1 cup/day) versus high consumption (≥ 3 cups/day). Despite these limitations and estimations, studies propose significant non-linear inverse associations between coffee consumption and the emerging oropharyngeal, gastric and colon tumors. In fact, the strongest data come from the hepatology field, which shows a linear inverse association between coffee beverage consumption and hepatocellular carcinoma (HCC) risk.

Although oropharyngeal cancers do not rank in the top ten most common malignant neoplasms, the annual estimated incidence is around half a million cases globally, mainly occurring in Asia, Europe, and South America. Tobacco and alcohol abuse cause $> 80\%$ of cases,

Table 1
Review of recent meta-analysis on the effects of coffee consumption against oropharyngeal and esophageal cancers.

Study	Countries/regions	Main findings	Sub group analysis
<i>Oropharyngeal</i>			
Miranda et al., 2017	Japan, Taiwan, Italy, Norway, Denmark, France, Switzerland, USA, Brazil	vs. low consumption ● 31% reduction for high consumption (OR: 0.69)	● Reduction remains in adjustment for Asian (OR: 0.65) countries
Wang et al., 2016	Japan, Norway, USA	vs. low consumption ● 31% reduction for high consumption (RR: 0.69)	● Reduction remains in adjustment for Asian (RR: 0.35) countries and smoking (RR: 0.68)
Li, Peng, & Li, 2016	Japan, Italy, Norway, Denmark, France, Switzerland, USA, Brazil	vs. low consumption ● 37% reduction for high consumption (OR: 0.63)	● Reduction remains in adjustment for Asian (OR: 0.64) and European (OR: 0.62) countries
Turati, Galeone, La Vecchia, Garavello, & Tavani, 2011	Japan, India, Italy, Switzerland, Denmark, Brazil, USA	vs. low consumption ● 36% reduction for high consumption (RR: 0.64) vs. ≤ one cup ● 35% reduction for 3 cups/day (OR: 0.65)	● Reduction remains in adjustment for Asian (RR: 0.74), South American (RR:0.58) and European (RR: 0.61) countries
<i>Esophagus</i>			
Zhang, Zhou, & Hao, 2018	Japan, Taiwan, Sweden, Italy, Greece, Switzerland, Norway, Argentina	vs. low consumption ● No association for high consumption in SCC (OR: 0.76) ● No association for high consumption in AC (OR: 0.90)	● 36% reduction for high consumption (OR: 0.64) in Asian countries (SCC and AC)
Wang et al., 2016	Japan, Norway, Denmark, France, Germany, Greece, Italy, Netherlands, Norway, Spain, Sweden, United Kingdom, USA	vs. low consumption ● No association for high consumption in SCC (RR: 0.89) ● No association for high consumption in AC (RR: 0.91)	● No association in adjustments for European countries (RR: 0.89), alcohol (RR: 0.84) and smoking (OR: 0.85)
Zheng et al., 2013	Japan, China, Iran, Turkey, India, Italy, Greece, Switzerland, Norway, Sweden, USA, Argentina, Brazil, Uruguay, Paraguay	vs. low consumption ● No association for high consumption in SCC (OR: 1.00) ● No association for high consumption in AC (OR: 0.90)	● 33% reduction for high consumption (OR: 0.67) in Asian countries (SCC and AC) ● No association in adjustments for European countries (OR: 0.95), men (OR: 0.82) and alcohol/smoking (OR: 0.89)
Turati et al., 2011	Japan, Taiwan, Italy, Switzerland, Greece, Sweden, USA, Argentina	vs. low consumption ● No association for high consumption in SCC (RR: 0.87) ● No association for high consumption in AC (RR: 1.18)	–

SCC = squamous cell carcinoma; AC = adenocarcinoma; RR = relative risk; OR = odds ratio.

and human papillomavirus infection may also be involved (Warnakulasuriya, 2009). Esophageal cancers, presenting ~572,000 new cases and ~508,000 related-deaths annually, are represented by 2 major subtypes, namely squamous cell carcinoma (SCC) and adenocarcinoma (AC). Both predominantly occur in men in Asian and European countries. Smoking and alcohol consumption are the main risk factors for esophageal SCC, while obesity and gastroesophageal reflux are also accounted for AC (Bray et al., 2018). Regarding coffee beverage consumption, many studies on oropharyngeal cancer present the same non-linear correlation describing that high consumption decreases the risk for this malignancy by 31% - 37% compared to low consumption. Moreover, this inverse association remains even if the data are adjusted for European, Asian countries or smoking (Table 1). For esophageal cancer data, meta-analysis results are inconsistent. Studies do not indicate any overall correlation between coffee consumption and the risk for esophageal SCC and AC development. Nonetheless, when data were subgrouped, high coffee consumption led to a 33%–36% risk reduction, considering both SCC and AC, in the highly affected Asian, but not in the European population (Table 1). Zheng et al. (2013) proposed that the genetic background difference between Europeans and Asians may

account for distinct nutritional responses for coffee intake. In this case, more in-depth experimental *in vitro* and *in vivo* findings are needed in order to confirm the biological plausibility of this effect of coffee consumption in different populational backgrounds.

Concerning gastric cancer, which is responsible for a million new cases and 800,000 deaths *per year*, the age-standardized incidence and mortality rates are higher in Eastern Asia, Central, and Eastern Europe and South America and 2-fold higher in men than women. > 90% of gastric cancers are AC, which can be classified according to the anatomic site as cardia and noncardia subtypes. Cardia AC has similar risk factors to esophageal AC, while almost 90% of noncardia AC cases are attributed to *Helicobacter pylori* infection. For both, smoking, alcohol, high salt and low fruit diet are also established risk factors (Bray et al., 2018). A single recent meta-analysis showed that any daily coffee intake significantly reduces the risk of gastric cancer by 7% when compared to non-consumers. A stronger association was observed in high consumers (3–4 cups/day), which displayed a 12% risk decrease. Nonetheless, most meta-analyses demonstrate that coffee consumption does not modulate overall gastric cancer risk, considering pooled RR and adjustments to smoking, alcohol drinking, Europe, and Asia

Table 2

Review of recent meta-analysis on the effects of coffee consumption against gastric and colorectal cancers.

Study	Countries/regions	Main findings	Sub group analysis
<i>Stomach</i>			
Deng et al., 2016	Japan, Korea, Singapore, Norway, Netherlands, Sweden, Denmark, France, Germany, Greece, Italy, Spain, United Kingdom, USA	vs. low consumption <ul style="list-style-type: none"> ● Increased risk for high consumption in cardia (RR: 1.50) ● No association for high consumption in non-cardia (RR: 0.99) 	<ul style="list-style-type: none"> ● Increased risk in adjustment for USA (RR: 1.36) ● No association in adjustments for Asia (RR: 0.96) and Europe (RR: 1.12)
Xie, Huang, He, & Su, 2016	Japan, Singapore, Taiwan, Turkey, India, Norway, Sweden, Finland, Poland, Italy, Spain, Uruguay, Venezuela	vs. non-consumption <ul style="list-style-type: none"> ● 7% reduction for any consumption (RR: 0.93) ● 12% reduction for 3–4 cups/day (RR: 0.88) ● 8% reduction for 1–2 cups/day (RR: 0.92) ● 5% reduction for < 1 cup day (RR: 0.95) 	–
Zeng et al., 2015	Singapore, Norway, Sweden, Finland, USA	vs. low consumption <ul style="list-style-type: none"> ● No linear association ● No association for 6.5 cups/day (RR: 1.18) ● No association for 3.5 cups/day (RR: 1.06) ● No association for 1.5 cups/day (RR: 0.97) 	<ul style="list-style-type: none"> ● Increased risk in adjustment for USA for 6.5 cups/day (RR: 1.36) ● No association in adjustments for Asia (RR: 0.96), Europe (RR: 1.07), smoking (RR: 0.95), and alcohol for 6.5 cups/day (RR: 1.24)
Xie et al., 2014	Japan, Singapore, Norway, Netherlands, Sweden, Finland, USA	vs. low consumption <ul style="list-style-type: none"> ● No association for high consumption for both (RR: 1.12) 	<ul style="list-style-type: none"> ● Increased risk in adjustment for USA (RR: 1.35), ● No association in adjustments for Europe (RR: 1.08), smoking (RR: 0.99), and alcohol (RR: 1.21)
<i>Colorectal</i>			
Gan et al., 2017	Japan, Singapore, Norway, Netherlands, Sweden, Finland, Denmark, France, Germany, Greece, Italy, Spain, United Kingdom, USA	vs. low consumption <ul style="list-style-type: none"> ● No association for high consumption for colorectal (RR: 0.98) ● No association for high consumption for colon (RR: 0.92) ● No association for high consumption for rectum (RR: 1.06) ● 7% reduction for 4 cups increment for colon (RR: 0.93) 	<ul style="list-style-type: none"> ● 11% reduction for colorectal in adjustment for high decaffeinated consumption (RR: 0.89) ● No associations for colorectal in adjustments for Europe (RR: 1.03), Asia (RR: 0.97), USA (RR: 0.92), smoking (RR: 0.96), alcohol (RR: 0.95), red meat consumption (RR: 0.98), low fruit intake (RR: 1.00), no physical activity (RR: 0.99)
Akter et al., 2016	Japan	vs. low consumption <ul style="list-style-type: none"> ● No association for high consumption for colorectal (RR: 0.95) ● No association for high consumption for colon (RR: 0.98) ● No association for high consumption for rectum (RR: 0.99) 	<ul style="list-style-type: none"> ● No associations for colorectal in adjustments for men (RR: 1.05) and women (RR: 0.82)
Wang et al., 2016	Japan, Singapore, Norway, Netherlands, Sweden, Finland, Denmark, France, Germany, Greece, Italy, Spain, United Kingdom, USA	vs. low consumption <ul style="list-style-type: none"> ● No association for high consumption for colorectal (RR: 0.96) ● 13% decrease for high consumption for colon (RR: 0.87) ● No association for high consumption for rectum (RR: 0.94) 	<ul style="list-style-type: none"> ● No associations in adjustments for Europe (RR: 0.97), Asia (RR: 1.03), USA (RR: 0.89), smoking (RR: 0.97), alcohol (RR: 0.96), red meat consumption (RR: 0.95), no fiber intake (RR: 0.93), no physical activity (RR: 0.93)
Je, Liu, & Giovannucci, 2009	Japan, Norway, Sweden, Finland, USA	vs. low consumption <ul style="list-style-type: none"> ● No association for high consumption for colorectal (RR: 0.91) ● 10% decrease for high consumption for colon (RR: 0.90) ● No association for high consumption for rectum (RR: 0.98) 	<ul style="list-style-type: none"> ● 38% reduction in adjustment for colon in Japanese women (0.62) ● No associations in adjustments in colorectal cancer for Europe (RR: 0.91), USA (RR: 0.93) and Japan (RR: 0.83)

RR = relative risk.

(Table 2). Although epidemiological data on coffee intake are not usually subgrouped considering different types of coffee (caffeinated or decaffeinated), a cohort study revealed that decaffeinated coffee consumption does not present a significant correlation with gastric cancer risk (Sanikini et al., 2015). In contrast, one subgroup analysis revealed that coffee may increase the risk for cardia, but not noncardia, gastric cancer. In addition, high coffee consumption (6.5 cups/day) also showed enhanced risk for both cardia and noncardia gastric cancers in U.S. adjustment (Table 2). However, Xie, Wang, Huang, and Guo (2014) and Deng et al. (2016) propose that these positive associations should not be overinterpreted, because residual confounding effects of other nutritional factors could exist, considering that coffee consumption tends to be related to the unhealthy behaviors of “western lifestyle”, such as smoking and high salt consumption. Furthermore, in comparison to HCC, there are few prospective studies available to establish a solid correlation for gastric cancer. Indeed, findings are inconsistent, and experimental *in vivo* and *in vitro* data point to the opposite direction, as will be further presented.

Colorectal cancer (CRC), considered the main type of digestive tract malignant neoplasm (accumulating 1.8 million cases and 880,000 deaths in each year), is usually linked to smoking, alcohol drinking, sedentary lifestyle and poor dietary habits (low fiber and vegetable and high red meat and fat intakes) (Bray et al., 2018). The occurrence of inflammatory bowel disease (IBD) (*i.e.* ulcerative colitis or Crohn's disease) is also suggested to increase CRC risk (Wang & Fang, 2014). Although CRC onset mainly involves environmental factors (~95%), hereditary risk factors, such as Familial Adenomatous Polyposis and Lynch syndrome (~5%), are also accounted for this malignancy (Bray et al., 2018). The highest age-standardized incidence/mortality rates for CRC are found in Europe, North America, and Eastern Asia, predominantly affecting men. Some of the recent meta-analyses on coffee consumption and CRC are focused on Asian populations (Table 2), considering that rates markedly increased in these regions over the last decades due to a “western lifestyle” turnover (Bray et al., 2018). Coffee drinking was not significantly associated with CRC risk in most studies (Table 2). Nonetheless, non-linear overall risk reductions of 7% to 13% were observed in high coffee consumers considering colon, but not rectal cancer. These marginal correlations appeared to be stronger only at higher ranges of intake, with 7% risk reductions for every 4 cups/day of coffee. Upon data adjustment for Japanese women, risk reduction is 38% (Table 2). On the other hand, high decaffeinated coffee consumption led to an 11% reduction for both colon and rectal cancer risks (Gan et al., 2017) (Table 2). Gan et al. (2017) suggested that this effect may be attributed to residual factors, since participants that drink decaffeinated coffee tend to have healthier lifestyles, with higher fruit/vegetable and low red meat intake. However, the direct contact of the colonic mucosa with common bioactive coffee compounds, rather than caffeine, should be addressed for this inverse association. As previously discussed, chlorogenic acid isomers are heavily metabolized by colonic microbiota, giving rise to many other bioactive compounds that have direct contact with the colonic mucosa. Although clinical findings on coffee consumption and CRC are missing, Kang et al. (2011) reported that any consumption (> 1 cup/day) of caffeinated or decaffeinated coffee showed similar responses on downregulating extracellular signal-regulated kinase (ERK) phosphorylation in CRC tissue compared to non-consumers. These parallel modulations of a key regulator on colon tumorigenesis underscore the importance of *in vivo* and *in vitro* approaches to unravel other mechanisms involved in caffeinated and decaffeinated coffee intake and decreased CRC risk, as will be discussed further on.

Liver cancers, mainly represented by HCC, accounted for about 840,000 incident cases and 780,000 deaths in 2018 (Bray et al., 2018). HCC, a poor prognosis malignancy that comprises 75%–85% of all liver cancer cases and deaths, usually occurs in a background of fibrosis or cirrhosis (> 90% of cases), which is considered the main risk factor. This cirrhotic context is mostly caused by chronic hepatitis B and/or C

virus (HBV/HCV) infections, alcohol abuse and non-alcoholic fatty liver disease (NAFLD) (Bray et al., 2018; Yang et al., 2011). Incidence data for HCC presents clear gender and geographic disparities, usually occurring in men and in Asian countries (Bray et al., 2018). In the last decade, there is increasing and accumulating evidence proposing an inverse linear dose-response correlation between coffee consumption and HCC risk in different populations (Table 3). In general, coffee consumption at any level leads to remarkable 27%–39% and 34%–43% reductions in fibrosis/cirrhosis and HCC risks when compared to non-consumers, respectively (Table 3). These inverse associations are stronger for high coffee consumers. Moreover, 1 to 2 extra cups per day on top of any consumption may lead to an additional 15%–27% reduction for HCC risk. Interestingly, when HCC data are stratified to specific risk conditions such as the history of chronic hepatitis and HCV or HBV serologic evidence or highly incident areas as Asia, these significant reductions are still observed (Table 3). In contrast, decaffeinated coffee consumption failed in showing a significant reduction for HCC risk in a recent meta-analysis (Godos et al., 2017). In addition, the daily consumption of 2 extra cups of decaffeinated coffee on top of any intake decreased HCC risk, but to a lesser extent in comparison to caffeinated coffee (14% vs. 27%) (Kennedy et al., 2017). These data suggest that decaffeinated coffee consumption presents a weak or none inverse association to HCC risk compared to caffeinated coffee consumption (Table 3). Thus, based on the epidemiological data available, one may raise the question if these protective effects majorly attributed to caffeine or to its combination or association to other highly abundant and bioavailable coffee compounds, as trigonelline and chlorogenic acid. Considering that a recent prospective cohort study also failed in showing that caffeine alone reduces HCC risk (Tamura et al., 2018), the combination of highly bioavailable coffee components may be accounted for the protective effects of coffee consumption against HCC. This insight should be considered for further translational investigations using *in vivo* and *in vitro* HCC models, since the available studies predominantly investigate the effects of coffee compounds individually, not in combination.

5. *In vitro* findings

In vitro studies demonstrate antiproliferative, antioxidant, anti-fibrotic or proapoptotic effects of coffee brews or major bioavailable coffee compounds on bioassays using SCC, AC, CRC, HCC and hepatic stellate cells (HSC) (Figs. 3 and 4). In general, these described beneficial effects are in line with the epidemiological evidence of inverse associations between gastrointestinal and liver cancer risks and coffee consumption, as pointed before. Interestingly, despite being administered individually, major coffee compounds exhibit a common modulation of key pathways involved in many cancer hallmarks (Figs. 3 and 4). Nonetheless, some insights based on human consumption and bioavailability of coffee compounds are necessary in order to improve novel experimental approaches. Most *in vitro* assays are based on exposing tumoral cells to bioactive coffee compounds individually, lacking the complexity of compound combination as observed in whole coffee beverages. Even when comparing the effects of whole coffee versus coffee compounds, these studies only focus on individually selected coffee compounds, and not on the combination of the most common and/or highly bioavailable ones (Kalthoff, Ehmer, Freiberg, Manns, & Strassburg, 2010; Nakayama, Funakoshi-Tago, & Tamura, 2017). Some studies evaluated the effects of cafestol and kahweol combinations (Kalthoff et al., 2010), although these lipids are almost completely absent in coffee brews after filtering. In addition, these assays applied coffee compounds in supraphysiological concentrations ranging from high micromolar (μM) to millimolar (mM) levels, usually mimicking the concentration observed in brewed coffee preparations (Kalthoff et al., 2010) (Fig. 2). Nonetheless, a “metabolic approach” should be considered for *in vitro* studies, such as the physiologically applicable concentrations based on serum or plasma peaks after coffee

Table 3

Review of recent meta-analysis on the effects of coffee consumption against liver fibrosis/cirrhosis and hepatocellular carcinoma (HCC).

Study	Countries/regions	Main findings	Sub group analysis
HCC			
Bravi, Tavani, Bosetti, Boffetta, & La Vecchia, 2017	China, Japan, Finland, multicentre Europe, USA	vs. low/non-consumption ● 34% reduction for any consumption (RR: 0.66) ● 50% reduction for high consumption (RR: 0.50) ● 15% reduction for 1 cup increment (RR: 0.85)	● Reduction remains in adjustment for Asian countries (RR: 0.68)
Godos et al., 2017	China, Japan, Finland, multicentre Europe, Italy, Greece, USA	vs. non-consumption ● Linear association: - 32% reduction for 2 cups/day (RR: 0.68) - 43% reduction for 3 cups/day (RR: 0.57) - 53% reduction for 4 cups/day (RR: 0.47) ● 15% reduction for 1 cup increment (RR: 0.85) ● 27% reduction for 2 cups increment (RR: 0.73)	● Non-significant reduction for decaffeinated (RR: 0.85) ● Significant reduction remains in adjustments for Asian countries (RR: 0.42) and chronic hepatitis (RR: 0.56)
Kennedy et al., 2017	China, Japan, Hong Kong, Singapore, Finland, multicentre Europe, Italy, Greece, France, USA	vs. non-consumption ● Linear association: - 24% reduction for 2 cups/day (RR: 0.76) - 33% reduction for 3 cups/day (RR: 0.67) - 42% reduction for 4 cups/day (RR: 0.58)	● 14% reduction for 2 decaffeinated cups increment (RR: 0.86)
Yu et al., 2016	Japan, Singapore, Finland, multicentre Europe, USA	vs. non-consumption ● Linear association: - 24% reduction for 2 cups/day (RR: 0.76) - 33% reduction for 3 cups/day (RR: 0.67) - 42% reduction for 4 cups/day (RR: 0.58)	● Reduction remains in adjustments for Asian countries (RR: 0.50), gender (male RR: 0.58, female RR: 0.57) and history of liver diseases (RR: 0.48)
Wang et al., 2016	Japan, Singapore, Finland, multicentre Europe, USA	vs. low consumption ● 54% reduction for high consumption (RR: 0.46) ● 27% reduction for 2 cups increment (RR: 0.73)	● Reduction remains in adjustments for Asian countries (RR: 0.51), men (RR: 0.29) and history of liver diseases (RR: 0.36)
Bravi, Bosetti, Tavani, Gallus, & La Vecchia, 2013	China, Japan, Finland, Italy, Greece, Serbia	vs. non-consumption ● 40% reduction for any consumption (RR: 0.60) ● 56% reduction for high consumption (RR: 0.44) ● 20% reduction for 1 cup increment (RR: 0.85)	● Reduction remains in adjustments for gender (male RR: 0.58, female RR: 0.70), serologic evidence of HBV and/or HCV (RR: 0.52) and history of hepatitis (RR: 0.70)
Bravi et al., 2007	Japan, Italy, Greece	vs. non-consumption ● 41% reduction for any consumption (RR: 0.59) ● 55% reduction for high consumption (RR: 0.45) ● 23% reduction for 1 cup increment (RR: 0.77)	● Reduction remains in adjustments for history of hepatitis (RR: 0.53)
Fibrosis/Cirrhosis			
Kennedy et al., 2016	Singapore, Norway, Finland, Italy, France, USA	● 44% reduction in all-cause cirrhosis for 2 cups increment (RR: 0.56) ● 42% reduction in alcoholic cirrhosis for 2 cups increment (RR: 0.58)	–
Liu et al., 2015	Hong Kong, Italy, France, UK, Brazil, USA	vs. non-consumption ● 39% reduction in cirrhosis for any consumption (OR: 0.61) ● 47% reduction in cirrhosis for high consumption (OR: 0.53) ● 27% reduction in fibrosis for any consumption (OR: 0.73)	● Reduction remains in adjustment for alcohol drinking in cirrhosis (OR: 0.49) and for HCV infection in fibrosis (OR: 0.65)

RR = relative risk; OR = odds ratio.

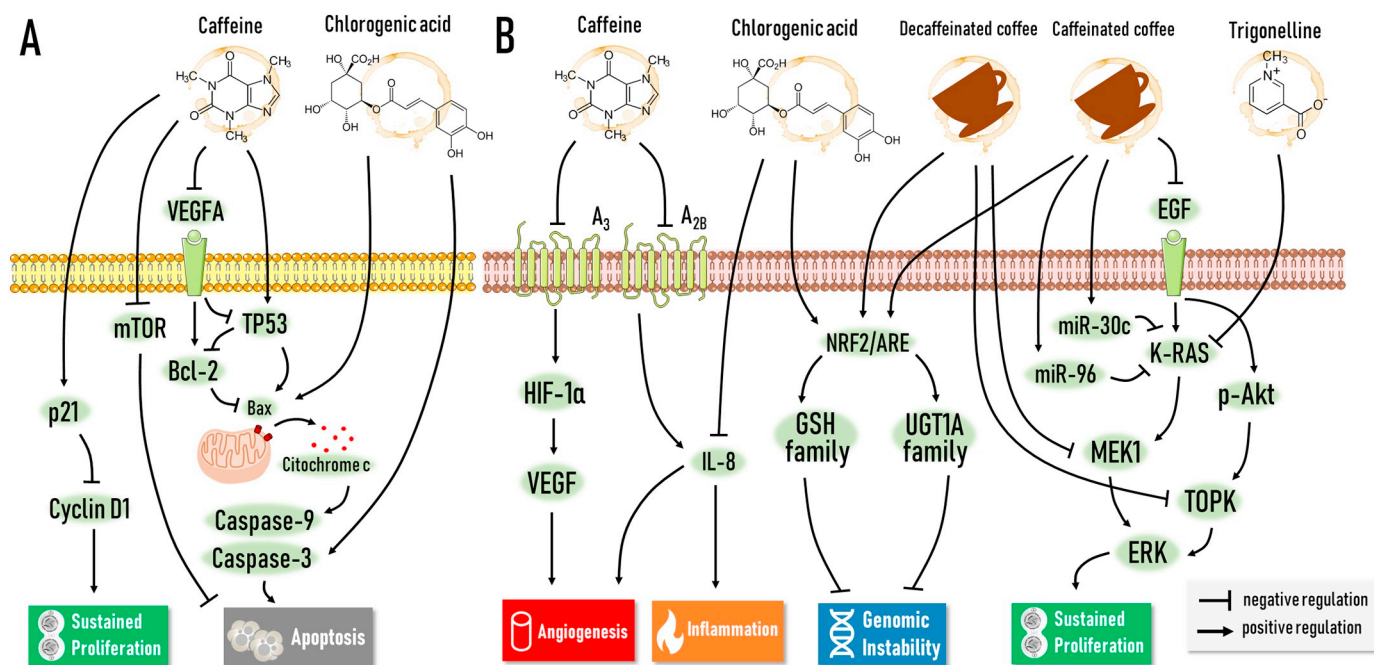


Fig. 3. Main molecular pathways modulated *in vitro* by whole caffeinated, decaffeinated coffee brews or highly bioavailable isolated coffee compounds in (A) gastric adenocarcinoma (AC) and (B) colon cancer cells. Caffeine and chlorogenic acid modulate common molecular targets in the proapoptotic axis in gastric AC cells. Caffeinated and decaffeinated coffee are suggested to share the regulation of pro-proliferative (K-RAS pathway) and antioxidant pathways (Nrf2 pathway), as well as both caffeine and chlorogenic acid, can commonly attenuate IL-8-mediated pro-inflammatory response.

compound biotransformation that range from mid to low micromolar (μ M) concentrations. Furthermore, the time points selected for parameter evaluation in these bioassays should be based on the half-life of the compounds in the human body, hence still simulating a physiologically reliable context. Finally, despite exerting antiproliferative and/or proapoptotic effects on different tumor cell lines, only few studies have included normal cell line controls to show a potential selective effect or absence of toxic effects in cells isolated from normal tissues

(Amigo-Benavent, Wang, Mateos, Sarriá, & Bravo, 2017; Liu, Zhou, & Tang, 2017; Saito et al., 2003).

5.1. Upper digestive tract cancer cells

There are few studies available on the effects of coffee brews and selected coffee compounds on upper digestive tract cancer *in vitro* models. With respect to whole brewed coffee exposure, both caffeinated

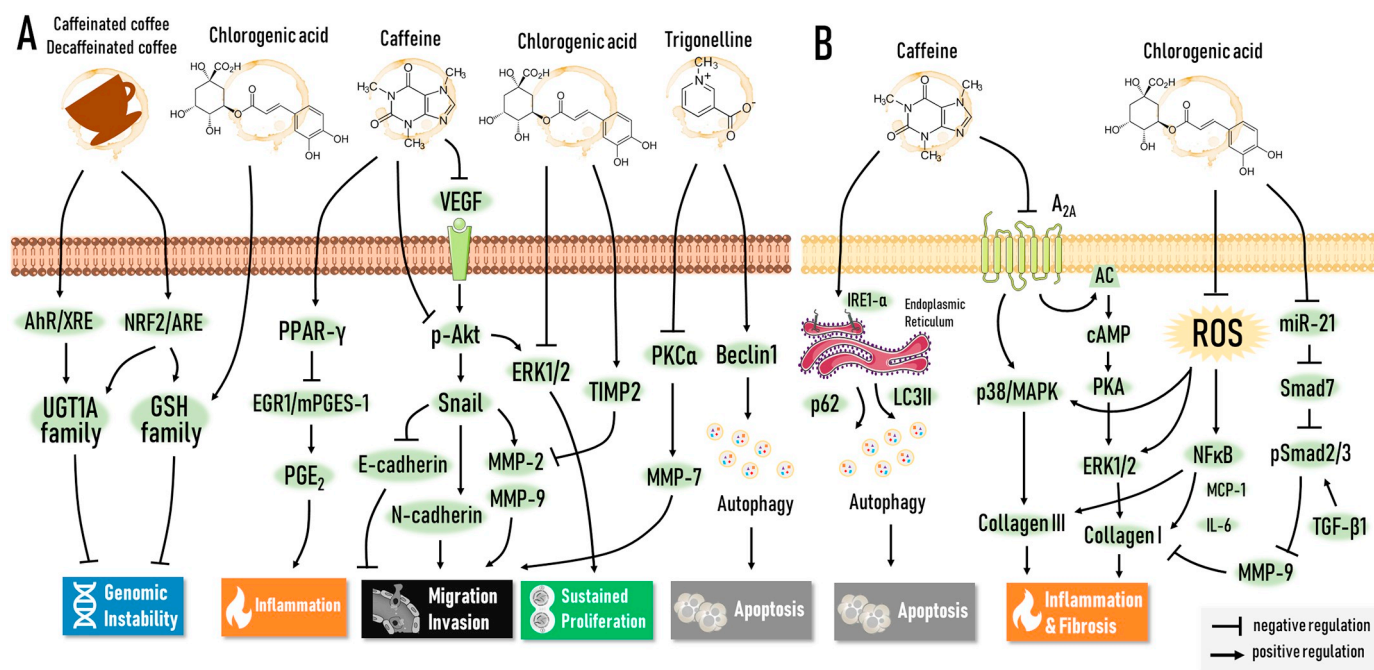


Fig. 4. Main molecular pathways modulated *in vitro* by whole caffeinated, decaffeinated coffee brews or highly bioavailable isolated coffee compounds in (A) hepatocellular carcinoma (HCC) cells and (B) hepatic stellate cells (HSC). Isolated coffee compounds share molecular targets implicated on important cancer hallmarks, such as migration/invasion in HCC cells (MMP modulation) and inflammation and fibrosis in HSC (p38/ERK1/2/collagen I/III pathway).

(12% in the medium, with ~400 μ M of caffeine) and decaffeinated coffee increased the transcription of genes encoding antioxidant UDP glucuronosyltransferases 1A (UGT1A) family through the upregulation of aryl hydrocarbon receptor (AhR), nuclear factor erythroid-related factor 2 (Nrf2) and antioxidant or xenobiotic response elements (ARE or XRE) proteins in esophageal SCC cells (KYSE70) (Kalthoff et al., 2010). In the same study, this important antioxidant pathway was not modulated by xanthines (including caffeine, 3.4 mM) and lipids present in coffee beverages, considering that these compounds individually did not increase UGT1A family mRNA. The contribution of chlorogenic acid and trigonelline to this antioxidant effect is still to be investigated. Recently, Amigo-Benavent et al. (2017) showed that chlorogenic acid (10, 100 and 1000 μ M) reduced cell viability and proliferation of esophageal SCC cells (OE-33) in a time- and concentration-dependent manner. However, chlorogenic acid also reduced the viability and proliferation of normal fibroblasts (CCD-18Co), mainly in the highest applied dose (1000 μ M), considered supraphysiological. In non-toxic doses to normal cells (0.1–1 μ M), chlorogenic acid also increased cytotoxicity in SCC cells (Amigo-Benavent et al., 2017). In the same study, caffeine (10, 100 and 1000 μ M) showed no effect on both normal and SCC cells. In accordance with these findings, high chlorogenic acid doses (0.1 to 10 mM) decreased the viability of oral SCC cells (HSC-2) in a concentration-dependent manner. Chlorogenic acid-treated cells displayed clear DNA fragmentation and nuclear condensation, typical features of apoptosis that were correlated with increased levels of the caspase cleavage product of cytokeratin 18 (Jiang et al., 2000). Molecular insights into the antiproliferative or proapoptotic effects of coffee compounds on SCC cell lines are still missing.

Caffeine showed beneficial effects on both well-differentiated (SGC-7901) poorly differentiated (MGC-803) human gastric AC cell lines. High doses of caffeine (0.5, 1, 2, 4 and 8 mM) showed similar results on both cell lines, reducing cell viability, inhibiting cell cycle progression and increasing apoptosis on a concentration-dependent way (Liu et al., 2017). Since caffeine treatment above 2 mM also exerted proapoptotic effects on normal gastric mucosa cells, the 0–2 mM range was selected for further analysis. In keeping with the cell cycle arrest effects, caffeine increased p21 protein production in poorly differentiated AC cells whereas decreasing cyclin D1 protein levels in both types of cell lines (Fig. 3A). In addition, a caffeine-mediated positive modulation of caspase 3 and 9 axis was suggested, corroborating with the pro-apoptotic effect in AC cells. Indeed, caffeine reduced vascular endothelial growth factor A (VEGFA) and mammalian target of rapamycin kinase (MTOR) expression, while it increased TP53 mRNA expression (Fig. 3A). In addition, caffeine decreased anti-apoptotic Bcl-2 protein quantities, but enhanced expression of pro-apoptotic Bax, cytochrome *c* and cleaved caspase-3 and 9 proteins (Fig. 3A). Notably, both protein and gene expression signatures in this proapoptotic axis were sustained even 24 h after caffeine withdrawal in the cell culture medium. Hence, it was suggested that caffeine may modulate the expression of microRNAs (miRs) involved in this pathway, yet further elucidation is warranted. Notably, chlorogenic acid exposure showed similar results as caffeine on increasing apoptosis and hindering cell cycle progression accompanied by the upregulation of Bax and caspase 3 gene expression in AC cells (Jafari, Zargar, Delnavazi, & Yassa, 2018) (Fig. 3A). These findings suggest that caffeine and chlorogenic acid share the induction of apoptosis as a mechanism for abrogating AC.

5.2. Colon cancer cells

In contrast to the upper digestive tract and liver cancer *in vitro* bioassays, literature is loaded with findings comparing the effects of coffee brews versus selected coffee compounds on CRC cell lines, as well as the effects of the most important compounds individually. Findings suggest that the combination of compounds in both caffeinated and decaffeinated coffee beverages may display the most pronounced antioxidant and antiproliferative effects on CRC cell lines (Fig. 3B). The

exposure to a common caffeinated coffee brew (at 0.31, 0.63, 1.25, 2.5, 3.75 or 5.0%) decreased both mRNA and protein expression of K-RAS in Caco-2 cells in a concentration-dependent manner through the upregulation of miR-30c and miR-96 expression (Fig. 3B), which are direct negative regulators of this oncogene (Nakayama et al., 2017). KRAS activating mutations are commonly found in CRC cases, exerting essential roles in the sustained proliferation of tumor cells (Vaughn, ZoBell, Furtado, Baker, & Samowitz, 2011). Coffee also reduced epidermal growth factor (EGF)-induced activation of phosphorylated protein kinase B (Akt) and ERK in these cells, reinforcing the negative modulation of K-RAS signaling (Fig. 3B). Of note, in the same study, most of the isolated components, including caffeic and chlorogenic acids and caffeine (100 μ M for 24 h), did not modulate K-RAS protein expression, except for a slight reduction observed in trigonelline treatment (100 μ M for 24 h) (Nakayama et al., 2017) (Fig. 3B). The authors also observed that the reduction in K-RAS protein expression was inversely correlated with the roasting of the beans used in brew preparation. These findings suggest that K-RAS-mediated malignant growth of CRC cells may be modulated by a sort of interaction between coffee compounds, especially those emerging during the roasting of the beans (Nakayama et al., 2017). Moreover, decaffeinated coffee exposure (5, 10, 20 and 40 μ g/mL) showed decreased mitogen-activated protein kinase (MEK1) and T-LAK cell-originated protein kinase (TOPK) activities, which are upstream activators of ERK (Fig. 3B), in a concentration dependent-manner, whereas chlorogenic acid displayed weak attenuation of TOPK in CT-26 cell line (Kang et al., 2011). In addition, caffeic acid showed stronger effects than chlorogenic acid, but the whole phenolic fraction of decaffeinated coffee, as well as interaction between these compounds, should be considered for explaining this effect. *In vitro* results of Nakayama et al. (2017) and Kang et al. (2011) are partially in line with clinical findings showing reduced ERK protein expression in colonic tissue of CRC patients that frequently consumed both caffeinated and decaffeinated coffee beverages (Kang et al., 2011).

Complex effects are also observed regarding the potential antioxidant activity of coffee brews. As addressed in SCC cells (KYSE70), Kalthoff et al. (2010) demonstrated that caffeinated and decaffeinated coffee exposures, (both 12% in the medium) similarly upregulated glucuronidation (UGT1A-related genes) via AhR/XRE and Nrf2/ARE induction in Caco-2 cells (Fig. 3B), an effect that was not accomplished by caffeine alone (~3.4 mM) and by cafestol combined with kahweol. Indeed, there is accumulating evidence regarding the positive modulation of AhR/Nrf2 pathways by different coffee brews on Caco-2 cells (Venkatasubramanian et al., 2017; Yazheng & Kitts, 2012). Findings from Bakuradze et al. (2010) suggest that the cellular antioxidant effectiveness of coffee beverages may be linked to the chlorogenic acid and *N*-methylpyridinium-derived (including trigonelline) fractions, present in both caffeinated and decaffeinated coffee brews. According to these authors, tert-butyl hydroperoxide (t-BOOH)-induced reactive oxygen species (ROS) levels were reduced in HT-29 cells by chlorogenic acid isomer 5-CQA (30 μ M), and mainly by chlorogenic acid- (1, 5, 10, 50 and 100 μ g/mL) or *N*-methylpyridinium-rich (1, 5 and 100 μ g/mL) fractions extracted from coffee. Interestingly, only the 5-CQA (most 1, 3, 10 and 30 μ M) and chlorogenic acid-rich fraction (1, 10 and 100 μ g/mL) of coffee increased the protein expression of ARE-dependent enzymes, such as NAD(P)H quinone dehydrogenase 1 (NQO1) and glutamate-cysteine ligase catalytic subunit (GCLC) (Fig. 3B). Recently, Liang and Kitts (2018) reinforced the antioxidant role of chlorogenic acid isomers (including the abundant 3-, 4- and 5-CQA) on phorbol-12-myristate-13-acetate or interferon- γ (IFN γ)-induced inflammation in Caco-2 cells, demonstrating that high concentrations (1 and 2 mM) of the most abundant isomers similarly increased Nrf2 protein expression (Fig. 3B), and 5-CQA upregulated gene expression of Nrf2 and its glutathione-related target genes (glutathione peroxidase 2, glutathione synthetase and glutathione-disulfide reductase). All isomers (0.2, 1.0 and 20 mM) similarly reduced interleukin-8 (IL-8) protein levels in a concentration-dependent manner. Shin et al. (2015) demonstrated that

chlorogenic acid not only decreased IL-8 secretion but also down-regulated mRNA and transcriptional activity of this proinflammatory mediator in Caco-2 cells (Fig. 3B). In addition to these effects, chlorogenic acid treatment (100–1000 μ M) decreased cell viability, increased cytotoxicity and induced S-phase cell-cycle arrest in a concentration-dependent manner, which was accompanied by the increased protein expression of the pro-apoptotic caspase-3 (Ekbatan, Li, Ghorbani, Azadi, & Kubow, 2018). In the same study, an equimolar mix of chlorogenic, caffeic acids and the selected microbial metabolites 3-phenylpropionic and benzoic acids in low concentrations showed more prominent results than isolated chlorogenic or caffeic acid individually in high concentrations (both at 500 and 1000 μ M), indicating that these compounds may function together on abrogating CRC.

Although caffeine is not likely to be involved in the antioxidant effects of coffee brews in CRC cell lines, low concentrations of this xanthine (10 μ M) modulated master regulators of tumor angiogenesis and migration in HT-29 cells under hypoxic conditions, a common feature of malignant tumors. This xanthine reduced the protein expression of (1) hypoxia-inducible factor-1 α (HIF-1 α) transcription factor and its downstream target VEGF via antagonism of adenosine A₃ receptor, and (2) IL-8 through blockade of adenosine A_{2B} receptor (Merighi et al., 2007) (Fig. 3B). Moreover, when combined with adenovirus-mediated transfer of phosphatase and tensin homolog (Ad-PTEN) treatment, caffeine administration attenuated growth and induced apoptosis through downregulation of Akt and modulation of p44/42 MAPK pathways in HCT116 cells in a synergistic manner, not exerting the same effects in normal CCD-18Co colon fibroblasts (Saito et al., 2003). Therefore, the authors proposed the combined treatment with Ad-PTEN and caffeine as a potential therapeutic alternative for CRC (Saito et al., 2003).

5.3. Liver cancer and hepatic stellate cells

There is a single report on the effects of whole brewed caffeinated (12% in the cell culture medium, with ~400 μ M of caffeine) and decaffeinated coffee on HCC cells (HepG2) (Kalthoff et al., 2010). In a similar manner to SCC (KYSE70) and CRC (Caco-2) cell lines, both types of coffee upregulated UGT1A-induced glucuronidation by AhR signaling and Nrf2 binding to ARE and XRE (Fig. 4A). Again, this antioxidant effect was not related to the xanthine fraction of coffee, since the treatment with caffeine (3.4 mM) and other coffee xanthines individually did not increase UGT1A expression in HepG2 cells (Kalthoff et al., 2010). The study did not investigate whether other common coffee compounds, like chlorogenic acid and trigonelline, are implicated in this potential antioxidant effect of brewed coffee. Nonetheless, previous findings suggest that this effect in HCC cells is related to the hydroxycinnamic acid fraction of the beverage, including chlorogenic acid (Baeza et al., 2014). Low concentrations of chlorogenic acid (1, 10 and 20 μ M) decreased t-BOOH-induced cytotoxicity, lipid peroxidation and protein oxidation in HepG2 cells by restoring reduced glutathione levels (GSH) and glutathione reductase (GR) and peroxidase (GSH-Px) activities (Fig. 4A), which are endogenous antioxidant agents modulated by the ARE/Nrf2 axis. In the same study, caffeine administration did not alter both oxidative stress and the antioxidant response. In addition, high concentrations of chlorogenic acid (0.5 and 1.0 mM) decreased cell viability and induced S-phase arrest in HepG2 cells in a dose-dependent manner (Yan, Liu, Hou, Dong, & Li, 2017). This antiproliferative effect was attributed to the down-regulation of active ERK1/2 protein expression (Fig. 4A). Furthermore, chlorogenic acid decreased the matrix metalloproteinase (MMP)-2/tissue inhibitor of metalloproteinase (TIMP)-2 ratio, suggesting an attenuation in MMP-2 activity, which plays a relevant role in extracellular matrix (ECM) degradation and remodeling essential for tissue invasion and metastasis (Yan et al., 2017) (Fig. 4A).

Caffeine alone (200, 400 and 600 μ M) reduced cell viability, invasion, and migration of two different HCC cell lines (HepG2 and Huh7)

in a concentration-dependent manner. These effects were associated with the downregulation of VEGF and Akt and suggest an abrogation of downstream VEGF and Akt-mediated signaling. In this respect, caffeine-treated HCC cells presented a reduction in the expression of MMP-2 and -9 proteins, both related to ECM degradation and remodeling, and reduced protein expression of Snail and N-cadherin, but increased expression of E-cadherin, which are involved in epithelial-mesenchymal transition (EMT) (Dong et al., 2015) (Fig. 4A). Concerning Akt signaling, caffeine-mediated (1.0, 1.5 and 2.0 mM) reduction of Akt phosphorylation was implied in the decrease of cell proliferation of HCC cells (SK-Hep-1) as well (Edling, Selvaggi, Ghonaim, Maffucci, & Falasca, 2014) (Fig. 4A). Caffeine has shown beneficial effects on abrogating pro-inflammatory signaling mediated by Hepatitis B virus x protein (HBx) in HepG2 cells (Ma, Wang, & Tang, 2015). This xanthine significantly reduced prostaglandin E₂ (PGE₂) levels by stimulating the protein expression of peroxisome proliferator-activated receptor gamma (PPAR- γ), which is a negative regulator of PGE₂ synthesis (Fig. 4A). The caffeine-mediated increase in PPAR γ is proposed to subsequently block protein expression and/or transcriptional activity of early growth response protein-1 (EGR1) and microsomal prostaglandin E synthase-1 (mPGES-1), ultimately leading to PGE₂ synthesis (Ma, Wang, & Tang, 2015). Interestingly, the treatment with trigonelline alone (50, 75 and 100 μ M) also decreased migration of HCC cells (Hep3B) in a concentration-dependent manner without altering cell viability by reducing the protein levels of protein kinase C α (PKC α) and mRNA levels of MMP-7 (Liao et al., 2015) (Fig. 4A). Recently, in a palmitic acid (PA)-induced model fatty liver disease in HepG2 cells, it was shown that trigonelline (50 μ M) downregulated the protein expression of sterol regulatory element-binding protein 1 (SREBP1) and PPAR- γ , suggesting decreased PA-induced lipotoxicity. Furthermore, trigonelline was able to enhance the protein expression of Beclin-1, a positive regulator of autophagy and apoptosis (Sharma, Lone, Knott, Hassan, & Abdullah, 2018) (Fig. 4A).

In addition to HCC cells, activated HSC, which produce collagen type I and III, are also regarded as key therapeutic targets for fibrosis and cirrhosis, the major risk factor for HCC development. Individually, caffeine treatment decreased the viability in a time and concentration-dependent manner and reduced the activation of human (LX-2) and rat (HSC-T6) HSCs by exerting antifibrotic and proapoptotic activities (Li et al., 2017; Shim et al., 2013; Wang et al., 2014) (Fig. 4B). This xanthine (4 mM) appears to block 2 distinct adenosine A_{2A} receptor-mediated signaling pathways: (1) cAMP/PKA/SRC/ERK1/2 activation leading to procollagen type I synthesis, and (2) p38/MAPK activation leading to procollagen type III production (Wang et al., 2014). In addition, Li et al. (2017) recently showed that caffeine (20 mM) induces inositol-requiring enzyme 1 alpha (IRE1- α)-mediated endoplasmic reticulum stress, with subsequent increases in autophagy (p62 and LC3II accumulation) and apoptosis. Similar to caffeine, chlorogenic acid diminishes HSC activation. This antioxidant molecule (~25, 50 and 100 μ M) attenuated oxidative stress in LX-2 and HSC-T6 cells, thus reducing the activation of the p38/ERK1/2/collagen I/III pathway and abrogating the redox-sensitive and profibrogenic nuclear factor κ B (NF- κ B) pathway as well (Shi et al., 2013, 2016). Moreover, chlorogenic acid exposure (~55, 110 and 220 μ M) upregulated the antifibrogenic Smad7/MMP-9 pathway by decreasing miR-21 expression, which is a negative regulator of Smad7 (Yang et al., 2017) (Fig. 4B). No data are available on the effects of whole decaffeinated and caffeinated coffee and trigonelline in HSC cells.

Although coffee compounds are usually administered individually, these data shed light onto common molecular targets of these compounds in both HCC (MMP modulation in migration and invasion activities) and HSC (p38/ERK1/2/collagen I/III pathway modulation in inflammation) (Fig. 4). These shared molecular targets and pathways suggest that the combination of highly bioavailable coffee compounds may underlie the protective effects of coffee consumption against fibrosis/cirrhosis and/or HCC, as suggested in caffeinated coffee data

from epidemiological studies. Nonetheless, monolayer *in vitro* models lack the complexity of the fibrosis or cirrhosis-associated hepatocarcinogenesis microenvironment. The use of complex *in vitro* models, as 3D HCC and HSC spheroids (Abu-Absi, Hansen, & Hu, 2004), is needed to confirm these molecular beneficial effects of the combination of bioactive coffee compounds.

6. *In vivo* findings

Evidence stemming from most *in vivo* studies predominantly demonstrate anti-carcinogenic effects of coffee brews or major bioavailable coffee compounds on tongue, esophagus, stomach, colon, and liver carcinogenesis preclinical bioassays, in keeping with the epidemiological and *in vitro* findings. Based on the available data, some critical points can be raised that might be helpful in designing future *in vivo* studies. Firstly, the dosages used in most studies do not usually mimic human coffee consumption and bioavailability of coffee compounds, and supraphysiological approaches are frequent. Allometric calculation approaches should be applied to suitably translate the dosage from one species to the another. The well-accepted Human Equivalent Dose (HED) calculation considers the body surface area (BSA) normalization for dose translation. BSA correlates well with important parameters of both rodent (rats and mice) and humans, such as basal metabolism, oxygen utilization and renal function (Reagan-Shaw, Nihal, & Ahmad, 2008). Thus, considering the data on average caffeine consumption from coffee in the USA, the 109.4–271 mg/day [1.82–4.52 mg/Kg body weight (b.wt.)/day in 60 Kg adults] range would correspond to 22.5–55.8 and 11.4–28.3 mg/Kg b.wt. doses in mice and rats, respectively. Secondly, several studies evaluated the anti-carcinogenic effects of the paper-filtered cafestol and kahweol lipids (Fig. 2), and these findings will not be included in this section. The main effects of coffee and most bioavailable coffee compounds (caffeine, chlorogenic acid, and trigonelline) on experimental tongue/esophagus, stomach, colon, and liver carcinogenesis are discussed in this section and summarized in Tables 4–6. Details on the experimental procedures (*i.e.*, carcinogen, dose, concentration, regimen of treatment, etc.) and the main effects on the endpoint lesions or cellular processes are also presented. In general, these studies focus on changes in incidence and/or multiplicity of preneoplastic and neoplastic lesions, with few data on potential related mechanisms. Indeed, the most prominent mechanistic findings come from hepatocarcinogenesis models or bioassays mimicking HCC main risk conditions, such as fibrosis and NAFLD. Therefore, the main pathways and biological processes commonly modulated by whole caffeinated coffee, decaffeinated coffee, and isolated compounds during these liver rodent bioassays are depicted in Fig. 5.

6.1. Upper digestive tract carcinogenesis bioassays

7,12-dimethylbenz[*a*]anthracene (DMBA), 4-nitroquinoline-1-oxide (4-NQO), diethylnitrosamine (DEN) and *N*-nitrosomethylbenzylamine (NMBA) are known carcinogens used for the induction of SCC in the oral cavity (tongue and buccal pouch) and esophagus (Nagini & Kowshik, 2016; Sallet, Zilberstein, Andreollo, Eshkenazy, & Pajecski, 2002; Tang, Knudsen, Bemis, Tickoo, & Gudas, 2004) while *N*-methyl-*N'*-nitro-*N*-nitrosoguanidine (MNNG) and *N*-methyl-*N*-nitrosourea (MNU) are used for the induction of SCC in forestomach and AC in glandular stomach of rodents (Tsukamoto, Mizoshita, & Tatematsu, 2007; Yu, Yang, & Nam, 2014). Due to their extensive similarities to human cancer, these animal models are usually applied to investigate multistage carcinogenesis and to assess the efficacy of chemopreventive agents (Nagini & Kowshik, 2016; Tsukamoto et al., 2007). A few studies on the effects of coffee, caffeine or chlorogenic acid on oral, esophageal and gastric carcinogenesis have been published (Table 4). The literature lacks animal studies investigating the effects of trigonelline on upper digestive tract carcinogenesis.

Miller, Formby, Rivera-Hidalgo, and Wright (1988) showed that

dietary supplementation with coffee bean powder is implicated in the attenuation of oral SCC development in a DMBA-induced buccal pouch painting hamster model, displaying a marked reduction (11-fold) in SCC mass (Table 4). Using a similar model, Saroja, Balasenthil, Ramachandran, and Nagini (2001) described that common coffee administration exerted no preventive effect on SCC development, resulting in increased mean tumor volume (Table 4). In the same study, common coffee treatment reduced lipid peroxidation and increased GSH levels and GSH-Px activity in oral pouch mucosa. The exact molecular mechanisms of these contrasting effects need further clarification. In a 4-NQO-induced tongue carcinogenesis model, Tanaka et al. (1993) demonstrated that the consumption of chlorogenic acid during the initiation step significantly reduces the incidence of squamous cell hyperplasia, moderate and severe dysplasia and total incidence of papillomas and SCC. In addition, chlorogenic acid reduced cell replication in non-neoplastic surrounding squamous epithelium. In a DEN-induced esophageal carcinogenesis model, Balansky, Blagoeva, Mircheva, and De Flora (1994) observed that caffeine intake does not interfere with the development of esophagus squamous cell papillomas in female BD6 rats. As in animal studies on oral and esophageal carcinogenesis, there are few animal studies on the effects of caffeine or chlorogenic acid on gastric carcinogenesis (Table 4). Nishikawa et al. (1995) observed that caffeine treatment reduced the incidence of pyloric AC and lipid hydroperoxide levels in the gastric mucosa of male Wistar rats submitted to MNNG and NaCl-induced carcinogenesis. Ultimately, the chlorogenic acid treatment led to a reduction of the incidence of MNU-induced adenomatous hyperplasia and AC, as well as to a decrease in proliferating cell nuclear antigen (PCNA) labeling indexes in non-neoplastic glandular areas (Shimizu et al., 1999). As could be observed in epidemiological studies, results from animal models also lack sufficiently strong evidence of beneficial effects of coffee and its main components on upper digestive tract carcinogenesis. Thus, these few findings indicate the need for additional animal studies to convincingly prove the beneficial effects and potential interactions of coffee bioactive compounds on oral and esophageal SCC and gastric AC development.

6.2. Colon carcinogenesis models

1,2-dimethylhydrazine hydrochloride (DMH) and its metabolites azoxymethane (AOM), methylazoymethanol (MAM) or MNNG and heterocyclic amines, such as 2-amino-1-methyl-6-phenylimidazo[4,5-*b*]pyridine (PhIP), are widely applied chemicals that promote the development of both preneoplastic (non-dysplastic and dysplastic aberrant crypt foci [ACF]) and neoplastic (adenomas and adenocarcinomas) lesions in the colon of rodents (Ward & Treuting, 2014). These lesions are mainly detected in the middle and distal colon and used as putative endpoints in short and medium-term rodent bioassays, enabling the evaluation of potential environmental and dietary factors or preventive compounds on different stages of colon carcinogenesis (Ward & Treuting, 2014).

Although epidemiological data show protective effects for both caffeinated and decaffeinated coffee consumption at higher levels, experimental animal data comparing these different types of coffee or isolated compounds are limited. Recently, Soares, Kannen, Jordão Junior, and Garcia (2018) showed that caffeinated coffee intake, but not decaffeinated coffee or caffeine, counteracted the development of dysplastic ACF during the initial stages of MNNG-induced colon carcinogenesis (Table 4). Rather than decaffeinated coffee, caffeinated coffee-treated rats also displayed fewer ACF positive for metallothionein, which is proposed as a stem cell mutation marker (Soares et al., 2018). In the same study, all treatments reduced DNA damage (phosphorylate H2A histone family/member X, γ -H2AX) and only caffeinated coffee and caffeine diminished proinflammatory cyclooxygenase 2 (COX-2) expression in colonic mucosa. The authors suggested that the anti-inflammatory and antigenotoxic effects exerted by caffeinated

Table 4
Review of the main studies on the effects of whole coffee or highly bioavailable isolated coffee compounds on oral, esophageal, gastric and colon carcinogenesis/colitis rodent models.

Carcinogen/Procedure (dose, exposure)	Animal	Coffee or specific compound	Dose/Concentration/Regimen	Before (1), during (2) or after (3) carcinogen exposure/model establishment	Main findings	Reference
<i>Oral cavity or esophagus</i>						
DMBA (0.5%, buccal pouch painting, 3 × /week for 16.5 weeks)	Female Syrian golden hamsters	Coffee powder	200 g/Kg in diet for 16.5 weeks	1	● Reduced SCC mass	Miller et al., 1988
DMBA (0.5%, buccal pouch painting, 3 × /week for 14 weeks)	Male Syrian golden hamsters	Common coffee	3 × /week, on alternate days to DMBA, i.g., for 14 weeks	1	● Increased SCC volume	Saroja et al., 2001
4-NQO, (20 mg/L in drinking water for 5 weeks)	Male F344 rats	Chlorogenic acid	500 mg/Kg in diet for 7 weeks	1, 2 and 3	● Reduced incidence of tongue hyperplasia and moderate/severe dysplasia	Tanaka et al., 1993
DEN (80 mg/kg b.wt., i.p., 1 × /week for 7 or 9 weeks)	Female BD6 rats	Caffeine	0.3 or 0.6 mg/mL in drinking water during 8–12 or 12–24 weeks	1 and 2 or 3	● Reduced incidence of tongue tumors (papillomas plus SCC)	
					● No effects on esophageal papilloma development	Balansky et al., 1994
<i>Stomach</i>						
MNNG (100 mg/L in drinking water for 8 weeks) and NaCl (50 g/Kg diet for 8 or 40 weeks)	Male Wistar rats	Caffeine	2.5 mg/mL in drinking water for 32 weeks	3	● Reduced incidence of pyloric AC	Nishikawa et al., 1995
MNU (400 mg/L) in drinking water for 12 weeks	Male F344 rats	Chlorogenic acid	250 or 500 mg/Kg in diet for 22 weeks	3	● Reduced incidence of adenomatous hyperplasia (500 mg/Kg)	Shimizu et al., 1999
					● Reduced incidence of gastric AC (250 mg/Kg)	
<i>Colon</i>						
MNNG, (2.5 mg/exposure, i.r., 2 × /week for 2 weeks)	Male Wistar rats	Caffeinated or decaffeinated coffee (instant powder) and caffeine	Coffee and decaffeinated at 200 mg/kg b.wt./day; caffeine at 5.4 mg/kg b.wt./day. All i.g. for 4 weeks	3	● Only coffee reduced dysplastic ACF number/mm ²	Soares et al., 2018
DMH (40 mg/Kg b.wt., s.c., 2 × /week for 2 weeks)	Male Wistar rats	Common coffee (commercial or organic)	Infusions: 5, 10 or 20 g of powder in 100 mL water/Kg diet for 12 weeks; Powder: 40 g /Kg diet for 12 weeks	1, 2 and 3	● No effects on conventional or mucin-depleted ACF development	Carvalho et al., 2011
–	<i>Apc</i> ^{Min/+} mice	Common coffee	Filtered or unfiltered coffee at 10 mg/Kg diet for 14 weeks	–	● No effects on colonic tumor development	Oikarinen et al., 2007
CT-26 xenograft model (i.v., single dose)	Male Balb/C mice	Decaffeinated coffee and chlorogenic acid	Decaffeinated coffee at 0.5, 1.0 and 2.0 g/Kg b.wt./day; chlorogenic acid at 0.1, 0.5 and 1.0 g/Kg b.wt./day. All i.v. for 2 weeks.	2 and 3	● Both reduced the number of CRC xenograft metastatic tumors in the lung	Kang et al., 2011
PhIP (100 mg/Kg b.wt., i.g., every other day for 2 weeks)	Male F344 rats	Caffeine	0.50 mg/mL in drinking water for 11 weeks	3	● Reduced number of total ACF	Carter et al., 2007
					● Reduced number of small ACF (< 4 crypts)	
PhIP (400 mg/Kg diet for 10 weeks)	Male F344 rats	Caffeine	0.01, 0.1 or 1.0 mg/mL in drinking water for 10 weeks	2	● Increased number of total ACF (1 mg/mL)	Tsuda et al., 1999
PhIP (200 mg/Kg in diet for 54 weeks)	Female F344/DuCrj rats	Caffeine	1.0 mg/mL in drinking water for 54 weeks	2	● Increased incidence of adenomas and adenocarcinomas;	Hagiwara et al., 1999
					● Increased multiplicity of tumors (all)	
DSS (35 mg/mL in drinking water for 5 days)	Male C57BL/6 mice	Caffeine	~0.49 mg/mL in drinking water for 18 days	1, 2 and 3	● Decreased colitis histological score	Lee et al., 2014
PhIP (three cycles of 50 mg/Kg b.wt./day, i.g. for 2 weeks) and high fat diet (three cycles for 4 weeks), in alternated cycles.	Male F344 rats	Caffeine	0.65 mg/mL in drinking water for 34 weeks	3	● Increased tumor incidence and volume	Wang et al., 2008
AOM (15 mg/Kg b.wt., s.c. 1 × /week for 3 weeks)	Male F344 rats	Chlorogenic acid	250 mg/Kg diet for 5 or 32 weeks	2 (5-week-long) or 3 (32-week-long)	● Reduced tumor multiplicity (5-week-long)	Matsunaga et al., 2002
AOM (15 mg/Kg b.wt., s.c., 1 × /week, for 3 weeks)	Male F344 rats	Chlorogenic acid	250 mg/Kg diet for 6 or 12 weeks	3	● Reduced number of total ACF;	Morishita et al., 1997
					● Reduced number of small ACF (< 3 crypts)	

(continued on next page)

Table 4 (continued)

Carcinogen/Procedure (dose, exposure)	Animal	Coffee or specific compound	Dose/Concentration/Regimen	Before (1), during (2) or after (3) carcinogen exposure/model establishment	Main findings	Reference
AOM (10 mg/kg, b.wt., i.p. 1 × /week, for 6 weeks)	Male A/J mice	Chlorogenic acid	100 or 1000 mg/kg in diet for 20 weeks	1, 2 and 3	<ul style="list-style-type: none"> • No effects on ACF and tumor development 	Park et al., 2010
DSS (25 mg/mL in drinking water for 8 days)	Female C57BL/6 mice	Chlorogenic acid	~0.35 mg/mL in drinking water for 15 days	2 and 3	<ul style="list-style-type: none"> • Decreased colitis activity index 	Zhang et al., 2017
DSS (30 mg/mL in drinking water for 8 days)	Female C57BL/6 mice	Chlorogenic acid	~0.35 mg/mL in drinking water for 15 days	2 and 3	<ul style="list-style-type: none"> • Decreased colitis histological score 	Shin et al., 2015

“.” = not applicable; DMBA = 7,12-dimethylbenz[*a*]anthracene; 4-NQO = 4-nitroquinoline-1-oxide; DEN = diethylnitrosamine; MNNG = *N*-methyl-*N*'-nitro-*N*-nitrosoguanidine; MNU = *N*-methyl-*N*-nitrosourea; DMH = 1,2-dimethylhydrazine; PhIP = 2-amino-1-methyl-6-phenylimidazo[4,5-*b*]pyridine; DSS = dextran sulphate sodium; i.g. = intragastrical route; i.r. = intrarectal route; s.c. = subcutaneous route; i.p. = intraperitoneal route. SCC = squamous cell carcinoma; ACF = aberrant crypt foci; AC = aberrant crypt.

coffee may be implicated in reducing ACF development. In keeping with these findings, Silva et al. (2014) demonstrated that the administration of common organic or commercial caffeinated coffee brews diminished DMH-induced mutagenicity (micronuclei) and toxicity (apoptotic cells) in colonocytes of male Swiss mice. Interestingly, the most pronounced results were observed in infusions prepared with organic coffee powder, despite presenting similar caffeine, chlorogenic acid, and trigonelline levels compared to the commercial preparation. The same research group reported that although similar organic and commercial common coffee brews reduced malondialdehyde (MDA) levels in the liver, the major organ responsible for DMH metabolism (Ward & Treuting, 2014), these treatments did not modulate the development of conventional or high-risk mucin-depleted ACF (Carvalho et al., 2011) (Table 4). Besides chemically-induced models, the dietary exposure to common caffeinated coffee did not exert antitumoral effects in multiple intestinal neoplasia (*Apc*^{Min/+}) mice and did not alter β -catenin and cyclin D1 protein levels in colonic adenomas either (Oikarinen, Erlund, & Mutanen, 2007) (Table 4). In a xenograft mice model using CT-26 CRC cell line, both decaffeinated coffee and chlorogenic acid treatments showed similar results on reducing the number of metastatic CT-26 tumors in the lung (Table 4), with stronger reductions at higher doses (Kang et al., 2011). This effect was possibly accomplished by reductions in COX-2 protein expression, corroborating with findings from an AOM-induced model (Soares et al., 2018). Additionally, reduced activity of matrix MMP-2 and MMP-9 and ERK phosphorylation was also observed, which are directly involved in the metastatic activity of CRC cells. Results were slightly stronger in decaffeinated coffee than chlorogenic acid treatment and the negative regulation of the ERK pathway corroborates with clinical and *in vitro* findings (Fig. 3B).

Concerning the most abundant coffee compounds, caffeine treatment right after PhIP exposure resulted in a significant reduction in the number of small ACF (< 4 aberrant crypts) and the total number of ACF (Carter et al., 2007) (Table 4). Despite not altering cleaved caspase-3 protein expression in colonocytes, this protective effect was accompanied by a significant reduction in cell proliferation index in the colonic crypts. In contrast, the co-administration of caffeine and PhIP resulted in a significant increase in colonic ACF development associated with a 2-fold enhancement in hepatic CYP1A2 protein expression in male rats (Tsuda et al., 1999) (Table 4). Similar findings were observed in a short-term study wherein Takeshita, Ogawa, Asamoto, and Shirai (2003) showed that caffeine intake simultaneously to PhIP exposure increased PhIP-induced DNA adduct formation as well as hepatic CYP1A2 mRNA levels in female rats. However, no alteration in cell proliferation, apoptosis or DNA repair enzymes were detected in the colon of PhIP- and caffeine-treated group. In addition to ACF, Hagiwara et al. (1999) demonstrated that caffeine intake during PhIP exposure significantly increases the incidence and multiplicity of colonic neoplastic lesions in female rats (Table 4). In addition to the increase in tumor incidence and volume, caffeine intake after cycles of PhIP exposure and HF diet intake increased the frequency of β -catenin mutations in colon tumors (79%, codon 34) compared to PhIP- and HF-exposed counterparts (36%, mainly in codons 32 and 34). Taken together, these findings suggest that caffeine exposure may modulate carcinogen metabolizing enzymes (as the universal CYP1A2) and, thus, the complex protective or promotional effects may depend on the time of administration of this xanthine (i.e., after, during and/or before carcinogen exposure) (Table 4). Other effects and mechanisms of caffeine on colon carcinogenesis, not considering the modification of carcinogen metabolism, should be evaluated in further studies using well-established transgenic and/or xenograft rodent models. Different from caffeine, most rodent bioassays point to a protective effect of chlorogenic acid on different stages of colon carcinogenesis. The administration of this polyphenol after AOM initiation resulted in a marked 43%–51% reduction in the total number of preneoplastic ACF in male rats (Morishita et al., 1997). In contrast, Park, Davis, Liang, Rosenberg, and

Table 5
Review of the main studies on the effects of whole caffeinated/decaffeinated coffee or highly bioavailable isolated coffee compounds on hepatocarcinogenesis, fibrosis or NAFLD rodent models.

Carcinogen/Procedure (dose, time)	Animal/ Liver Disease	Coffee or coffee compound	Dose/Concentration/Regimen	Before (1), during (2) or after (3) model establishment	Main findings	Reference
DEN (single, 200 mg/Kg b.wt., i.p.) and CCl ₄ (1 × /week, 0.5–1.0 mL/Kg b.wt., gavage, for 21 weeks)	Male Wistar rats, Fibrosis-associated Hepatocarcinogenesis	Common coffee or caffeine	Common coffee with 1.00, 0.51 and 0.41 mg/mL of caffeine, trigonelline and chlorogenic acid, respectively. Caffeine at 1 mg/mL. All in drinking water for 23 weeks.	2	<ul style="list-style-type: none"> Only caffeine reduced the size and area of GST-P+ preneoplastic lesions and the number of neoplastic lesions; Both reduced collagen area and collagen I mRNA; only common coffee reduced collagen III mRNA Only common coffee reduced the number of GST-P+ preneoplastic lesions All treatments reduced collagen area 	Furtado et al., 2014
TAA (2 × /week, 200 mg/Kg b.wt., i.p., for 8 weeks)	Male Wistar rats, Fibrosis-associated Hepatocarcinogenesis	Common coffee, decaffeinated coffee or caffeine	Common coffee containing with 1.00 and 0.41 mg/mL of caffeine and chlorogenic acid, respectively. Decaffeinated coffee with 0.09 and 0.30 mg/mL of caffeine and 5-CQA, respectively. Caffeine 1 mg/mL. All in drinking water for 8 weeks.	2	<ul style="list-style-type: none"> Reduced size, area and number of total, persistent and remodeling G6Pase- preneoplastic lesions 	Furtado et al., 2012
DEN (single, 200 mg/Kg b.wt., i.p.) followed by 2-AAF (1 × /day, 20 mg/Kg b.wt., gavage, for 6 days) and PH	Male Wistar rats, Hepatocarcinogenesis	Common coffee	Lyophilized, 15 mg/Kg diet for ~13 weeks	1, 2 and 3	<ul style="list-style-type: none"> Reduced number of small GST-P+ preneoplastic lesions 	Silva-Oliveira et al., 2010
-	Long Evans Cinnamon rats, Inflammation associated Hepatocarcinogenesis	Common coffee	Common coffee with ~0.5 and ~0.09 mg/mL of caffeine and chlorogenic acid, respectively in drinking water for 27 weeks	-	<ul style="list-style-type: none"> Both common and decaffeinated coffee reduced the number of GST-P+ preneoplastic lesions; Only common coffee reduced the area of GST-P+ preneoplastic lesions 	Katayama et al., 2014
AFB1 (single, 0.75 mg/Kg b.wt., i.p.)	Male Wistar rats, Hepatocarcinogenesis	Common coffee or decaffeinated coffee	Common coffee with 0.045–0.065 mg/mL of caffeine. Decaffeinated coffee with 0.003 mg/mL of caffeine. Both in 25% and 50% solutions in drinking water for 8 days	1	<ul style="list-style-type: none"> Only common coffee and caffeine reduced collagen I protein and mRNA 	Arauz et al., 2017
BDL procedure	Male Wistar rats, Fibrosis	Common coffee, decaffeinated coffee or caffeine	Common coffee and decaffeinated coffee at 200 mg/Kg b.wt., caffeine at 50 mg/Kg b.wt. i.g., or 4 weeks.	2 and 3	<ul style="list-style-type: none"> Both common and decaffeinated coffee reduced collagen area All treatments reduced both lipid droplets, inflammatory infiltrate and fibrosis 	Arauz et al., 2013
TAA (2 × /week, 200 mg/Kg b.wt., i.p., for 8 weeks)	Male Wistar rats, Fibrosis	Common coffee or decaffeinated coffee	Decaffeinated coffee with 2.8 and 1.5 mg/mL of polyphenols and melanoidins, respectively.	2	<ul style="list-style-type: none"> Reduced NAFLD score 	Brandt et al., 2019
HFD (for 3 months)	Male Wistar rats, NAFLD	Decaffeinated coffee, or melanoidin combination	Polyphenol combination with 2.8 mg/mL, Melanoidin combination with 1.5 mg/mL. All in drinking water for 2 months	2	<ul style="list-style-type: none"> Reduced steatosis, ballooning, inflammatory infiltration, fibrosis and liver triglycerides 	Salomone et al., 2014
Fat-, fructose- and cholesterol-rich diet for 6 weeks	Female C57BL/6 J mice, NAFLD	Decaffeinated coffee	~Freeze-dried decaffeinated coffee, 6 g/Kg diet for 6 weeks	2	<ul style="list-style-type: none"> Both treatments decreased liver triglycerides 	Takahashi et al., 2014
HFD (for 3 months)	Male Wistar rats, NAFLD	Decaffeinated coffee	1.5 mL /day in drinking water for 2 months	2	<ul style="list-style-type: none"> Only common coffee reduced liver steatosis grades and triglyceride levels 	
HFD (for 9 weeks)	Male C57BL/6 mice, NAFLD	Common coffee and decaffeinated coffee	Lyophilized common coffee, 20 g/Kg diet, with trigonelline and chlorogenic acid. Lyophilized decaffeinated coffee, 20 g/Kg diet, with 0.02, 0.18 and 0.18 g/Kg diet of caffeine, trigonelline and chlorogenic acid. Both for 9 weeks.	2		
HFD and fructose in drinking water (for 14 weeks)	Male Sprague-Dawley rats, NAFLD	Common coffee or chlorogenic acid, caffeic acid and trigonelline combination	Common coffee i.g. for 14 weeks, 24, 12 and 7 mg/rat/day of chlorogenic acid, caffeic acid and trigonelline, respectively, i.g. for 14 weeks.	2		

(continued on next page)

Table 5 (continued)

Carcinogen/Procedure (dose, time)	Animal/ Liver Disease	Coffee or coffee compound	Dose/Concentration/Regimen	Before (1), during (2) or after (3) model establishment	Main findings	Reference
“-“ = not applicable; AFB1 = Aflatoxin B1; BDL = bile duct ligation; GST-P = placental glutathione-S-transferase; G6Pase = glucose 6-phosphatase; DEN = diethylnitrosamine; CCl ₄ = carbon tetrachloride; TAA = thioacetamide; 2-AAF = 2-acetylaminofluorene; pH = partial hepatectomy; HFD = high fat diet; NAFLD = non-alcoholic fatty liver disease; i.g. = intragastric route; b.wt. = body weight; i.p. = intraperitoneal route; s.c. = subcutaneous route.						Shokouh et al., 2018

Bruno (2010) observed that chlorogenic acid intake before, during and after AOM exposure did not influence ACF and tumor development in male mice. Matsunaga et al. (2002) have also shown that chlorogenic acid treatment during AOM initiation phase reduced colon tumor multiplicity, while both exposures during initiation and post-initiation phases diminished PCNA labeling index in colonocytes in non-tumorous mucosa areas (Table 4).

Apart from the chemically-induced colon carcinogenesis models, some studies have shown similar protective effects of caffeine and chlorogenic acid on dextran sulfate sodium (DSS)-induced colitis in mice models (Lee, Low, Kamba, Llado, & Mizoguchi, 2014; Shin et al., 2015; Zhang et al., 2017) (Table 4). In patients with IBD, chronic mucosal inflammation is a key factor for carcinogenesis onset (Wang & Fang, 2014). Caffeine attenuated colitis by reducing bacterial and inflammatory cell infiltration, modulating cytokine production, including decreasing tumor necrosis factor α (TNF- α), IFN γ and IL-17F while increasing IL-10 and downregulating chitinase 3-like 1-associated Akt signaling pathway activation (Lee et al., 2014). Similarly, chlorogenic acid administration also attenuated colitis by reducing colonic infiltration of macrophages, neutrophils and CD3+ T cells, decreasing pro-inflammatory NF- κ B, IFN γ , TNF- α , IL-1b, and IL-6 signaling, and modulating colonic microbiota (i.e. decreased *Firmicutes* and *Bacteroidetes* whereas increased mucin-degrading *Akkermansia* spp.) (Shin et al., 2015; Zhang et al., 2017).

6.3. Hepatocarcinogenesis, fibrosis, cirrhosis, and NAFLD models

In the past decade, increasing evidence from rodent models of hepatocarcinogenesis or from bioassays mimicking its main risk conditions (fibrosis, cirrhosis and NASH) allowed insight into the molecular pathways modulated by common filtered caffeinated, decaffeinated coffee and the most common and bioavailable compounds (Fig. 5). In general, data from these preclinical bioassays are in line with the findings of epidemiological studies showing beneficial effects of coffee consumption, especially caffeinated coffee intake (Tables 5 and 6). Different whole common coffee treatments reduced the mean number, size and/or relative area of placental glutathione-S-transferase (GST-P)-positive or glucose 6-phosphatase (G6Pase)-negative hepatocyte foci in several rodent studies (Table 5). These foci are well-established pre-neoplastic lesions (PNL) observed in models of chemically-induced hepatocarcinogenesis, featuring the absence (as some DEN-induced models) or presence of a fibrotic or cirrhotic [as in thioacetamide (TAA) or carbon tetrachloride (CCl₄)-induced ones] background (Silva-Oliveira, Fernandes, & Moraes-Santos, 2010; Furtado et al., 2012; 2014). These classical biomarkers, especially GST-P-positive foci, are prone to neoplastic transformation or regression under adequate stimuli, enabling the *in vivo* short-term screening of modulators of chemical hepatocarcinogenesis (Tatematsu, Tsuda, Shirai, Masui, & Ito, 1987), such as coffee beverages and its isolated compounds.

Only a few studies compared the effects of different types of coffee and/or isolated compounds on the fate of these lesions. Some findings suggested that caffeinated coffee displays more pronounced attenuation of PNL development compared to decaffeinated coffee and caffeine alone (Ferk et al., 2014; Furtado et al., 2012) (Table 5), but the precise mechanisms involved in these different responses are still unclear. Nonetheless, during hepatocarcinogenesis, whole coffee and caffeine increased GSH levels without altering GST-P-positive PNL and whole coffee reduced DNA strand breaks in the liver, while decaffeinated coffee exerted none of these effects (Ferk et al., 2014; Furtado et al., 2012) (Fig. 5). Both caffeinated and decaffeinated coffee, (without altering GST-P positive PNL) coffee also increased the activity of the antioxidant UGT enzyme (Fig. 5), an effect equally addressed in HCC cells (Kalthoff et al., 2010) (Fig. 4A). In the absence of fibrosis/cirrhosis, while caffeinated coffee diminished the levels of IL-6 and TNF- α (Katayama et al., 2014), which are considered potent hepatomitogenic cytokines, and reduced the number of PCNA-positive hepatocytes

Table 6
Review of the main studies on the effects of on highly bioavailable isolated coffee compounds on hepatocarcinogenesis, fibrosis or NAFLD rodent models.

Carcinogen/Procedure (dose, time)	Animal/ Liver Disease	Coffee compound	Dose/Concentration/Regimen	Before (1), during (2) or after (3) model establishment	Main findings	Reference
DEN (40 mg/Kg b.wt./day, i.p., for 10 or 14 weeks)	Male Wistar rats, Hepatocarcinogenesis	Caffeine	0.2 mg/mL in drinking water, for 10 and 14 weeks	2	● Reduced number/size of GST-P+ preneoplastic lesions	Fujise et al., 2012
Alcohol (2 × /day, 5–8 g/Kg b.wt., gavage, for 8 or 12 weeks)	Male Sprague-Dawley rats, Alcoholic liver fibrosis	Caffeine	5, 10 and 20 mg/Kg b.wt./day, i.g., for 8 or 12 weeks	2	● All treatments reduced collagen area, protein and mRNA (time- and dose-dependent manner) ● Reduced collagen levels	Wang et al., 2015
TAA (2 × /week, 200 mg/Kg, b.wt., i.p., for 8 weeks)	Male Wistar rats, Cirrhosis	Caffeine	50 mg/Kg b.wt./day, i.g., for 8 weeks.	2	● Reduced fibrosis and inflammation scores	Arauz et al., 2014
TAA (2 × /week, 200 mL/Kg, b.wt., i.p., for 8 weeks)	Male Sprague-Dawley rats, Cirrhosis	Caffeine	50 mg/Kg b.wt./day, i.g., for 4 weeks.	2	● Reduced fibrosis and inflammation scores	Shim et al., 2013
HFD (for 4 weeks)	Male C57BL/6 J mice, NAFLD	Caffeine	0.5 mg/mL in drinking water, for 4 weeks	3	● Reduced lipid accumulation and liver triglyceride levels	Sinha et al., 2014
HFD (for 16 weeks)	Male Wistar rats, NAFLD	Caffeine	20 or 30 mg/Kg/day, i.g., for 8 weeks	2	● Reduced liver inflammation, lipid accumulation, serum cholesterol and triglyceride levels	Helal et al., 2018
HepG2 xenograft model (single, s.c.)	Male nude mice, Hepatocarcinogenesis	Chlorogenic acid	30, 60 or 120 mg/Kg b.wt., i.p./day for 6 weeks	3	● Reduced xenograft tumor volume and weight	Yan et al., 2017
CCl ₄ (2 × /week, 4–2 mL/Kg b.wt., 40% solution, i.p., for 8 weeks)	Male Sprague-Dawley rats, Fibrosis	Chlorogenic acid	15, 30 and 60 mg/Kg b.wt./day, i.g., for 4 weeks.	2	● Reduced collagen I area (dose-dependent manner)	Yang et al., 2017
CCl ₄ (2 × /week, 3 mL/Kg b.wt., 40% solution, i.p., for 8 weeks)	Male Sprague-Dawley rats, Fibrosis	Chlorogenic acid	60 mg/Kg b.wt./day, i.g., for 8 weeks.	2	● Reduced collagen area and hydroxyproline levels	Shi et al., 2016
HFD (for 15 weeks)	Male C57BL/6 J mice, NAFLD	Chlorogenic acid	100 mg/Kg b.wt., i.p., 2 × /week for 15 weeks	2	● Reduced lipid accumulation, serum cholesterol and triglyceride levels	Ma, Wang, & Tang, 2015
High cholesterol and HFD (for 16 weeks)	Male C57BL/6 J mice, NAFLD	Trigonelline	50 mg/Kg b.wt., 3 × /week, i.g., for 16 weeks	2	● Decreased liver triglycerides and steatosis	Sharma et al., 2018
HFD (for 8 weeks)	Male Sprague-Dawley rats, NAFLD	Trigonelline	40 mg/Kg b.wt./day, i.g., for 8 weeks.	3	● Decreased cholesterol, triglycerides and steatosis	Zhang, Zhang, Zhang, Zhang, & Li, 2015

GST-P = placental glutathione-S-transferase; DEN = diethylnitrosamine; CCl₄ = carbon tetrachloride; TAA = thioacetamide; HFD = high fat diet; NAFLD = non-alcoholic fatty liver disease; b.wt. = body weight; i.g. = intragastric route; i.p. = intraperitoneal route; s.c. = subcutaneous route.

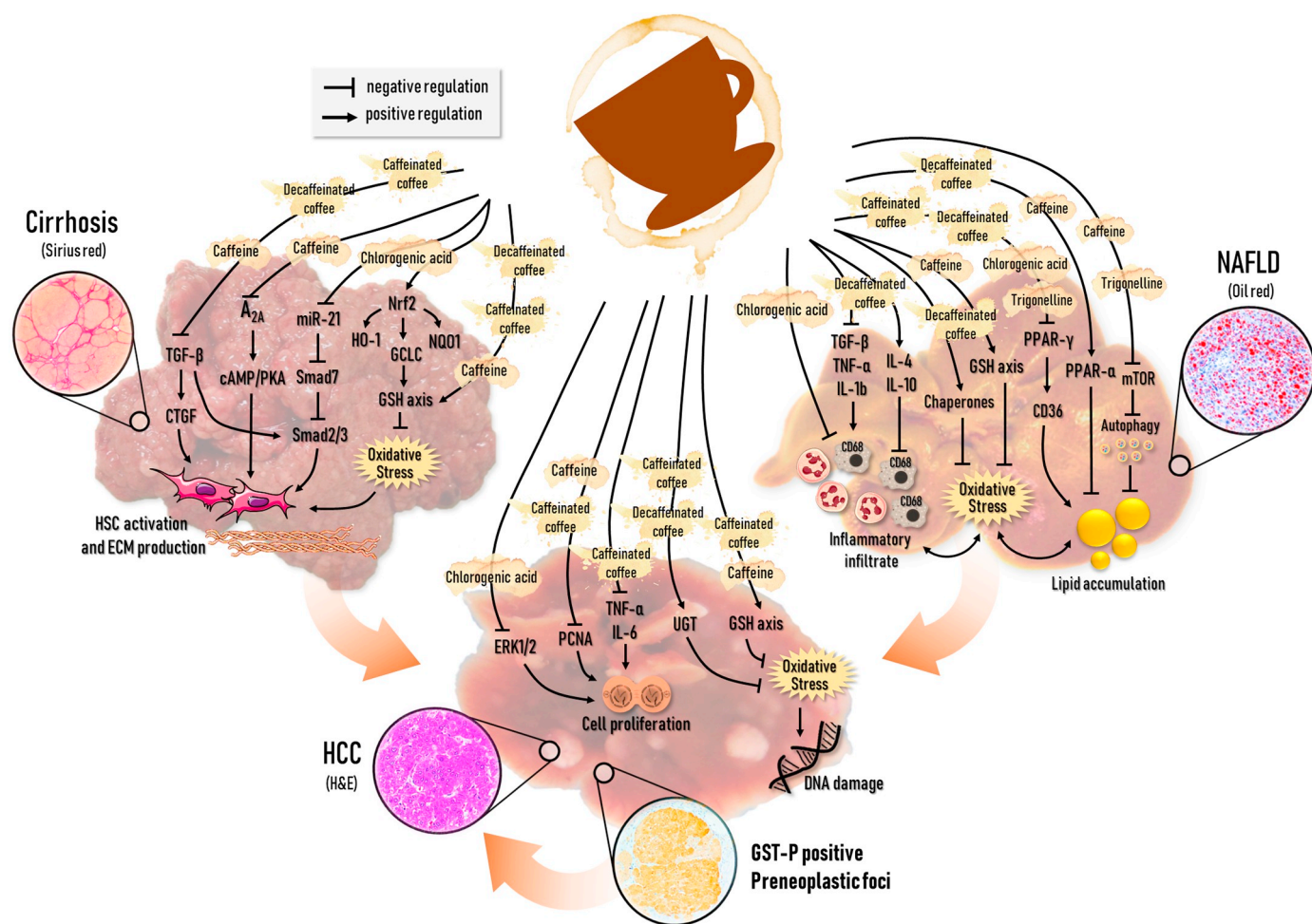


Fig. 5. Main molecular pathways and biological processes modulated by whole caffeinated, decaffeinated coffee brews or highly bioavailable isolated coffee compounds in fibrosis/cirrhosis (left), non-alcoholic fatty liver disease (NAFLD) (right) and hepatocarcinogenesis (down) *in vivo* models. Caffeinated/decaffeinated coffee and highly bioavailable isolated coffee compounds share many molecular targets. Notably, some modulated pathways *in vivo* are also addressed *in vitro*, as summarized in Fig. 4.

(Fig. 5), decaffeinated coffee did not (Furtado et al., 2012). These antioxidant, antigenotoxic and antiproliferative effects, especially exerted by whole coffee, may contribute to lessening GST-P-positive PNL development. However, other underlying mechanisms should be considered as well. Indeed, a single study comparing whole coffee *versus* caffeine reported that only caffeine reduced the size and area of GST-P-positive PNL and the number of neoplastic lesions, (including adenomas and HCC) (Furtado et al., 2014) (Table 5). In the same study, despite not altering antiapoptotic Bcl-2 protein expression, caffeine administration increased protein levels of proapoptotic Bax, whereas common caffeinated coffee did not. In line with these findings, caffeine showed similar results when administered alone, reducing GST-P-positive PNL and PCNA protein levels in the liver (Fujise et al., 2012) (Table 6, Fig. 5). Chlorogenic acid administration alone attenuated the progression of HepG2 xenograft tumors in mice, reducing tumor volume and weight in a dose-dependent manner (Yan et al., 2017) (Table 6). In xenograft tumors, chlorogenic acid reduced ERK1/2 phosphorylation (Fig. 5) and MMP-2/TIMP2 and MMP-9/TIMP2 ratios, which are implicated in sustained cell proliferation and invasion of tumor cells, respectively (Yan et al., 2017). Interestingly, the same effects on the ERK1/2 and MMP-2/TIMP2 pathways were observed when chlorogenic acid was added to the cell culture medium of HepG2 cells (Yan et al., 2017) (Fig. 4A). Regrettably, no studies on the effects of trigoneanine treatment in hepatocarcinogenesis in *in vivo* models are available. Altogether, these studies underscore the complexity of understanding the

effects of coffee beverages on hepatocarcinogenesis, since beneficial effects are not restricted to whole coffee and/or caffeine alone. Thus, additive or synergistic effects of the most common or highly bioavailable compounds may be considered. As it follows, complex similar responses were also observed in models recapitulating HCC risk conditions.

Featured in 75–80% of human HCC cases (Bray et al., 2018), the fibrotic/cirrhotic background associated to chronic liver disease is recapitulated by well-established experimental rodent models, especially in those induced by chemicals, (e.g. TAA/CCl₄) (Tables 5 and 6). Considering that the profibrotic microenvironment is essential to preneoplastic and neoplastic lesion development, alleviating this feature may indirectly slow down hepatocarcinogenesis. Some studies report that whole coffee and caffeine have stronger effects than decaffeinated coffee on diminishing profibrogenic signaling mediated by transforming growth factor β (TGF- β) and downstream connective tissue growth factor (CTGF), thus reducing HSC activation, fibrotic areas and collagen I mRNA production (Arauz et al., 2017). Furtado et al. (2012, 2014) demonstrated that only whole coffee administration diminished collagen III mRNA expression and total and active MMP-2 levels compared to decaffeinated and/or caffeine alone. In contrast, other authors addressed similar effects of whole coffee, decaffeinated coffee and caffeine on reducing oxidative stress (reducing lipid peroxidation and increasing GSH axis) (Fig. 5), profibrogenic signaling (TGF- β and CTGF) (Fig. 5) and ECM remodeling (MMP-2, 9 and -13) (Arauz et al., 2014;

Arauz, Moreno, Cortés-Reynosa, Salazar, & Muriel, 2013; Furtado et al., 2012). In line with *in vitro* studies with HSC (Fig. 4B), caffeine treatment alone attenuated fibrosis/cirrhosis presumably via interaction with adenosine A_{2A} receptors and reduction of the downstream cAMP/PKA/CREB signaling pathway (Chan et al., 2006; Wang et al., 2015) (Fig. 5). In fact, adenosine A_{2A} receptor plays a central role in the pathogenesis of hepatic fibrosis, since knockout mice (A_{2A}^{-/-}) showed a 10-fold decrease in collagen areas during TAA-induced fibrosis (Chan et al., 2006). Due to these effects, some authors pointed caffeine as the main antifibrotic agent in coffee, supporting the “caffeine hypothesis” (Dranoff, 2018). Nonetheless, the effects of chlorogenic acid on the antifibrotic miR-21-regulated Smad7 signaling pathway and antioxidant Nrf2 axis should also be considered for explaining the effects of coffee beverages (caffeinated coffee and, especially, decaffeinated coffee) on liver fibrosis. When administered to rats individually, this polyphenol reduced HSC activation, fibrosis areas, collagen I and III mRNA production and hydroxyproline levels (Shi et al., 2016; Yang et al., 2017). Chlorogenic acid may suppress fibrosis through the attenuation of oxidative stress (MDA levels) in liver tissue, increasing the protein expression of Nrf2 transcription factor, and gene expression of its downstream targets, heme oxygenase-1 (HO-1), NQO1 and GCLC, resulting in augmented GSH levels (Fig. 5), superoxide dismutase and catalase activities (Shi et al., 2016). Furthermore, chlorogenic acid treatment downregulates miR-21 expression in liver, subsequently increasing the mRNA and protein expression of Smad7, a direct miR-21 target (Yang et al., 2017) (Fig. 5). Smad7 upregulation was implicated in decreasing profibrotic Smad2 and Smad3 signaling in rat liver (Yang et al., 2017). Of note, the modulation of the miR-21/Smad7 axis by chlorogenic acid was also observed in HSC *in vitro* (Yang et al., 2017) (Fig. 4B).

Being a growing risk factor for human HCC in high-income countries, experimentally-induced NAFLD was found to be alleviated by whole and decaffeinated coffee interventions, as well as caffeine, chlorogenic acid and trigonelline individually (Tables 5 and 6). A limited number of studies compared the effects of different types of coffee in dietary-induced NAFLD models (Table 5). Shokouh et al. (2018) showed that common whole coffee treatment reduced both plasma and liver triglycerides levels as well as steatosis scores in the liver, while a combination of chlorogenic acid, trigonelline, and caffeic acid did not (Table 5). The molecular events underlying this pronounced response in common coffee treatment are still to be unveiled. On the other hand, another study showed that both caffeinated and decaffeinated coffee regimens triggered strikingly similar responses in reducing the expression of lipid metabolism-related genes, especially PPAR- γ and PPAR- γ -regulated genes, such as CD36, which positively correlated with fatty acid uptake in the liver (Takahashi et al., 2014) (Fig. 5).

Vitaglione et al. (2010) compared decaffeinated coffee treatment with combinations of polyphenols or melanoidins individually (Table 5). In general, all treatments showed similar responses in reducing liver fat accumulation through increased PPAR- α mRNA and protein expression, which is responsible for lipid β -oxidation and clearance, decreased oxidative stress (decreased MDA levels and increased GSH axis) and inflammation (increased levels of IL-4 and IL-10 and decreased mRNA and protein of TNF- α and TGF- β) (Fig. 5). Decaffeinated coffee treatment individually, presumably containing chlorogenic acid and trigonelline, also counteracted NAFLD development in high fat diet (HFD)-fed rats (Brandt et al., 2019; Salomone et al., 2014; Takahashi et al., 2014) (Table 5). Salomone et al. (2014) proposed that these protective effects may be attributed to the reduction of lipid peroxidation and DNA oxidative damage through the upregulation of antioxidant agents (peroxiredoxin 1, glutathione S-transferase α 2, and D-dopachrome tautomerase) and chaperones that maintain endoplasmic reticulum or mitochondrial homeostasis (GRP78, PDI-A3, mtHSP70, and DJ-1) (Fig. 5). Decaffeinated coffee reduced the protein expression of electron transfer flavoprotein subunit α , which is

part of the mitochondrial respiratory chain and directly relates to *de novo* lipogenesis (Salomone et al., 2014). Alterations in the intestinal barrier permeability with subsequent translocation of bacterial endotoxins to the liver are proposed to trigger inflammatory responses and insulin resistance in the liver, contributing to the multifactorial development of NAFLD (Miele et al., 2009). Decaffeinated coffee treatment is also suggested to attenuate NAFLD development by maintaining small intestine barrier integrity, reducing endotoxin translocation to the liver and subsequently decreasing proinflammatory response (reduced granulocyte infiltration and IL-1 β mRNA) and insulin resistance (decreased insulin receptor mRNA) (Brandt et al., 2019).

The administration of the most common and highly bioavailable coffee compounds alone unraveled both distinct (autophagy induction) and similar (PPAR- γ axis downregulation) mechanisms implicated in experimental NAFLD attenuation compared to whole or decaffeinated coffee approaches. Caffeine treatment alone enhanced lipids autophagy by abrogating mTOR negative regulation (enhanced LC3-II protein and lipase A gene expression) (Fig. 5), which was followed by β -oxidation of fatty acids (increased carnitine palmitoyltransferase I α gene expression and ketones and ATP levels) that culminated in lipid clearance and NAFLD attenuation (Sinha et al., 2014). Interestingly, trigonelline alone showed similar results as caffeine in inducing liver autophagy by the modulation of the mTOR pathway (Sharma et al., 2018) (Fig. 5). In addition to autophagy, caffeine also reduced oxidative stress (reduced malondialdehyde, nitrogen oxide and increased GSH levels) and *de novo* lipogenesis (fatty acid synthase and acetyl CoA carboxylase genes), while increasing lipid β -oxidation (gene expression of PPAR- α) (Helal, Ayoub, Elkashefand, & Ibrahim, 2018) (Fig. 5). Similarly to whole caffeinated or decaffeinated coffee regimens, chlorogenic acid alone reduced proinflammatory responses by downregulating macrophage-related genes and decreasing PPAR- γ axis (Ma, Gao, & Liu, 2015) (Fig. 5). The downregulation of PPAR- γ pathway was also featured when trigonelline was individually administered to high-fat diet-fed rats (Sharma et al., 2018) (Fig. 5).

7. Conclusions and future perspectives

Taken together, epidemiological (Tables 1–3), *in vitro* (Figs. 3 and 4) and *in vivo* (Tables 4–6, and Fig. 5) findings predominantly address protective effects of coffee beverages and of its most common and bioavailable individual compounds in gastrointestinal and liver cancer development. Some mechanistic glimpses on their antiproliferative, antioxidant, proapoptotic and antifibrotic actions are also described, mostly *in vitro* (Figs. 3 and 4). It is also noteworthy mentioning that caffeine, chlorogenic acid, and trigonelline, when individually administered, modulate common molecular targets directly implicated in key cancer hallmarks, suggesting that the combination of coffee compounds (as seen in whole coffee beverages), may account for the beneficial effects of coffee consumption. It should be stressed that *in vivo* studies are sometimes mechanistically limited. Hopefully, translational approaches using different preclinical rodent models, such as genetically modified and patient-derived xenograft (PDX), will overcome these limitations. As far as *in vitro* approaches are concerned, caution should be taken in data interpretation, as supraphysiological and non-translatable concentrations are often used. Therefore, more physiologically relevant administration based on coffee compound metabolism and bioavailability should be considered in these studies. Considering that naturally-occurring polyphenols (as chlorogenic acid) and alkaloids (as trigonelline and caffeine) are proposed to target epigenetic processes (Bishayee & Bhatia, 2018), the modulation of the epigenetic machinery by coffee or selected coffee compounds, including DNA methylation, histone modifications and non-coding RNAs, should be definitely investigated in further experiments on gastrointestinal and liver carcinogenesis.

In general, the consumption of common and/or espresso coffee brews is considered a safe and popular dietary habit, especially among

adult and older people. Moreover, coffee bean production and consumption displayed remarkable 70% and 160% increases in the past 3 decades (1990–2018) (International Coffee Organization, 2018), respectively, eliciting the need and relevance of future research on the beneficial effects of coffee on cancer development. On the other hand, some concern on the presence of heat-derived contaminants in coffee beverages (polycyclic aromatic hydrocarbons, furan, acrylamide), as well as the potential risk of hot-beverage intake on esophageal cancer, have been recently raised (Loomis et al., 2016). Nonetheless, according to the International Agency for Research on Cancer (IARC) report, there is lack of evidence for carcinogenicity in humans, and along with experimental data, coffee intake was classified into group 3 (not classifiable as to its carcinogenicity to humans) (Loomis et al., 2016). Although coffee consumption can be incorporated as a healthy habit for most of the adult population, side effects of coffee consumption should be considered in potential “sensitive” populational subgroups. Poole et al. (2017) described harmful associations between high coffee ingestion and pregnancy outcomes (increased risk of low birth weight, pregnancy loss, and 1st and 3rd semester preterm birth). Indeed, EFSA (2015) indicates that caffeine consumption in pregnant women should be limited to 200 mg/day (corresponding to 1–2 cups of common or espresso brews), half the habitual caffeine consumption (400 mg/day). Other health consequences should be considered, since coffee consumption is proposed to cause sleep disruption (Clark & Landolt, 2017) and to slightly increase peripheral arterial stiffness (Echeverri, Pizano, Montes, & Forcada, 2017).

Funding information

Guilherme R. Romualdo and Ariane B. Rocha were recipients of fellowships and grants from São Paulo Research Foundation (FAPESP) (#2016/12015-0 and #2017/26217-7, respectively). Guilherme R. Romualdo was the recipient of a doctoral exchange program fellowship from Coordenação de Aperfeiçoamento de Pessoal de Nível Superior - Brasil (CAPES) (#88881.188786/2018-01). This study was financed in part by CAPES - Finance Code 001. Luis F. Barbisan was the recipient of support research from FAPESP (grant #2016/14420-0). The funders had no influence on the writing and interpretation of data.

Declaration of competing interests

The authors have no conflict of interest to report.

Acknowledgments

The authors would like to thank Prof. Amedeo Columbano and Dr. Pia Sulas - for their suggestions during the preparation of this manuscript. The authors are also grateful to Ms. Rebecca Pandolph and Ms. Sarah Friend, members of the International Coffee Organization, for providing global data on coffee production and consumption.

References

Abu-Absi, S. F., Hansen, L. K., & Hu, W. S. (2004). Three-dimensional co-culture of hepatocytes and stellate cells. *Cytotechnology*, 45, 125–140. <https://doi.org/10.1007/s10616-004-7996-6>.

Akter, S., Kashino, I., Mizoue, T., Matsuo, K., Ito, H., Wakai, K., ... Nishino, Y. (2016). Coffee drinking and colorectal cancer risk: An evaluation based on a systematic review and meta-analysis among the Japanese population. *Japanese Journal of Clinical Oncology*, 46, 781–787. <https://doi.org/10.1093/jjco/hyw059>.

Amigo-Benavent, M., Wang, S., Mateos, R., Sarriá, B., & Bravo, L. (2017). Antiproliferative and cytotoxic effects of green coffee and yerba mate extracts, their main hydroxycinnamic acids, methylxanthine and metabolites in different human cell lines. *Food and Chemical Toxicology*, 106, 125–138. <https://doi.org/10.1016/j.fct.2017.05.019>.

Arauz, J., Moreno, M. G., Cortés-Reynosa, P., Salazar, E. P., & Muriel, P. (2013). Coffee attenuates fibrosis by decreasing the expression of TGF- β and CTGF in a murine model of liver damage. *Journal of Applied Toxicology*, 33, 970–979. <https://doi.org/10.1002/jat.2788>.

Arauz, J., Zarco, N., Hernández-Aquino, E., Galicia-Moreno, M., Favari, L., Segovia, J., & Muriel, P. (2017). Coffee consumption prevents fibrosis in a rat model that mimics secondary biliary cirrhosis in humans. *Nutrition Research*, 40, 65–74. <https://doi.org/10.1016/j.nutres.2017.03.008>.

Arauz, J., Zarco, N., Segovia, J., Shibayama, M., Tsutsumi, V., & Muriel, P. (2014). Caffeine prevents experimental liver fibrosis by blocking the expression of TGF- β . *European Journal of Gastroenterology & Hepatology*, 26, 164–173. <https://doi.org/10.1097/MEG.0b013e3283644e26>.

Baeza, G., Amigo-Benavent, M., Sarriá, B., Goya, L., Mateos, R., & Bravo, L. (2014). Green coffee hydroxycinnamic acids but not caffeine protect human HepG2 cells against oxidative stress. *Food Research International*, 62, 1038–1046. <https://doi.org/10.1016/j.foodres.2014.05.035>.

Bakuradze, T., Lang, R., Hofmann, T., Stiebitz, H., Bytof, G., Lantz, J., ... Janzowski, C. (2010). Antioxidant effectiveness of coffee extracts and selected constituents in cell-free systems and human colon cell lines. *Molecular Nutrition & Food Research*, 54, 1734–1743. <https://doi.org/10.1002/mnfr.201000147b>.

Balansky, R. M., Blagoeva, P. M., Mircheva, Z. I., & De Flora, S. (1994). Modulation of diethylnitrosamine carcinogenesis in rat liver and oesophagus. *Journal of Cellular Biochemistry*, 56, 449–454. <https://doi.org/10.1002/jcb.240560405>.

Bartel, C., Mesias, M., & Morales, F. J. (2015). Investigation on the extractability of melanoidins in portioned espresso coffee. *Food Research International*, 67, 356–365. <https://doi.org/10.1016/j.foodres.2014.11.053>.

Bishayee, A., & Bhatia, D. (2018). *Epigenetics of Cancer prevention* (1st ed.). Academic Press.

Bispo, M. S., Veloso, M. C. C., Pinheiro, H. L. C., De Oliveira, R. F. S., Reis, J. O. N., & Andrade, J. B. D. (2002). Simultaneous determination of caffeine, theobromine, and theophylline by high-performance liquid chromatography. *Journal of Chromatographic Science*, 40, 45–48. <https://doi.org/10.1093/chromsci/40.1.45>.

Brandt, A., Nier, A., Jin, C. J., Baumann, A., Jung, F., Ribas, V., ... Berghelm, I. (2019). Consumption of decaffeinated coffee protects against the development of early non-alcoholic steatohepatitis: Role of intestinal barrier function. *Redox Biology*, 21, 101092. <https://doi.org/10.1016/j.redox.2018.101092>.

Bravi, F., Bosetti, C., Tavani, A., Bagnardi, V., Gallus, S., Negri, E., ... La Vecchia, C. (2007). Coffee drinking and hepatocellular carcinoma risk: A meta-analysis. *Hepatology*, 46, 430–435. <https://doi.org/10.1002/hep.21708>.

Bravi, F., Bosetti, C., Tavani, A., Gallus, S., & La Vecchia, C. (2013). Coffee reduces risk for hepatocellular carcinoma: An updated meta-analysis. *Clinical Gastroenterology and Hepatology*, 11. <https://doi.org/10.1016/j.cgh.2013.04.039> 1413–1421.e1.

Bravi, F., Tavani, A., Bosetti, C., Boffetta, P., & La Vecchia, C. (2017). Coffee and the risk of hepatocellular carcinoma and chronic liver disease: A systematic review and meta-analysis of prospective studies. *European Journal of Cancer Prevention*, 26, 368–377. <https://doi.org/10.1097/CEJ.0000000000000252>.

Bray, F., Ferlay, J., Soerjomataram, I., Siegel, R. L., Torre, L. A., & Jemal, A. (2018). Global cancer statistics 2018: GLOBOCAN estimates of incidence and mortality worldwide for 36 cancers in 185 countries. *CA: a Cancer Journal for Clinicians*, 68, 394–424. <https://doi.org/10.3322/caac.21492>.

Campa, C., Doubeau, S., Dussert, S., Hamon, S., & Noirot, M. (2005). Diversity in bean caffeine content among wild *Coffea* species: Evidence of a discontinuous distribution. *Food Chemistry*, 91, 633–637. <https://doi.org/10.1016/j.foodchem.2004.06.032>.

Caporaso, N., Genovese, A., Canela, M. D., Civitella, A., & Sacchi, R. (2014). Neapolitan coffee brew chemical analysis in comparison to espresso, Moka and American brews. *Food Research International*, 61, 152–160. <https://doi.org/10.1016/j.foodres.2014.01.020>.

Caprioli, G., Cortese, M., Maggi, F., Minnetti, C., Odello, L., Sagratini, G., & Vittori, S. (2014). Quantification of caffeine, trigonelline and nicotinic acid in espresso coffee: The influence of espresso machines and coffee cultivars. *International Journal of Food Sciences and Nutrition*, 65, 465–469. <https://doi.org/10.3109/09637486.2013.873890>.

Caprioli, G., Cortese, M., Odello, L., Ricciutielli, M., Sagratini, G., Tomassoni, G., ... Vittori, S. (2013). Importance of espresso coffee machine parameters on the extraction of chlorogenic acids in a certified Italian espresso by using SPE-HPLC-DAD. *Journal of Food Research*, 2(3), 55–64. <https://doi.org/10.5539/jfr.v2n3p55>.

Carter, O., Wang, R., Dashwood, W. M., Orner, G. A., Fischer, K. A., Löhr, C. V., ... Dashwood, R. H. (2007). Comparison of white tea, green tea, epigallocatechin-3-gallate, and caffeine as inhibitors of PhIP-induced colonic aberrant crypts. *Nutrition and Cancer*, 58, 60–65. <https://doi.org/10.1080/01635580701308182>.

Carvalho, D. C., Brigagão, M. R. P. L., dos Santos, M. H., de Paula, F. B. A., Giusti-Paiva, A., & Azevedo, L. (2011). Organic and conventional *Coffea arabica* L.: A comparative study of the chemical composition and physiological, biochemical and toxicological effects in Wistar rats. *Plant Foods for Human Nutrition*, 66, 114–121. <https://doi.org/10.1007/s11130-011-0221-9>.

Chan, E. S., Montesinos, M. C., Fernandez, P., Desai, A., Delano, D. L., Yee, H., ... Cronstein, B. N. (2006). Adenosine A_{2A} receptors play a role in the pathogenesis of hepatic cirrhosis. *British Journal of Pharmacology*, 148, 1144–1155. <https://doi.org/10.1038/sj.bjp.0706812>.

Clark, I., & Landolt, H. P. (2017). Coffee, caffeine, and sleep: A systematic review of epidemiological studies and randomized controlled trials. *Sleep Medicine Reviews*, 31, 70–78. <https://doi.org/10.1016/j.smrv.2016.01.006>.

Crozier, T. W. M., Stalmach, A., Lean, M. E. J., & Crozier, A. (2012). Espresso coffees, caffeine and chlorogenic acid intake: potential health implications. *Food & Function*, 3, 30–33. <https://doi.org/10.1039/c1fo10240k>.

Deng, W., Yang, H., Wang, J., Cai, J., Bai, Z., Song, J., & Zhang, Z. (2016). Coffee consumption and the risk of incident gastric cancer - a meta-analysis of prospective cohort studies. *Nutrition and Cancer*, 68, 40–47. <https://doi.org/10.1080/01635581.2016.1115093>.

Derossi, A., Ricci, I., Caporizzi, R., Fiore, A., & Severini, C. (2018). How grinding level and

- brewing method (Espresso, American, Turkish) could affect the antioxidant activity and bioactive compounds in a coffee cup. *Journal of the Science of Food and Agriculture*, 98, 3198–3207. <https://doi.org/10.1002/jsfa.8826>.
- Diaz-Rubio, M. E., & Saura-Calixto, F. (2007). Dietary fiber in brewed coffee. *Journal of Agricultural and Food Chemistry*, 55, 1999–2003. <https://doi.org/10.1021/jf062839p>.
- Dong, S., Sun, W., Zheng, L., Kong, J., Kong, J., Kong, F., & Shen, Q. (2015). Low concentration of caffeine inhibits the progression of the hepatocellular carcinoma via Akt signaling pathway. *Anti-Cancer Agents in Medicinal Chemistry*, 15, 484–492. <https://doi.org/10.2174/1871520615666150209110832>.
- Dranoff, J. A. (2018). Coffee consumption and prevention of cirrhosis: In support of the caffeine hypothesis. *Gene Expression*, 18, 1–3. <https://doi.org/10.5221617/X15046391179559>.
- Echeverri, D., Pizano, A., Montes, F. R., & Forcada, P. (2017). Acute effect of coffee consumption on arterial stiffness, evaluated using an oscillometric method. *Artery Research*, 17, 16–32. <https://doi.org/10.1016/j.artres.2017.01.001>.
- Edling, C. E., Selvaggi, F., Ghonaim, R., Maffucci, T., & Falasca, M. (2014). Caffeine and the analog CGS 15943 inhibit cancer cell growth by targeting the phosphoinositide 3-kinase/Akt pathway. *Cancer Biology & Therapy*, 15, 524–532. <https://doi.org/10.4161/cbt.28018>.
- Ekbatan, S. S., Li, X. Q., Ghorbani, M., Azadi, B., & Kubow, S. (2018). Chlorogenic acid and its microbial metabolites exert anti-proliferative effects, S-phase cell-cycle arrest and apoptosis in human colon cancer caco-2 cells. *International Journal of Molecular Sciences*, 19, 1–13. <https://doi.org/10.3390/ijms19030723>.
- European Food Safety Authority (2015). Scientific opinion on the safety of caffeine. *EFSA Journal*, 13, 4102–4222. <https://doi.org/10.2903/j.efsa.2015.4102>.
- Farah, A., Monteiro, M. C., Calado, V., Franca, A. S., & Trugo, L. C. (2006). Correlation between cup quality and chemical attributes of Brazilian coffee. *Food Chemistry*, 98, 373–380. <https://doi.org/10.1016/j.foodchem.2005.07.032>.
- Ferk, F., Huber, W. W., Grasl-Kraupp, B., Speer, K., Buchmann, S., Bohacek, R., ... Knasmüller, S. (2014). Protective effects of coffee against induction of DNA damage and pre-neoplastic foci by aflatoxin B(1). *Molecular Nutrition & Food Research*, 58, 229–238. <https://doi.org/10.1002/mnfr.201300154>.
- Fogliano, V., & Morales, F. J. (2011). Estimation of dietary intake of melanoidins from coffee and bread. *Food & Function*, 2, 117–123. <https://doi.org/10.1039/c0fo00156b>.
- Frary, C. D., Johnson, R. K., & Wang, M. Q. (2005). Food sources and intakes of caffeine in the diets of persons in the United States. *Journal of the American Dietetic Association*, 105, 110–113. <https://doi.org/10.1016/j.jada.2004.10.027>.
- Fujise, Y., Okano, J. I., Nagahara, T., Abe, R., Imamoto, R. Y. U., & Murawaki, Y. (2012). Preventive effect of caffeine and curcumin on hepatocarcinogenesis in diethylnitrosamine-induced rats. *International Journal of Oncology*, 40, 1779–1788. <https://doi.org/10.3892/ijo.2012.1343>.
- Fuller, M., & Rao, N. Z. (2017). The effect of time, roasting temperature, and grind size on caffeine and chlorogenic acid concentrations in cold brew coffee. *Scientific Reports*, 7, 1–9. <https://doi.org/10.1038/s41598-017-18247-4>.
- Furtado, K. S., Polletini, J., Dias, M. C., Rodrigues, M. A. M., & Barbisan, L. F. (2014). Prevention of rat liver fibrosis and carcinogenesis by coffee and caffeine. *Food and Chemical Toxicology*, 64, 20–26. <https://doi.org/10.1016/j.fct.2013.11.011>.
- Furtado, K. S., Prado, M. G., Aguiar e Silva, M. A., Dias, M. C., Rivelli, D. P., Rodrigues, M. A. M., & Barbisan, L. F. (2012). Coffee and caffeine protect against liver injury induced by thioacetamide in male Wistar rats. *Basic & Clinical Pharmacology & Toxicology*, 111, 339–347. <https://doi.org/10.1111/j.1742-7843.2012.00903.x>.
- Gan, Y., Wu, J., Zhang, S., Li, L., Cao, S., Mkwandire, N., ... Lu, Z. (2017). Association of coffee consumption with risk of colorectal cancer: A meta-analysis of prospective cohort studies. *Oncotarget*, 8, 18699–18711. <https://doi.org/10.18632/oncotarget.8627>.
- Gennaro, M. C., & Abrigo, C. (1992). Caffeine and theobromine in coffee, tea and cola-beverages - simultaneous determination by reversed-phase ion-interaction HPLC. *Fresenius' Journal of Analytical Chemistry*, 343, 523–525. <https://doi.org/10.1007/BF00322162>.
- Gillies, M. E., & Birkbeck, J. A. (1983). Tea and coffee as sources of some minerals in the New Zealand diet. *The American Journal of Clinical Nutrition*, 38, 936–942. <https://doi.org/10.1093/ajcn/38.6.936>.
- Godos, J., Micek, A., Marranzano, M., Salomone, F., Del Rio, D., & Ray, S. (2017). Coffee consumption and risk of biliary tract cancers and liver cancer: A dose-response meta-analysis of prospective cohort studies. *Nutrients*, 9. <https://doi.org/10.3390/nu9090950> pii: E950.
- Gross, G., Jaccaud, E., & Huggett, A. C. (1997). Analysis of the content of the diterpenes cafestol and kahweol in coffee brews. *Food and Chemical Toxicology*, 35, 547–554. <https://doi.org/10.1016/B978-0-12-160280-2.50011-0>.
- Gu, L., Gonzalez, F. J., Kalow, W., & Tang, B. K. (1992). Biotransformation of caffeine, paraxanthine, theobromine and theophylline by cDNA-expressed human CYP1A2 and CYP2E1. *Pharmacogenetics*, 2, 73–77. <https://doi.org/10.1097/00008571-199204000-00004>.
- Hagiwara, A., Boonyaphiphat, P., Tanaka, H., Kawabe, M., Kaneko, H., Tamano, S., ... Shirai, T. (1999). Organ-dependent modifying effects of caffeine, and two naturally occurring antioxidants α -tocopherol and n-tritriacontane-16,18-dione, on 2-amino-1-methyl-6-phenylimidazo [4,5-b] pyridine (PhIP)-induced mammary and colonic carcinogenesis in female F344 rats. *Japanese Journal of Cancer Research*, 90, 399–405. <https://doi.org/10.1111/j.1349-7006.1999.tb00761.x>.
- Helal, M. G., Ayoub, S. E., Elkashefand, W. F., & Ibrahim, T. M. (2018). Caffeine affects HFD-induced hepatic steatosis by multifactorial intervention. *Human & Experimental Toxicology*, 37, 983–990. <https://doi.org/10.1177/0960327117747026>.
- International Coffee Organization (2016). Country data on the global coffee trade. http://www.ico.org/profiles_e.asp, Accessed date: 8 January 2018.
- International Coffee Organization (2018). Historical data on the global coffee trade. http://www.ico.org/new_historical.asp?section=Statistics, Accessed date: 8 January 2018.
- Jafari, N., Zargar, S. J., Delnavazi, M.-R., & Yassa, N. (2018). Cell cycle arrest and apoptosis induction of phloracetophenone glycosides and caffeoylquinic acid derivatives in gastric adenocarcinoma (ags) cells. *Anti-Cancer Agents in Medicinal Chemistry*, 18, 610–616. <https://doi.org/10.2174/1871520618666171219121449>.
- Je, Y., Liu, W., & Giovannucci, E. (2009). Coffee consumption and risk of colorectal cancer: A systematic review and meta-analysis of prospective cohort studies. *International Journal of Cancer*, 124, 1662–1668. <https://doi.org/10.1002/ijc.24124>.
- Jiang, Y., Kusama, K., Satoh, K., Takayama, E., Watanabe, S., & Sakagami, H. (2000). Induction of cytotoxicity by chlorogenic acid in human oral tumor cell lines. *Phytomedicine*, 7, 483–491. [https://doi.org/10.1016/S0944-7113\(00\)80034-3](https://doi.org/10.1016/S0944-7113(00)80034-3).
- Kalthoff, S., Ehmer, U., Freiberg, N., Manns, M. P., & Strassburg, C. P. (2010). Coffee induces expression of glucuronosyltransferases by the aryl hydrocarbon receptor and Nrf2 in liver and stomach. *Gastroenterology*, 139(5), 1699–1710. <https://doi.org/10.1053/j.gastro.2010.06.048>.
- Kang, N. J., Lee, K. W., Kim, B. H., Bode, A. M., Lee, H. J., Heo, Y. S., ... Dong, Z. (2011). Coffee phenolic phytochemicals suppress colon cancer metastasis by targeting MEK and TOPK. *Carcinogenesis*, 32, 921–928. <https://doi.org/10.1093/carcin/bgr022>.
- Kaster, M. P., Machado, N. J., Silva, H. B., Nunes, A., Ardaís, A. P., Santana, M., ... Cunha, R. A. (2015). Caffeine acts through neuronal adenosine A_{2A} receptors to prevent mood and memory dysfunction triggered by chronic stress. *Proceedings of the National Academy of Sciences*, 112, 7833–7838. <https://doi.org/10.1073/pnas.1423088112>.
- Katayama, M., Donai, K., Sakakibara, H., Ohtomo, Y., Miyagawa, M., Kuroda, K., ... Fukuda, T. (2014). Coffee consumption delays the hepatitis and suppresses the inflammation related gene expression in the Long-Evans Cinnamon rat. *Clinical Nutrition*, 33, 302–310. <https://doi.org/10.1016/j.clnu.2013.05.006>.
- Kennedy, O. J., Roderick, P., Buchanan, R., Fallowfield, J. A., Hayes, P. C., & Parkes, J. (2016). Systematic review with meta-analysis: Coffee consumption and the risk of cirrhosis. *Alimentary Pharmacology & Therapeutics*, 43, 562–574. <https://doi.org/10.1111/apt.13523>.
- Kennedy, O. J., Roderick, P., Buchanan, R., Fallowfield, J. A., Hayes, P. C., & Parkes, J. (2017). Coffee, including caffeinated and decaffeinated coffee, and the risk of hepatocellular carcinoma: A systematic review and dose-response meta-analysis. *BMJ Open*, 7, e013739. <https://doi.org/10.1136/bmjopen-2016-013739>.
- Knight, C. A., Knight, I., Mitchell, D. C., & Zepp, J. E. (2004). Beverage caffeine intake in US consumers and subpopulations of interest: estimates from the share of intake panel survey. *Food and Chemical Toxicology*, 42, 1923–1930. <https://doi.org/10.1016/j.fct.2004.05.002>.
- Kuhn, M., Lang, S., Bezold, F., Minceva, M., & Briesen, H. (2017). Time-resolved extraction of caffeine and trigonelline from finely-ground espresso coffee with varying particle sizes and tamping pressures. *Journal of Food Engineering*, 206, 37–47. <https://doi.org/10.1016/j.jfoodeng.2017.03.002>.
- Lafay, S., Gil-Izquierdo, A., Manach, C., Morand, C., Besson, C., & Scalbert, A. (2006). Chlorogenic acid is absorbed in its intact form in the stomach of rats. *The Journal of Nutrition*, 136, 1192–1197. <https://doi.org/10.1093/jn/136.5.1192>.
- Lang, R., Dieminger, N., Beusch, A., Lee, Y. M., Dunkel, A., Suess, B., ... Hofmann, T. (2013). Bioappearance and pharmacokinetics of bioactives upon coffee consumption. *Analytical and Bioanalytical Chemistry*, 405, 8487–8503. <https://doi.org/10.1007/s00216-013-7288-0>.
- Lee, I.-A., Low, D., Kamba, A., Llado, V., & Mizoguchi, E. (2014). Oral caffeine administration ameliorates acute colitis by suppressing chitinase 3-like 1 expression in intestinal epithelial cells. *Journal of Gastroenterology*, 49, 1206–1216. <https://doi.org/10.1007/s00535-013-0865-3>.
- Li, Y., Chen, Y., Huang, H., Shi, M., Yang, W., Kuang, J., & Yan, J. (2017). Autophagy mediated by endoplasmic reticulum stress enhances the caffeine-induced apoptosis of hepatic stellate cells. *International Journal of Molecular Medicine*, 1405–1414. <https://doi.org/10.3892/ijmm.2017.3145>.
- Li, Y. M., Peng, J., & Li, L. Z. (2016). Coffee consumption associated with reduced risk of oral cancer: A meta-analysis. *Oral Surgery, Oral Medicine, Oral Pathology, Oral Radiology*, 121, 381–389. <https://doi.org/10.1016/j.oooo.2015.12.006>.
- Liang, N., & Kitts, D. D. (2018). Amelioration of oxidative stress in caco-2 cells treated with pro-inflammatory proteins by chlorogenic acid isomers via activation of the Nrf2-Keap1-ARE-signaling pathway. *Journal of Agricultural and Food Chemistry*, 66, 11008–11017. <https://doi.org/10.1021/acs.jafc.8b03983>.
- Liao, J.-C., Lee, K. T., You, B. J., Lee, C. L., Chang, W. T., Wu, Y. C., & Lee, H. Z. (2015). Raf/ERK/Nrf2 signaling pathway and MMP-7 expression involvement in the trigonelline-mediated inhibition of hepatocarcinoma cell migration. *Food & Nutrition Research*, 22(59), 29884. <https://doi.org/10.3402/fnr.v59.29884>.
- Liguori, A., Hughes, J. R., & Grass, J. A. (1997). Absorption and subjective effects of caffeine from coffee, cola and capsules. *Pharmacology Biochemistry and Behavior*, 58, 721–726. [https://doi.org/10.1016/S0091-3057\(97\)00003-8](https://doi.org/10.1016/S0091-3057(97)00003-8).
- Lim, H. S., Hwang, J. Y., Choi, J. C., & Kim, M. (2015). Assessment of caffeine intake in the Korean population. *Food Additives & Contaminants*, 32, 1786–1798. <https://doi.org/10.1080/19440049.2015.1077396>.
- Lin, Y. S., Wu, S. S., & Lin, J. K. (2003). Determination of tea polyphenols and caffeine in tea flowers (*Camellia sinensis*) and their hydroxyl radical scavenging and nitric oxide suppressing effects. *Journal of Agricultural and Food Chemistry*, 51, 975–980. <https://doi.org/10.1021/jf020870v>.
- Liu, F., Wang, X., Wu, G., Chen, L., Hu, P., Ren, H., & Hu, H. (2015). Coffee consumption decreases risks for hepatic fibrosis and cirrhosis: A meta-analysis. *PLoS One*, 10, e0142457. <https://doi.org/10.1371/journal.pone.0142457>.
- Liu, H., Zhou, Y., & Tang, L. (2017). Caffeine induces sustained apoptosis of human gastric cancer cells by activating the caspase-9/caspase-3 signalling pathway. *Molecular Medicine Reports*, 16, 2445–2454. <https://doi.org/10.3892/mmr.2017.6894>.
- Loomis, D., Guyton, K. Z., Grosse, Y., Lauby-Secretan, B., El Ghissassi, F., Bouvard, V.,

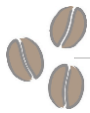
- Benbrahim-Tallaa, L., ... Straif, K. (2016). Carcinogenicity of drinking coffee, mate, and very hot beverages. *The Lancet Oncology*, 17, 877–878. [https://doi.org/10.1016/s1470-2045\(16\)30239-x](https://doi.org/10.1016/s1470-2045(16)30239-x).
- Lopes, G. R., Ferreira, A. S., Pinto, M., Passos, C. P., Coelho, E., Rodrigues, C., ... Coimbra, M. A. (2016). Carbohydrate content, dietary fibre and melanoidins: Composition of espresso from single-dose coffee capsules. *Food Research International*, 89, 989–996. <https://doi.org/10.1016/j.foodres.2016.01.018>.
- López-Galilea, I., De Peña, M. P., & Cid, C. (2007). Correlation of selected constituents with the total antioxidant capacity of coffee beverages: Influence of the brewing procedure. *Journal of Agricultural and Food Chemistry*, 55, 6110–6117. <https://doi.org/10.1021/jf070779x>.
- Ludwig, I. A., Mena, P., Calani, L., Cid, C., Del Rio, D., Lean, M. E. J., & Crozier, A. (2014). Variations in caffeine and chlorogenic acid contents of coffees: What are we drinking? *Food & Function*, 5, 1718–1726. <https://doi.org/10.1039/c4fo00290c>.
- Ma, Y., Gao, M., & Liu, D. (2015). Chlorogenic acid improves high fat diet-induced hepatic steatosis and insulin resistance in mice. *Pharmaceutical Research*, 32, 1200–1209. <https://doi.org/10.1007/s11095-014-1526-9>.
- Ma, Y., Wang, X., & Tang, N. (2015). Downregulation of mPGES-1 expression via EGRI plays an important role in inhibition of caffeine on PGE2 synthesis of HBx(+) hepatocytes. *Mediators of Inflammation*, 2015, 372750. <https://doi.org/10.1155/2015/372750>.
- Martyn, D., Lau, A., Richardson, P., & Roberts, A. (2018). Temporal patterns of caffeine intake in the United States. *Food and Chemical Toxicology*, 111, 71–83. <https://doi.org/10.1016/j.fct.2017.10.059>.
- Matsunaga, K., Katayama, M., Sakata, K., Kuno, T., Yoshida, K., Yamada, Y., ... Mori, H. (2002). Inhibitory effects of chlorogenic acid on azoxymethane-induced colon carcinogenesis in male F344 rats. *Asian Pacific Journal of Cancer Prevention*, 3, 163–166.
- McCusker, R. R., Fuehrlein, B., Goldberger, B. A., Gold, M. S., & Cone, E. J. (2006). Caffeine content of decaffeinated coffee. *Journal of Analytical Toxicology*, 30, 611–613. <https://doi.org/10.1093/jat/30.8.611>.
- McCusker, R. R., Goldberger, B. A., & Cone, E. J. (2003). Caffeine content of specialty coffees. *Journal of Analytical Toxicology*, 27, 520–522. <https://doi.org/10.1093/jat/27.7.520>.
- Merighi, S., Benini, A., Mirandola, P., Gessi, S., Varani, K., Simioni, C., ... Borea, P. A. (2007). Caffeine inhibits adenosine-induced accumulation of hypoxia-inducible factor-1, vascular endothelial growth factor, and interleukin-8 expression in hypoxic human colon cancer cells. *Molecular Pharmacology*, 72, 395–406. <https://doi.org/10.1124/mol.106.032920>.
- Midttun, Ø., Ulvik, A., Nygård, O., & Ueland, P. M. (2018). Performance of plasma trigonelline as a marker of coffee consumption in an epidemiologic setting. *The American Journal of Clinical Nutrition*, 107, 941–947. <https://doi.org/10.1093/ajcn/nqy059>.
- Miele, L., Valenza, V., La Torre, G., Montalto, M., Cammarota, G., Ricci, R., ... Grieco, A. (2009). Increased intestinal permeability and tight junction alterations in nonalcoholic fatty liver disease. *Hepatology*, 49, 1877–1887. <https://doi.org/10.1002/hep.22848>.
- Miller, E. G., Formby, W. A., Rivera-Hidalgo, F., & Wright, J. M. (1988). Inhibition of hamster buccal pouch carcinogenesis by green coffee beans. *Oral Surgery, Oral Medicine, Oral Pathology and Oral Radiology*, 65, 745–749. [https://doi.org/10.1016/0030-4220\(88\)90022-9](https://doi.org/10.1016/0030-4220(88)90022-9).
- Miranda, J., Monteiro, L., Albuquerque, R., Pacheco, J. J., Khan, Z., Lopez-Lopez, J., & Warnakulasuriya, S. (2017). Coffee is protective against oral and pharyngeal cancer: A systematic review and meta-analysis. *Medicina Oral Patologia Oral y Cirugia Bucal*, 22, e554–e561. <https://doi.org/10.4317/medoral.21829>.
- Mitchell, D. C., Knight, C. A., Hockenberry, J., Teplansky, R., & Hartman, T. J. (2014). Beverage caffeine intakes in the U.S. *Food and Chemical Toxicology*, 63, 136–142. <https://doi.org/10.1016/j.fct.2013.10.042>.
- Morishita, Y., Yoshimi, N., Kawabata, K., Matsunaga, K., Sugie, S., Tanaka, T., & Mori, H. (1997). Regressive effects of various chemopreventive agents on azoxymethane-induced aberrant crypt foci in the rat colon. *Japanese Journal of Cancer Research*, 88, 815–820. <https://doi.org/10.1111/j.1349-7006.1997.tb00456.x>.
- Nagini, S., & Kowshik, J. (2016). The hamster buccal pouch model of oral carcinogenesis. *Methods in Molecular Biology*, 1422, 341–350. https://doi.org/10.1007/978-1-4939-3603-8_29.
- Nakayama, T., Funakoshi-Tago, M., & Tamura, H. (2017). Coffee reduces KRAS expression in Caco-2 human colon carcinoma cells via regulation of miRNAs. *Oncology Letters*, 14, 1109–1114. <https://doi.org/10.3892/ol.2017.6227>.
- Nardini, M., Cirillo, E., Natella, F., & Scaccini, C. (2002). Absorption of phenolic acids in humans after coffee consumption. *Journal of Agricultural and Food Chemistry*, 50, 5735–5741. <https://doi.org/10.1021/jf0257547>.
- Nehlig, A. (2018). Interindividual differences in caffeine metabolism and factors driving caffeine consumption. *Pharmacological Reviews*, 70, 384–411. <https://doi.org/10.1124/pr.117.014407>.
- Nishikawa, A., Furukawa, F., Imazawa, T., Ikezaki, S., Hasegawa, T., & Takahashi, M. (1995). Effects of caffeine on glandular stomach carcinogenesis induced in rats by N-methyl-N-nitrosoguanidine and sodium chloride. *Food and Chemical Toxicology*, 33, 21–26. [https://doi.org/10.1016/0278-6915\(95\)80243-6](https://doi.org/10.1016/0278-6915(95)80243-6).
- Oikarinen, S. I., Erlund, I., & Mutanen, M. (2007). Tumour formation in multiple intestinal neoplasia (*Apc^{Min/+}*) mice fed with filtered or unfiltered coffee. *Scand. Journal of Food and Nutrition*, 51, 167–173. <https://doi.org/10.1080/17482970701757119>.
- Oliveira, M., Ramos, S., Delerue-Matos, C., & Morais, S. (2015). Espresso beverages of pure origin coffee: Mineral characterization, contribution for mineral intake and geographical discrimination. *Food Chemistry*, 177, 330–338. <https://doi.org/10.1016/j.foodchem.2015.01.061>.
- Olthof, M. R., Hollman, P. C. H., & Katan, M. B. (2001). Chlorogenic acid and caffeic acid are absorbed in humans. *The Journal of Nutrition*, 131, 66–71. <https://doi.org/10.1093/jn/131.1.66>.
- Panda, S., Biswas, S., & Kar, A. (2013). Trigonelline isolated from fenugreek seed protects against isoproterenol-induced myocardial injury through down-regulation of Hsp27 and αB-crystallin. *Nutrition*, 29, 1395–1403. <https://doi.org/10.1016/j.nut.2013.05.006>.
- Park, H. J., Davis, S. R., Liang, H. Y., Rosenberg, D. W., & Bruno, R. S. (2010). Chlorogenic acid differentially alters hepatic and small intestinal thiol redox status without protecting against azoxymethane-induced colon carcinogenesis in mice. *Nutrition & Cancer*, 62, 362–370. <https://doi.org/10.1080/101635580903407239>.
- Pendergrast, M. (2010). *Uncommon grounds: The history of coffee and how it transformed our world*. revised ed. New York: Basic Books.
- Perrone, D., Farah, A., & Donangelo, C. M. (2012). Influence of coffee roasting on the incorporation of phenolic compounds into melanoidins and their relationship with antioxidant activity of the brew. *Journal of Agricultural and Food Chemistry*, 60, 4265–4275. <https://doi.org/10.1021/jf205388x>.
- Poole, R., Kennedy, O. J., Roderick, P., Fallowfield, J. A., Hayes, P. C., & Parkes, J. (2017). Coffee consumption and health: Umbrella review of meta-analyses of multiple health outcomes. *BMJ*, 359. <https://doi.org/10.1136/bmj.j5024>.
- Reagan-Shaw, S., Nihal, M., & Ahmad, N. (2008). Dose translation from animal to human studies revisited. *FASEB Journal*, 22, 659–661. <https://doi.org/10.1096/fj.07-9574LSF>.
- Risner, C. H. (2008). Simultaneous determination of theobromine, (+)-catechin, caffeine, and (–)-epicatechin in standard reference material baking chocolate 2384, cocoa, cocoa beans, and cocoa butter. *Journal of Chromatographic Science*, 46, 892–899. <https://doi.org/10.1093/chromsci/46.10.892>.
- Saito, Y., Gopalan, B., Mhashilkar, A. M., Roth, J. A., Chada, S., Zumstein, L., & Ramesh, R. (2003). Adenovirus-mediated PTEN treatment combined with caffeine produces a synergistic therapeutic effect in colorectal cancer cells. *Cancer Gene Therapy*, 10, 803–813. <https://doi.org/10.1038/sj.cgt.7700644>.
- Sallet, J. A., Zilberstein, B., Andreollo, N. A., Eshkenazy, R., & Pajcecki, D. (2002). Experimental esophageal carcinogenesis: technical standardization and results. *Diseases of the Esophagus*, 15, 278–281. <https://doi.org/10.1046/j.1442-2050.2002.00273.x>.
- Salomone, F., Li Volti, G., Vitaglione, P., Morisco, F., Fogliano, V., Zappalà, A., ... Galvano, F. (2014). Coffee enhances the expression of chaperones and antioxidant proteins in rats with nonalcoholic fatty liver disease. *Translational Research*, 163, 593–602. <https://doi.org/10.1016/j.trsl.2013.12.001>.
- Sanikini, H., Dik, V. K., Siersema, P. D., Bhoo-Pathy, N., Uiterwaal, C. S. P. M., Peeters, P. H. M., ... Bueno-de-Mesquita, H. B. (2015). Total, caffeinated and decaffeinated coffee and tea intake and gastric cancer risk: Results from the EPIC cohort study. *International Journal of Cancer*, 136, E720–E730. <https://doi.org/10.1002/ijc.29223>.
- Saroja, M., Balasenthil, S., Ramachandran, C. R., & Nagini, S. (2001). Coffee enhances the development of 7,12-dimethylbenz[*a*]anthracene (DMBA)-induced hamster buccal pouch carcinomas. *Oral Oncology*, 37, 172–176. [https://doi.org/10.1016/S1368-8375\(00\)00084-1](https://doi.org/10.1016/S1368-8375(00)00084-1).
- Sharma, L., Lone, N. A., Knott, R. M., Hassan, A., & Abdullah, T. (2018). Trigonelline prevents high cholesterol and high fat diet induced hepatic lipid accumulation and lipo-toxicity in C57BL/6J mice, via restoration of hepatic autophagy. *Food and Chemical Toxicology*, 121, 283–296. <https://doi.org/10.1016/j.fct.2018.09.011>.
- Shi, H., Dong, L., Dang, X., Liu, Y., Jiang, J., Wang, Y., ... Guo, X. (2013). Effect of chlorogenic acid on LPS-induced proinflammatory signaling in hepatic stellate cells. *Inflammation Research*, 62, 581–587. <https://doi.org/10.1007/s00011-013-0610-7>.
- Shi, H., Shi, A., Dong, L., Lu, X., Wang, Y., Zhao, J., ... Guo, X. (2016). Chlorogenic acid protects against liver fibrosis *in vivo* and *in vitro* through inhibition of oxidative stress. *Clinical Nutrition*, 35, 1366–1373. <https://doi.org/10.1016/j.clnu.2016.03.002>.
- Shim, S. G., Jun, D. W., Kim, E. K., Saeed, W. K., Lee, K. N., Lee, H. L., ... Yoon, B. C. (2013). Caffeine attenuates liver fibrosis via defective adhesion of hepatic stellate cells in cirrhotic model. *Journal of Gastroenterology and Hepatology*, 28, 1877–1884. <https://doi.org/10.1111/jgh.12317>.
- Shimizu, M., Yoshimi, N., Yamada, Y., Matsunaga, K., Kawabata, K., Hara, A., ... Mori, H. (1999). Suppressing effects of chlorogenic acid on N-methyl-N-nitrosourea-induced glandular stomach carcinogenesis in male F344 rats. *The Journal of Toxicological Sciences*, 24, 433–439. <https://doi.org/10.2131/jts.24.5.433>.
- Shin, H. S., Satsu, H., Bae, M. J., Zhao, Z., Ogiwara, H., Totsuka, M., & Shimizu, M. (2015). Anti-inflammatory effect of chlorogenic acid on the IL-8 production in Caco-2 cells and the dextran sulphate sodium-induced colitis symptoms in C57BL/6 mice. *Food Chemistry*, 168, 167–175. <https://doi.org/10.1016/j.foodchem.2014.06.100>.
- Shokouh, P., Jeppesen, P. B., Hermansen, K., Laustsen, C., Stodkilde-Jørgensen, H., Hamilton-Dutoit, S. J., ... Gregersen, S. (2018). Effects of unfiltered coffee and bioactive coffee compounds on the development of metabolic syndrome components in a high-fat–/high-fructose-fed rat model. *Nutrients*, 10, 1547. <https://doi.org/10.3390/nu10101547>.
- Silva, J. P. L., Ferreira, E. B., Barbisani, L. F., Brigagao, M. R. P. L., Paula, F. B. A., Moraes, G. O. I., ... Azevedo, L. (2014). Organically produced coffee exerts protective effects against the micronuclei induction by mutagens in mouse gut and bone marrow. *Food Research International*, 61, 272–278. <https://doi.org/10.1016/j.foodres.2013.07.006>.
- Silva-Oliveira, E. M., Fernandes, P. A., & Moraes-Santos, T. (2010). Effect of coffee on chemical hepatocarcinogenesis in rats. *Nutrition & Cancer*, 62, 336–342. <https://doi.org/10.1080/101635580903407205>.
- Sinha, R. A., Farah, B. L., Singh, B. K., Siddique, M. M., Li, Y., Wu, Y., ... Yen, P. M. (2014). Caffeine stimulates hepatic lipid metabolism by the autophagy-lysosomal pathway in mice. *Hepatology*, 59, 1366–1380. <https://doi.org/10.1002/hep.26667>.
- Soares, P. V., Kannen, V., Jordão Junior, A. A., & Garcia, S. B. (2018). Coffee, but neither decaffeinated coffee nor caffeine, elicits chemoprotection against a direct carcinogen in the colon of Wistar rats. *Nutrition & Cancer*, 26, 1–9. <https://doi.org/10.1080/>

- 01635581.2018.1506489.
- Stalmach, A., Mullen, W., Barron, D., Uchida, K., Yokota, T., Cavin, C., ... Crozier, A. (2009). Metabolite profiling of hydroxycinnamate derivatives in plasma and urine after the ingestion of coffee by humans: Identification of biomarkers of coffee consumption. *Drug Metabolism & Disposition*, 37, 1749–1758. <https://doi.org/10.1124/dmd.109.028019>.
- Stalmach, A., Steiling, H., Williamson, G., & Crozier, A. (2010). Bioavailability of chlorogenic acids following acute ingestion of coffee by humans with an ileostomy. *Archives of Biochemistry and Biophysics*, 501, 98–105. <https://doi.org/10.1016/j.abb.2010.03.005>.
- Sunarharum, W. B., Williams, D. J., & Smyth, H. E. (2014). Complexity of coffee flavor: A compositional and sensory perspective. *Food Research International*, 62, 315–325. <https://doi.org/10.1016/j.foodres.2014.02.030>.
- Tadesse, M. (2017). *Ethiopia - home of Arabica coffee: Early use, folklore, coffee ceremony, origin and biology* (1st ed.). Scotts Valley: CreateSpace Independent Publishing Platform.
- Takahashi, S., Egashira, K., Saito, K., Jia, H., Abe, K., & Kato, H. (2014). Coffee intake down-regulates the hepatic gene expression of peroxisome proliferator-activated receptor gamma in C57BL/6J mice fed a high-fat diet. *Journal of Functional Foods*, 6, 157–167. <https://doi.org/10.1016/j.jff.2013.10.002>.
- Takeshita, F., Ogawa, K., Asamoto, M., & Shirai, T. (2003). Mechanistic approach of contrasting modifying effects of caffeine on carcinogenesis in the rat colon and mammary gland induced with 2-amino-1-methyl-6-phenylimidazo[4,5-b]pyridine. *Cancer Letters*, 194, 25–35. [https://doi.org/10.1016/S0304-3835\(03\)00051-X](https://doi.org/10.1016/S0304-3835(03)00051-X).
- Tamura, T., Wada, K., Konishi, K., Goto, Y., Mizuta, F., Koda, S., ... Nagata, C. (2018). Coffee, green tea, and caffeine intake and liver cancer risk: A prospective cohort study. *Nutrition & Cancer*, 20, 1–7. <https://doi.org/10.1080/01635581.2018.1512638>.
- Tanaka, T., Kojima, T., Kawamori, T., Wang, A., Suzui, M., Okamoto, K., & Mori, H. (1993). Inhibition of 4-nitroquinoline-1-oxide-induced rat tongue carcinogenesis by the naturally occurring plant phenolics caffeic, ellagic, chlorogenic and ferulic acids. *Carcinogenesis*, 14, 1321–1325. <https://doi.org/10.1093/carcin/14.7.1321>.
- Tang, X. H., Knudsen, B., Bemis, D., Tickoo, S., & Gudas, L. J. (2004). Oral cavity and esophageal carcinogenesis modeled in carcinogen-treated mice. *Clinical Cancer Research*, 10, 301–313. <https://doi.org/10.1158/1078-0432.CCR-0999-3>.
- Tatematsu, M., Tsuda, H., Shirai, T., Masui, T., & Ito, N. (1987). Placental glutathione S-transferase (GST-P) as a new marker for hepatocarcinogenesis: *In vivo* short-term screening for hepatocarcinogenesis. *Toxicologic Pathology*, 15, 60–68. <https://doi.org/10.1177/019262338701500107https://onlinelibrary.wiley.com/journal/13652621>.
- Tfouni, S. A. V., Carreiro, L. B., Teles, C. R. A., Furlani, R. P. Z., Cipolli, K. M. V. A. B., & Camargo, M. C. R. (2014). Caffeine and chlorogenic acids intake from coffee brew: Influence of roasting degree and brewing procedure. *International Journal of Food Science & Technology*, 49, 747–752. <https://doi.org/10.1111/ijfs.12361>.
- Tolessa, K., D'heer, J., Duchateau, L., & Boeckx, P. (2017). Influence of growing altitude, shade and harvest period on quality and biochemical composition of Ethiopian specialty coffee. *Journal of the Science of Food and Agriculture*, 97, 2849–2857. <https://doi.org/10.1002/jsfa.8114>.
- Tsuda, H., Sekine, K., Uehara, N., Takasuka, N., Moore, M. A., Konno, Y., ... Degawa, M. (1999). Heterocyclic amine mixture carcinogenesis and its enhancement by caffeine in F344 rats. *Cancer Letters*, 143, 229–234. [https://doi.org/10.1016/S0304-3835\(99\)00130-5](https://doi.org/10.1016/S0304-3835(99)00130-5).
- Tsakamoto, T., Mizoshita, T., & Tatematsu, M. (2007). Animal models of stomach carcinogenesis. *Toxicologic Pathology*, 35, 636–648. <https://doi.org/10.1080/01926230701420632>.
- Turati, F., Galeone, C., La Vecchia, C., Garavello, W., & Tavani, A. (2011). Coffee and cancers of the upper digestive and respiratory tracts: Meta-analyses of observational studies. *Annals of Oncology*, 22, 536–544. <https://doi.org/10.1093/annonc/mdq603>.
- Upadhyay, R., & Mohan Rao, L. J. (2013). An outlook on chlorogenic acids-occurrence, chemistry, technology, and biological activities. *Critical Reviews in Food Science and Nutrition*, 53, 968–984. <https://doi.org/10.1080/10408398.2011.576319>.
- Vaughn, C. P., ZoBell, S. D., Furtado, L. V., Baker, C. L., & Samowitz, W. S. (2011). Frequency of KRAS, BRAF, and NRAS mutations in colorectal cancer. *Genes, Chromosomes and Cancer*, 50, 307–312. <https://doi.org/10.1002/gcc.20854>.
- Venkatasubramanian, P. B., Toydemir, G., De Wit, N., Saccenti, E., Martins Dos Santos, V. A. P., Van Baarlen, P., ... Mes, J. J. (2017). Use of microarray datasets to generate caco-2-dedicated networks and to identify reporter genes of specific pathway activity. *Scientific Reports*, 7, 1–12. <https://doi.org/10.1038/s41598-017-06355-0>.
- Vitaglione, P., Morisco, F., Mazzone, G., Amoroso, D. C., Ribocco, M. T., Romano, A., ... D'Argenio, G. (2010). Coffee reduces liver damage in a rat model of steatohepatitis: The underlying mechanisms and the role of polyphenols and melanoidins. *Hepatology*, 52, 1652–1661. <https://doi.org/10.1002/hep.23902>.
- Walton, K., Dorne, J. L., & Renwick, A. G. (2001). Uncertainty factors for chemical risk assessment: Interspecies differences in the *in vivo* pharmacokinetics and metabolism of human CYP1A2 substrates. *Food and Chemical Toxicology*, 39, 667–680. [https://doi.org/10.1016/S0278-6915\(01\)00006-0](https://doi.org/10.1016/S0278-6915(01)00006-0).
- Wang, A., Wang, S., Zhu, C., Huang, H., Wu, L., Wan, X., ... Zhao, H. (2016). Coffee and cancer risk: A meta-analysis of prospective observational studies. *Scientific Reports*, 6, 1–13. <https://doi.org/10.1038/srep33711>.
- Wang, H., Guan, W., Yang, W., Wang, Q., Zhao, H., Yang, F., ... Li, J. (2014). Caffeine inhibits the activation of hepatic stellate cells induced by acetaldehyde via adenosine A2A receptor mediated by the cAMP/PKA/SRC/ERK1/2/P38 MAPK signal pathway. *PLoS One*, 9, 1–11. <https://doi.org/10.1371/journal.pone.0092482>.
- Wang, Q., Dai, X., Yang, W., Wang, H., Zhao, H., Yang, F., ... Lv, X. (2015). Caffeine protects against alcohol-induced liver fibrosis by dampening the cAMP/PKA/CREB pathway in rat hepatic stellate cells. *International Immunopharmacology*, 25, 340–352. <https://doi.org/10.1016/j.intimp.2015.02.012>.
- Wang, R., Dashwood, R. H., Löhr, C. V., Fischer, K. A., Pereira, C. B., Louderback, M., ... Dashwood, W. M. (2008). Protective versus promotional effects of white tea and caffeine on PhIP-induced tumorigenesis and β -catenin expression in the rat. *Carcinogenesis*, 29, 834–839. <https://doi.org/10.1093/carcin/bgn051>.
- Wang, Z.-H., & Fang, J.-Y. (2014). Colorectal cancer in inflammatory bowel disease: Epidemiology, pathogenesis and surveillance. *Gastrointestinal Tumors*, 1, 146–154. <https://doi.org/10.1159/000365309>.
- Ward, J. M., & Treuting, P. M. (2014). Rodent intestinal epithelial carcinogenesis: Pathology and preclinical models. *Toxicology Pathology*, 42, 148–161. <https://doi.org/10.1177/0192623313505156>.
- Warnakulasuriya, S. (2009). Global epidemiology of oral and oropharyngeal cancer. *Oral Oncology*, 45, 309–316. <https://doi.org/10.1016/j.oraloncology.2008.06.002>.
- White, J. R., Jr., Padowski, J. M., Zhong, Y., Chen, G., Luo, S., Lazarus, P., ... McPherson, S. (2016). Pharmacokinetic analysis and comparison of caffeine administered rapidly or slowly in coffee chilled or hot versus chilled energy drink in healthy young adults. *Clinical Toxicology*, 54, 308–312. <https://doi.org/10.3109/15563650.2016.1146740>.
- Wiseman, M. J. (2018). Nutrition and cancer: Prevention and survival. *British Journal of Nutrition*, 14, 1–7. <https://doi.org/10.1017/S0007114518002222>.
- Xie, F., Wang, D., Huang, Z., & Guo, Y. (2014). Coffee consumption and risk of gastric cancer: A large updated meta-analysis of prospective studies. *Nutrients*, 6, 3734–3746. <https://doi.org/10.3390/nu6093734>.
- Xie, Y., Huang, S., He, T., & Su, Y. (2016). Coffee consumption and risk of gastric cancer: An updated meta-analysis. *Asia Pacific Journal of Clinical Nutrition*, 25, 578–588. <https://doi.org/10.6133/apjcn.092015.07>.
- Yan, Y., Liu, N., Hou, N., Dong, L., & Li, J. (2017). Chlorogenic acid inhibits hepatocellular carcinoma *in vitro* and *in vivo*. *The Journal of Nutritional Biochemistry*, 46, 68–73. <https://doi.org/10.1016/j.jnutbio.2017.04.007>.
- Yang, F., Luo, L., de Zhu, Z., Zhou, X., Wang, Y., Xue, J., ... Zhao, L. (2017). Chlorogenic acid inhibits liver fibrosis by blocking the miR-21-regulated TGF- β 1/Smad7 signaling pathway *in vitro* and *in vivo*. *Frontiers in Pharmacology*, 8, 1–13. <https://doi.org/10.3389/fphar.2017.00929>.
- Yang, J. D., Kim, W. R., Coelho, R., Mettler, T. A., Benson, J. T., Sanderson, S. O., ... Roberts, L. R. (2011). Cirrhosis is present in most patients with hepatitis B and hepatocellular carcinoma. *Clinical Gastroenterology and Hepatology*, 9, 64–70. <https://doi.org/10.1016/j.cgh.2010.08.019>.
- Yazheng, L., & Kitts, D. D. (2012). Activation of antioxidant response element (ARE)-dependent genes by roasted coffee extracts. *Food & Function*, 3, 950–954. <https://doi.org/10.1039/c2fo30021d>.
- Yoshinari, O., Sato, H., & Igarashi, K. (2009). Anti-diabetic effects of pumpkin and its components, trigonelline and nicotinic acid, on Goto-Kakizaki rats. *Bioscience, Biotechnology, and Biochemistry*, 73, 1033–1041. <https://doi.org/10.1271/bbb.80805>.
- Yu, C., Cao, Q., Chen, P., Yang, S., Deng, M., Wang, Y., & Li, L. (2016). An updated dose-response meta-analysis of coffee consumption and liver cancer risk. *Scientific Reports*, 6, 1–8. <https://doi.org/10.1038/srep37488>.
- Yu, S., Yang, M., & Nam, K. T. (2014). Mouse models of gastric carcinogenesis. *Journal of Gastric Cancer*, 14, 67–86. <https://doi.org/10.5230/jgc.2014.14.2.67>.
- Yu, X., Bao, Z., Zou, J., & Dong, J. (2011). Coffee consumption and risk of cancers: A meta-analysis of cohort studies. *BMC Cancer*, 11, 96. <https://doi.org/10.1186/1471-2407-11-96>.
- Yuyama, S. (1999). Absorption of Trigonelline from the small intestine of the specific pathogen-free (Spf) and germ-free (Gf) rats *In Vivo*. In G. Huether, W. Kochen, T. J. Simat, & H. Steinhart (Eds.), *Tryptophan, serotonin, and melatonin. Advances in experimental medicine and biology* (pp. 723–727). Boston: Springer.
- Zeng, S. B., Weng, H., Zhou, M., Duan, X. L., Shen, X. F., & Zeng, X. T. (2015). Long-term coffee consumption and risk of gastric cancer: A PRISMA-compliant dose-response meta-analysis of prospective cohort studies. *Medicine*, 94, e1640. <https://doi.org/10.1097/MD.0000000000001640>.
- Zhang, D. F., Zhang, F., Zhang, J., Zhang, R. M., & Li, R. (2015). Protection effect of trigonelline on liver of rats with non-alcoholic fatty liver diseases. *Asian Pacific Journal of Tropical Medicine*, 8, 651–654. <https://doi.org/10.1016/j.apjtm.2015.07.012>.
- Zhang, J., Zhou, B., & Hao, C. (2018). Coffee consumption and risk of esophageal cancer incidence: A meta-analysis of epidemiologic studies. *Medicine*, 97, e0514. <https://doi.org/10.1097/MD.00000000000010514>.
- Zhang, Z., Wu, X., Cao, S., Cromie, M., Shen, Y., Feng, Y., ... Li, L. (2017). Chlorogenic acid ameliorates experimental colitis by promoting growth of *Akkermansia* in mice. *Nutrients*, 9, 677. <https://doi.org/10.3390/nu9070677>.
- Zheng, J. S., Yang, J., Fu, Y. Q., Huang, T., Huang, Y. J., & Li, D. (2013). Effects of green tea, black tea, and coffee consumption on the risk of esophageal cancer: A systematic review and meta-analysis of observational studies. *Nutrition & Cancer*, 65, 1–16. <https://doi.org/10.1080/01635581.2013.741762>.



Capítulo 2

Artigo científico



O artigo a seguir foi submetido ao periódico “Journal of Nutritional Biochemistry” (fator de impacto 4,490, JCR 2018) atualmente está sob revisão (JB_2019_1093). O certificado de submissão pode ser encontrado abaixo.

The Journal of Nutritional Biochemistry



Luís Fernando Barbisan | My Journa

Home

Reports



JNB_2019_1093 | Research Paper

The combination of coffee compounds attenuates early fibrosis-associated hepatocarcinogenesis in mice: involvement of miRNA profile modulation



Luís Fernando Barbisan

São Paulo State University (UNESP), . Prof. Dr. Antônio Celso Wagner Zanin, 250, Distrito de Rubião Junior, null, Brazil.

Status: Under Review (17 days) | Submitted: 16/Dec/2019

Your co-authored submission > Caixa de entrada x



The Journal of Nutritional Biochemistry <Evisesupport@elsevier.com>
para eu ▾

seg., 16 de dez. de 2019 17:53



Dear Mr. Romualdo,

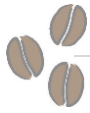
You have been listed as a Co-Author of the following submission:

Journal: The Journal of Nutritional Biochemistry

Title: The combination of coffee compounds attenuates early fibrosis-associated hepatocarcinogenesis in mice: involvement of miRNA profile modulation

Corresponding Author: Luís Fernando Barbisan

Co-Authors: Bruno Cogliati, Fernando Salvador Moreno, Tereza Da Silva, Guilherme Romualdo, Gabriel Bacil, Adriane Evangelista, Rui Reis, Mathieu Vinken



1 **The combination of coffee compounds attenuates early fibrosis-associated**
2 **hepatocarcinogenesis in mice: involvement of miRNA profile modulation**

3
4 Guilherme Ribeiro Romualdo¹; Gabriel Bacil Prata²; Tereza Cristina da Silva³; Adriane Feijó Evangelista⁴; Rui Manuel
5 Reis^{4,7,8}; Mathieu Vinken⁵; Fernando Salvador Moreno⁶; Bruno Cogliati³; Luís Fernando Barbisan^{2*}

6
7 ¹Department of Pathology, Botucatu Medical School, São Paulo State University (UNESP), Botucatu - SP, Brazil.

8 ²Department of Morphology, Biosciences Institute, São Paulo State University (UNESP), Botucatu - SP, Brazil.

9 ³Department of Pathology, School of Veterinary Medicine and Animal Science, University of São Paulo (USP), São Paulo -
10 SP, Brazil.

11 ⁴Molecular Oncology Research Center, Barretos Cancer Hospital, Barretos –SP, Brazil.

12 ⁵Department of *In Vitro* Toxicology and Dermato-Cosmetology, Faculty of Medicine and Pharmacy, Vrije Universiteit Brussel,
13 Brussels, Belgium

14 ⁶Department of Food and Experimental Nutrition, Faculty of Pharmaceutical Sciences, University of São Paulo (USP), São
15 Paulo – SP, Brazil.

16 ⁷Life and Health Sciences Research Institute (ICVS), School of Medicine, University of Minho, Braga, Portugal;

17 ⁸3B's - PT Government Associate Laboratory, Braga/Guimarães, Portugal

18
19
20 * To whom correspondence should be addressed.

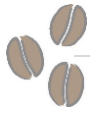
21 Department of Morphology, Biosciences Institute, São Paulo State University (UNESP). Prof. Dr. Antonio Celso Wagner
22 Zanin, 250, 18618-689, Botucatu, São Paulo, Brazil. Phone: +55 14 38800469. E-mail address: luis.barbisan@unesp.br
23 (L.F. Barbisan).

24

25

26

27

**1 Abstract**

2 Aberrant microRNA expression implicates on hepatocellular carcinoma (HCC) development. Conversely, daily
3 coffee consumption reduces by ~40% the risk for fibrosis/cirrhosis and HCC, while decaffeinated coffee does not. It is
4 currently unknown whether these protective effects are solely related to caffeine (CAF), or to its combination with other
5 common and/or highly bioavailable coffee compounds, such as trigonelline (TRI) and chlorogenic acid (CGA). We evaluated
6 whether CAF individually or combined with TRI and/or CGA alleviates fibrosis-associated hepatocarcinogenesis, examining
7 the involvement of miRNA profile modulation. Male C3H/HeJ mice were submitted to a diethylnitrosamine/carbon
8 tetrachloride-induced model. Animals received CAF (50 mg/kg), CAF+TRI (50 and 25 mg/kg), CAF+CGA (50 and 25 mg/kg)
9 or CAF+TRI+CGA (50, 25 and 25 mg/kg), intragastrically, 5x/week, for 10 weeks. Only CAF+TRI+CGA combination reduced
10 the incidence, number and proliferation (Ki-67) of hepatocellular preneoplastic foci while enhanced apoptosis (cleaved
11 caspase-3) in adjacent tissue. CAF+TRI+CGA treatment also decreased hepatic oxidative stress by enhancing the
12 antioxidant Nrf2 axis. CAF+TRI+CGA had the most pronounced effects on decreasing hepatic pro-inflammatory IL-17/NFκB
13 signaling, contributing to reduce CD68-positive macrophage number, stellate cell activation, and collagen deposition. The
14 miRNAomic profile revealed that CAF+TRI+CGA upregulated tumor suppressors miR-144-3p and antifibrotic miR-15b-5p,
15 frequently altered in human HCC. CAF+TRI+CGA reduced protein levels of pro-proliferative EGFR (miR-144-3p target) and
16 antiapoptotic Bcl-2 family members (miR-15b-5p targets). Our results suggest that the combination of most common and
17 highly bioavailable coffee compounds, rather than CAF individually, attenuates early fibrosis-associated
18 hepatocarcinogenesis by modulating miRNA expression profile.

19

20 **Keywords:** Caffeine; trigonelline; chlorogenic acid; liver fibrosis; hepatocarcinogenesis; miRNA.

21

22

23

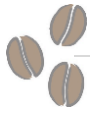
24

25

26

27

28

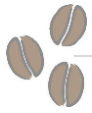


1 1. Background

2 Hepatocellular carcinoma (HCC), the main type of primary liver cancer, ranks as the sixth most incident and fourth
3 deadliest cancer worldwide (841,080 new cases and 781,631 deaths *per year*) [1]. HCC is considered a poor prognosis
4 disease, with an overall median survival of 11 months after clinical diagnosis [2]. Most HCC cases (70 - 90%) arise in the
5 setting of liver fibrosis/cirrhosis, mainly caused by chronic hepatitis B (HBV) and C (HCV) virus infections, alcoholic liver
6 disease (ALD) and non-alcoholic fatty liver disease (NAFLD) [3,4]. This malignancy emerges due to the accumulation of
7 multiple molecular alterations, including the deregulation of microRNA (miRNA) expression [5,6]. miRNAs are noncoding,
8 single-stranded molecules of ~22 nucleotides that constitute a class of gene regulators [7]. In general, miRNAs canonically
9 interact with the 3' untranslated region (3' UTR) of target mRNAs, inducing their degradation or promoting translational
10 repression [7]. It is estimated that ~60% of protein-coding genes in the human genome are controlled miRNA expression
11 [7]. A wealth of evidence points out to the pivotal involvement of miRNAs during hepatocarcinogenesis, as either potential
12 tumor suppressors or onco-miRNAs [8]. In order to unveil the molecular aspects involved in liver fibrosis and
13 carcinogenesis, chemically-induced murine models have been established as suitable tools for pre-clinical research [9-
14 11]. These bioassays display striking morphological and molecular similarities to the corresponding human diseases,
15 including aberrant miRNA expression profile [12], enabling the translational screening of preventive and therapeutic
16 strategies for this liver malignancy [9-11].

17 In contrast, epidemiological and experimental data suggest that nutritional habits and interventions may reduce
18 the incidence of different types of cancer, including HCC [13]. The “common” brewed and espresso coffee beverages,
19 prepared from roasted and grounded seeds of *Coffea* genus plant species, are widely consumed worldwide and exhibit
20 impressive impact on the economy of producing/exporting countries [14]. Indeed, there is a spectrum of epidemiological
21 data evidencing the clear inverse correlation between coffee consumption and fibrogenesis and/or hepatocarcinogenesis
22 risks [15-17]. Overall, coffee consumption (>1 cup/day) reduces by ~40% the risk for fibrosis/cirrhosis and HCC, even upon
23 adjustments for risk factors or highly incident areas [16,17]. In contrast, decaffeinated coffee intake leads to none or less
24 pronounced risk reduction [18,19]. Thus, could this protection be attributed to caffeine (CAF) individually, or, to CAF
25 combination with other common constituents of coffee beverages? The inherent mechanisms and exact compounds
26 involved in this differential response are still unclear.

27 The brewed and espresso coffees are complex mixtures that include many compounds of different chemical
28 classes [20,21]. Particularly, the alkaloids CAF and trigonelline (TRI), and the polyphenol chlorogenic acid (CGA) are some



1 of the most abundant bioactive compounds in coffee beverages [20,21]. After coffee consumption, these compounds
2 present high bioavailability and may accumulate in the plasma due to their long half-life times during regular consumption
3 of many coffee cups along the day [22]. In our previous studies, CAF intake attenuated liver fibrosis and carcinogenesis in
4 rats [23,24]. Furthermore, CGA and TRI are also proposed to reduce liver fibrosis and NAFLD in rats, respectively [25,26].
5 Despite presenting beneficial effects individually, the literature lacks mechanistical studies concerning the combination of
6 these abundant and highly bioavailable compounds on liver fibrosis/carcinogenesis models. Besides, as recently reviewed
7 by our group [15], many *in vivo* and *in vitro* interventions do not resemble human consumption and/or bioavailability, as
8 well as coffee compound concentrations and/or doses are usually overestimated. Finally, since naturally occurring
9 phytochemicals are recently proposed to modulate epigenetic machinery, contributing to cancer prevention, the modifying
10 effects of common coffee compounds on non-coding RNA expression should be unraveled in the context of liver disease
11 [15, 27].

12 Thus, we assessed whether CAF administration individually or combined with TRI and/or CGA alleviates fibrosis-
13 associated hepatocarcinogenesis in a diethylnitrosamine (DEN)/carbon tetrachloride (CCl₄)-induced mice model. In
14 parallel, hepatic miRNA profiling was evaluated to unveil the underlying involvement of these non-coding RNAs, correlating
15 the changes in miRNA expression with fibrosis-associated hepatocarcinogenesis outcomes. Also considering a
16 physiological plausible approach, we evaluated the cytotoxic effects of the same compounds on a human HCC cell line.
17 Our study could provide a translational insight into potential preventive strategies based on tumor suppressor or onco-
18 miRNAs modulated by bioactive coffee compounds. This study constitutes the first scientific report on the beneficial effects
19 of coffee compounds on the miRNAomic profile of a common end-stage liver disease mice model.

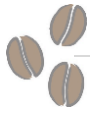
20

21 **2. Materials & Methods**

22 **2.1 *In vivo* experiments**

23 **2.1.1 *Experimental design***

24 The liver-cancer susceptible C3H/HeJ mice strain was submitted to a previously established fibrosis-associated
25 hepatocarcinogenesis model [11]. Briefly, male mice (n = 5 to 10 animals/group) were initiated for liver carcinogenesis by
26 receiving a single intraperitoneal (i.p.) injection of DEN [10 mg/kg body weight (b.wt.) in 0.9% saline, Sigma-Aldrich, USA]
27 or just saline vehicle at 14 postnatal day (PND) (week 2) (Fig. 1). Mice were weaned at PND 28 (week 4). In order to
28 promote DEN-initiated hepatocytes in a fibrotic background, resembling 70-90% of HCC cases in humans [3], mice



1 received three weekly i.p. increasing CCl₄ doses (0.25 to 1.50 µL/g b.wt. 10% solution in corn oil, Sigma-Aldrich, USA)
2 from week 8 to 16 or corn oil vehicle (4-6 p.m.), as previously established by our group [11]. In addition, from week 7 to
3 17, mice received CAF alone (50 mg/kg b.wt.), CAF and TRI (50 and 25 mg/kg b.wt./day, respectively); CAF and CGA (50
4 and 25 mg/kg b.wt./day, respectively); CAF, TRI and CGA treatments (50, 25 and 25 mg/kg b.wt./day, respectively) or just
5 distilled water as vehicle (intragastrically, five times *per week*) (8-10 a.m.) (Fig. 1). Solutions containing bioactive coffee
6 compounds were prepared on a daily basis. All mice were euthanized by exsanguination under ketamine/xylazine
7 anesthesia (100/16 mg/kg b.wt., i.p.) at 17 weeks of age, a week after the last CCl₄ administration. Blood was collected in
8 heparinized syringes from cardiac puncture, centrifuged (1503×g, 10 min.) and serum samples were collected and stored
9 at -80°C for further analysis. At necropsy, the liver was removed, weighted and representative samples from left lateral,
10 right medial and caudate liver lobes were collected for histological analysis, according to previous trimming
11 recommendations [28]. Additional samples from the left lateral and medial lobes were collected, snap-frozen in liquid
12 nitrogen and stored at -80°C.

13 The animals were obtained from School of Veterinary Medicine and Animal Science of the University of São Paulo
14 (FMVZ, USP, São Paulo-SP, Brazil) and were kept in Botucatu Medical School of São Paulo State University (FMB,
15 UNESP, São Paulo-SP, Brazil). Mice were kept in a room with continuous ventilation (16-18 air changes/hour), relative
16 humidity (45-65%), controlled temperature (20-24°C) and light/dark cycle 12:12h and were given water and diet (Nuvital -
17 Nuvilab, Brazil) *ad libitum*. Body weight and food consumption were recorded once a week during the experimental period.
18 The animal experiment was carried out under protocols approved by Botucatu Medical School/UNESP Ethics Committee
19 on Use of Animals (CEUA) (Protocol number 1186/2016) and all animals received humane care according to the criteria
20 outlined in the “Guide for the Care and Use of Laboratory Animals” [29].

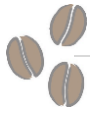
21

22 **2.1.2 Dose determination of bioactive coffee compounds**

23 High coffee consumption, as observed in the USA and in many European countries, leads to an estimated CAF
24 intake range of 200-300 mg/day (~2.8 to 4.0 mg/Kg b.wt./day, considering 70 Kg adults) [30,31]. Therefore, the CAF dose
25 (50 mg/Kg b.wt.) was calculated based on the allometric translation of Human Equivalent Dose (HED) [32], considering
26 the dose of 4.0 mg/Kg b.wt./day, as it follows:

27

28



1
$$(I) HED (mg/kg/day) = Animal\ dose (mg/kg/day) \times \frac{Mice\ Km^*}{Animal\ Km}$$

2
$$(II) HED = 50 \times \frac{3}{37}$$

3
$$(III) HED = 4\ mg/kg/day\ or\ 280\ mg/day\ (70\ kg\ adult)$$

4 *K_m = species-related constant based on body weight and surface area [32]

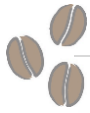
5

6 The administered dose corresponded to the consumption of 280 mg CAF/day, equivalently to 2-3 cups of common
7 coffee brew [15,21]. Moreover, this dose was previously applied and showed no toxic effect on chemically-induced cirrhosis
8 in rodents [33]. Since the epidemiological studies are focused on CAF consumption from coffee beverages, both TRI and
9 CGA doses (25 mg/kg b.wt.) were based on TRI or CGA/CAF ratio found in filtered coffee, as previously determined by
10 our research group [24]. TRI (0.51 mg/mL of coffee), CGA (0.41 mg/mL of coffee) and CAF (1.0 mg/mL of coffee)
11 concentrations in filtered coffee display a ratio of 1/2, resembling previous studies [20,21]. The administration of coffee
12 compounds from the seventh week of age on (sexual maturity) resembles human exposure to coffee/CAF, which starts
13 from puberty and extends over the adult age [31,32].

14

15 **2.1.3 Preneoplastic hepatocyte foci screening and collagen morphometry**

16 Liver samples were fixed in 10% neutral buffered formalin for 24 h at room temperature, stored in 70% ethanol
17 and embedded in paraffin. Five-micron thick liver sections from paraffin-embedded blocks were obtained and stained with
18 Hematoxylin and Eosin (H&E), the gold standard staining to identify preneoplastic liver lesions in mice. The altered
19 hepatocyte foci (AHF), considered the main endpoint lesions for the 17-week time-point, were identified by the blind reading
20 of coded slides, using well-established criteria [11,28]. The analyzed sections had representative fragments of left lateral,
21 right medial and caudate lobes (one slide/animal). Then, the total number of AHF/liver section area (cm²), the mean size
22 (mm²), the relative area (sum of all AHF areas/liver section area, in mm²/cm²) and the incidence of these lesions were
23 calculated. The liver section areas were measured by Stemi 2000 stereo zoom microscope (Zeiss, Germany) using a Dino
24 Capture (ANMO Electronics Corporations, USA) image analysis system. The AHF size was measured by Olympus CellSens
25 software (Olympus Corporation, Japan). Quantitative analysis of collagen fibers was performed in Sirius red-stained sections
26 using Leica QWin V3 software (Leica Microsystems, Germany), selecting 10 random microscopic fields (20× objective) per
27 section (left lobe), comprising portal areas [Collagen area (%) = Sirius red area / total 20× field area analyzed].



1 **2.1.4 Immunohistochemistry**

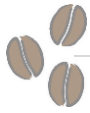
2 For immunohistochemistry, deparaffinated 5- μ m liver sections on silane-covered microscope slides were subject
3 to antigen retrieval in 0.01M citrate buffer (pH 6.0, 120°C, 5 min) in a Pascal Pressure Chamber (Dako Cytomation,
4 Denmark). After endogenous peroxidase blockade with 1% H₂O₂ in phosphate-buffered saline (PBS) (15 min.), the slides
5 were treated with skim milk (60 min.) and incubated in a humidified chamber (4°C, overnight) with anti- α -smooth muscle
6 actin (α -SMA, *i.e.* hepatic stellate cell marker, ab124964, 1:500 dilution, Abcam, UK), anti-CD68 (*i.e.* macrophage/ Kupffer
7 cell marker, ab125212, 1:1000 dilution, Abcam, UK), anti-Ki-67 (*i.e.* cell proliferation marker, ab16667, 1:100 dilution,
8 Abcam, UK), anti-Proliferating Cell Nuclear Antigen (PCNA, *i.e.* cell proliferation marker, PC10, 1:100 dilution, Dako
9 Cytomation, Denmark), anti-cleaved caspase-3 (*i.e.* apoptosis marker, 5A1E, 1:100 dilution, Cell Signaling, USA), anti-NF κ B
10 p65 (sc-372, 1:100 dilution, Santa Cruz Biotechnology, USA) primary antibodies. Then, slides were incubated with one-step
11 horseradish peroxidase (HRP)-polymer (EasyPath - Erviegas, Brazil) (20 min). Reactions were visualized with 3'-3'-
12 diaminobenzidine (DAB) chromogen (Sigma–Aldrich, USA) and counterstained with Harris hematoxylin.

13 The semiquantitative analysis of α -SMA immunostained sections was performed as described for collagen
14 morphometry. In adjacent liver (avoiding preneoplastic foci), 10 random fields (20 \times objective) were assessed in left hepatic
15 lobe sections, mainly comprising portal areas. Ki-67 and PCNA positive hepatocytes; cleaved caspase-3 positive cells; and
16 CD68 positive macrophages were counted and divided by the liver area analyzed (mm²). In preneoplastic foci (considering
17 all types), all Ki-67 and PCNA-positive hepatocytes or cleaved caspase-3-positive cells were counted and divided by the
18 lesion area analyzed (mm²). All analyses were performed in Olympus CellSens (Olympus Corporation, Japan) and Image J
19 software (National Institutes of Health, USA).

20

21 **2.1.5 Enzyme-Linked Immunosorbent Assay (ELISA)**

22 Liver samples (~100 mg) of the left medial lobe were homogenized in RIPA buffer (Cell Signaling, USA) containing
23 1% protease inhibitor cocktail (Sigma-Aldrich, USA), in proportion 30 mg tissue/100 μ l buffer, and maintained at 4°C for 2
24 h. Then, the homogenate was centrifuged (10,000 \times g, 4°C, 30 min.) and the supernatant was collected for protein
25 quantification by the Bradford method. The levels of tumor necrosis factor alpha (TNF- α), interleukin-6 (IL-6) and 17 (IL-17)
26 were determined by the Luminex multiple analyte profiling (xMAP) methodology using a 96-well plate containing specific
27 magnetic beads for each of the cytokines, following the manufacturer's instructions (MICYTOMAG-70K, Millipore, USA).



1 Before normalization by the amount of protein (mg or g), liver samples followed the limits of detection of the kit: IL-6 (1134
2 - 107 pg/mL), IL-17 (1074 - 103 pg/mL), and TNF- α (1200-110 pg/ml).

3

4 **2.1.6 TBARS and antioxidant enzymes**

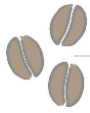
5 For thiobarbituric acid reactive species (TBARS) determination, left medial lobe samples (50 mg) were
6 homogenized with magnetic beads in 0.5 mL of 3% sulfosalicylic acid solution and centrifuged (18.000 \times g, 4°C, 3 min.) Then,
7 samples were mixed with 0.67% thiobarbituric acid solution (1:1 proportion) [34]. For antioxidant profiling, other samples of
8 the left medial lobe (50 mg) were homogenized in 50 mM phosphate buffer (pH 7.4) using a motor-driven Teflon glass Potter
9 Elvehjem (100 \times g/min) and centrifuged (12000 \times g, 4°C, 15 min). The supernatant was collected for antioxidant enzyme
10 determination. Catalase activity was assayed in sodium and potassium phosphate buffer with 10 mM hydrogen peroxide
11 [35]. Glutathione peroxidase (GSH-Px) determination followed the oxidation of 0.16 mM NADPH in the presence of
12 glutathione reductase (GR) [36]. Superoxide dismutase (SOD) was determined by the reduction of hydroxylamine-generated
13 nitro blue tetrazolium (NBT), in a medium containing 0.1 mM EDTA, 50 mM NTB, 78 mM NADH and 33 mM phenazine
14 methosulfate [37]. All determinations were performed using a microplate reader (25°C) (mQuant-Gen5 2.0 software, Bio-
15 Tec Instruments, USA).

16

17 **2.1.7 RNA extraction and miRNA global expression assay**

18 Liver samples (~30 mg) of the left lateral lobe were homogenized in 1 mL QIAzol (Qiagen, UK). Total RNA was
19 isolated separately using a QIAGEN RNeasy column-based system following the manufacturer's instructions (Qiagen,
20 UK). RNA quantification and integrity were assessed in Qubit 2.0 Fluorometer (Invitrogen, USA) and Agilent 2100
21 Bioanalyzer platform (Agilent Technologies, USA), respectively. Samples with RNA integrity number (RIN) >7.0 were
22 profiled for miRNA expression [7.65 \pm 0.43, mean \pm standard deviation (S.D.)] Reports on RIN are presented in
23 Supplementary Fig. 1. The RNA samples were stored at -80°C until further analysis.

24 An amount of 100 ng of total RNA (each sample/mouse) was used for nCounter Mouse v1.5 miRNA global
25 expression assay (detecting 600 murine and murine-related viral miRNAs) in an automated system (NanoString
26 Technologies, USA). These analyses were performed at the Molecular Oncology Research Center, Barretos Cancer
27 Hospital (Barretos - SP, Brazil). Briefly, total RNA samples were incubated with specific tags that bind the 3' end of each
28 mature miRNA, in order to normalize miRNA melting temperatures. The tag excess was removed, and the miRNA-tag



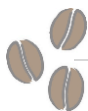
1 complexes were incubated with 10 μ L and 5 μ L of reporter and capture probes, respectively, at 64°C for 18 h. Reporter
2 probes had specific fluorescent signals for each miRNA in 5' end and capture probes are biotinylated in 3' end. The mix
3 was purified and then pipetted in a streptavidin-covered cartridge by nCounter Prep Station. Finally, cartridges were
4 analyzed in nCounter Digital Analyzer, which acquired 280 fields of view *per* sample and counted the miRNA-reporter
5 probe complexes. For miRNA expression analysis, raw counting of miRNA-reporter probe complexes was normalized by
6 the median of the top-ten miRNAs presenting the lowest coefficient of variation (low CV values) using NanostringNorm
7 package [38]. Student *t*-test was used for pair comparison, considering $p < 0.05$ and fold change (FC) > 1.5 . The heat
8 maps were performed using the ComplexHeatmap package in Galaxy computational environment (<https://usegalaxy.org/>)
9 [39]. Pair comparisons were crossed using Venn's diagram, distinguishing the differentially expressed miRNAs related to
10 the treatments.

11 12 **2.1.8 miRNA target analysis and Gene Ontology/KEGG pathway analysis**

13 After the identification of differentially expressed miRNAs, Ingenuity Pathway Analysis software (IPA, Qiagen, USA)
14 was applied for miRNA target analysis, restricting outcome target lists to experimentally validated data. The output list was
15 submitted to functional enrichment analysis using the Gene Ontology (GO) Consortium online platform
16 (<https://geneontology.org>) [40] and KEGG pathway analysis in DAVID Bioinformatics Resources 6.8 online platform
17 (<https://david.ncifcrf.gov/>) [41]. The main biological process (BP) annotations and KEGG terms were ranked by the lowest
18 adjusted p values, considering $p < 0.05$. STRING v11 (<https://string-db.org>) was applied for drawing association networks,
19 considering curated databases and experimentally determined interactions among targets [42].

20 21 **2.1.9 Immunoblotting**

22 Aliquots containing 7 μ g of total protein (extracted as described in item 2.1.5) were heated (95°C, 5 min) in Laemmli
23 sample buffer (2.5 mM Tris, 2% SDS, 10% glycerol, 0.01% bromophenol blue, 5% 2-mercaptoethanol) and then
24 electrophoretically separated in a 10% SDS-PAGE gel under reducing conditions and transferred to nitrocellulose
25 membranes (Bio-rad Laboratories, USA). Membranes were blocked with skim milk in Tris-Buffered Saline-Tween (TBS-T,
26 1 M Tris, 5 M NaCl, pH 7.2, 500 μ L Tween-20) (1 h). Membranes were subsequently incubated with anti-NF κ B p65 (sc-372,
27 65 kDa, 1:1000 dilution, Santa Cruz Biotechnology, USA), anti- α -SMA (ab124964, 43 kDa, 1:1000 dilution, Abcam, UK),
28 anti-Nrf2 (PA5-27882, ~95–110 kDa, 1:1000, Thermo Fisher Scientific, USA), anti-HIF-1 α (PA1-16601, 93 kDa, 1:1000



1 dilution, Thermo Fisher Scientific, USA), anti-Bcl2l2 (PA5-78865, 21 kDa, 1:250 dilution, Thermo Fisher Scientific, USA),
2 anti-Mcl-1 (PA5-11389, 37 kDa, 1:4000 dilution, Thermo Fisher Scientific, USA), anti-VEGF (PA5-16754, 37 kDa, 1:700,
3 Thermo Fisher Scientific, USA), anti-Bcl-2 (PA5-20068, 26 kDa, 1:2000, Thermo Fisher Scientific, USA), anti-total EGFR
4 (ab2430, 170 kDa, 1:250, Santa Cruz Biotechnology, USA), anti-PCNA (PC10, 36 kDa, 1:1000 dilution, Dako Cytomation,
5 Denmark), or anti- β -actin (sc1615, 43 kDa, 1:1000 dilution, Santa Cruz Biotechnology, USA) primary antibodies diluted in
6 TBS-T overnight. After 5 wash steps with TBS-T, membranes were incubated with specific HRP-conjugated secondary
7 antibodies, according to the primary antibodies used (2 h). Finally, membranes were submitted to immunoreactive protein
8 signals detected using Clarity Max ECL Substrate (Bio-Rad Laboratories, USA). Signals were captured by a G:BOX Chemi
9 system (Syngene, UK) controlled by an automatic software (GeneSys, Syngene, UK). Band intensities were quantified using
10 densitometry analysis Image J software (National Institutes of Health, USA). Finally, protein expression was reported as
11 fold change according to β -actin protein expression used as a normalizer.

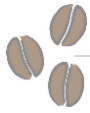
12

13 **2.2 In vitro experiments**

14 **2.2.1 Cell culture, treatments, and cytotoxicity assay**

15 HCC C3A cell line (clonal derivative of human HepG2 cells) (ATCC, CRL-10741TM, USA) were grown in Eagle's
16 Minimum Essential Medium (MEM) (Vitrocell, Brazil) supplemented with 10% fetal bovine serum (FBS) (Gibco, USA), 100
17 U/ml penicillin and 100 μ g/ml streptomycin (Gibco, USA) in a humidified atmosphere of 5% CO₂ at 37°C. C3A cells were
18 seeded in 96-well plates at a density of 7×10^4 cells/mL. Twenty-four hours after seeding, tumor cells were treated with
19 medium supplemented with varying concentrations of CAF alone or combined with TRI and/or CGA (Sigma-Aldrich, USA)
20 (6 subcultures *per* treatment) for 24 or 48 h, according to the Supplementary Table 1. All compounds were diluted with MEM
21 to the desired concentrations. CAF concentrations were based on serum peak ($\sim 40 \mu$ M) after the ingestion of 280 mg of
22 CAF, equivalently to 2-3 cups of common coffee brew [15,21,22].

23 For cytotoxicity assessment, lactate dehydrogenase (LDH) levels were measured using a colorimetric kit (Roche
24 Diagnostics, Germany). Positive control for cell lysis was established by adding 100 μ L of 2% Triton X-100 solution (Thermo
25 Fisher Scientific, USA). Plates were centrifuged (250 \times g, 10 min.) in order to obtain a cell-free supernatant. Then, the
26 supernatant (100 μ L/well) was transferred from the top of all the wells to the LDH assay plate. Next, the supernatant was
27 mixed with the kit working solution (100 μ L/well) and assay plates were then incubated at room temperature in the dark for
28 20 min. The absorbance (abs.) was measured at 340 nm using an automated ELISA plate reader (Varioskan Flash, Thermo



1 Scientific, USA). The results were calculated by the following relation: (sample abs. value – untreated control abs. value) /
2 (positive control abs. value – untreated control abs. value) × 100. Three independent experiments were performed.

3

4 **2.3 Statistical analysis**

5 Data were analyzed by One-way ANOVA or Kruskal-Wallis and *post hoc* Tukey's test. Data on incidence were
6 analyzed by Fisher's Exact test. Differences were considered significant when $p < 0.05$. Statistical analyses were performed
7 using GraphPad Prism software 6.0 (GraphPad, USA). Data are presented as mean \pm standard deviation (S.D.), box plot
8 or the proportion of affected animals (percentage). The number of replicates (n) *per* group for each analysis is determined
9 in the results section.

10

11 **3. Results**

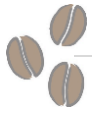
12 **3.1 General findings**

13 All treatments with bioactive coffee compounds did not significantly alter final body weight and food consumption
14 compared to vehicle and DEN/CCl₄ groups (Table 1). Indeed, all groups showed similar body weight evolution curves
15 during the 17 weeks of the experiment (Supplementary Fig. 2). As expected, DEN/CCl₄-induced fibrosis-associated
16 hepatocarcinogenesis model increased absolute ($p < 0.001$) and relative ($p = 0.019$) liver weights, as well as elevated serum
17 ALT levels ($p = 0.027$), compared to the untreated counterpart. In contrast, all coffee compound interventions reduced
18 absolute liver weight compared to DEN/CCl₄ model ($p < 0.001$) (Table 1). CAF and CAF+TRI+CGA oral treatments
19 diminished relative liver weight as well ($p = 0.019$) (Table 1). Despite presenting 7% to 20% reductions in ALT levels
20 compared to DEN/CCl₄ group, coffee compound-treated groups did not significantly alter ALT levels (Table 1).

21

22 **3.2 The combination of coffee compounds attenuates preneoplastic lesion development**

23 In the early stages of mouse hepatocarcinogenesis, the AHF are considered putative preneoplastic lesions and
24 were identified in H&E-stained sections as eosinophilic, basophilic and clear cell phenotypes (Fig. 2A). DEN-induced AHF
25 frequently displays *Hras* and *Braf* (97.3% of basophilic foci) oncogene mutations, predisposing these hepatocellular lesions
26 to neoplastic progression under promoting stimuli [43,44]. In the established DEN/CCl₄-induced model, the basophilic
27 phenotype prevails [11]. As expected, the established DEN/CCl₄-induced model increased the incidence of preneoplastic
28 foci compared to the untreated counterpart ($p < 0.001$) (Table 2). Interestingly, only the CAF+TRI+CGA combination reduced



1 the incidence of clear cell foci compared to DEN/CCl₄ group ($p=0.011$) (Table 2). Moreover, only the combination of all
2 coffee compounds reduced by 43% and 38% the number of all AHF ($p=0.024$) and basophilic phenotype ($p=0.029$) *per* liver
3 area compared to DEN/CCl₄ group, respectively (Fig. 2B). The decreased number of lesions also led to diminished relative
4 foci area in the CAF+TRI+CGA group ($p=0.032$) (Supplementary Fig. 3A). Due to the carcinogen effect on glycogen
5 metabolism, the glycogenotic eosinophilic and clear cell foci phenotypes are the first to arise in hepatocarcinogenesis [44].
6 Progressively, these lesions tend to a “metabolic turnover”, giving rise to the basophilic foci with a glycogenolytic profile [45].
7 These metabolic changes, as well as *Braf* and *Hras* mutations, are the stimulus to promote cell proliferation, a cancer
8 hallmark [44, 45]. Thus, our findings indicate that the combination of coffee compounds, rather than CAF individually, may
9 modulate different steps of hepatic preneoplasia development.

10

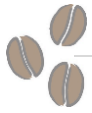
11 **3.3 The combination of coffee compounds reduces proliferation in preneoplastic foci and increases apoptosis in** 12 **adjacent tissue**

13 Sustained cell proliferation into preneoplastic lesions could favor the accumulation of genetic and epigenetic
14 alterations, predisposing AHF to neoplastic progression [46]. DEN/CCl₄ model induced an increase ($p<0.0001$) in hepatocyte
15 proliferation (Ki-67-positive cells) in adjacent tissue, compared to the untreated counterpart (Fig. 3). Although all coffee
16 compound treatments did not modulate cell proliferation in adjacent tissue, only the combination of CAF+TRI+CGA
17 diminished the number Ki-67+ hepatocytes inside all types of preneoplastic lesions compared to CAF and DEN/CCl₄ groups
18 ($p=0.0059$) (Fig. 4A). Negative modulation of cell proliferation into AHF can slow lesion development [46], resulting in
19 diminished incidence and number of lesions *per* liver area. In addition, the CAF+TRI+CGA intervention presented
20 significantly more cleaved caspase-3-positive cells in adjacent liver tissue when compared to the other groups ($p<0.0001$)
21 (Fig. 3). Treatments did not modulate the number of apoptotic cells inside AHF (Fig. 4B).

22

23 **3.4 The combination of coffee compounds attenuates fibrosis by decreasing IL-17/ NFκB p65 axis**

24 In keeping with the increased liver weight and ALT levels, the applied DEN/CCl₄-induced model displayed typical
25 features of chronic liver disease, within enhanced collagen area showed by fibrous expansions and bridging ($p<0.0001$),
26 HSC activation indicated by the increased α -SMA protein expression ($p<0.0001$) and increased number of CD68-positive
27 hepatic macrophages, predominantly concentrated in fibrous expansions ($p=0.0004$) when compared to the untreated
28 counterpart (Fig. 5A, B and C). In accordance, DEN/CCl₄ model presented 2.4-fold higher hepatic levels of pro-inflammatory



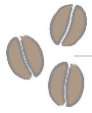
1 cytokine IL-17 compared to the untreated group ($p=0.007$) (Fig. 5B). Conversely, only the combination of CAF+TRI+CGA,
2 rather than CAF individually, reduced by 25% the collagen area compared to the DEN/CCl₄ group ($p<0.0001$), displaying
3 more delicate collagen fibers in Sirius red-stained liver sections (Fig.s 5A and B). Moreover, only the combination of all
4 coffee compounds decreased the number of CD68-positive macrophages in comparison to CAF, CAF+TRI-treated and
5 DEN/CCl₄ groups ($p=0.0004$) (Fig. 5B). The CAF+TRI, CAF+CGA and especially, CAF+TRI+CGA treatment reduced IL-17
6 hepatic levels compared to DEN/CCl₄ group as well ($p=0.007$) (Fig. 5B). IL-6 and TNF- α hepatic levels were similar in all
7 groups (Supplementary Fig. 3B). All coffee compound combinations, including CAF+TRI+CGA, decreased α -SMA protein
8 expression in the liver compared to DEN/CCl₄ ($p<0.0001$), indicating an attenuation in HSC activation by the coffee
9 compound combination that corroborates with reduced collagen deposition in CAF+TRI+CGA group (Fig. 5C). Lastly, only
10 the combination of all coffee compounds significantly reduced pro-inflammatory NF κ B p65 protein expression in the liver
11 compared to DEN/CCl₄ group ($p=0.015$) (Fig. 5C).

12 Liver resident (Kupffer cells, KC) and recruited macrophages play pivotal roles in inducing pro-inflammatory and
13 pro-fibrogenic responses in HSC through the production of cytokines and subsequent paracrine signaling [47]. The pro-
14 inflammatory IL-17 production, mainly mediated by KC, directly contributes to HSC activation and collagen production, being
15 essential on undergoing liver fibrosis [48]. The IL-17 signaling, as well as increased oxidative stress, are stimuli for NF κ B
16 transcription factor (including p65 subunit) upregulation and nuclear translocation, eliciting pro-survival and pro-inflammatory
17 and responses in both HSC and KC [48]. NF κ B signaling may not only contribute to the profibrogenic response but is also
18 proposed to induce a pro-survival response in hepatocytes, promoting preneoplastic and neoplastic lesion development
19 [49]. Indeed, immunohistochemistry for NF κ B p65 revealed both cytoplasmic/nuclear staining in hepatocytes of basophilic
20 lesions and nuclear staining in adjacent hepatocytes, mainly in DEN/CCl₄ group (Supplementary Fig. 4). On the other hand,
21 IL-17 receptor α knockout (IL17RA^{-/-}) or antagonism, as well as the selective inactivation of NF κ B using a decoy, are
22 proposed to ameliorate CCl₄-induced liver fibrosis [48,50]. Thus, when combined (CAF+TRI+CGA) and administered in
23 physiological applicable doses, coffee compounds showed more pronounced results on attenuating the pro-fibrogenic IL-
24 17/NF κ B axis in the liver, in keeping with the reduction on HSC activation and collagen deposition.

25

26 **3.5 The combination of coffee compounds attenuates oxidative stress and induces antioxidant response**

27 Oxidative stress plays pivotal roles in both human and experimental fibrosis/cirrhosis-associated
28 hepatocarcinogenesis [10,11,51]. DEN and CCl₄ hepatic metabolisms generate reactive oxygen species (ROS) and



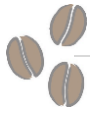
1 nucleophilic metabolites [52,53]. The DEN-induced DNA oxidative damage is implicated in genomic instability,
2 predisposing hepatocytes to preneoplastic and neoplastic lesion development [52]. Moreover, the byproducts of CCl₄
3 metabolism, as well as ROS produced by CD68-positive macrophages, contribute to oxidative stress-mediated signaling
4 that leads to HSC activation and fibrosis [48,53,54]. TBARS, formed as byproducts of lipid peroxidation, are well-accepted
5 markers of oxidative stress [55]. All coffee compound treatments showed a trend in decreasing TBARS and increasing
6 Nrf2 protein levels, but only CAF+TRI+CGA reached significance when compared to untreated and/or DEN/CCl₄ groups
7 ($p=0.013$ and $p=0.010$, respectively) (Fig. 6A and B). DEN/CCl₄ model significantly decreased catalase and GSH-Px
8 activities while presented a trend on reducing SOD activity (Fig. 6C). Although all coffee compound treatments did not alter
9 catalase activity, all treatments GSH-Px activity compared to DEN/CCl₄ ($p<0.0001$) (Fig. 6C). Of note, only CAF+TRI+CGA
10 treatment increased SOD activity compared to DEN/CCl₄ and CAF+TRI groups ($p=0.0011$) (Fig. 6C).

11 The nuclear factor erythroid-related factor 2 (Nrf2) is a transcription factor that controls the expression enzymatic
12 antioxidant agents, including GSH system, catalase, and SOD, which are accounted for ROS and lipid hydroperoxide
13 neutralization [56,57]. *In vitro*, both caffeinated (containing CAF, TRI, and CGA) and decaffeinated coffee (containing TRI
14 and CGA) treatments similarly induced antioxidant response through the upregulation of Nrf2 and downstream antioxidant
15 response element (ARE) axis in HCC cells (HepG2) [58]. Other *in vitro* findings suggest that this antioxidant effect is related
16 to the hydroxycinnamic acid fraction of the beverage, including CGA, and not to CAF [59]. Nonetheless, several *in vivo*
17 reports have shown the individual ability of CAF, TRI or CGA to induce Nrf2 and/or downstream antioxidant agents [26,60],
18 although the exact mechanisms remain to be fully elucidated. Here, findings suggest that the combination of the most
19 common and bioavailable coffee compounds (as seen in caffeinated coffee beverages), rather than caffeine alone, is
20 responsible for reducing oxidative stress and increasing hepatic endogenous antioxidant Nrf2 axis. The individual free
21 radical scavenging capacity of these molecules, mainly CAF and CGA, and their metabolites should be considered to
22 understand the decrease in MDA levels as well [61]. Thus, decreased oxidative stress in the CAF+TRI+CGA group may
23 be in part attributed to the induction of Nrf2 axis and SOD/GSH-Px enzymes, ultimately contributing to reduce fibrosis and
24 to decrease the incidence/number of preneoplastic lesion in this group.

25

26 **3.6 The combination of coffee compounds upregulates miR-144-3p, miR-376a-3p and miR-15b-5p**

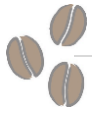
27 Since CAF+TRI+CGA treatment displayed the most pronounced effects on attenuating preneoplastic lesion
28 development and liver fibrosis in comparison to DEN/CCl₄ group, we performed global miRNA expression in this group in



1 order to unveil the potential implications and correlations of miRNA modulation on the previously observed outcomes. We
2 also analyzed the global miRNA expression in the CAF-treated group to identify CAF-modulated miRNAs in the
3 CAF+TRI+CGA-related miRNA signature. DEN/CCl₄-induced fibrosis-associated hepatocarcinogenesis model displayed 19
4 differentially expressed miRNAs compared to the untreated group (14 up and 5 downregulated) (Table 3). Interestingly, both
5 miR-144-3p (FC=0.57; p=0.0054) and miR-376a-3p (FC=0.53; p=0.0008) were downregulated in the liver of DEN/CCl₄-
6 submitted mice. In keeping with our data, miR-144-3p levels were decreased in HCC in a similar DEN-induced
7 hepatocarcinogenesis model in neonatal C3H mice [62]. In human HCC and fibrotic liver, miR-144-3p is downregulated as
8 well, being inversely correlated with tumor staging and profibrotic HSC-related transforming growth factor (TGF)- β 1 marker,
9 respectively [63,64]. Moreover, miR-144-3p (HepG2, Hep3B, and Huh7) and miR-376a-3p (HepG2 and Huh7) expressions
10 are decreased in classical human HCC cell lines [63,65].

11 Conversely, we found that CAF+TRI+CGA treatment upregulated 9/19 (~50%) of the differentially expressed
12 miRNAs in fibrosis-associated hepatocarcinogenesis model, including miR-144-3p (FC=2.14, p=0.001), miR-376a-3p
13 (FC=1.62, p=0.0035) and miR-15b-5p (FC=1.52, p=0.0011) (Table 4, Fig. 7A, Supplementary Fig. 5). CAF treatment
14 upregulated only 5/19 (26%) (Fig. 7A, Supplementary Table 2). Using Venn's diagram (Fig. 7A), we observed that
15 CAF+TRI+CGA and CAF comparisons to DEN/CCl₄ group shared the upregulation of 5 miRNAs (mmu-miR-199a-3p, miR-
16 199a-5p, miR-132-3p, miR-144-3p, miR-376a-3p). Since CAF+TRI+CGA vs. CAF comparison showed no statistical contrast
17 regarding these 5 miRNAs, these are probably modulated by CAF administration. The other 4 miRNAs were exclusively
18 upregulated by CAF+TRI+CGA treatment (miR-15b-5p, miR-342-3p, miR-350-3p and miR-335-5p) (Fig. 7A). Therefore, we
19 considered all 9 miRNAs as part of the CAF+TRI+CGA-related miRNA signature for further target analysis.

20 Noteworthy, treatment with miR-144-3p by intravenous administration diminished HCC size in a DEN-induced
21 neonatal hepatocarcinogenesis model in C3H mice by targeting and decreasing the protein expression of proliferation-
22 related growth factor receptor (EGFR) [62]. Similar findings on attenuating cell proliferation were observed after miR-144-
23 3p or miR-376a-3p mimic transfection to human HCC cells and xenograft mice model [64,65]. Although miR-15b-5p is
24 upregulated in our DEN/CCl₄-induced model (Table 3), as well as in HCC samples and tumor cell lines, previous findings
25 suggest that this miRNA may act a tumor suppressor/antifibrotic miRNA when the expression is way up increased by mimetic
26 transfection. Indeed, miR-15b-5p transfection induced endoplasmic reticulum stress and apoptosis in HCC cells and
27 xenograft mice model [66]. Moreover, miR-15b-5p transfection induced apoptosis in activated rat HSC by targeting



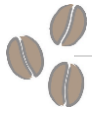
1 antiapoptotic Bcl-2 and enhancing the caspase axis [67]. Thus, the upregulation of miR-144-3p, miR-376a-3p, miR-15b-5p
2 by CAF+TRI+CGA may have direct implications on the attenuation of both fibrosis and preneoplastic lesion development.

3

4 **3.7 Target genes are associated with negative regulation of apoptosis and positive regulation of proliferation**

5 The target analysis of the 9 miRNAs modulated by CAF+TRI+CGA revealed an output of 232 validated genes.
6 Interestingly, according to IPA analysis, most of these validated targets are modulated by miR-15b-5p (197/232)
7 (Supplementary Table 3). Gene enrichment analysis regarding biological processes (BP) evidenced that 18-25% of the
8 target genes were significantly associated with cell death or proliferation functional annotations (Fig. 7B). Especially, 20%
9 (47/232) were associated with “negative regulation of cell death”, while ~18% (43/232) were associated with “positive
10 regulation of cell population proliferation” annotation (Fig. 7B). In addition, KEGG pathway analysis revealed that ~18%
11 (43/232), 12% (28/232), and 7% (17/232) were linked to “pathways in cancer”, “microRNAs in cancer” and “Hepatocellular
12 Carcinoma”, respectively (Fig. 7B). Among other significant terms, we observed that ~14% (32/232), ~9% (21/232) and ~6%
13 (14/232) of genes were associated to the pro-proliferative PI3K-Akt, Ras and HIF-1 pathways, respectively, corroborating
14 with proliferation-related annotations in GO analysis (Fig. 7B).

15 Network analysis using STRING depicted many experimentally determined interactions among the proteins coded
16 by the target genes (Supplementary Fig. 6). Among interactions regarding cell death annotations, we observed key members
17 of the Bcl-2 family, including myeloid cell leukemia sequence 1 (*Mcl1*), B cell leukemia/lymphoma 2 (*Bcl2*) and BCL2-like 2
18 (*Bcl2l2*), which are responsible for a strong anti-apoptotic (pro-survival) signaling (Supplementary Fig. 6 and Supplementary
19 Table 3). These Bcl-2 family members are experimentally validated targets of miR-15b-5p in different tissues, including
20 mouse liver, rat HSCs and human HCC cell lines (Supplementary Tables 3 and 4). Network analysis also evidenced the
21 central role of the epidermal growth factor receptor (*Egfr*) on target interactions in cell proliferation annotations
22 (Supplementary Fig. 6). In the early stages of DEN-induced hepatocarcinogenesis, particularly in preneoplastic foci and
23 adenomas, the downstream signaling mediated by EGFR, which is a target of miR-144-3p (Supplementary Tables 3 and 4),
24 activates of PI3K-Akt and Ras pathways (Fig. 7B), promoting cell proliferation in these lesions [67]. EGFR activation is also
25 proposed to induce the hypoxia-independent overexpression of hypoxia-inducible factor 1 (HIF-1 α) transcription factor and
26 its downstream targets, including vascular endothelial growth factor (VEGF) and c-Met [67]. This interaction was also
27 depicted in our network analysis (Supplementary Fig. 6). It is worthy of note that HIF-1 α and VEGF are miR-144-3p and
28 miR-15b-5p targets, respectively (Supplementary Tables 3 and 4). The EGFR-mediated HIF-1 α activation may be crucial in

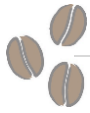


1 the expansion of preneoplastic hepatocyte population and neoplastic progression as well as EGFR-mediated PI3K-Akt/Ras
2 induction [68]. Indeed, *Egfr* shared both positive regulation of cell population proliferation and hepatocellular carcinoma
3 annotations in network analysis (Supplementary Fig. 7), eliciting the importance of this miR-144-3p target on
4 hepatocarcinogenesis.

6 **3.8 The combination of coffee compounds reduces protein levels of Bcl-2 family members and EGFR**

7 In line with target analysis, we observed that the combination of all coffee compounds reduced the protein levels of
8 Bcl-2 family members evaluated (Fig. 8A). In the CAF+TRI+CGA group, Mcl-1 was significantly reduced compared to
9 untreated and DEN/CCl₄ groups ($p=0.019$), whereas Bcl-2 and Bcl2l2 were significantly reduced compared to the untreated
10 group ($p=0.017$ and $p=0.032$, respectively) (Fig. 8A). As expected, CAF treatment did not reduce the protein levels of Bcl-2
11 family members. These findings could indicate coffee compound-mediated upregulation of miR-15b-5p may reduce the
12 protein expression of these key anti-apoptotic proteins, contributing to an increased number of apoptotic cells (cleaved
13 caspase-3 positive) in the adjacent liver (Fig. 3A). Since a miR-15b-5p mimic induced apoptosis in activated HSC in rats by
14 diminishing Bcl-2 mRNA and protein expressions and increasing caspase axis [67], a coffee compound-induced pro-
15 apoptotic signal in HSC may contribute on alleviating fibrosis in this intervention group, as observed (Fig. 5). Indeed, as seen
16 in Sirius red-stained, α -SMA and cleaved caspase-3 immunostained sections, apoptotic cells were found near the regions
17 of increased α -SMA expression (activated HSCs) and collagen accumulation (Supplementary Fig. 8).

18 Moreover, CAF+TRI+CGA treatment reduced by 54% the DEN/CCl₄-mediated increase in EGFR protein levels
19 ($p=0.018$) (Fig. 8B). Our results indicate that coffee compound combination-mediated upregulation of miR-144-3p may
20 alleviate EGFR signaling activation during the early stages of mouse hepatocarcinogenesis, contributing to decrease
21 proliferation (Ki-67-positive hepatocytes) inside preneoplastic foci (Fig. 4A), ultimately attenuating preneoplastic foci
22 development (Fig. 2B, Table 2). Our findings suggest that EGFR-mediated activation of HIF-1 α transcription factor may not
23 be involved in this effect since HIF-1 α and VEGF protein expressions were not modified by CAF+TRI+CGA treatment
24 (Supplementary Fig. 9). The downstream modulation of the PI3K-Akt/Ras axis is hypothesized (Fig. 7B), but complementary
25 studies are warranted. Regarding cell proliferation, we also evaluated the beneficial effects of the coffee compound
26 combination on proliferating nuclear cell antigen (PCNA), a miR-376a-3p target widely accepted as a proliferation marker
27 [69] (Supplementary Table 3). Although CAF+TRI+CGA intervention failed on reducing the number of PCNA-positive
28 hepatocytes in adjacent liver, also presenting a statistical trend ($p=0.051$) on decreasing hepatic PCNA protein levels



1 (Supplementary Fig. 9), only CAF+TRI+CGA reduced the number of PCNA- positive hepatocytes in preneoplastic foci
2 ($p=0.039$) (Fig. 8B), in keeping with Ki-67 findings (Fig. 3B). Despite sharing the upregulation of miR-144-3p and miR-376a-
3 3p, CAF treatment failed on reducing EGFR protein levels and the number of PCNA-positive hepatocytes inside
4 preneoplastic foci (Fig. 8B). Therefore, we hypothesize that other mechanisms, independently from miR-144-3p and miR-
5 376a-3p modulation, may contribute to decreasing the number of preneoplastic lesions in the CAF+TRI+CGA group, as
6 reduced oxidative stress (Fig. 6A).

7

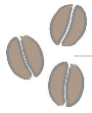
8 **3.9 The combination of coffee compounds enhances cytotoxicity in human HCC cells**

9 The exposure to all concentrations of CAF individually (160, 80, 40 and 20 μM) significantly increased cytotoxicity
10 in C3A cells after 48h of exposure ($p<0.001$), not after 24h (Supplementary Fig. 10). In general, the combination of all coffee
11 compounds (CAF+TRI+CGA) in all tested concentrations displayed more pronounced results on enhancing cytotoxicity
12 compared to untreated-, CAF-treated and/or two drug-treated cells after both 24 and 48h of exposure ($p<0.001$)
13 (Supplementary Fig. 10). LDH *in vitro* findings are in keeping with the *in vivo* results suggesting that the combination of
14 coffee compounds, rather than CAF individually, may attenuate HCC. Increased LDH levels may indicate a disruption of the
15 cell membrane which occurs in necrosis or in late stages of apoptosis [70]. Pro-apoptotic effects of CAF, TRI or CGA are
16 not well-described in HCC cell lines [15], but miR-15b-5p transfection increased the number of late apoptotic cells in human
17 HCC Hep3B cell line by targeting and suppressing Rab1A oncogene [67]. Nonetheless, the correlation between coffee
18 compound-induced cytotoxicity and miR-15b-5p expression *in vitro* needs further evaluation.

19

20 **4. Discussion**

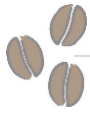
21 In the current study, we aimed at evaluating the effects of CAF individually or combined with TRI and/or CGA on a
22 well-established chemically-induced model of fibrosis-associated hepatocarcinogenesis in C3H/HeJ mice. The modulation
23 of miRNA profile by these compounds was also investigated, correlating changes in expression with liver
24 fibrosis/carcinogenesis outcomes. In summary (Fig. 9), the combination of all compounds displayed the most pronounced
25 effects on alleviating preneoplastic foci development. This treatment also reduced hepatocyte proliferation in preneoplastic
26 lesions and enhanced apoptosis in adjacent tissue. In addition, CAF+TRI+CGA combination alleviated fibrosis, reducing
27 hepatic pro-inflammatory IL-17/NF κ B signaling. Moreover, CAF+TRI+CGA decreased hepatic oxidative stress and
28 enhanced the antioxidant Nrf2 axis. miRNAomic profile showed the upregulation of miR-144-3p and miR-15b-5p, which were



1 in accordance with the reduction of pro-proliferative EGFR (miR-144-3p target) and antiapoptotic Bcl-2 family members (Bcl-
2, Mcl-1, and Bcl2l2, miR-15b-5p targets) were reduced in this group. Noteworthy, this is the first report on the modulation
3 of miRNA expression by bioactive coffee compounds administered in physiologically-based doses during fibrosis-associated
4 hepatocarcinogenesis. Especially, results indicate that miR-15b-5p and miR-144-3p upregulation are potentially implicated
5 in liver fibrosis and carcinogenesis outcomes.

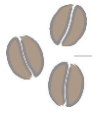
6 Globally, coffee beverage consumption is a popular and safe dietary habit, presenting a growing cultural and
7 economic impact [14,15]. In fact, from 1960 to 2017, global coffee bean production increased by ~100% [71]. There is a
8 wealth of epidemiological evidence pointing out to the hepatoprotective effects of coffee consumption on liver fibrosis and
9 cancer [15-17]. On the other hand, recent data evidenced that decaffeinated coffee, compositionally identical to caffeinated
10 coffee apart from not having CAF, showed none or less pronounced protection [18,19]. In this context, some authors support
11 the “caffeine hypothesis”, directly correlating the hepatoprotective effects of coffee beverages to the widely reported bioactive
12 properties of this xanthine [72]. Nonetheless, coffee is a complex pharmacopeia, and the potential effects of other abundant
13 compounds, as TRI and CGA, were also considered in the present investigation. In previous chemically-induced models of
14 fibrosis and hepatocarcinogenesis in rats, caffeinated coffee resulted in more pronounced attenuation of preneoplastic foci
15 development and collagen III mRNA expression than decaffeinated coffee and CAF alone [23], suggesting that the
16 combination of CAF with other common coffee compounds may account for this protective effect. However, the mechanisms
17 and exact compounds involved in this differential response were still to be unveiled. As highlighted before, both *in vivo* and
18 *in vitro* experimental approaches designed herein reflected this widespread dietary habit. CAF dose was based on average
19 CAF consumption from coffee in the USA and European countries, which are top coffee consuming nations, corresponding
20 to ~280 mg CAF/day (2-3 cups) [30,31]. As reviewed by our group, the allometric HED calculation approach for CAF was
21 not applied in previous fibrosis/hepatocarcinogenesis bioassays, and doses/concentrations are usually above human intake
22 [15]. *In vitro*, the corresponding serum peak of the same CAF intake was chosen (~40 μ M) [22]. Regarding TRI and CGA
23 doses, since epidemiological data on human consumption of these compounds from coffee are scant, we considered the
24 concentration ratio compared with CAF found in coffee beverages [15,22].

25 As hypothesized, only the combination of the most common and highly bioavailable coffee compounds attenuated
26 collagen deposition and preneoplastic foci development (Fig. 9), the main outcomes observed in the DEN-initiated/CCl₄-
27 promoted mouse model at this time point (week 17). DEN is an initiating agent for liver carcinogenesis that causes DNA
28 damage and genomic instability in hepatocytes, while multiple CCl₄ administrations lead to lipid peroxidation and cell death,



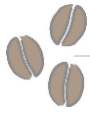
1 providing the necessary necro inflammatory background for HSC activation, collagen deposition and preneoplastic lesion
2 growth [11,52,53]. This short/medium-term bioassay combining DEN and CCl₄ regimens, rather than only DEN-induced
3 models, resembles molecular and morphological features of the corresponding human disease in its early stages since most
4 HCC cases (70 - 90%) are set up on fibrosis/cirrhosis context [3]. Although coffee compounds (8-10 a.m.) and CCl₄ (4-6
5 p.m) were concomitantly administered for 8 weeks, CCl₄ is biotransformed by cytochrome (CYP) 2E1, while CAF is majorly
6 metabolized (90%) by CYP1A2, TRI is methylated by nicotinamide N-methyltransferase (NNMT), and CGA is heavily
7 metabolized by colonic microbiota [15, 52]. Thus, it is unlikely that coffee compound intervention interfered with CCl₄ phase
8 I metabolism.

9 In addition to the reduction in liver fibrosis and preneoplastic foci development, the miRNomic profile of the
10 CAF+TRI+CGA group revealed an upregulation of the tumor suppressors miR-144-3p and miR-376a-3p, and
11 antifibrotic/tumor suppressor miR-15b-5p (Fig. 9). While miRNAs are directly implicated in physiological processes in the
12 liver, including postnatal growth, regeneration, and functioning, their abnormal expression is pivotal in different stages of
13 fibrosis/cirrhosis-associated hepatocarcinogenesis in humans, contributing to sustained cell proliferation, epithelial-
14 mesenchymal transition, invasion, metastasis, angiogenesis, and drug resistance hallmarks [8]. In chemically-induced
15 rodent models of fibrosis and hepatocarcinogenesis, the importance of miRNA deregulation is also reported [6, 12].
16 Especially, the DEN/CCl₄ approach used recapitulated some miRNomic features of the corresponding human disease, as
17 the downregulation of miR-144-3p and miR-376a-3p, eliciting the translational value of the present short/medium-term
18 bioassay. As briefly discussed, miR-144-3p downregulation is also a feature of more advanced stages of DEN-induced
19 mouse hepatocarcinogenesis since it is also observed in HCC [62]. He et al. [62] showed that the intravenous treatment with
20 miR-144-3p increased its levels in tumor and adjacent tissue. When enhanced, miR-144-3p targeted EGFR and decreased
21 downstream pro-proliferative Akt signaling pathway, acting as a tumor suppressor by reducing HCC size. In contrast, miR-
22 144-3p knockout increased EGFR/Akt axis [62]. Noteworthy, 85% of human HCC cases present miR-144-3p downregulation,
23 while 32–66% and 45% display EGFR overexpression and amplification, correspondingly, evoking the importance of this
24 pathway in human liver tumorigenesis as well [64,73]. Here, we reported that the combination of coffee compounds
25 upregulated miR-144-3p while decreased EGFR protein levels (Fig. 9). In line with these findings, CAF+TRI+CGA
26 combination reduced cell proliferation inside preneoplastic foci. These findings suggest that even in the early stages of
27 hepatocarcinogenesis, miR-144-3p upregulation may target EGFR, decreasing cell proliferation and resulting in lower
28 preneoplastic foci development (Fig. 9).



1 The roles of miR-367a-3p on rodent models of liver fibrosis and carcinogenesis are not described yet. However,
2 the downregulation of this miRNA is featured in both physiological and pathological liver contexts. Around 80% of human
3 HCC samples displayed decreased levels of this miRNA, and similar findings were observed in HCC cell lines [65].
4 Interestingly, this non-coding RNA was also downregulated during liver regeneration after partial hepatectomy in mice,
5 suggesting underlying roles in controlling hepatocyte proliferation [65]. Our findings are the first to report the downregulation
6 of this miRNA during the early stages of chemically-induced fibrosis-associated hepatocarcinogenesis. *In vitro*, the
7 transfection of miR-376a-3p mimics exerted a tumor-suppressive effect in the Huh7 HCC cell line by targeting p85 α [65]. In
8 mice, the only experimentally validated target of this miRNA is PCNA, which is an auxiliary protein of DNA polymerase δ , an
9 enzyme necessary for DNA synthesis during cell replication [69]. We found that CAF+TRI+CGA combination upregulated
10 miR-376a-3p while decreased the number of PCNA-positive hepatocytes in preneoplastic foci, indicating that, along with
11 miR-144-3p, the modulation this miRNA could result on a reduced number of preneoplastic foci (Fig. 9). Interestingly, we
12 found a reduction in cell proliferation indexes (Ki-67-and PCNA-positive hepatocytes) just inside preneoplastic foci, whereas
13 CAF+TRI+CGA treatment did not alter proliferation in adjacent tissue. Since preneoplastic foci display increased cell
14 proliferation compared to adjacent tissue, in part due to mutations in *Braf* and *Hras* [43,44], our findings could indicate that
15 these lesions may be sensitive to CAF+TRI+CGA-mediated modulation of these tumor suppressor miRNAs.

16 The combination of all coffee compounds upregulated miR-15b-5p in the liver as well. On activated HSC isolated
17 from rat liver, the upregulation of miR-15 family by the transfection of mimics (including miR-15a, miR-15b, and miR-16)
18 contributed to cell death by targeting anti-apoptotic proteins, such as Bcl-2, and subsequently increasing caspase levels
19 (caspase-3, -8 and -9) [67]. Hence, the modulation of the miR-15 family is proposed as a novel therapeutic strategy for liver
20 fibrosis, considering that HSC death could attenuate collagen deposition [67]. In line with increased miR-15b-5p expression,
21 we observed that protein levels of antiapoptotic Bcl-2 family members were reduced while apoptosis (cleaved caspase-3-
22 positive cells) was increased in adjacent tissue in CAF+TRI+CGA treatment (Fig. 9). Bcl-2, Mcl-1 and Bcl2l2, proteins placed
23 in the mitochondrial membrane, bind to pro-apoptotic BH3 sensitizers, initiators, or pore formers, avoiding mitochondrial
24 permeability, cytochrome release and activation of caspase cascade [74]. Then, results indicate that CAF+TRI+CGA-
25 mediated upregulation of miR-15b-5p and decrease of Bcl-2 family may lead to HSC apoptotic cell death (thus reduced α -
26 SMA protein expression), contributing to decreased collagen deposition (Fig. 9). Nonetheless, the negative modulation of
27 oxidative stress and proinflammatory IL-17/NF- κ B axis should also be accounted for decreased liver fibrosis, since it appears



1 to be independent of miRNA modulation (Fig. 9). Along with miR-144-3p and miR-376a-3p modulation, the amelioration of
2 hepatic fibrotic context by CAF+TRI+CGA may indirectly contribute to slow preneoplastic foci development (Fig. 9).

3 Finally, none is reported on how alkaloids and polyphenols could directly alter canonical and non-canonical miRNA
4 biogenesis, but the modulation of the crosstalk between cellular pathways and miRNA biogenesis is speculated. The
5 activation of the pro-inflammatory NF- κ B transcription factor is responsible for upregulating some anti-inflammatory miRNA
6 families in negative feedback [75]. EGFR upregulation is also responsible for argonaute 2 (AGO2) phosphorylation, reducing
7 its binding to Dicer and thus inhibiting miRNA processing from precursor to mature miRNAs, which could hinder the
8 maturation of specific tumor-suppressor-like miRNAs [76]. In addition, oxidative stress is proposed to cause miRNA
9 deregulation at the level of transcription, processing, cellular localization and functioning [75]. Thus, the relationship between
10 CAF+TRI+CGA-mediated effects on oxidative stress, NF- κ B, EGFR and miRNA biogenesis should be evaluated on future
11 investigations.

12 In conclusion, findings suggest that the combination of the most common and bioavailable coffee compounds as
13 seen in coffee beverages, rather than CAF alone, attenuates chemically-induced fibrosis and hepatocarcinogenesis. Results
14 also indicate that these beneficial effects may be mediated by alterations in miRNA expression and provide mechanistical
15 insights on the hepatoprotective population-level effects attributed to caffeinated coffee consumption. Finally, the modulation
16 of tumor suppressor and antifibrotic miRNAs by naturally occurring compounds may open a preventive avenue, as these
17 non-coding RNAs should be considered potential new targets for further translational investigations on early fibrosis-
18 associated hepatocarcinogenesis.

19

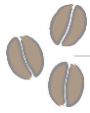
20 **5. Conflicts of interest**

21 The authors declare no conflict of interest.

22

23 **6. Acknowledgments**

24 The authors would like to thank Professor Amedeo Columbano for his suggestions during manuscript preparation.
25 We are grateful to Dr. Pia Sulas' and Dr. Lucas Tadeu Bidinotto's assistance during miRNomic data interpretation. We also
26 express our gratitude to Professor Débora Cristina Damasceno and Professor Ana Angélica Henrique Fernandes for their
27 help during TBARS and antioxidant agent determination, respectively. The authors also would like to thank the employees
28 of Unidade de Pesquisa Experimental (Unipex, Botucatu Medical School) for their support during animal experimentation.



1 **7. Funding information**

2 Guilherme R. Romualdo and Gabriel B. Prata were the recipient of fellowships and grants from the São Paulo
3 Research Foundation (FAPESP)(#2016/12015-0 and #2017/16596-0, respectively). Guilherme R.Romualdo was the
4 recipient of a doctoral exchange program fellowship from Coordenação de Aperfeiçoamento de Pessoal de Nível Superior
5 -Brasil (CAPES) (#88881.188786/2018-01). This study was financed in part by CAPES - Finance Code 001. Luis F. Barbisan
6 was the recipient of support research from FAPESP (grant #2016/14420-0). The funders had no influence on the writing and
7 interpretation of data

8

9

10

11

12

13

14

15

16

17

18

19

20

21

22

23

24

25

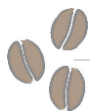
26

27

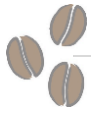


References

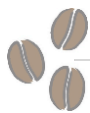
- [1] Global Cancer Observatory - World Health Organization. Estimated number of incident cases and deaths worldwide, <https://gco.iarc.fr/today/online-analysis-multi-bars>; 2018 [accessed 9 September 2019].
- [2] Greten TF, Papendorf F, Bleck JS, Kirchhoff T, Wohlbered T, Kubicka S, et al. Survival rate in patients with hepatocellular carcinoma: A retrospective analysis of 389 patients. *Br J Cancer* 2005;92:1862–8. doi:10.1038/sj.bjc.6602590.
- [3] Yang JD, Kim WR, Coelho R, Mettler TA, Benson JT, Sanderson SO, et al. Cirrhosis is present in most patients with Hepatitis B and Hepatocellular Carcinoma. *Clin Gastroenterol Hepatol* 2011;9:64–70. doi: 10.1016/j.cgh.2010.08.019.
- [4] Baecker A, Liu X, La Vecchia C and Zhang Z-F. Worldwide incident hepatocellular carcinoma cases attributable to major risk factors. *Eur J Cancer Prev* 2018; 27(3):205–212. doi: 10.1097/CEJ.0000000000000428
- [5] The Cancer Genome Atlas Research Network. Comprehensive and Integrative Genomic Characterization of Hepatocellular Carcinoma. *Cell* 2017;169:1327–1341.e23. doi: 10.1016/j.cell.2017.05.046.
- [6] Sulas P, Di Tommaso L, Novello C, Rizzo F, Rinaldi A, Weisz A, et al. A Large Set of miRNAs Is Dysregulated from the Earliest Steps of Human Hepatocellular Carcinoma Development. *Am J Pathol* 2018;188:785–94. doi:10.1016/j.ajpath.2017.10.024.
- [7] O'Brien J, Hayder H, Zayed Y, Peng C. Overview of microRNA biogenesis, mechanisms of actions, and circulation. *Front Endocrinol* 2018;9:1–12. doi:10.3389/fendo.2018.00402.
- [8] Otsuka M, Kishikawa T, Yoshikawa T, Ohno M, Takata A, Shibata C, et al. The role of microRNAs in hepatocarcinogenesis: Current knowledge and future prospects. *J Gastroenterol* 2014;49:173–84. doi:10.1007/s00535-013-0909-8.
- [9] Crespo Yanguas S, Cogliati B, Willebrords J, Maes M, Colle I, van den Bossche B, et al. Experimental models of liver fibrosis. *Arch Toxicol* 2016;90:1025–48. doi:10.1007/s00204-015-1543-4.
- [10] Romualdo GR, Grassi TF, Goto RL, Tablas MB, Bidinotto LT, Fernandes AAH, et al. An integrative analysis of chemically-induced cirrhosis-associated hepatocarcinogenesis: Histological, biochemical and molecular features. *Toxicol Lett* 2017;281:84–94. doi:10.1016/j.toxlet.2017.09.015.
- [11] Romualdo GR, Prata GB, da Silva TC, Fernandes AAH, Moreno FS, Cogliati B, et al. Fibrosis-associated hepatocarcinogenesis revisited: Establishing standard medium-term chemically-induced male and female models. *PLoS One* 2018;13:1–26. doi:10.1371/journal.pone.0203879.
- [12] Hyun J, Park J, Wang S, Kim J, Lee HH, Seo YS, et al. MicroRNA expression profiling in CCl₄-induced liver fibrosis of *Mus musculus*. *Int J Mol Sci* 2016;17:1–21. doi:10.3390/ijms17060961.
- [13] Wiseman MJ. Nutrition and cancer: Prevention and survival. *Br J Nutr* 2018;14:1-7. doi:10.1017/S0007114518002222.
- [14] International Coffee Organization. Historical data on the global coffee trade, http://www.ico.org/new_historical.asp?section=Statistics; 2018 [accessed 9 September 2019].
- [15] Romualdo GR, Rocha AB, Vinken M, Cogliati B, Moreno FS, Chaves MAG, et al. Drinking for protection? Epidemiological and experimental evidence on the beneficial effects of coffee or major coffee compounds against gastrointestinal and liver carcinogenesis. *Food Res Int* 2019;123:567–89. doi:10.1016/j.foodres.2019.05.029.
- [16] Liu F, Wang X, Wu G, Chen L, Hu P, Ren H, et al. Coffee Consumption Decreases Risks for Hepatic Fibrosis and Cirrhosis: A Meta-Analysis. *PLoS One* 2015;10:e0142457. doi:10.1371/journal.pone.0142457.



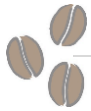
- [17] Bravi F, Tavani A, Bosetti C, Boffetta P, La Vecchia C. Coffee and the risk of hepatocellular carcinoma and chronic liver disease: A systematic review and meta-analysis of prospective studies. *Eur J Cancer Prev* 2017;26:368–77. doi:10.1097/CEJ.0000000000000252.
- [18] Godos J, Micek A, Marranzano M, Salomone F, Del Rio D, Ray S. Coffee consumption and risk of biliary tract cancers and liver cancer: A dose–response meta-analysis of prospective cohort studies. *Nutrients* 2017; 28:9(9) E950. doi:10.3390/nu9090950.
- [19] Kennedy OJ, Roderick P, Buchanan R, Fallowfield JA, Hayes PC, Parkes J. Coffee, including caffeinated and decaffeinated coffee, and the risk of hepatocellular carcinoma: A systematic review and dose-response meta-analysis. *BMJ Open* 2017;7:e013739. doi:10.1136/bmjopen-2016-013739.
- [20] Caprioli G, Cortese M, Maggi F, Minnetti C, Odello L, Sagratini G, et al. Quantification of caffeine, trigonelline and nicotinic acid in espresso coffee: The influence of espresso machines and coffee cultivars. *Int J Food Sci Nutr* 2014;65:465–9. doi:10.3109/09637486.2013.873890.
- [21] Caporaso N, Genovese A, Canela MD, Civitella A, Sacchi R. Neapolitan coffee brew chemical analysis in comparison to espresso, moka and American brews. *Food Res Int* 2014;61:152–60. doi:10.1016/j.foodres.2014.01.020.
- [22] Lang R, Dieminger N, Beusch A, Lee YM, Dunkel A, Suess B, et al. Bioappearance and pharmacokinetics of bioactives upon coffee consumption. *Anal Bioanal Chem* 2013;405:8487–503. doi:10.1007/s00216-013-7288-0.
- [23] Furtado KS, Prado MG, Aguiar e Silva MA, Dias MC, Rivelli DP, Rodrigues MAM, et al. Coffee and caffeine protect against liver injury induced by thioacetamide in male wistar rats. *Basic Clin Pharmacol Toxicol* 2012;111:339–47. doi:10.1111/j.1742-7843.2012.00903.x.
- [24] Furtado KS, Polletini J, Dias MC, Rodrigues MAM, Barbisan LF. Prevention of rat liver fibrosis and carcinogenesis by coffee and caffeine. *Food Chem Toxicol* 2014;64:20–6. doi:10.1016/j.fct.2013.11.011.
- [25] Zhang DF, Zhang F, Zhang J, Zhang RM, Li R. Protection effect of trigonelline on liver of rats with non-alcoholic fatty liver diseases. *Asian Pac J Trop Med* 2015;8:651–4. doi:10.1016/j.apjtm.2015.07.012.
- [26] Shi H, Shi A, Dong L, Lu X, Wang Y, Zhao J, et al. Chlorogenic acid protects against liver fibrosis *in vivo* and *in vitro* through inhibition of oxidative stress. *Clin Nutr* 2016;35:1366–73. doi:10.1016/j.clnu.2016.03.002.
- [27] Bishayee A, Bhatia D. Epigenetics of Cancer prevention. 1st ed., New York: Academic Press; 2018.
- [28] Thoolen B, Maronpot RR, Harada T, Nyska A, Rousseaux C, Nolte T, et al. Proliferative and nonproliferative lesions of the rat and mouse hepatobiliary system. *Toxicol Pathol* 2010;38:5S–81S. doi:10.1177/0192623310386499.
- [29] National Research Council. Committee for the Update of the Guide for the Care and Use of Laboratory Animals. Guide for the Care and Use of Laboratory Animals. 8th ed. Washington (DC): National Academies Press; 2011.
- [30] Mitchell DC, Knight CA, Hockenberry J, Teplansky R, Hartman TJ. Beverage caffeine intakes in the U.S. *Food Chem Toxicol* 2014;63:136–42. doi:10.1016/j.fct.2013.10.042.
- [31] European Food Safety Authority. Scientific opinion on the safety of caffeine. *EFSA J* 2015;13:4102–4222. doi:10.2903/j.efsa.2015.4102.
- [32] Reagan-Shaw S, Nihal M, Ahmad N. Dose translation from animal to human studies revisited. *FASEB J* 2008;22:659–61. doi:10.1096/fj.07-9574LSF.
- [33] Hsu SJ, Lee FY, Wang SS, Hsin IF, Lin TY, Huang HC, et al. Caffeine ameliorates hemodynamic derangements and portosystemic collaterals in cirrhotic rats. *Hepatology* 2015;61:1672–84. doi:10.1002/hep.27679.
- [34] Ferreira ALA, Machado PEA, Matsubara LS. Lipid peroxidation, antioxidant enzymes and glutathione levels in human erythrocytes exposed to colloidal iron hydroxide *in vitro*. *Braz J Med Biol Res* 1999;32, 689–94. doi:10.1590/S0100-879X1999000600004



- [35] Bergmeyer HU. *Methods of Enzymatic Analysis*. 2nd ed. New York: Academic Press; 1974.
- [36] Nakamura W, Hojoda S, Hayashi K. Purification and properties of rat liver glutathione peroxidase. *Biochim Biophys Acta* 1974;358:251–61. doi: 10.1016/0005-2744(74)90455-0
- [37] Ewing JF, Janero DR. Microplate superoxide dismutase assay employing a nonenzymatic superoxide generator. *Anal Biochem* 1995;232:243–8. doi:10.1006/abio.1995.0014
- [38] Waggott D, Chu K, Yin S, Wouters BG, Liu FF, Boutros PC. NanoStringNorm: An extensible R package for the pre-processing of nanostring mRNA and miRNA data. *Bioinformatics* 2012;28:1546–1548. <https://doi.org/10.1093/bioinformatics/bts188>.
- [39] Afgan E, Baker D, Batut B, Van Den Beek M, Bouvier D, Ech M, et al. The Galaxy platform for accessible, reproducible and collaborative biomedical analyses: 2018 update. *Nucleic Acids Res* 2018;46:W537–44. doi:10.1093/nar/gky379.
- [40] The Gene Ontology Consortium. Expansion of the gene ontology knowledgebase and resources: The gene ontology consortium. *Nucleic Acids Res* 2017;45:D331–8. doi:10.1093/nar/gkw1108.
- [41] Huang DW, Sherman BT, Lempicki RA. Systematic and integrative analysis of large gene lists using DAVID bioinformatics resources. *Nat Protoc* 2009;4:44–57. doi:10.1038/nprot.2008.211.
- [42] Szklarczyk D, Gable AL, Lyon D, Junge A, Wyder S, Huerta-Cepas J, et al. STRING v11: Protein-protein association networks with increased coverage, supporting functional discovery in genome-wide experimental datasets. *Nucleic Acids Res* 2019;47:D607–13. doi:10.1093/nar/gky1131.
- [43] Buchmann A, Mahr J, Bauer-Hofmann R, Schwarz M. Mutations at codon 61 of the *Ha-ras* proto-oncogene in precancerous liver lesions of the B6C3F1 mouse. *Mol Carcinog* 1989;2:121–5. doi:10.1002/mc.2940020303.
- [44] Yamamoto M, Tanaka H, Xin B, Nishikawa Y, Yamazaki K, Shimizu K, et al. Role of the *BrafV637E* mutation in hepatocarcinogenesis induced by treatment with diethylnitrosamine in neonatal B6C3F1 mice. *Mol Carcinog* 2017;56:478–88. doi:10.1002/mc.22510.
- [45] Bannasch P, Haertel T, Su Q. Significance of Hepatic Preneoplasia in Risk Identification and Early Detection of Neoplasia. *Toxicol Pathol* 2003;31:134–9. doi:10.1080/01926230390173923.
- [46] Klaunig JE, Kamendulis LM. Mechanisms of cancer chemoprevention in hepatic carcinogenesis: modulation of focal lesion growth in mice. *Toxicol Sci* 1999;52:101–6.
- [47] Tsuchida T, Friedman SL. Mechanisms of hepatic stellate cell activation. *Nat Rev Gastroenterol Hepatol* 2017;14:397–411. doi:10.1038/nrgastro.2017.38.
- [48] Meng F, Wang K, Aoyama T, Grivennikov SI, Paik Y, Scholten D, et al. Interleukin-17 signaling in inflammatory, Kupffer cells, and hepatic stellate cells exacerbates liver fibrosis in mice. *Gastroenterology* 2012;143:765–776.e3. doi:10.1053/j.gastro.2012.05.049.
- [49] Luedde T, Schwabe RF. NF- κ B in the liver—linking injury, fibrosis and hepatocellular carcinoma. *Nat Rev Gastroenterol Hepatol* 2011;8:108–18. doi:10.1038/nrgastro.2010.213.
- [50] Son G, Imuro Y, Seki E, Hirano T, Kaneda Y, Fujimoto J. Selective inactivation of NF- κ B in the liver using NF- κ B decoy suppresses CCl₄-induced liver injury and fibrosis. *Am J Physiol Liver Physiol* 2007;293:G631–9. doi:10.1152/ajpgi.00185.2007.
- [51] Marra M, Sordelli IM, Lombardi A, Lamberti M, Tarantino L, Giudice A, et al. Molecular targets and oxidative stress biomarkers in hepatocellular carcinoma: An overview. *J Transl Med* 2011;9:1–14. doi:10.1186/1479-5876-9-171.
- [52] Verna L, Whysner J, Williams GM. N-Nitrosodiethylamine mechanistic data and risk assessment: Bioactivation, DNA-adduct formation, mutagenicity, and tumor initiation. *Pharmacol Ther* 1996;71:57–81. doi:10.1016/0163-7258(96)00062-9.



- [53] Weber LWD, Boll M, Stampfl A. Hepatotoxicity and mechanism of action of haloalkanes: carbon tetrachloride as a toxicological model. *Crit Rev Toxicol* 2003;33:105–36. doi:10.1080/713611034.
- [54] Kinoshita M, Uchida T, Sato A, Nakashima M, Nakashima H, Shono S, et al. Characterization of two F4/80-positive Kupffer cell subsets by their function and phenotype in mice. *J Hepatol* 2010;53:903–10. doi:10.1016/j.jhep.2010.04.037.
- [55] Ayala A, Muñoz MF, Argüelles S. Lipid peroxidation: production, metabolism, and signaling mechanisms of malondialdehyde and 4-hydroxy-2-nonenal *Oxid Med Cell Longev*. 2014;2014:360438. doi: 10.1155/2014/360438.
- [56] Zhu H, Itoh K, Yamamoto M, Zweier JL, Li Y. Role of Nrf2 signaling in regulation of antioxidants and phase 2 enzymes in cardiac fibroblasts: Protection against reactive oxygen and nitrogen species-induced cell injury. *FEBS Lett* 2005;579:3029–36. doi:10.1016/j.febslet.2005.04.058.
- [57] Marengo B, Nitti M, Furfaro AL, Colla R, Ciucis C De, Marinari UM, et al. Redox homeostasis and cellular antioxidant systems: Crucial players in cancer growth and therapy. *Oxid Med Cell Longev* 2016;2016: 2016: 6235641. doi:10.1155/2016/6235641.
- [58] Kalthoff S, Ehmer U, Freiberg N, Manns MP, Strassburg C P. Coffee induces expression of glucuronosyltransferases by the aryl hydrocarbon receptor and Nrf2 in liver and stomach. *Gastroenterol* 2010;139:1699–1710. doi:10.1053/j.gastro.2010.06.048
- [59] Baeza G, Amigo-Benavent M, Sarriá B, Goya L, Mateos R, Bravo L. Green coffee hydroxycinnamic acids but not caffeine protect human HepG2 cells against oxidative stress. *Food Res Int* 2014;62:1038–46. doi:10.1016/j.foodres.2014.05.035
- [60] Zhou J, Zhou S, Zeng S. Experimental diabetes treated with trigonelline: effect on β cell and pancreatic oxidative parameters. *Fundam Clin Pharmacol* 2013;27:279–87. doi: 10.1111/j.1472-8206.2011.01022.x.
- [61] Liang N, Kitts DD. Antioxidant property of coffee components: assessment of methods that define mechanisms of action. *Molecules* 2014;19:19180–208. doi: 10.3390/molecules191119180.
- [62] He Q, Wang F, Honda T, Lindquist DM, Dillman JR, Timchenko NA, et al. Intravenous miR-144 inhibits tumor growth in diethylnitrosamine-induced hepatocellular carcinoma in mice. *Tumor Biol* 2017;39:1–8. doi:10.1177/1010428317737729.
- [63] Liu Z, Yi J, Ye R, Liu J, Duan Q, Xiao J, et al. miR-144 regulates transforming growth factor- β 1 induced hepatic stellate cell activation in human fibrotic liver. *Int J Clin Exp Pathol* 2015;8:3994–4000.
- [64] Yu M, Lin Y, Zhou Y, Jin H, Hou B, Wu Z, et al. MiR-144 suppresses cell proliferation, migration, and invasion in hepatocellular carcinoma by targeting SMAD4. *Onco Targets Ther* 2016;9:4705–14. doi:10.2147/OTT.S88233.
- [65] Zheng Y, Yin L, Chen H, Yang S, Pan C, Lu S, et al. miR-376a suppresses proliferation and induces apoptosis in hepatocellular carcinoma. *FEBS Lett* 2012;586:2396–403. doi:10.1016/j.febslet.2012.05.054.
- [66] Yang Y, Hou N, Wang X, Wang L, Chang S, He K, et al. miR-15b-5p induces endoplasmic reticulum stress and apoptosis in human hepatocellular carcinoma, both *in vitro* and *in vivo*, by suppressing Rab1A. *Oncotarget* 2015;6. doi:10.18632/oncotarget.3970.
- [67] Guo CJ, Pan Q, Li DG, Sun H, Liu BW. miR-15b and miR-16 are implicated in activation of the rat hepatic stellate cell: An essential role for apoptosis. *J Hepatol* 2009;50:766–78. doi:10.1016/j.jhep.2008.11.025.
- [68] Tanaka H, Yamamoto M, Hashimoto N, Miyakoshi M, Tamakawa S, Yoshie M, et al. Hypoxia-independent overexpression of hypoxia-inducible factor 1 α as an early change in mouse hepatocarcinogenesis. *Cancer Res* 2006;66:11263–70. doi:10.1158/0008-5472.CAN-06-1699.



[69] Eldrige SR, Butterworth BE, Goldsworthy TL. Proliferating cell nuclear antigen: a marker for hepatocellular proliferation in rodents. *Environ Health Perspect* 1993;101:211-8.

[70] Maes M, Vanhaecke T, Cogliati B, Yanguas SC, Willebrords J, et al. Measurement of apoptotic and necrotic cell death in primary hepatocyte cultures. *Methods Mol Biol.* 2015;1250:349-61. doi: 10.1007/978-1-4939-2074-7_27.

[71] Food and Agriculture Organization of the United Nations. Production quantities of Coffee, green by country Average 1961-2017, <http://www.fao.org/faostat/en/#data/QC/visualize>; 2017 [accessed 21 October 2019]

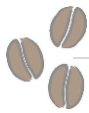
[72] Dranoff JA. Coffee consumption and prevention of cirrhosis: In support of the caffeine hypothesis. *Gene Expr* 2018;18:1–3. doi:10.5221617/X15046391179559.

[73] Buckley AF, Burgart LJ, Sahai V, Kakar S. Epidermal growth factor receptor expression and gene copy number in conventional hepatocellular carcinoma. *Am J Clin Pathol* 2008;129:245–51. doi:10.1309/WF10QAAED3PP93BH.

[74] Kale J, Osterlund EJ, Andrews DW. BCL-2 family proteins: changing partners in the dance towards death. *Cell Death Differ* 2017;25:65–80. doi:10.1038/cdd.2017.186.

[75] Olejniczak M, Kotowska-Zimmer A, Krzyzosiak W. Stress-induced changes in miRNA biogenesis and functioning. *Cell Mol Life Sci* 2018;75:177–91. doi:10.1007/s00018-017-2591-0.

[76] Shen J, Xia W, Khotskaya YB, Huo L, Nakanishi K, Lim SO, et al. EGFR modulates microRNA maturation in response to hypoxia through phosphorylation of AGO2. *Nature* 2013;497:383–7. doi:10.1038/nature12080.



9. Figures

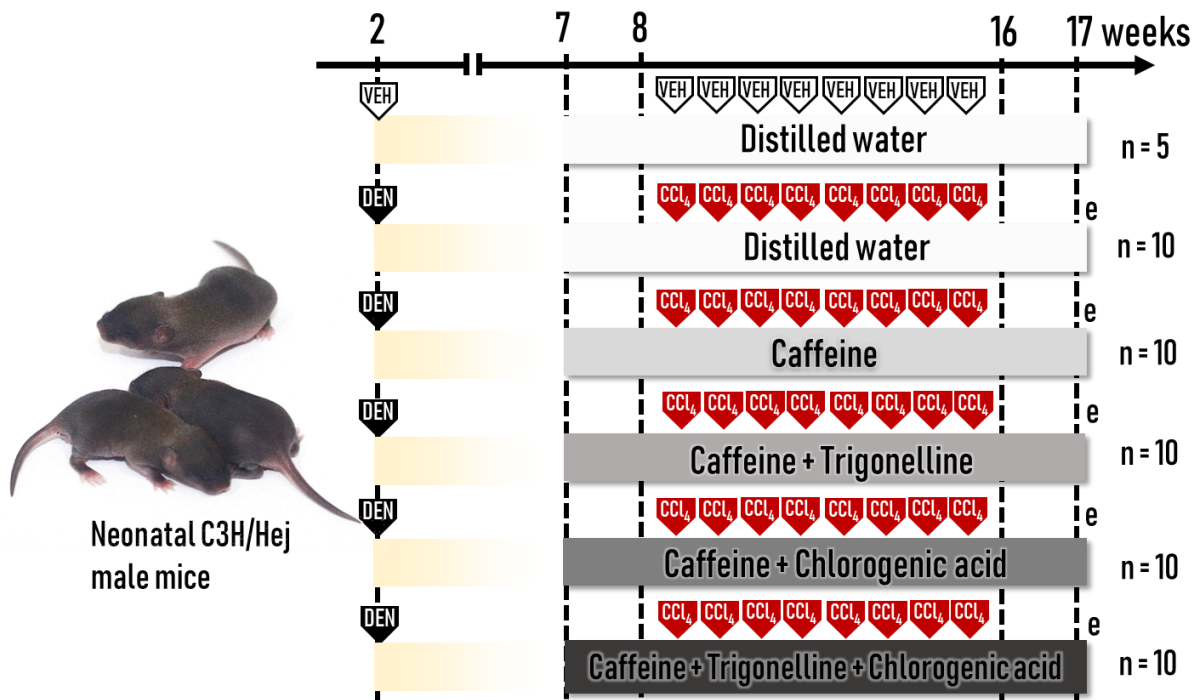


Figure 1. Animal study diagram. DEN = 1x diethylnitrosamine [10 mg/Kg body weight (b.wt.), intraperitoneal injections]; CCl₄ = 3x/week carbon tetrachloride (0.25 to 1.50 μ L/g b.wt., intraperitoneal injections); VEH = saline 0.9% or corn oil vehicle; CAF = caffeine (50 mg/Kg b.wt., intragastrically administered, 5x/week); TRI, CGA = trigonelline and/or chlorogenic acid (25 mg/Kg b.wt., intragastrically administered, 5x/week); n = number of mice/group; e = euthanasia.

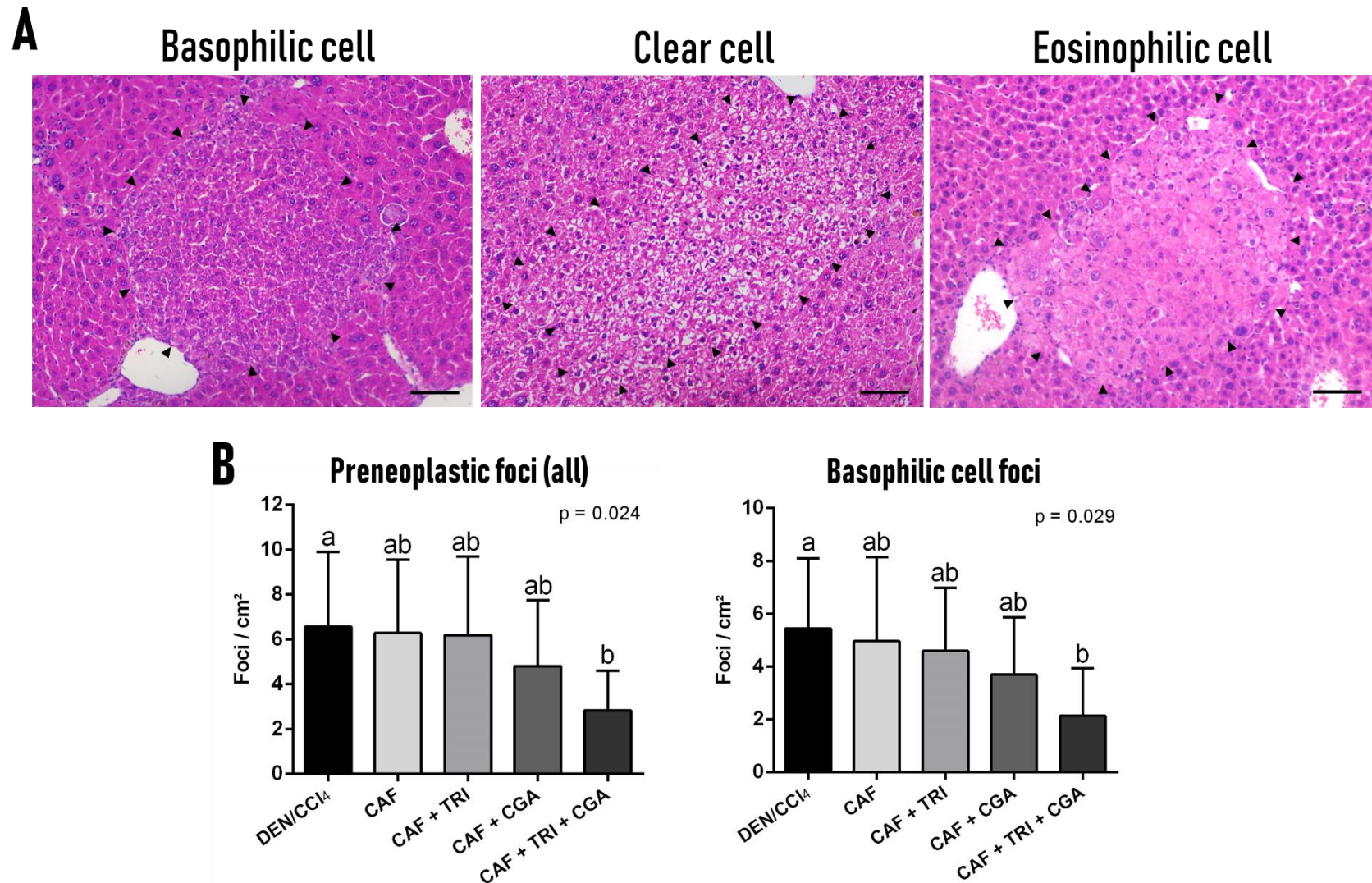
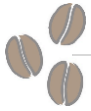


Figure 2. Effects of caffeine (CAF) individually or combined to trigonelline (TRI) and/or chlorogenic acid (CGA) on preneoplastic foci development during DEN/CCl₄-induced fibrosis-associated hepatocarcinogenesis. **(A)** Representative photomicrographs of H&E-stained sections showing basophilic, clear and eosinophilic cell foci (arrowheads, 20× objective, scale bar=50 μm). **(B)** Number of preneoplastic foci (all types) and basophilic foci *per* liver area. Data are mean ± S.D. n = 5 (untreated) to 10 (other groups) mice/group. DEN/CCl₄ = diethylnitrosamine 10 mg/kg b.wt. i.p. at week 2 and carbon tetrachloride 0.25 to 1.50 μL/g b.wt. i.p. from week 8 to 16. CAF = caffeine (50 mg/Kg b.wt.) and TRI, CGA = trigonelline and/or chlorogenic acid (25 mg/Kg b.wt., both) intragastrically administered from week 7 to 17 (see Material & Methods section). Different letters correspond to statistical difference among groups by ANOVA and *post hoc* Tukey test (p<0.05).

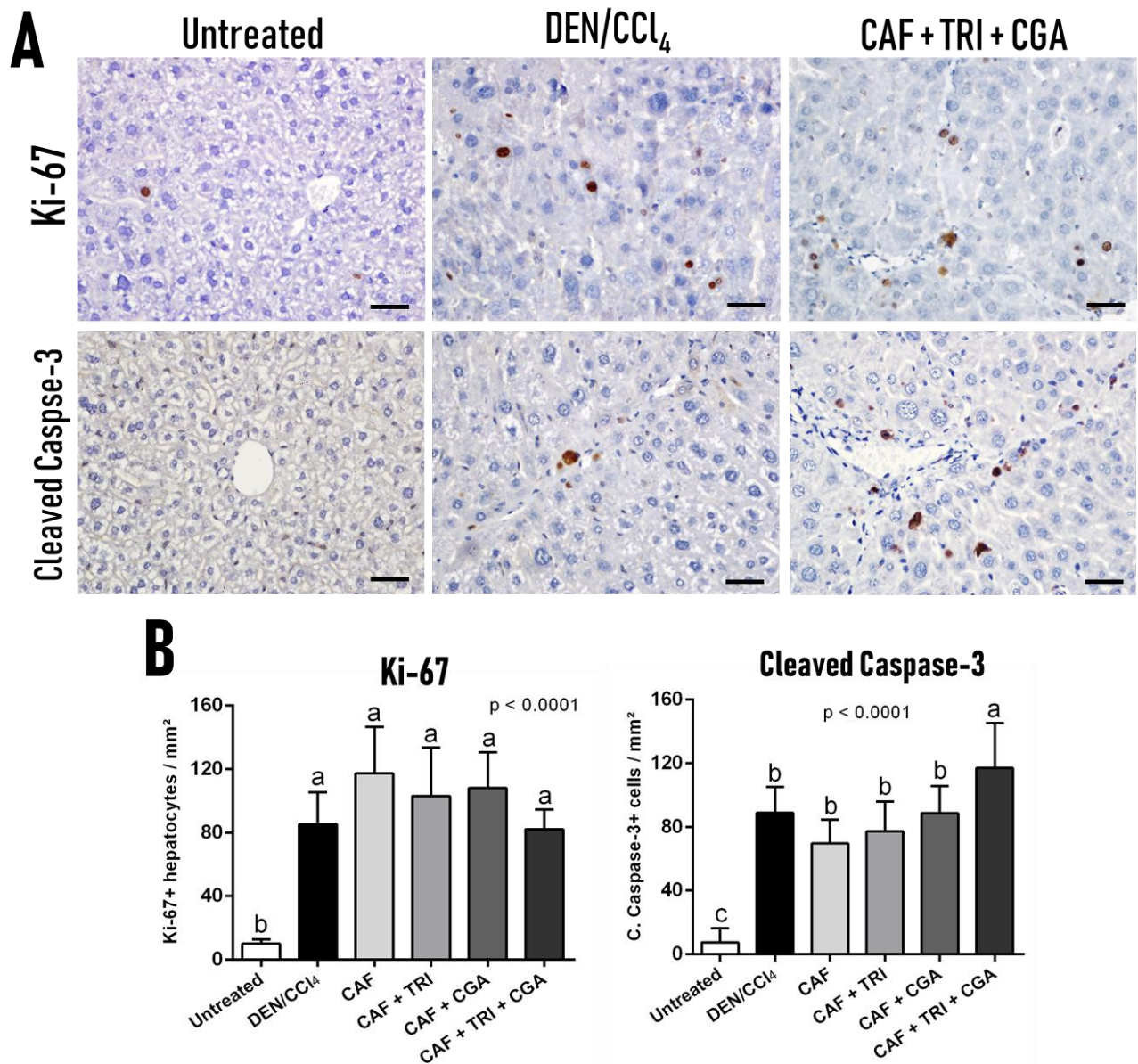
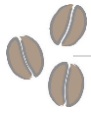


Figure 3. Effects of caffeine (CAF) individually or combined to trigonelline (TRI) and/or chlorogenic acid (CGA) on cell proliferation (Ki-67) and apoptosis (Cleaved Caspase-3) in adjacent liver tissue during DEN/CCl₄-induced fibrosis-associated hepatocarcinogenesis. **(A)** Representative photomicrographs (40× objective, scale bar=25 μm). **(B)** Semiquantitative analysis. Data are mean ± S.D. n= 5 (untreated) to 8 (other groups) mice/group. DEN/CCl₄ = diethylnitrosamine 10 mg/kg b.wt. i.p. at week 2 and carbon tetrachloride 0.25 to 1.50 μL/g b.wt. i.p. from week 8 to 16. CAF = caffeine (50 mg/Kg b.wt.) And TRI, CGA = trigonelline and/or chlorogenic acid (25 mg/Kg b.wt., both) intragastrically administered from week 7 to 17 (see Material & Methods section). Different letters correspond to statistical difference among groups by ANOVA and *post hoc* Tukey test ($p < 0.05$).

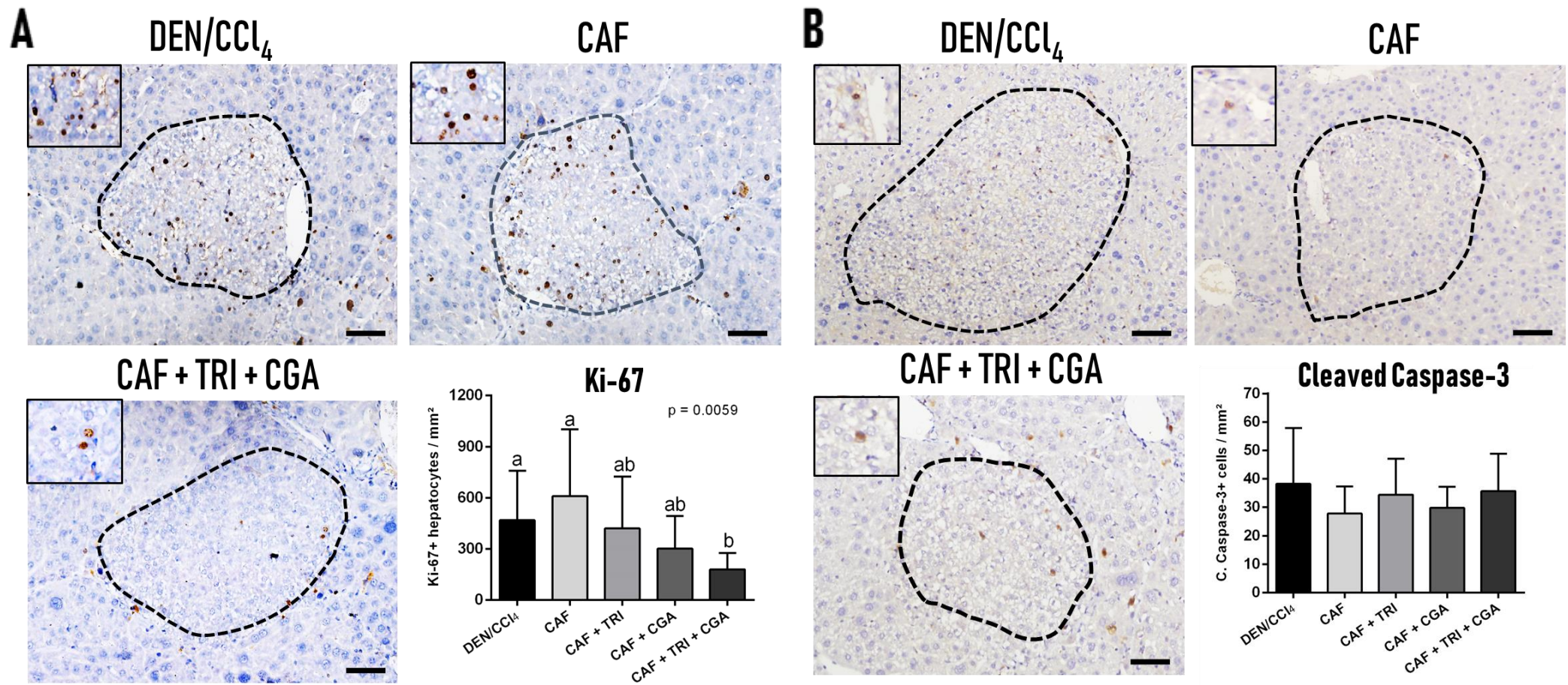
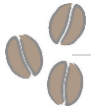


Figure 4. Effects of caffeine (CAF) individually or combined to trigonelline (TRI) and/or chlorogenic acid (CGA) on (A) cell proliferation (Ki-67) and (B) apoptosis (Cleaved Caspase-3) in preneoplastic foci during DEN/CCl₄-induced fibrosis-associated hepatocarcinogenesis. Representative photomicrographs (20× objective, scale bar=50 μm) and semiquantitative analysis are presented. Data are mean ± S.D. n = 5 (untreated) to 8 (other groups) mice/group. DEN/CCl₄ = diethylnitrosamine 10 mg/kg b.wt. i.p. at week 2 and carbon tetrachloride 0.25 to 1.50 μL/g b.wt. i.p. from week 8 to 16. CAF = caffeine (50 mg/Kg b.wt.) and TRI, CGA = trigonelline and/or chlorogenic acid (25 mg/Kg b.wt., both) intragastrically administered from week 7 to 17 (see Material & Methods section). Different letters correspond to statistical difference among groups by ANOVA and *post hoc* Tukey test ($p < 0.05$).

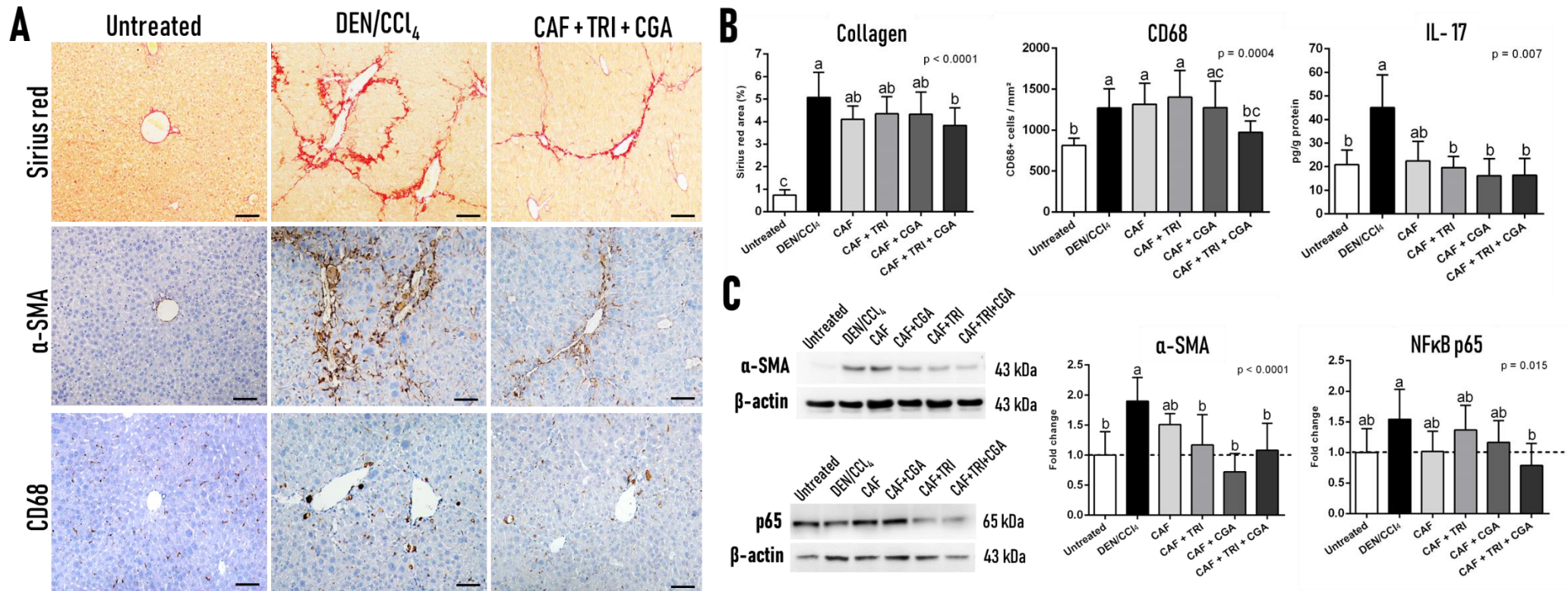
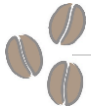


Figure 5. Effects of caffeine (CAF) individually or combined to trigonelline (TRI) and/or chlorogenic acid (CGA) on fibrosis markers during DEN/CCl₄-induced fibrosis-associated hepatocarcinogenesis. **(A)** Representative photomicrographs of collagen fibers in Sirius red-stained sections and α-smooth muscle actin (α-SMA) and CD68 immunostaining (20× objective, scale bar=50 μm). **(B)** Collagen area (Sirius red-stained sections), number of CD68-positive macrophages and interleukin-17 (IL-17) levels (ELISA). **(C)** Representative blot bands and semiquantitative analysis of α-SMA and NFκB p65 protein levels. Data are mean ± S.D. n = 5 (untreated) to 8 (other groups) mice/group. DEN/CCl₄ = diethylnitrosamine 10 mg/kg b.wt. i.p. at week 2 and carbon tetrachloride 0.25 to 1.50 μL/g b.wt. i.p. from week 8 to 16. CAF = caffeine (50 mg/Kg b.wt.) And TRI, CGA = trigonelline and/or chlorogenic acid (25 mg/Kg b.wt., both) intragastrically administered from week 7 to 17 (see Material & Methods section). Different letters correspond to statistical difference among groups by ANOVA and *post hoc* Tukey test (p<0.05).

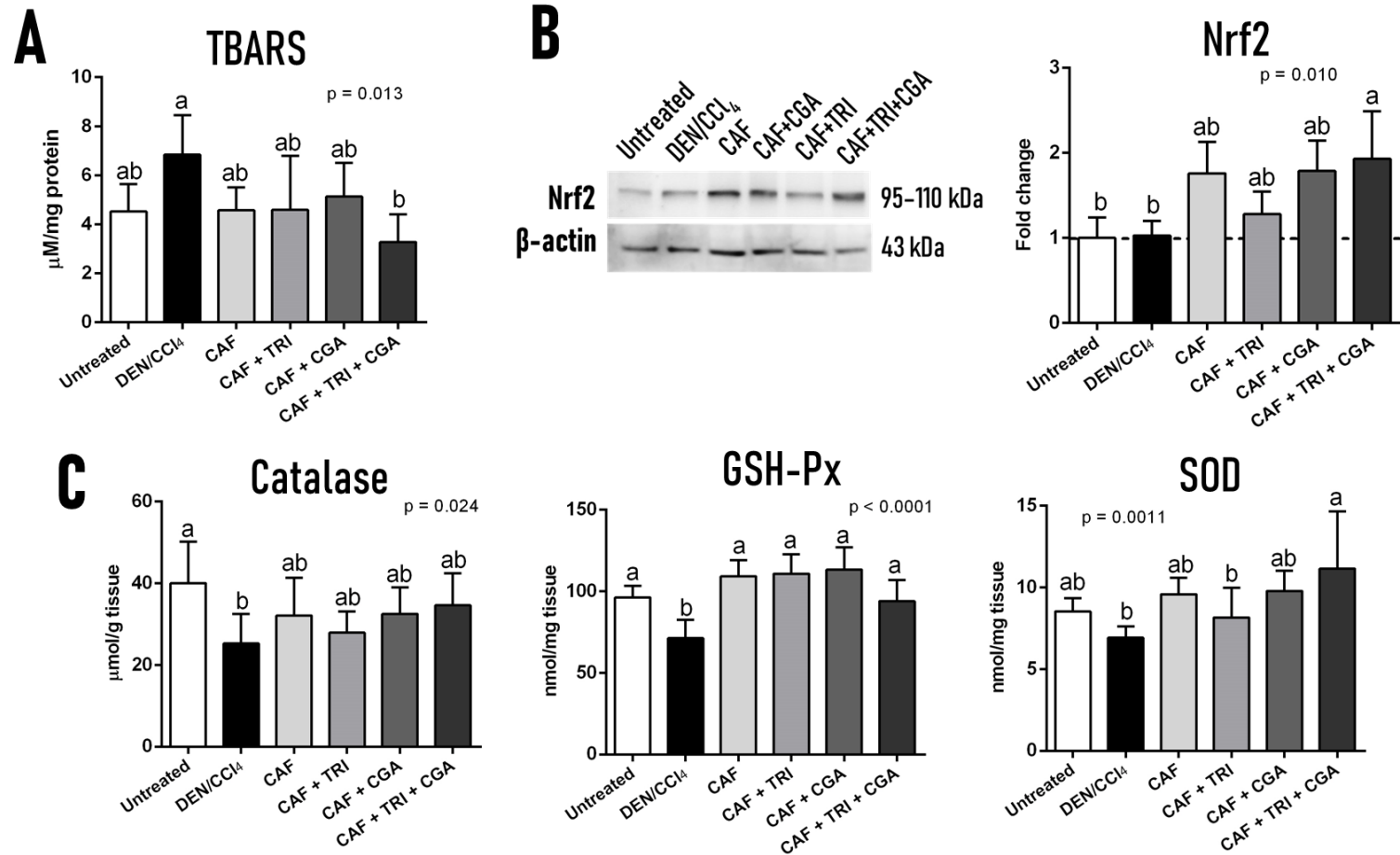
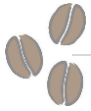


Figure 6. Effects of caffeine (CAF) individually or combined to trigonelline (TRI) and/or chlorogenic acid (CGA) on (A) thiobarbituric acid reactive species (TBARS), (B) Nrf2 protein levels and (C) catalase, glutathione peroxidase (GSH-Px), and superoxide dismutase (SOD) activities during DEN/CCl₄-induced fibrosis-associated hepatocarcinogenesis. Data are mean \pm S.D. n (TBARS and enzymes) = 5 (untreated) to 8 (other groups) mice/group. n (immunoblot) = 5 (untreated) to 6 (other groups) mice/group. DEN/CCl₄ = diethylnitrosamine 10 mg/kg b.wt. i.p. at week 2 and carbon tetrachloride 0.25 to 1.50 $\mu\text{L}/\text{g}$ b.wt. i.p. from week 8 to 16. CAF = caffeine (50 mg/Kg b.wt.) And TRI, CGA = trigonelline and/or chlorogenic acid (25 mg/Kg b.wt., both) intragastrically administered from week 7 to 17 (see Material & Methods section). Different letters correspond to statistical difference among groups by ANOVA and *post hoc* Tukey test ($p < 0.05$).

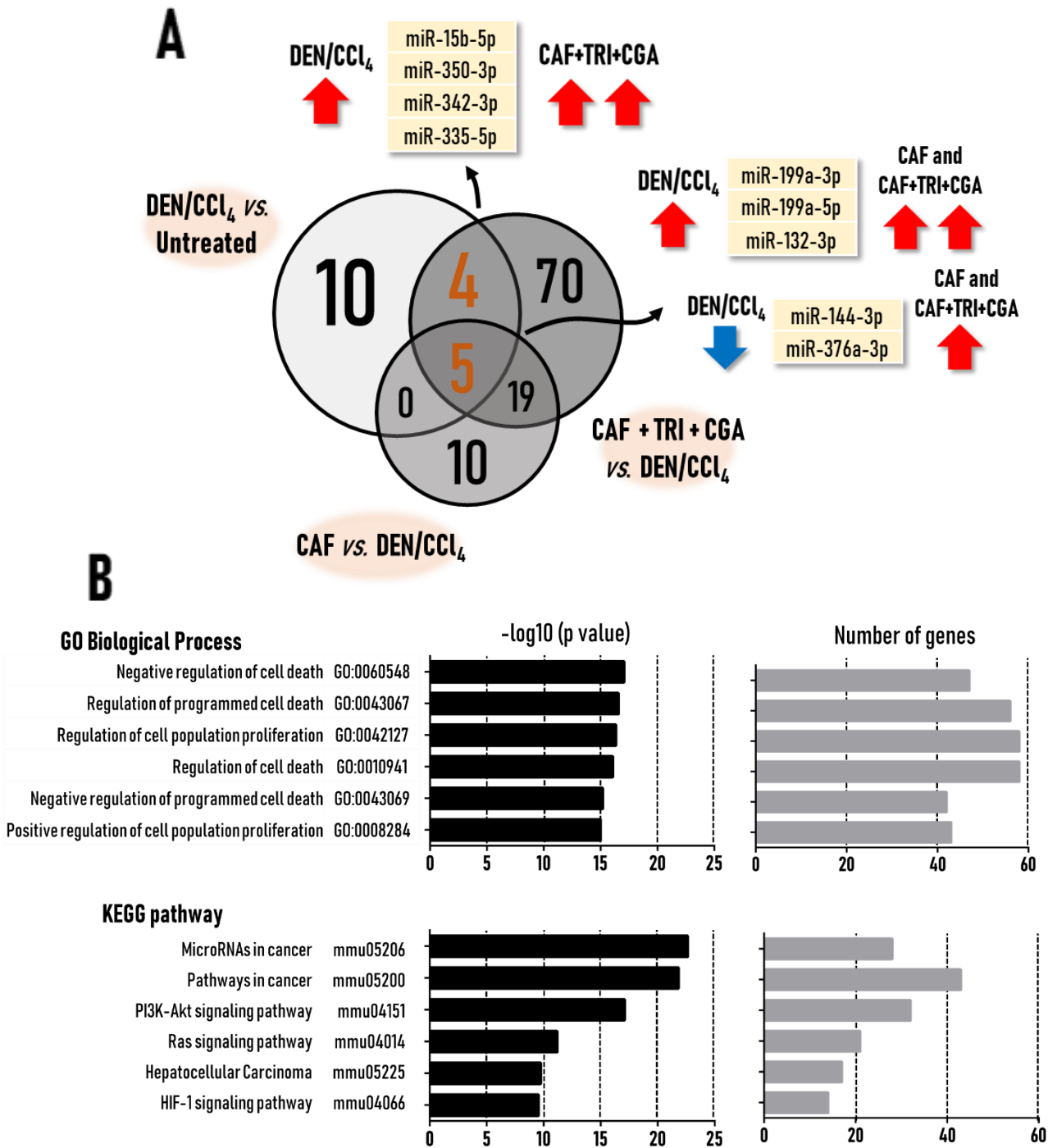
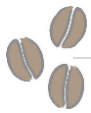


Figure 7. (A) Venn's diagram analysis of global miRNA expression by NanoString. Nineteen miRNAs were differentially expressed in DEN/CCl₄-induced fibrosis associated carcinogenesis hepatocarcinogenesis, including the downregulation of tumor suppressor miR-144-3p and miR-376a-3p. CAF+TRI+CGA treatment upregulated 9/19 (~50%) of the differentially expressed miRNAs in DEN/CCl₄ group, including the tumor suppressors miR-144-3p, miR-376a-3p and antifibrotic miR-15b-5p. CAF+TRI+CGA-related miRNA signature (9 miRNAs) involved 4 miRNAs exclusively upregulated in this treatment and 5 miRNAs also upregulated in CAF-treated group. ↑: upregulation; ↓: downregulation. **(B)** Gene ontology and KEGG pathway analysis of the 232 experimentally validated target genes associated with CAF+TRI+CGA treatment miRNA signature, ranked by adjusted -log₁₀ (p value).

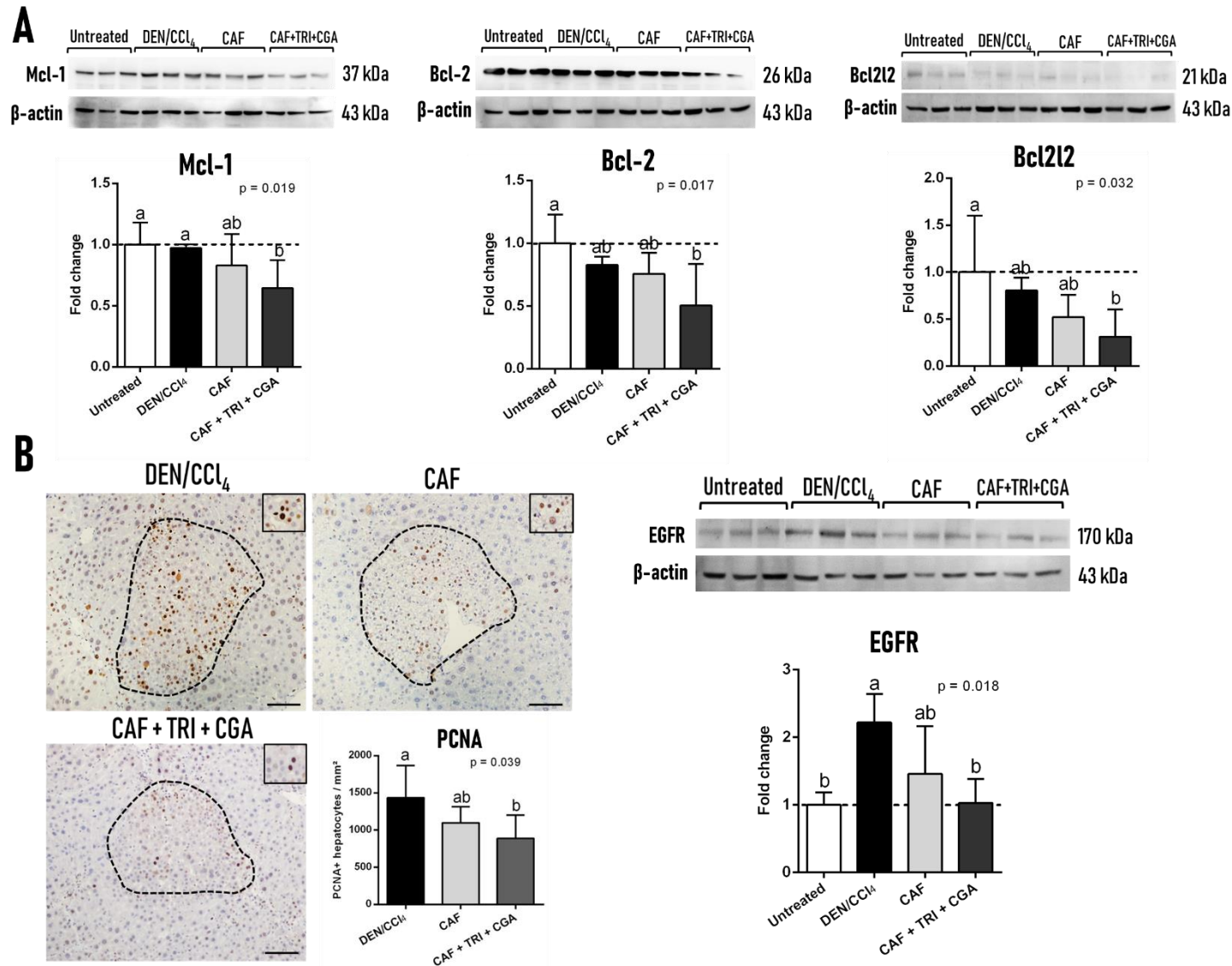
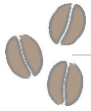


Figure 8. Effects of caffeine (CAF) individually or combined to trigonelline (TRI) and chlorogenic acid (CGA) on (A) Mcl-1, Bcl-2, Bcl212 (miR-15b-5p targets) hepatic protein levels, (B) PCNA (miR-376a-3p target) immunostaining in preneoplastic foci and EGFR (miR-144-3p target) hepatic protein levels during DEN/CCl₄-induced fibrosis-associated hepatocarcinogenesis. Representative blot bands and semiquantitative analysis are presented. 20× objective, scale bar=50 μm. Data are mean ± S.D. n= 5 (untreated) to 6 (other groups) mice/group. DEN/CCl₄ = diethylnitrosamine 10 mg/kg b.wt. i.p. at week 2 and carbon tetrachloride 0.25 to 1.50 μL/g b.wt. i.p. from week 8 to 16. CAF = caffeine (50 mg/Kg b.wt.) and TRI, CGA = trigonelline and/or chlorogenic acid (25 mg/Kg b.wt., both) intragastrically administered from week 7 to 17 (see Material & Methods section). Different letters correspond to statistical difference among groups by ANOVA and *post hoc* Tukey test (p<0.05).

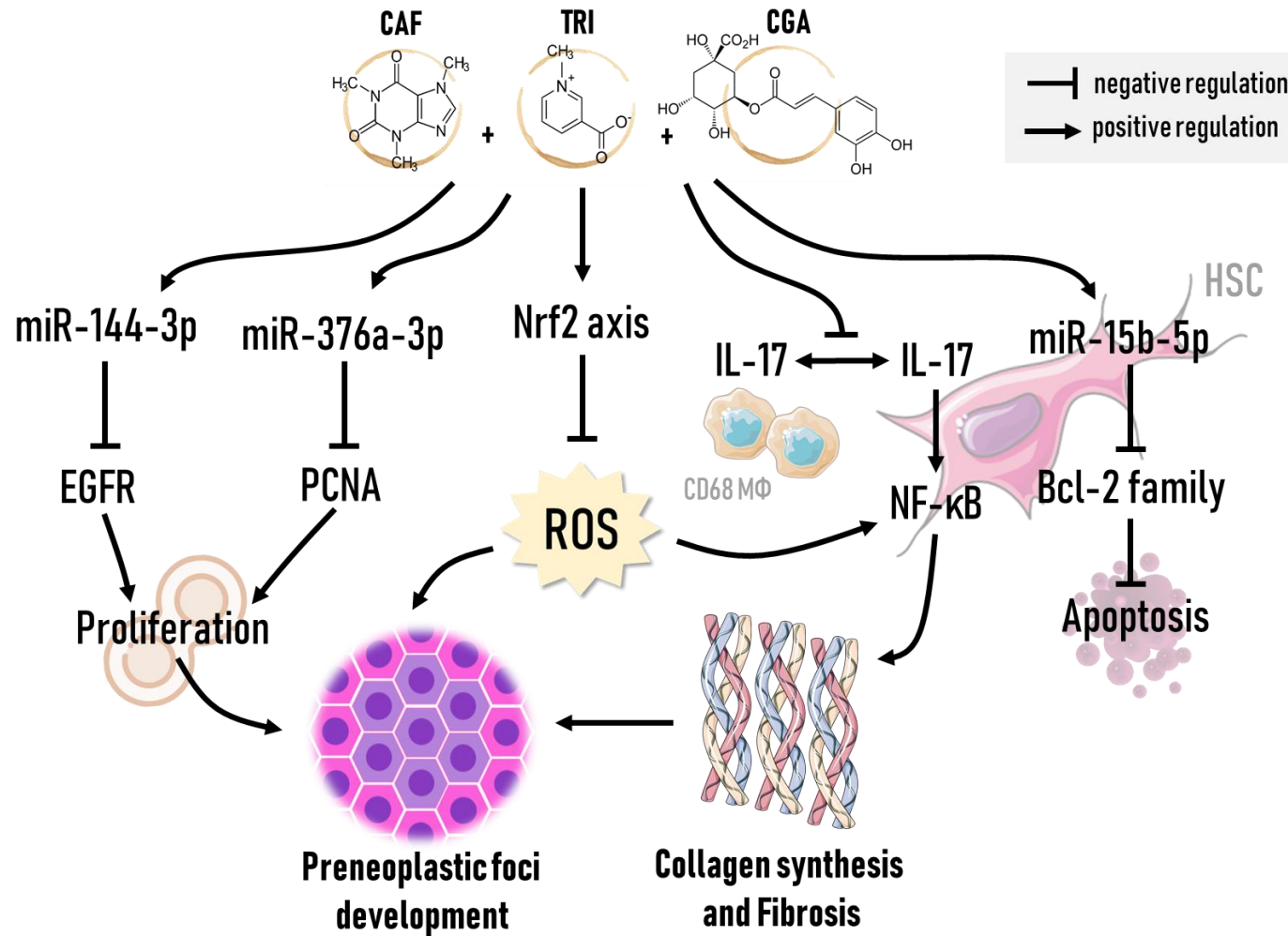
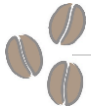


Figure 9. Summary of the main effects of caffeine (CAF), trigonelline (TRI) and chlorogenic acid (CGA) combination on fibrosis-associated hepatocarcinogenesis. The combination of coffee compounds upregulated tumor suppressor miR-144-3p and miR-376a-3p and decreased EGFR protein expression (miR-144-3p target) and the number of PCNA (miR-376a-3p target) positive hepatocytes in preneoplastic foci. Decreased cell proliferation contribute to the attenuation of preneoplastic foci development. Treatment upregulated miR-15b-5p and increased protein expression of Bcl-2 family members (miR-15b-5p targets), promoting apoptosis. Along with the attenuation of pro-inflammatory CD68 macrophages (MΦ)/IL-17/NF-κB axis, hepatic stellate cell (HSC) death may alleviate collagen accumulation and fibrosis. The induction of Nrf2 antioxidant axis is also proposed to attenuate oxidative stress, implicating on decreased fibrosis/carcinogenesis outcomes.

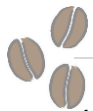


Table 1. Effects of caffeine (CAF) individually or combined to trigonelline (TRI) and/or chlorogenic acid (CGA) on food consumption, final body weight, liver relative and absolute weights, and alanine aminotransferase (ALT) levels during DEN/CCl₄-induced fibrosis-associated hepatocarcinogenesis.

Parameters	Groups ¹					
	Untreated	DEN/CCl ₄	CAF	CAF + TRI	CAF + CGA	CAF + TRI + CGA
Food consumption (g/mice/day)	4.54 (5.17 - 4.22)	4.25 (4.68 - 4.07)	4.61 (4.77 - 3.88)	4.13 (4.33 - 4.05)	4.01 (4.28 - 3.89)	4.26 (4.40 - 3.87)
Final body weight (g)	26.98 ± 1.31	27.40 ± 1.33	26.82 ± 1.02	26.80 ± 1.35	26.16 ± 1.64	27.14 ± 1.74
Liver absolute weight (g)	1.54 ± 0.11 b	1.75 ± 0.14 a	1.56 ± 0.10 b	1.58 ± 0.09 b	1.55 ± 0.11 b	1.59 ± 0.14 b
Liver relative weight (%)	5.71 ± 0.29 b	6.34 ± 0.37 a	5.83 ± 0.48 b	5.93 ± 0.29 ab	5.93 ± 0.34 ab	5.87 ± 0.48 b
ALT (U/L)	33.80 ± 8.15 b	60.88 ± 15.08 a	51.00 ± 17.38 ab	48.57 ± 11.19 ab	51.16 ± 14.54 ab	56.00 ± 9.96 ab

Data are mean ± S.D. or median (q75-q25). n = 5 (untreated) to 10 (other groups) mice/group. ¹DEN/CCl₄ = diethylnitrosamine 10 mg/kg b.wt. i.p. at week 2 and carbon tetrachloride 0.25 to 1.50 µL/g b.wt. i.p. from week 8 to 16. CAF = caffeine (50 mg/Kg b.wt.) and TRI, CGA = trigonelline and/or chlorogenic acid (25 mg/Kg b.wt., both) intragastrically administered from week 7 to 17 (see Material & Methods section). Different letters correspond to statistical difference among groups by ANOVA and *post hoc* Tukey test (p<0.05).

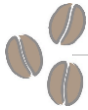


Table 2. Effects of caffeine (CAF) individually or combined to trigonelline (TRI) and/or chlorogenic acid (CGA) on preneoplastic foci incidence during fibrosis-associated hepatocarcinogenesis.

Parameters	Groups ¹					
	Untreated	DEN/CCl ₄	CAF	CAF + TRI	CAF + CGA	CAF + TRI + CGA
Foci (all types)	0/5 (0) b	10/10 (100%) a	10/10 (100%) a	10/10 (100%) a	9/10 (90%) a	8/10 (80%) a
Basophilic foci	-	10/10 (100%)	9/10 (90%)	10/10 (100%)	9/10 (90%)	7/10 (70%)
Eosinophilic foci	-	0/10 (0)	3/10 (30%)	3/10 (30%)	4/10 (40%)	2/10 (20%)
Clear cell foci	-	6/10 (60%) a	3/10 (30%) ab	3/10 (30%) ab	3/10 (30%) ab	0/10 (0) b

Data are the proportion of affected animals (percentage). ¹DEN/CCl₄ = diethylnitrosamine 10 mg/kg b.wt. i.p. at week 2 and carbon tetrachloride 0.25 to 1.50 µL/g b.wt. i.p. from week 8 to 16. CAF = caffeine (50 mg/Kg b.wt.)and TRI, CGA = trigonelline and/or chlorogenic acid (25 mg/Kg b.wt., both) intragastrically administered from week 7 to 17 (see Material & Methods section). Different letters correspond to statistical difference by Fisher Exact test (p<0.05).

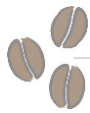


Table 3. Differentially expressed miRNAs in DEN/CCl₄-induced fibrosis-associated hepatocarcinogenesis group compared to untreated group.

Upregulated (14)			
miRNAs	MIMATIDs	p value	FC
miR-199a-3p	MIMAT0000230	0.0011	2.29
miR-125a-5p	MIMAT0000135	9.90E-06	2.14
miR-883b-3p	MIMAT0004851	0.0470	2.14
miR-199a-5p	MIMAT0000229	0.0200	2.00
miR-342-3p	MIMAT0000590	0.0040	2.00
miR-466a-3p	MIMAT0002107	0.0330	1.86
miR-223-3p	MIMAT0000665	0.0140	1.74
miR-132-3p	MIMAT0000144	3.50E-05	1.62
miR-34a-5p	MIMAT0000542	0.0003	1.62
miR-669a-5p	MIMAT0003477	0.0250	1.62
miR-150-5p	MIMAT0000160	0.0350	1.51
miR-15b-5p	MIMAT0000124	0.0039	1.51
miR-335-5p	MIMAT0000766	0.0150	1.51
miR-350-3p	MIMAT0000605	0.0001	1.51
Downregulated (5)			
miRNAs	MIMATIDs	p value	FC
miR-451a	MIMAT0001632	0.0140	0.61
miR-496a-3p	MIMAT0003738	0.0130	0.61
miR-144-3p	MIMAT0000156	0.0054	0.57
miR-486a-5p	MIMAT0003130	0.0067	0.57
miR-376a-3p	MIMAT0000740	0.0008	0.53

p<0.05 and fold change (FC) >1.5. n= 5 (Untreated) or 6 (DEN/CCl₄) mice/group. DEN/CCl₄ = diethylnitrosamine 10 mg/kg b.wt. i.p. at week 2 and carbon tetrachloride 0.25 to 1.50 µL/g b.wt. i.p. from week 8 to 16.

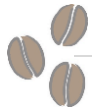
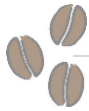


Table 4. miRNAs modulated by CAF+TRI+CGA treatment during fibrosis-associated hepatocarcinogenesis (vs. DEN/CCl₄ group).

Upregulated (9)			
miRNAs	MIMATIDs	p value	FC
miR-199a-5p	MIMAT0000229	0.00008	2.30
miR-144-3p	MIMAT0000156	0.00100	2.14
miR-199a-3p	MIMAT0000230	0.00001	1.87
miR-335-5p	MIMAT0000766	0.00610	1.62
miR-342-3p	MIMAT0000590	0.03400	1.62
miR-376a-3p	MIMAT0000740	0.00350	1.62
miR-132-3p	MIMAT0000144	0.00037	1.52
miR-15b-5p	MIMAT0000124	0.00110	1.52
miR-350-3p	MIMAT0000605	0.00011	1.52

$p < 0.05$ and fold change (FC) > 1.5 . $n = 6$ (DEN/CCl₄) or 7 (CAF+TRI+CGA) mice/group. DEN/CCl₄ = diethylnitrosamine 10 mg/kg b.wt. i.p. at week 2 and carbon tetrachloride 0.25 to 1.50 $\mu\text{L/g}$ b.wt. i.p. from week 8 to 16. CAF = caffeine (50 mg/Kg b.wt.) and TRI, CGA = trigonelline and/or chlorogenic acid (25 mg/Kg b.wt., both) intragastrically administered from week 7 to 17 (see Material & Methods section).



11. Supplementary material

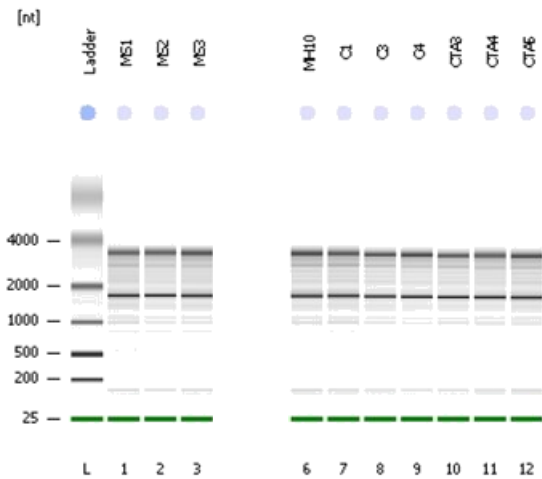
2100 expert_Eukaryote Total RNA Nano_DE72905390_2018-05-16_16-08-45.xad

Page 1 of 16

Assay Class: Eukaryote Total RNA Nano
Data Path: C:\...Eukaryote Total RNA Nano_DE72905390_2018-05-16_16-08-45.xad

Created: 16/5/2018 16:08:45
Modified: 16/5/2018 16:32:42

Electrophoresis File Run Summary

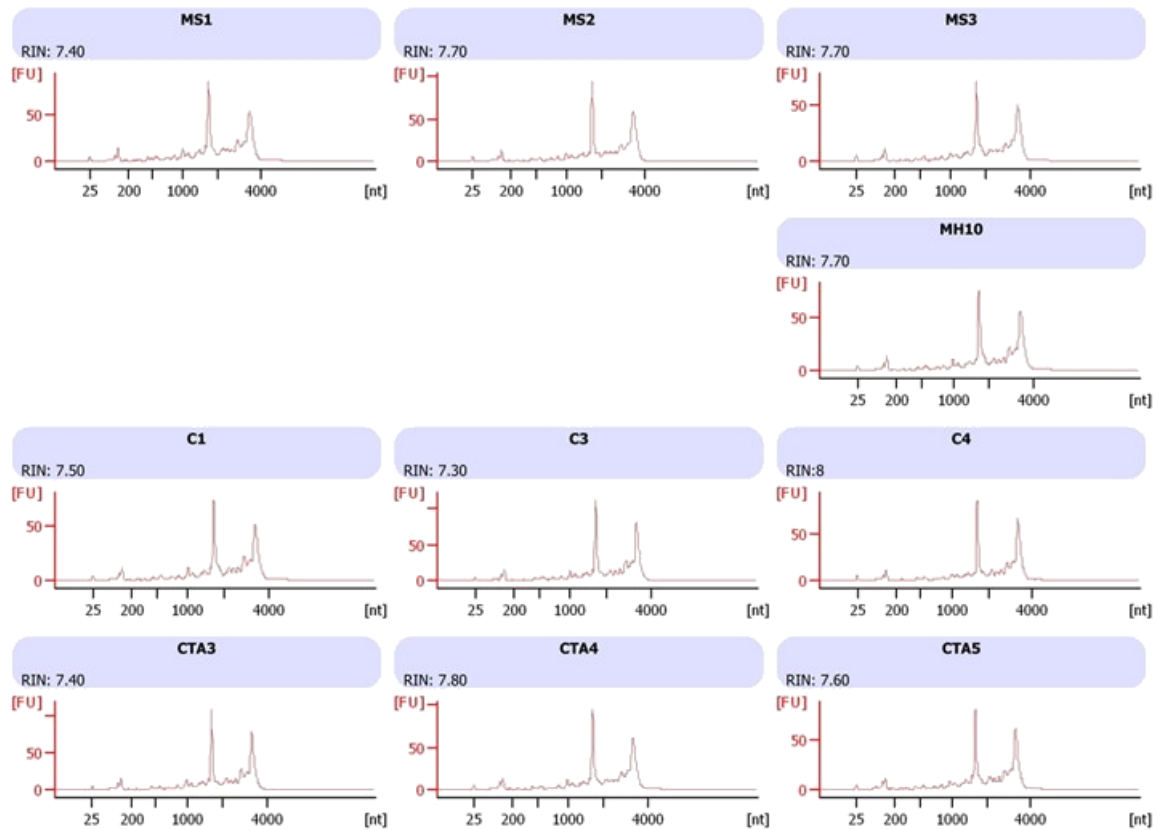


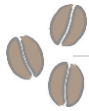
Instrument Information:
 Instrument Name: DE72905390 Firmware: C.01.069
 Serial#: DE72905390 Type: G2938C

Assay Information:
 Assay Origin Path: C:\Program Files\Agilent\2100 bioanalyzer\2100 expert\assays\RNA\Eukaryote Total RNA Nano Series II.xsy
 Assay Class: Eukaryote Total RNA Nano
 Version: 2.6
 Assay Comments: Total RNA Analysis ng sensitivity (Eukaryote)

Chip Information:
 Chip Lot #:
 Reagent Kit Lot #:
 Chip Comments:

© Copyright 2003 - 2009 Agilent Technologies, Inc.

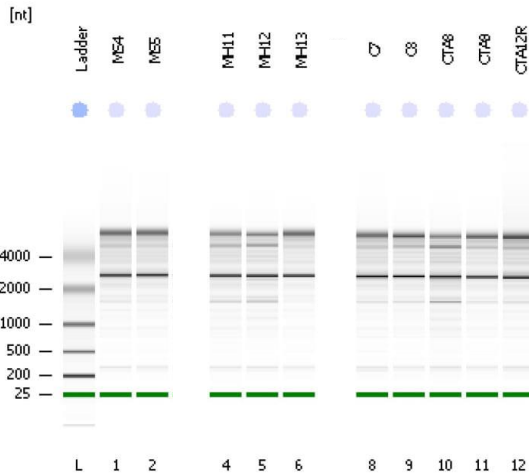




Assay Class: Eukaryote Total RNA Nano
Data Path: C:\...Eukaryote Total RNA Nano_DE72905390_2018-05-16_16-44-23.xad

Created: 16/5/2018 16:44:23
Modified: 16/5/2018 17:08:18

Electrophoresis File Run Summary



Instrument Information:

Instrument Name: DE72905390 Firmware: C.01.069
Serial#: DE72905390 Type: G2938C

Assay Information:

Assay Origin Path: C:\Program Files\Agilent\2100 bioanalyzer\2100 expert\assays\RNA\Eukaryote Total RNA Nano Series II.xsy

Assay Class: Eukaryote Total RNA Nano

Version: 2.6

Assay Comments: Total RNA Analysis ng sensitivity (Eukaryote)

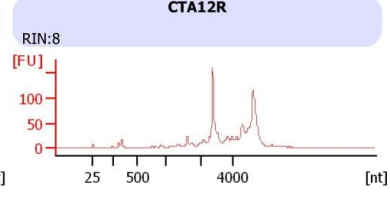
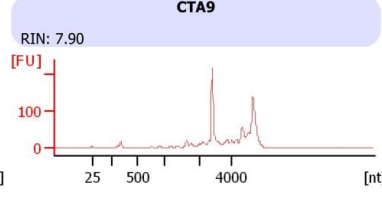
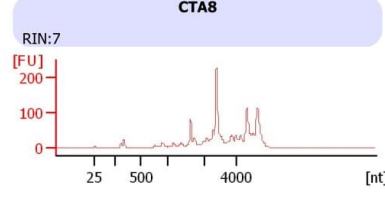
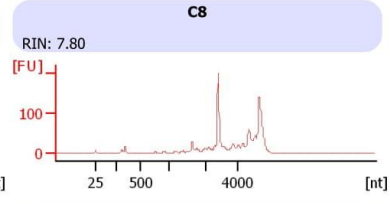
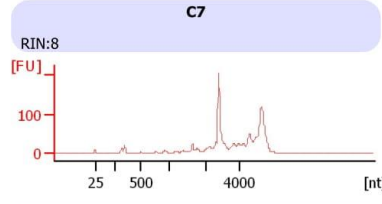
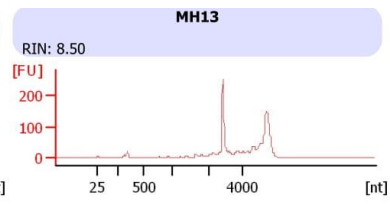
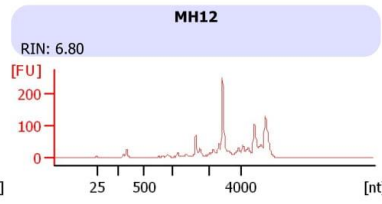
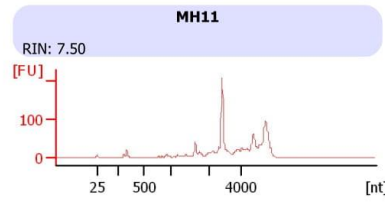
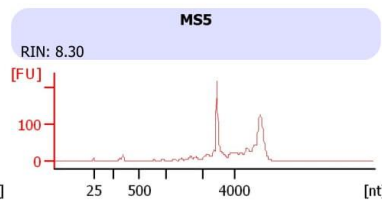
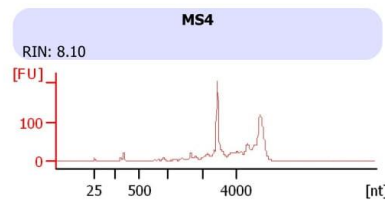
© Copyright 2003 - 2009 Agilent Technologies, Inc.

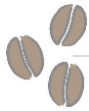
Chip Information:

Chip Lot #:

Reagent Kit Lot #:

Chip Comments:





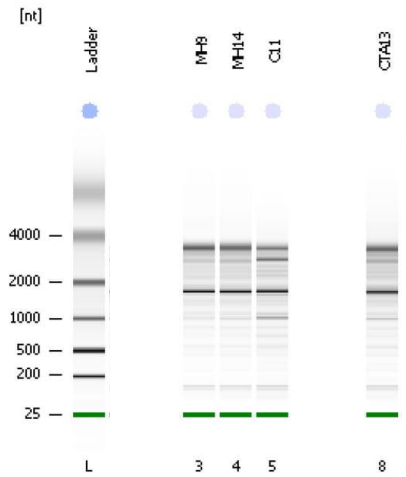
2100 expert_Eukaryote Total RNA Nano_DE72905390_2018-05-16_17-25-26.xad

Page 1 of 16

Assay Class: Eukaryote Total RNA Nano
Data Path: C:\...Eukaryote Total RNA Nano_DE72905390_2018-05-16_17-25-26.xad

Created: 16/5/2018 17:25:26
Modified: 16/5/2018 17:49:21

Electrophoresis File Run Summary



Instrument Information:

Instrument Name: DE72905390 Firmware: C.01.069
Serial#: DE72905390 Type: G2938C

Assay Information:

Assay Origin Path: C:\Program Files\Agilent\2100 bioanalyzer\2100 expert\assays\RNA\Eukaryote Total RNA Nano Series II.xsy

Assay Class: Eukaryote Total RNA Nano

Version: 2.6

Assay Comments: Total RNA Analysis ng sensitivity (Eukaryote)

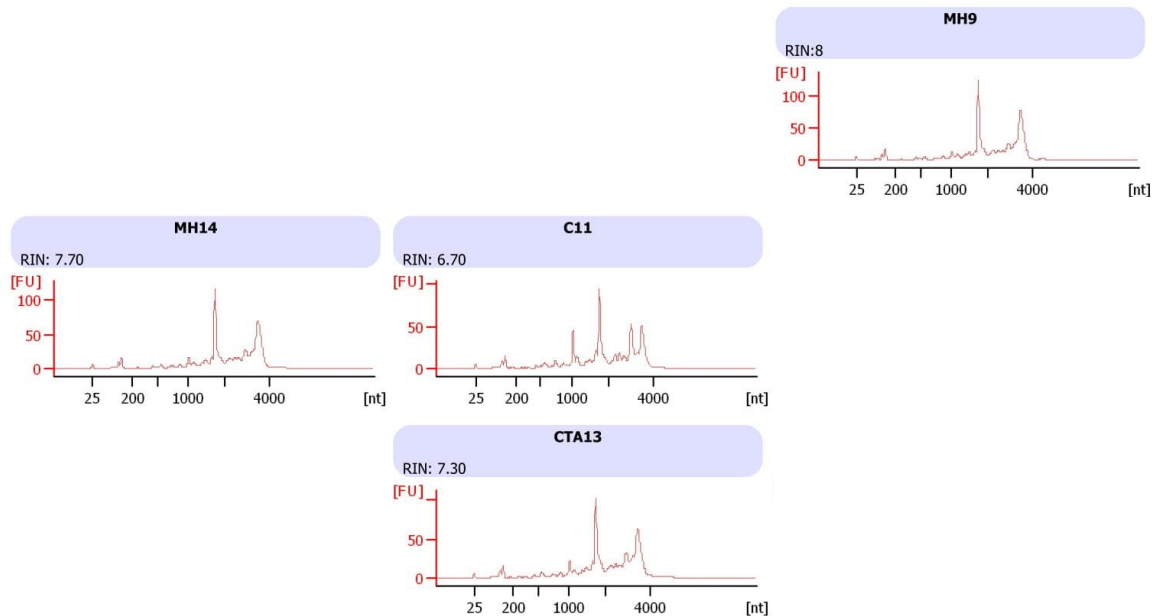
© Copyright 2003 - 2009 Agilent Technologies, Inc.

Chip Information:

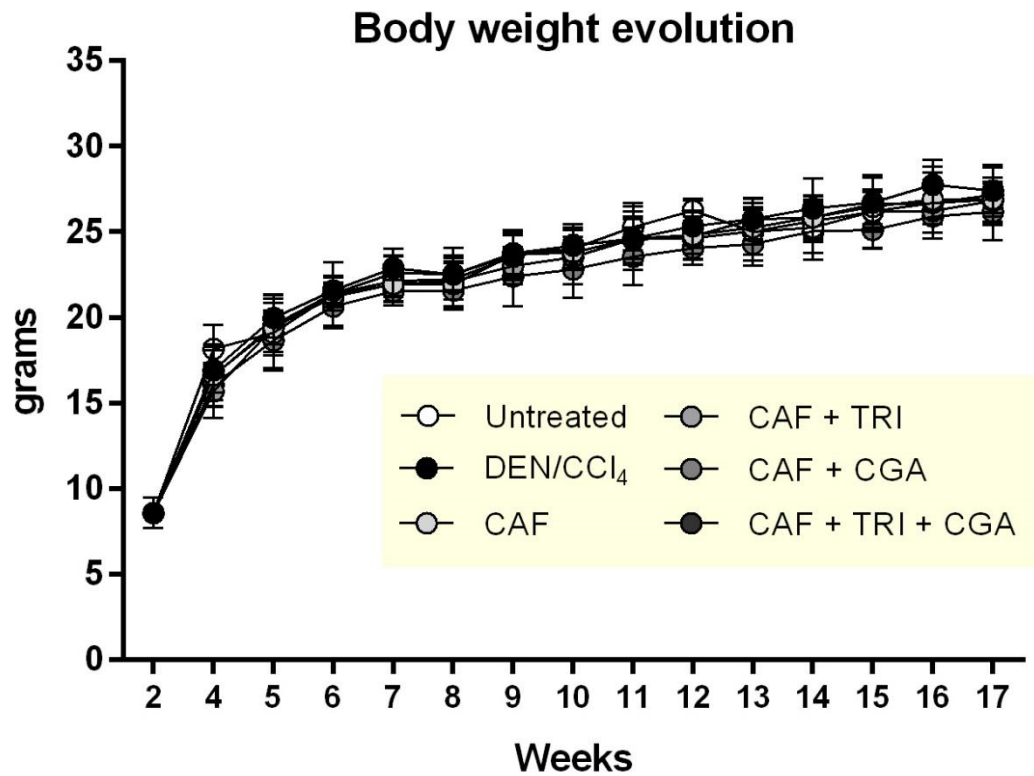
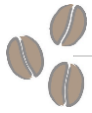
Chip Lot #:

Reagent Kit Lot #:

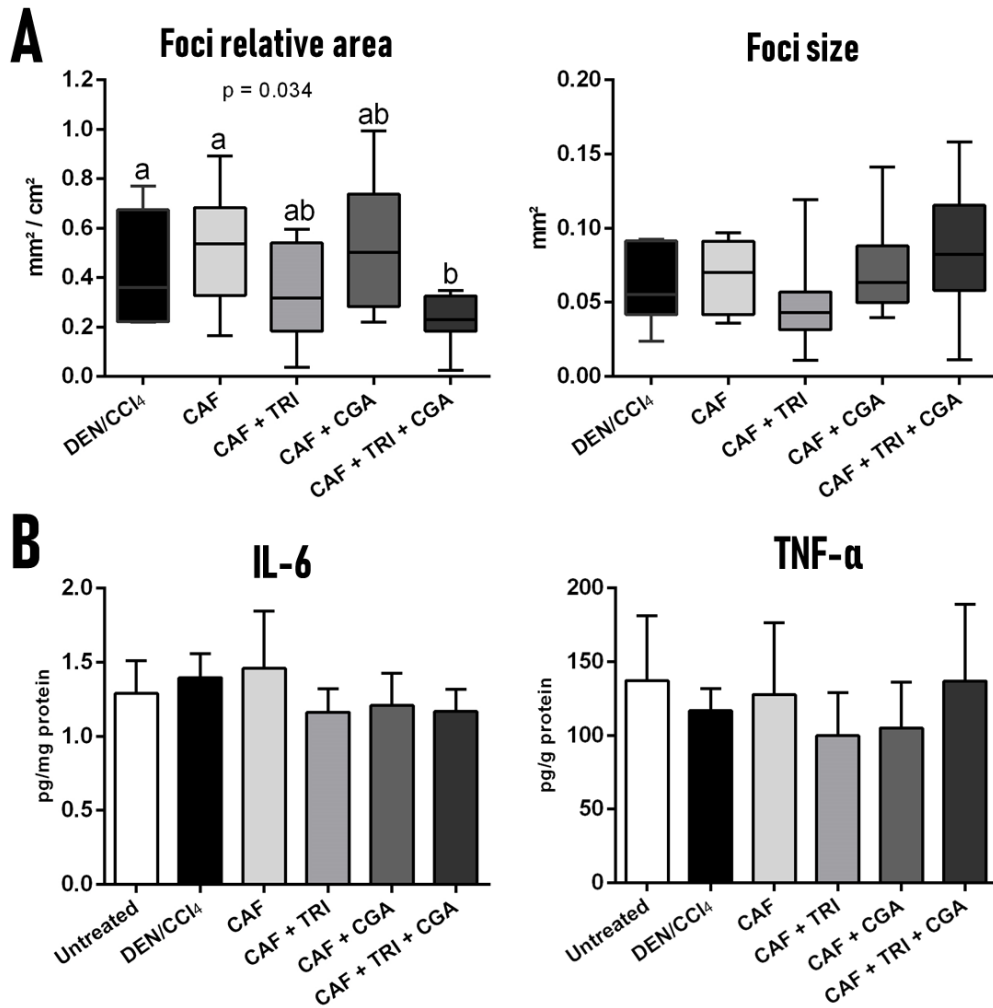
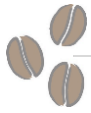
Chip Comments:



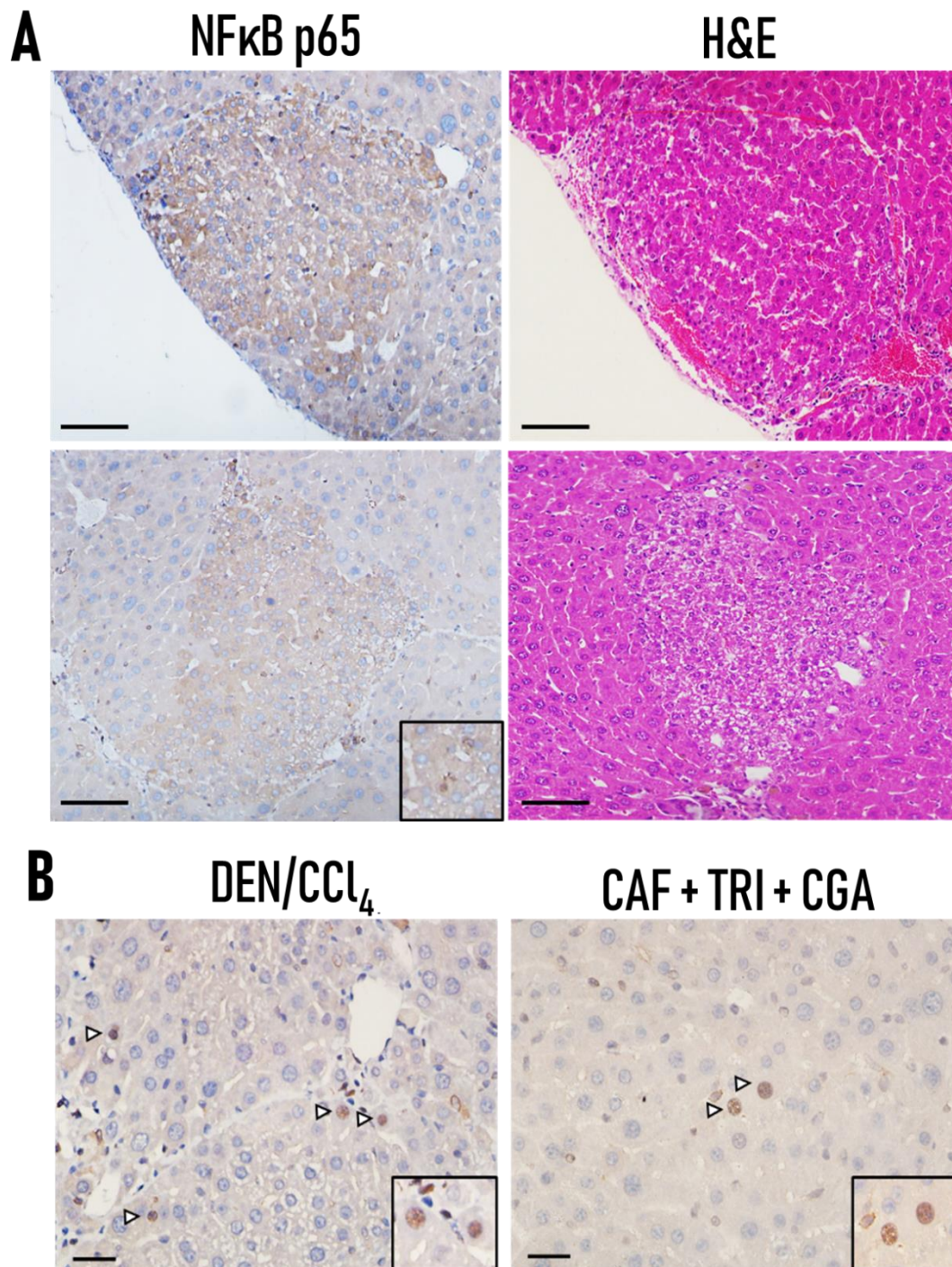
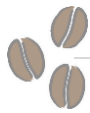
Supplementary Figure 1. Reports on RNA quality control analysis performed by Agilent 2100 Bioanalyzer platform (Agilent Technologies, USA). RIN = RNA Integrity Number; MS = untreated group samples; MH = DEN/CCl₄; C = caffeine-treated group samples; CTA = caffeine + trigonelline + chlorogenic acid-treated group samples.



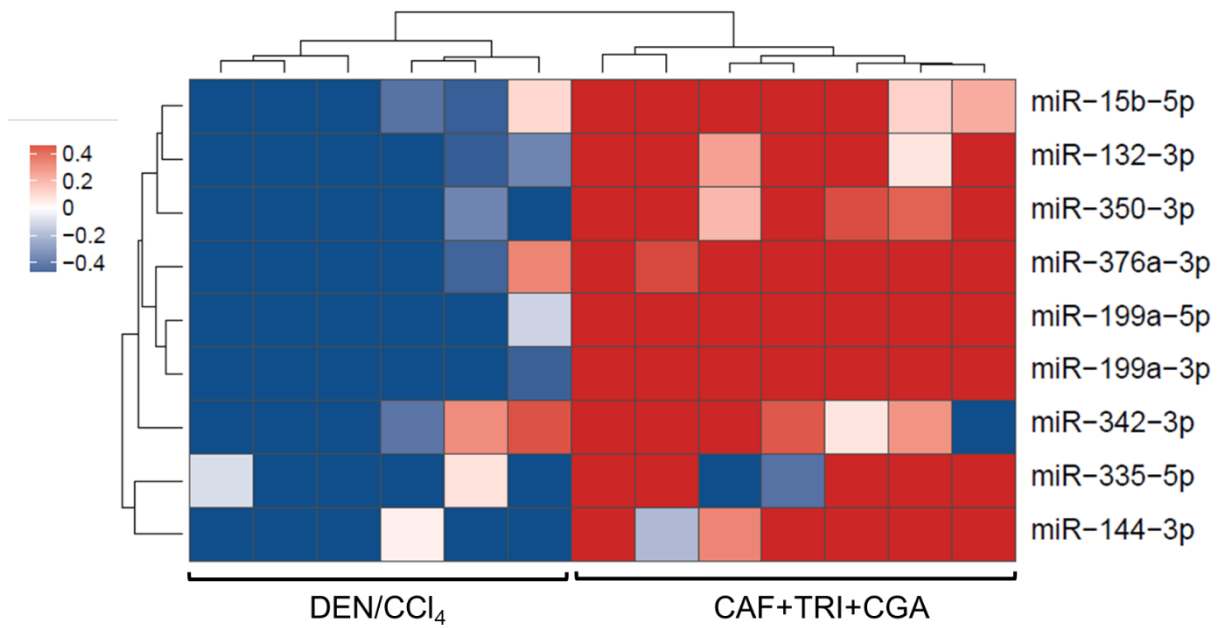
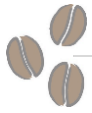
Supplementary Figure 2. Effects of caffeine (CAF) individually or combined to trigonelline (TRI) and/or chlorogenic acid (CGA) on body weight evolution during DEN/CCl₄-induced fibrosis-associated hepatocarcinogenesis. Data are the mean \pm S.D. n = 5 (untreated) to 10 (other groups) mice/group. DEN/CCl₄ = diethylnitrosamine 10 mg/kg b.wt. i.p. at week 2 and carbon tetrachloride 0.25 to 1.50 μ L/g b.wt. i.p. from week 8 to 16. CAF = caffeine (50 mg/Kg b.wt.) and TRI, CGA = trigonelline and/or chlorogenic acid (25 mg/Kg b.wt., both) intragastrically administered from week 7 to 17 (see Material & Methods section). Data were analyzed by ANOVA ($p < 0.05$).



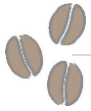
Supplementary Figure 3. Effects of caffeine (CAF) individually or combined to trigonelline (TRI) and/or chlorogenic acid (CGA) on (A) preneoplastic foci size, relative area, and (B) interleukin-6 (IL-6) and tumor necrosis factor α (TNF- α) levels during DEN/CCl₄-induced fibrosis-associated hepatocarcinogenesis. Data are the mean \pm S.D or box plots. n (ELISA) = 5 (untreated) to 8 (other groups) mice/group. n (Foci screening) = 5 (untreated) to 10 (other groups) mice/group. DEN/CCl₄ = diethylnitrosamine 10 mg/kg b.wt. i.p. at week 2 and carbon tetrachloride 0.25 to 1.50 μ L/g b.wt. i.p. from week 8 to 16. CAF = caffeine (50 mg/Kg b.wt.) and TRI, CGA = trigonelline and/or chlorogenic acid (25 mg/Kg b.wt., both) intragastrically administered from week 7 to 17 (see Material & Methods section). Data were analyzed by ANOVA and *post hoc* Tukey test ($p < 0.05$).



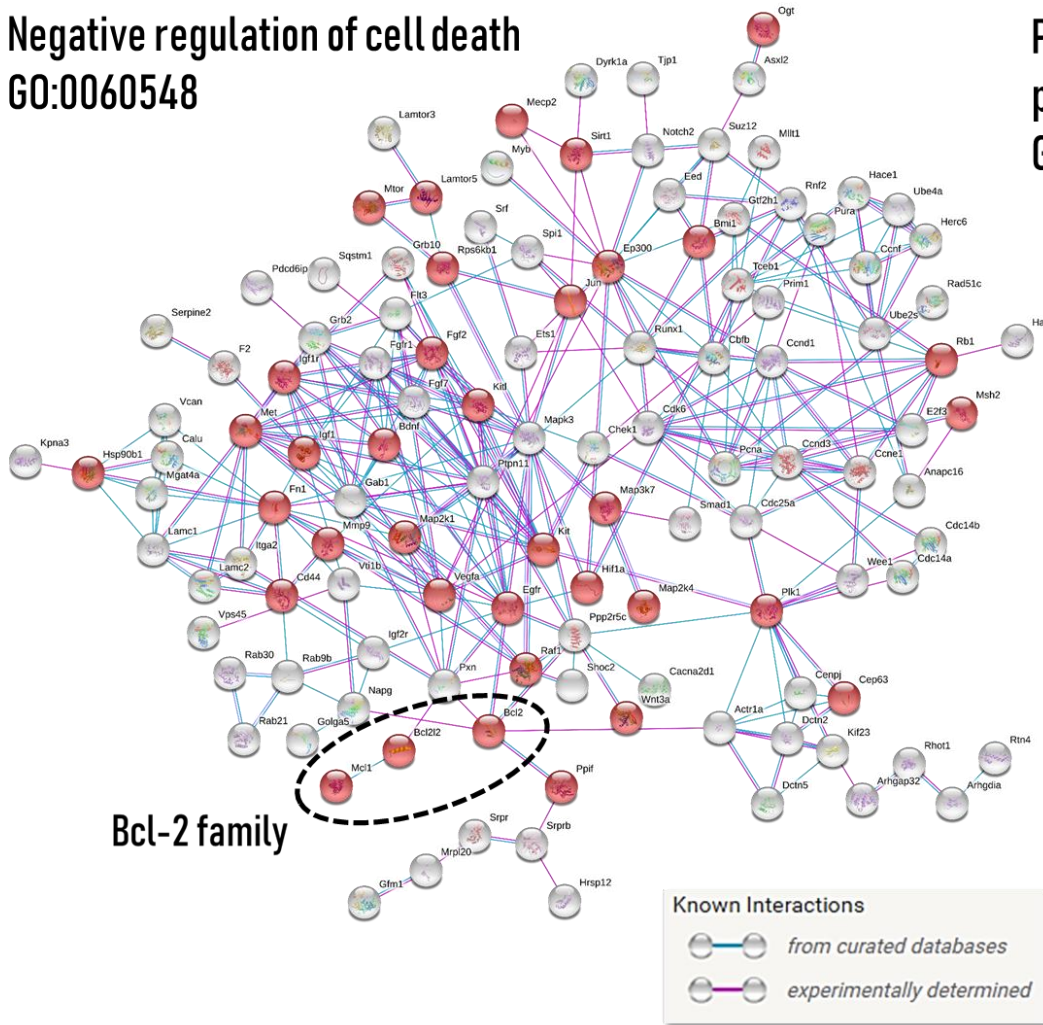
Supplementary Figure 4. (A) Representative photomicrographs of NF- κ B p65 immunostained sections and respective H&E-stained sections of basophilic preneoplastic foci (20 \times objective, scale bar=50 μ m). Hepatocytes of preneoplastic foci displayed stronger cytoplasmatic p65 immunostaining than adjacent liver tissue, with eventual nuclear staining (detail). (B) Representative photomicrographs of NF- κ B p65 immunostained sections of adjacent hepatocytes (40 \times objective, scale bar=25 μ m). Eventual hepatocytes showing nuclear staining (arrowheads and detail) were found. DEN/CCl₄ = diethylnitrosamine 10 mg/kg b.wt. i.p. at week 2 and carbon tetrachloride 0.25 to 1.50 μ L/g b.wt. i.p. from week 8 to 16. CAF = caffeine (50 mg/Kg b.wt.) and TRI, CGA = trigonelline and/or chlorogenic acid (25 mg/Kg b.wt., both) intragastrically administered from week 7 to 17 (see Material & Methods section).



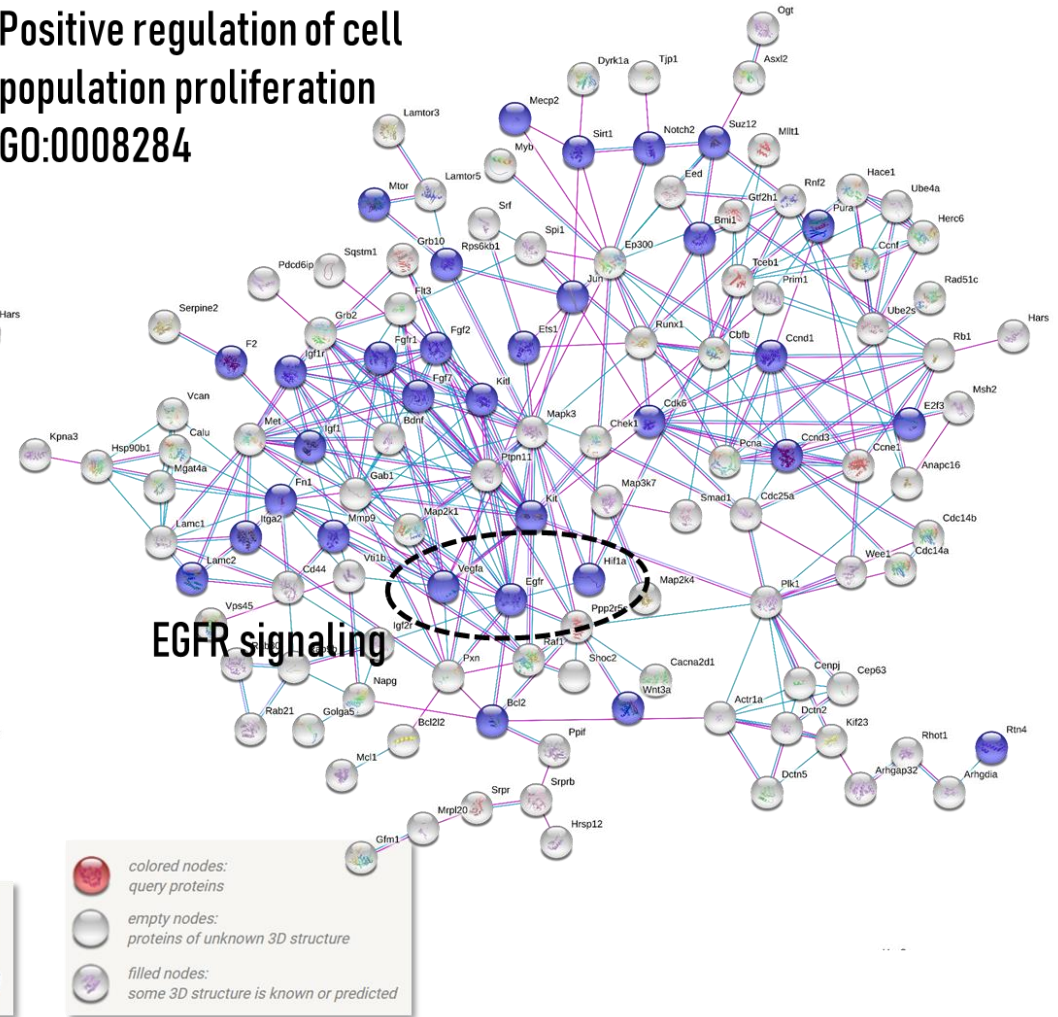
Supplementary Figure 5. Heatmap of the miRNAs upregulated by CAF+TRI+CGA treatment during fibrosis-associated hepatocarcinogenesis (vs. DEN/CCl₄ group), considering $p < 0.05$ and fold change (FC) > 1.5 .



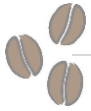
Negative regulation of cell death GO:0060548



Positive regulation of cell population proliferation GO:0008284

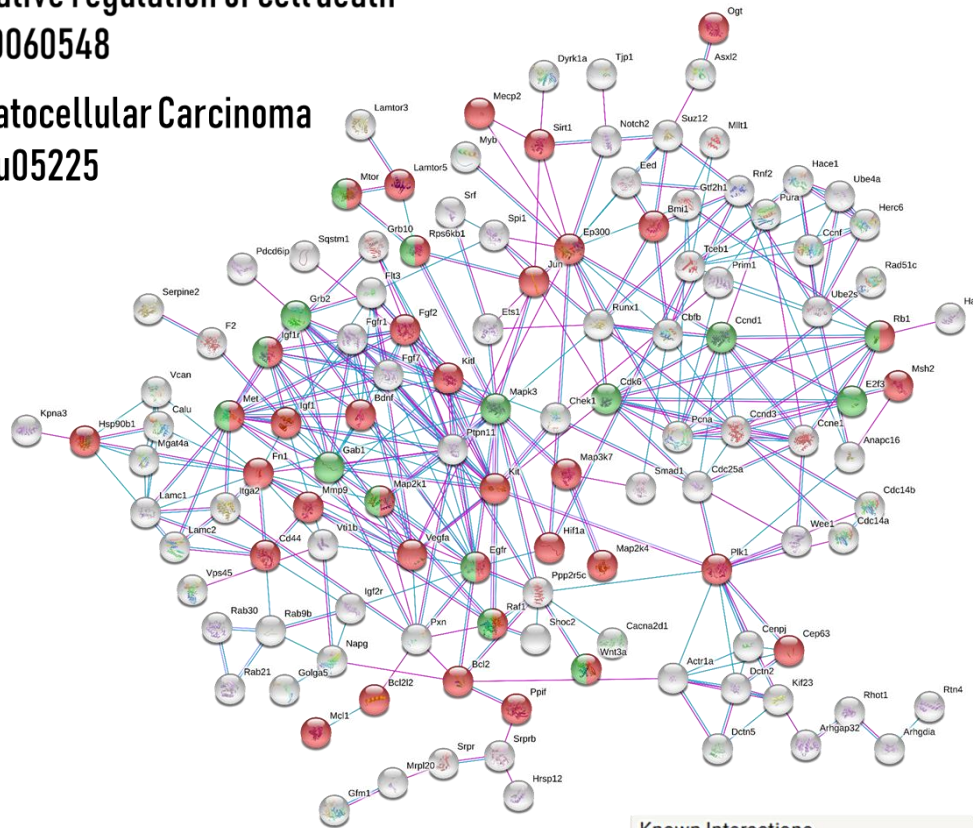


Supplementary Figure 6. Network analysis of the validated target genes of the differentially expressed miRNAs in CAF+TRI+CGA treatment. The interactions among the nodes (physical or functional) considered curated databases and/or experimentally determined data. Functional annotations regarding negative regulation of cell death (red) and positive regulation of cell population proliferation (blue) were highlighted in the network. The importance of key members of antiapoptotic Bcl-2 family (*Bcl-2*, *Bcl2l2* and *Mcl1*) and pro-proliferative EGFR signaling (*Egfr*, *Vegf*, *Hif1a*) is depicted in the networks.



Negative regulation of cell death GO:0060548

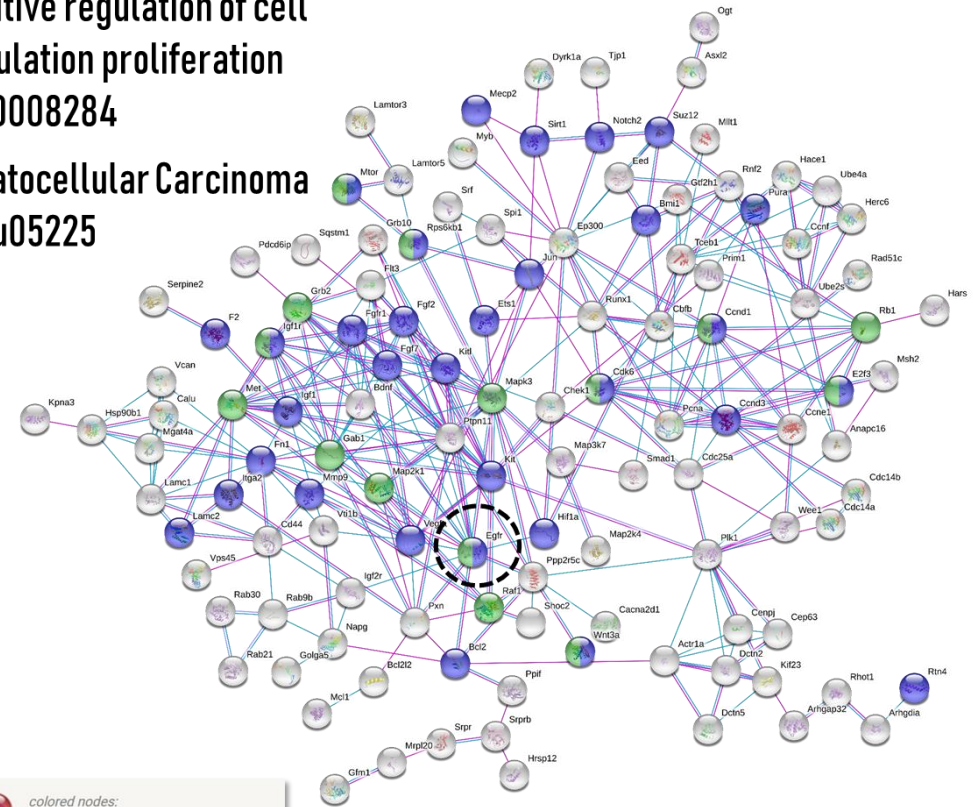
Hepatocellular Carcinoma
mmu05225



Known Interactions
— from curated databases
— experimentally determined

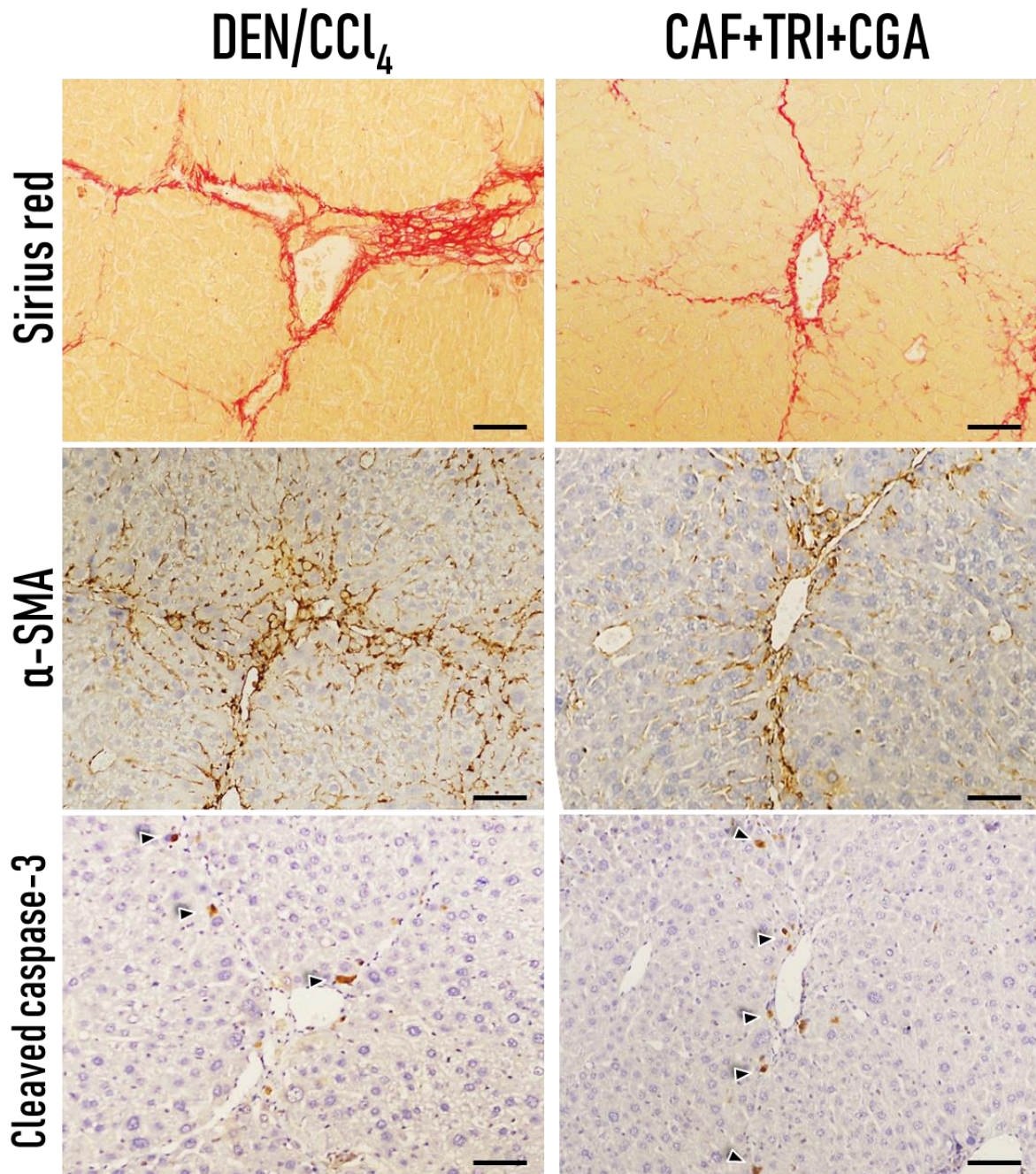
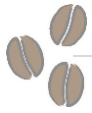
Positive regulation of cell population proliferation GO:0008284

Hepatocellular Carcinoma
mmu05225

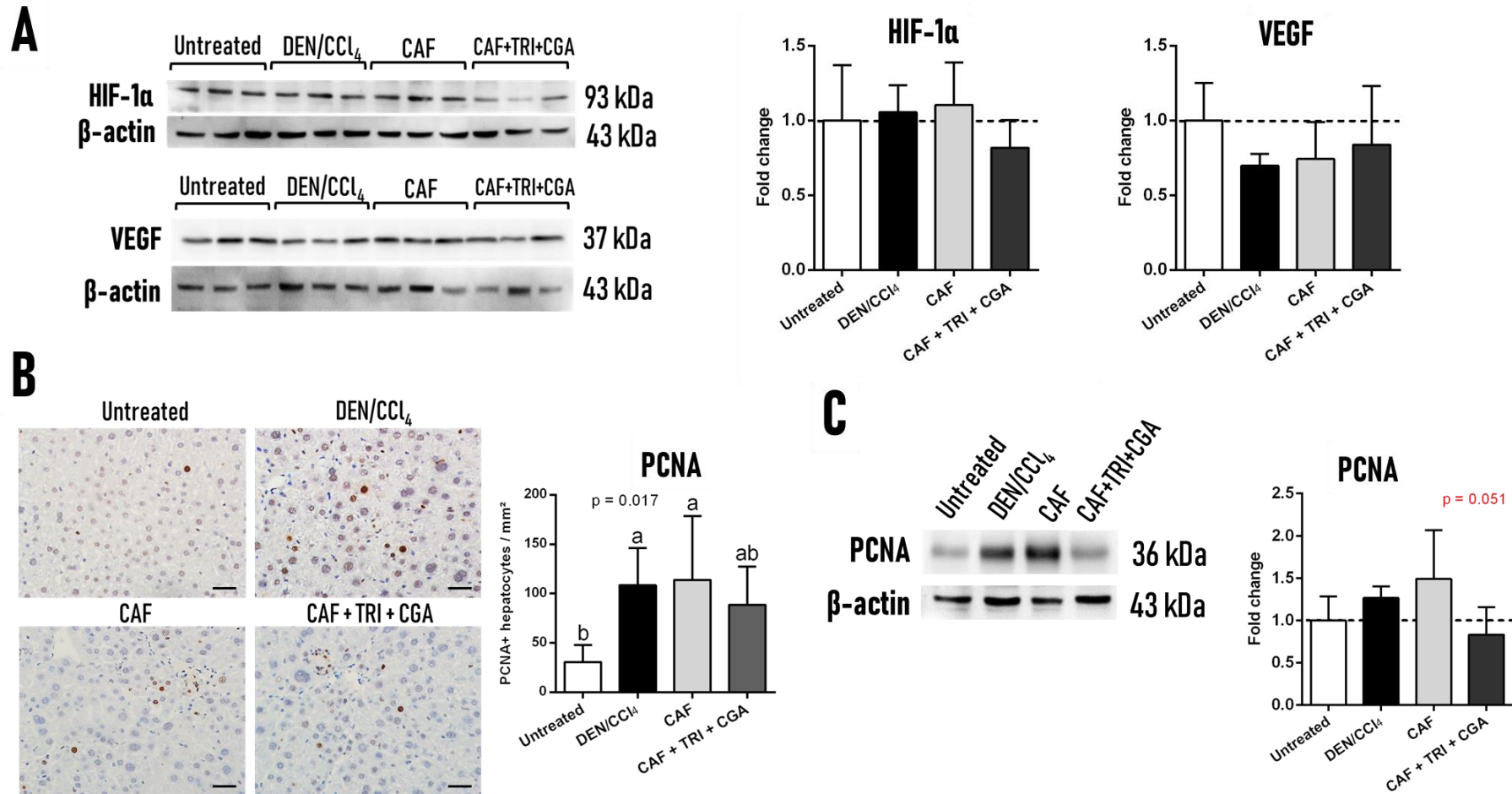
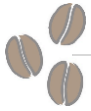


colored nodes:
query proteins
empty nodes:
proteins of unknown 3D structure
filled nodes:
some 3D structure is known or predicted

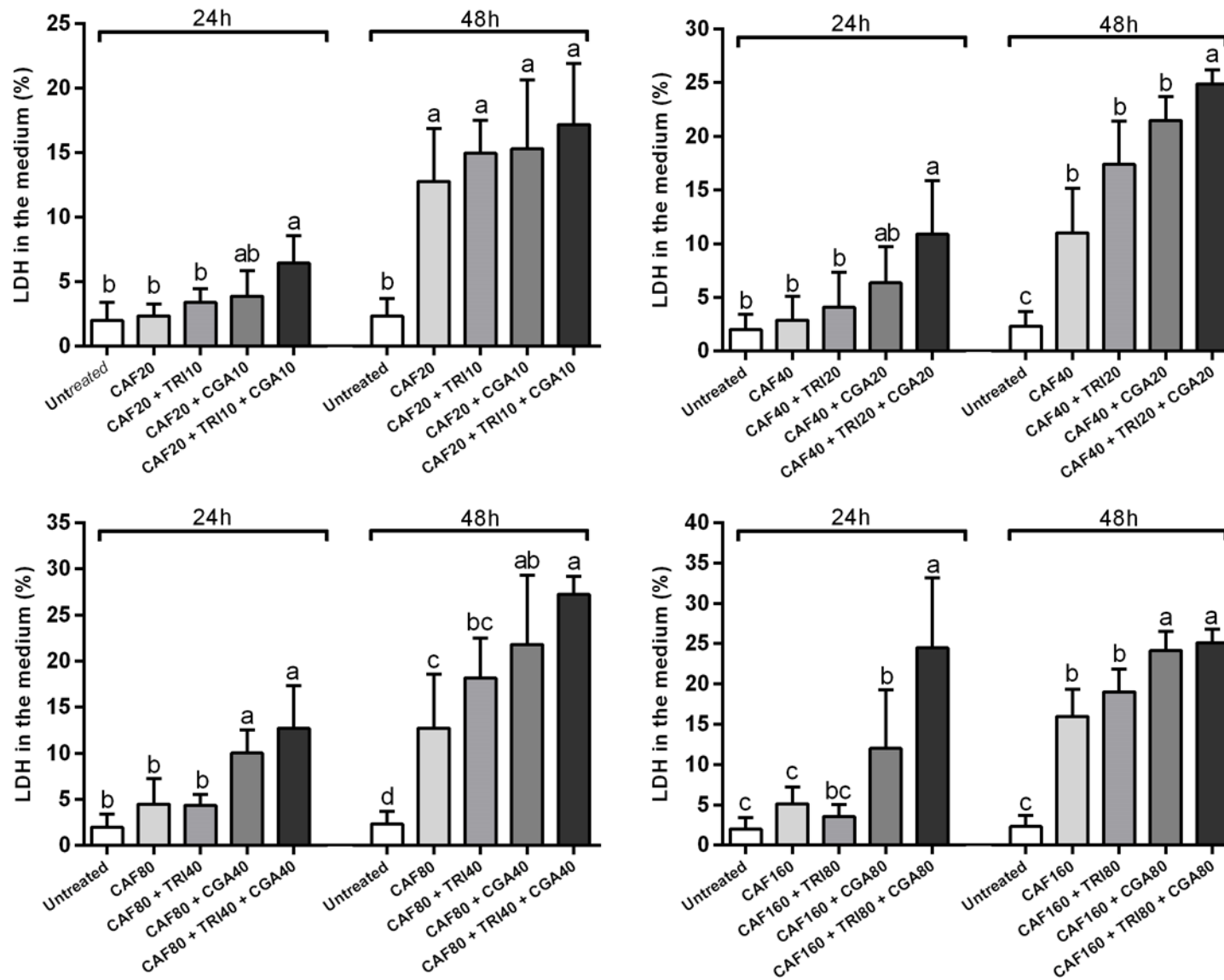
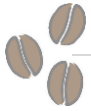
Supplementary Figure 7. Network analysis of the validated target genes of the differentially expressed miRNAs in CAF+TRI+CGA treatment. The interactions among the nodes (physical or functional) considered curated databases and/or experimentally determined data. Functional annotations regarding negative regulation of cell death (red) or positive regulation of cell population proliferation (blue) and Hepatocellular Carcinoma (green) were highlighted in the network. *Egrf* (dotted circle) shared both positive regulation of cell population proliferation and Hepatocellular Carcinoma annotations, eliciting the importance of this miR-144-3p target on hepatocarcinogenesis.



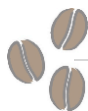
Supplementary Figure 8. Representative photomicrographs of Sirius red-stained sections and respective α -SMA and cleaved caspase-3 immunostained sections (20 \times objective, scale bar=50 μ m). In CAF+TRI+CGA group, apoptotic bodies (cleaved caspase-3 positive cells, arrowheads) are distributed over the region of activated hepatic stellate cells (α -SMA) and collagen deposition (Sirius red). α -SMA = alpha smooth muscle actin. DEN/ CCl_4 = diethylnitrosamine 10 mg/kg b.wt. i.p. at week 2 and carbon tetrachloride 0.25 to 1.50 μ L/g b.wt. i.p. from week 8 to 16. CAF = caffeine (50 mg/Kg b.wt.) and TRI, CGA = trigonelline and/or chlorogenic acid (25 mg/Kg b.wt., both) intragastrically administered from week 7 to 17 (see Material & Methods section).



Supplementary Figure 9. Effects of caffeine (CAF) individually or combined to trigonelline (TRI) and chlorogenic acid (CGA) on **(A)** HIF- α (miR-144-3p target) and VEGF (miR-15b-5p target) hepatic protein levels, **(B)** PCNA (miR-376a-3p target) immunostaining in preneoplastic foci and EGFR (miR-144-3p target) hepatic protein levels during DEN/CCl₄-induced fibrosis-associated hepatocarcinogenesis. Representative blot bands and semiquantitative analysis are presented. 40 \times objective, scale bar=25 μ m. Data are mean \pm S.D. n = 5 (untreated) to 6 (other groups) mice/group. DEN/CCl₄ = diethylnitrosamine 10 mg/kg b.wt. i.p. at week 2 and carbon tetrachloride 0.25 to 1.50 μ L/g b.wt. i.p. from week 8 to 16. CAF = caffeine (50 mg/Kg b.wt.) and TRI, CGA = trigonelline and/or chlorogenic acid (25 mg/Kg b.wt., both) intragastrically administered from week 7 to 17 (see Material & Methods section). Different letters correspond to statistical difference among groups by ANOVA and *post hoc* Tukey test ($p < 0.05$).



Supplementary Figure 10. Effects of varying concentrations of caffeine (CAF, 20, 40, 80 or 160 µM) alone or combined with trigonelline (TRI, 10, 20, 40 or 80 µM) and/or chlorogenic acid (CGA, 10, 20, 40 or 80 µM) on the cytotoxicity of C3A cells after 24 or 48 h of exposure. LDH = lactate dehydrogenase. Values are Mean + S.D. Different letters correspond to statistical difference by ANOVA and *post hoc* Tukey test ($p < 0.05$).



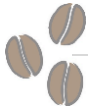
Supplementary Table 1. Concentrations of caffeine (CAF), trigonelline (TRI) and chlorogenic acid (CGA) used *in vitro*.

Combinations	Concentration (μM)		
	CAF	TRI	CGA
CAF	20	-	-
	40	-	-
	80	-	-
	160	-	-
CAF + TRI	20	10	-
	40	20	-
	80	40	-
	160	80	-
CAF + CGA	20	-	10
	40	-	20
	80	-	40
	160	-	80
CAF + TRI + CGA	20	10	10
	40	20	20
	80	40	40
	160	80	80

Supplementary Table 2. miRNAs modulated by CAF treatment during fibrosis-associated hepatocarcinogenesis (vs. DEN/ CCl_4 group).

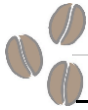
Upregulated (5)			
miRNAs	MIMATIDs	p value	FC
miR-144-3p	MIMAT0000156	0.008	1.74
miR-199a-5p	MIMAT0000229	0.004	1.74
miR-199a-3p	MIMAT0000230	0.002	1.62
miR-132-3p	MIMAT0000144	0.024	1.52
miR-376a-3p	MIMAT0000740	0.013	1.52

$p < 0.05$ and fold change (FC) > 1.5 . $n = 6$ mice/group. DEN/ CCl_4 = diethylnitrosamine 10 mg/kg b.wt. i.p. at week 2 and carbon tetrachloride 0.25 to 1.50 $\mu\text{L/g}$ b.wt. i.p. from week 8 to 16. CAF = caffeine (50 mg/Kg b.wt.) and TRI, CGA = trigonelline and/or chlorogenic acid (25 mg/Kg b.wt., both) intragastrically administered from week 7 to 17 (see Material & Methods section).

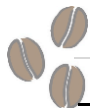


Supplementary Table 3. Experimentally validated targets of the 9 differentially expressed miRNAs in CAF+TRI+CGA treatment during fibrosis-associated hepatocarcinogenesis according to Ingenuity Pathway Analysis (IPA) output.

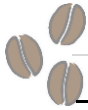
miRNA	Source	Confidence	Target gene
miR-132-3p	Ingenuity Expert Findings, TarBase, miRecords	Experimentally Observed	<i>Arhgap32</i>
miR-132-3p	miRecords	Experimentally Observed	<i>Capn8</i>
miR-132-3p	miRecords	Experimentally Observed	<i>Mecp2</i>
miR-132-3p	miRecords	Experimentally Observed	<i>Mmp9</i>
miR-132-3p	TarBase	Experimentally Observed	<i>Pgc</i>
miR-132-3p	Ingenuity Expert Findings, TargetScan Human	Experimentally Observed, High (predicted)	<i>Rb1</i>
miR-132-3p	Ingenuity Expert Findings, TargetScan Human	Experimentally Observed, Moderate (predicted)	<i>Sox4</i>
miR-132-3p	miRecords	Experimentally Observed	<i>Tjp1</i>
miR-144-3p	miRecords	Experimentally Observed	<i>Enpp6</i>
miR-144-3p	TarBase	Experimentally Observed	<i>Met</i>
miR-144-3p	TarBase	Experimentally Observed	<i>Hif1a</i>
miR-144-3p	TarBase	Experimentally Observed	<i>Egfr</i>
miR-15b-5p	TarBase, TargetScan Human	Experimentally Observed, Moderate (predicted)	<i>Abcf2</i>
miR-15b-5p	TarBase	Experimentally Observed	<i>Abhd10</i>
miR-15b-5p	TarBase, TargetScan Human	Experimentally Observed, Moderate (predicted)	<i>Acp2</i>
miR-15b-5p	miRecords	Experimentally Observed	<i>Actr1a</i>
miR-15b-5p	TarBase	Experimentally Observed	<i>Adss</i>
miR-15b-5p	miRecords	Experimentally Observed	<i>Anapc16</i>
miR-15b-5p	Ingenuity Expert Findings, TargetScan Human	Experimentally Observed, Moderate (predicted)	<i>Anln</i>
miR-15b-5p	TarBase, TargetScan Human	Experimentally Observed, Moderate (predicted)	<i>Arhgdia</i>
miR-15b-5p	TarBase, TargetScan Human, miRecords	Experimentally Observed, High (predicted)	<i>Arl2</i>



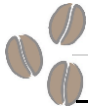
miR-15b-5p	miRecords	Experimentally Observed	<i>Asx12</i>
miR-15b-5p	Ingenuity Expert Findings,TargetScan Human	Experimentally Observed,Moderate (predicted)	<i>Atf6</i>
miR-15b-5p	TarBase,TargetScan Human	Experimentally Observed,High (predicted)	<i>Atg9a</i>
miR-15b-5p	Ingenuity Expert Findings,TarBase,TargetScan Human,miRecords	Experimentally Observed,Moderate (predicted)	<i>Bcl2</i>
miR-15b-5p	Ingenuity Expert Findings,TargetScan Human,miRecords	Experimentally Observed,High (predicted)	<i>Bcl2l2</i>
miR-15b-5p	TargetScan Human,miRecords	Experimentally Observed,High (predicted)	<i>Bdnf</i>
miR-15b-5p	miRecords	Experimentally Observed	<i>Bmi1</i>
miR-15b-5p	miRecords	Experimentally Observed	<i>C17orf80</i>
miR-15b-5p	miRecords	Experimentally Observed	<i>C2orf74</i>
miR-15b-5p	TarBase,TargetScan Human	Experimentally Observed,Moderate (predicted)	<i>Ca12</i>
miR-15b-5p	TarBase,TargetScan Human	Experimentally Observed,Moderate (predicted)	<i>Cacna2d1</i>
miR-15b-5p	miRecords	Experimentally Observed	<i>Cadm1</i>
miR-15b-5p	Ingenuity Expert Findings,TargetScan Human,miRecords	Experimentally Observed,Moderate (predicted)	<i>Caprin1</i>
miR-15b-5p	miRecords	Experimentally Observed	<i>Card8</i>
miR-15b-5p	Ingenuity Expert Findings,TargetScan Human,miRecords	Experimentally Observed,High (predicted)	<i>Ccnd1</i>
miR-15b-5p	TargetScan Human,miRecords	Experimentally Observed,High (predicted)	<i>Ccnd3</i>
miR-15b-5p	Ingenuity Expert Findings,TargetScan Human,miRecords	Experimentally Observed,High (predicted)	<i>Ccne1</i>
miR-15b-5p	Ingenuity Expert Findings	Experimentally Observed	<i>Ccnf</i>
miR-15b-5p	Ingenuity Expert Findings,TargetScan Human	Experimentally Observed,High (predicted)	<i>Cdc14a</i>
miR-15b-5p	miRecords	Experimentally Observed	<i>Cdc14b</i>
miR-15b-5p	Ingenuity Expert Findings,TargetScan Human	Experimentally Observed,Moderate (predicted)	<i>Cdc25a</i>
miR-15b-5p	TarBase,TargetScan Human	Experimentally Observed,Moderate (predicted)	<i>Cdk5rap1</i>
miR-15b-5p	TargetScan Human,miRecords	Experimentally Observed,Moderate (predicted)	<i>Cdk6</i>
miR-15b-5p	miRecords	Experimentally Observed	<i>Cenpj</i>
miR-15b-5p	miRecords	Experimentally Observed	<i>Cep63</i>
miR-15b-5p	miRecords	Experimentally Observed	<i>Cfl2</i>



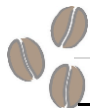
miR-15b-5p	Ingenuity Expert Findings,TargetScan Human	Experimentally Observed,High (predicted)	<i>Chek1</i>
miR-15b-5p	TarBase,TargetScan Human	Experimentally Observed,Moderate (predicted)	<i>Chordc1</i>
miR-15b-5p	TargetScan Human,miRecords	Experimentally Observed,High (predicted)	<i>Cldn12</i>
miR-15b-5p	miRecords	Experimentally Observed	<i>Crebl2</i>
miR-15b-5p	miRecords	Experimentally Observed	<i>Crhbp</i>
miR-15b-5p	miRecords	Experimentally Observed	<i>Csh1</i>
miR-15b-5p	TarBase,TargetScan Human,miRecords	Experimentally Observed,Moderate (predicted)	<i>Dmtf1</i>
miR-15b-5p	TarBase,TargetScan Human	Experimentally Observed,High (predicted)	<i>Dnajb4</i>
miR-15b-5p	TarBase	Experimentally Observed	<i>Dtd1</i>
miR-15b-5p	TargetScan Human,miRecords	Experimentally Observed,Moderate (predicted)	<i>E2f3</i>
miR-15b-5p	miRecords	Experimentally Observed	<i>Echdc1</i>
miR-15b-5p	TarBase	Experimentally Observed	<i>Egfr</i>
miR-15b-5p	TarBase,TargetScan Human	Experimentally Observed,Moderate (predicted)	<i>Eif4e</i>
miR-15b-5p	TarBase	Experimentally Observed	<i>F2</i>
miR-15b-5p	TargetScan Human,miRecords	Experimentally Observed,Moderate (predicted)	<i>Fam122c</i>
miR-15b-5p	miRecords	Experimentally Observed	<i>Fam69a</i>
miR-15b-5p	Ingenuity Expert Findings,TarBase,TargetScan Human	Experimentally Observed,High (predicted)	<i>Fgf2</i>
miR-15b-5p	Ingenuity Expert Findings,TargetScan Human	Experimentally Observed,High (predicted)	<i>Fgf7</i>
miR-15b-5p	Ingenuity Expert Findings,TargetScan Human,miRecords	Experimentally Observed,Moderate (predicted)	<i>Fgfr1</i>
miR-15b-5p	Ingenuity Expert Findings,TargetScan Human	Experimentally Observed,Moderate (predicted)	<i>Flt3</i>
miR-15b-5p	TarBase	Experimentally Observed	<i>Fndc3b</i>
miR-15b-5p	Ingenuity Expert Findings	Experimentally Observed	<i>Galnt13</i>
miR-15b-5p	TarBase,TargetScan Human	Experimentally Observed,High (predicted)	<i>Galnt7</i>
miR-15b-5p	TarBase	Experimentally Observed	<i>Gfm1</i>
miR-15b-5p	TarBase,TargetScan Human	Experimentally Observed,Moderate (predicted)	<i>Gfpt1</i>
miR-15b-5p	TarBase	Experimentally Observed	<i>Gnl3l</i>



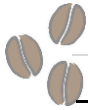
miR-15b-5p	miRecords	Experimentally Observed	<i>Golga5</i>
miR-15b-5p	miRecords	Experimentally Observed	<i>Golph3l</i>
miR-15b-5p	TarBase	Experimentally Observed	<i>Gpam</i>
miR-15b-5p	Ingenuity Expert Findings,TargetScan Human	Experimentally Observed,Moderate (predicted)	<i>Grb10</i>
miR-15b-5p	Ingenuity Expert Findings,TargetScan Human	Experimentally Observed,Moderate (predicted)	<i>Grb2</i>
miR-15b-5p	TarBase	Experimentally Observed	<i>Gstm4</i>
miR-15b-5p	miRecords	Experimentally Observed	<i>Gtf2h1</i>
miR-15b-5p	miRecords	Experimentally Observed	<i>H3f3a/h3f3b</i>
miR-15b-5p	miRecords	Experimentally Observed	<i>Hace1</i>
miR-15b-5p	TarBase	Experimentally Observed	<i>Hars</i>
miR-15b-5p	miRecords	Experimentally Observed	<i>Hdhd2</i>
miR-15b-5p	TargetScan Human,miRecords	Experimentally Observed,Moderate (predicted)	<i>Herc6</i>
miR-15b-5p	Ingenuity Expert Findings,TargetScan Human,miRecords	Experimentally Observed,High (predicted)	<i>Hmga1</i>
miR-15b-5p	TarBase	Experimentally Observed	<i>Hmox1</i>
miR-15b-5p	miRecords	Experimentally Observed	<i>Hpf1</i>
miR-15b-5p	miRecords	Experimentally Observed	<i>Hsdl2</i>
miR-15b-5p	miRecords	Experimentally Observed	<i>Hsp90b1</i>
miR-15b-5p	TarBase,TargetScan Human,miRecords	Experimentally Observed,High (predicted)	<i>Hspa1a/hspa1b</i>
miR-15b-5p	TarBase	Experimentally Observed	<i>Hyal3</i>
miR-15b-5p	TarBase	Experimentally Observed	<i>lfrd1</i>
miR-15b-5p	Ingenuity Expert Findings	Experimentally Observed	<i>lgf1</i>
miR-15b-5p	Ingenuity Expert Findings,TargetScan Human	Experimentally Observed,Moderate (predicted)	<i>lgf1r</i>
miR-15b-5p	TarBase	Experimentally Observed	<i>lgf2r</i>
miR-15b-5p	TarBase	Experimentally Observed	<i>lpo4</i>
miR-15b-5p	TarBase,TargetScan Human	Experimentally Observed,Moderate (predicted)	<i>ltga2</i>
miR-15b-5p	miRecords	Experimentally Observed	<i>Jun</i>



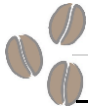
miR-15b-5p	Ingenuity Expert Findings	Experimentally Observed	<i>Jun/junb/jund</i>
miR-15b-5p	TarBase, TargetScan Human	Experimentally Observed, High (predicted)	<i>Kcnn4</i>
miR-15b-5p	Ingenuity Expert Findings, TargetScan Human	Experimentally Observed, High (predicted)	<i>Kif23</i>
miR-15b-5p	Ingenuity Expert Findings	Experimentally Observed	<i>Kitlg</i>
miR-15b-5p	TarBase	Experimentally Observed	<i>Kpna3</i>
miR-15b-5p	TarBase, TargetScan Human	Experimentally Observed, Moderate (predicted)	<i>Lamc1</i>
miR-15b-5p	TarBase, TargetScan Human	Experimentally Observed, Moderate (predicted)	<i>Lamtor3</i>
miR-15b-5p	TarBase	Experimentally Observed	<i>Lamtor5</i>
miR-15b-5p	miRecords	Experimentally Observed	<i>Ldah</i>
miR-15b-5p	TarBase, TargetScan Human	Experimentally Observed, High (predicted)	<i>Luzp1</i>
miR-15b-5p	TarBase, TargetScan Human	Experimentally Observed, Moderate (predicted)	<i>Lypla2</i>
miR-15b-5p	TargetScan Human, miRecords	Experimentally Observed, High (predicted)	<i>Map2k1</i>
miR-15b-5p	miRecords	Experimentally Observed	<i>Map2k4</i>
miR-15b-5p	Ingenuity Expert Findings	Experimentally Observed	<i>Mapk3</i>
miR-15b-5p	miRecords	Experimentally Observed	<i>Mcl1</i>
miR-15b-5p	Ingenuity Expert Findings	Experimentally Observed	<i>Mgat4a</i>
miR-15b-5p	Ingenuity Expert Findings	Experimentally Observed	<i>Mir-9</i>
miR-15b-5p	TarBase	Experimentally Observed	<i>Mlit1</i>
miR-15b-5p	TarBase	Experimentally Observed	<i>Mlit11</i>
miR-15b-5p	TarBase	Experimentally Observed	<i>Mrpl20</i>
miR-15b-5p	miRecords	Experimentally Observed	<i>Msh2</i>
miR-15b-5p	TargetScan Human, miRecords	Experimentally Observed, High (predicted)	<i>Myb</i>
miR-15b-5p	TarBase, TargetScan Human	Experimentally Observed, Moderate (predicted)	<i>Naa15</i>
miR-15b-5p	TarBase, TargetScan Human	Experimentally Observed, Moderate (predicted)	<i>Napg</i>
miR-15b-5p	Ingenuity Expert Findings, miRecords	Experimentally Observed	<i>Nfia</i>
miR-15b-5p	miRecords	Experimentally Observed	<i>Nipal2</i>



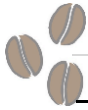
miR-15b-5p	TarBase,TargetScan Human	Experimentally Observed,Moderate (predicted)	<i>Notch2</i>
miR-15b-5p	TarBase	Experimentally Observed	<i>Npr3</i>
miR-15b-5p	miRecords	Experimentally Observed	<i>Nt5dc1</i>
miR-15b-5p	Ingenuity Expert Findings	Experimentally Observed	<i>Ogt</i>
miR-15b-5p	miRecords	Experimentally Observed	<i>Oma1</i>
miR-15b-5p	miRecords	Experimentally Observed	<i>Osgepl1</i>
miR-15b-5p	TarBase,TargetScan Human	Experimentally Observed,Moderate (predicted)	<i>Pafah1b2</i>
miR-15b-5p	TarBase	Experimentally Observed	<i>Panx1</i>
miR-15b-5p	TargetScan Human,miRecords	Experimentally Observed,Moderate (predicted)	<i>Pdcd4</i>
miR-15b-5p	TargetScan Human,miRecords	Experimentally Observed,Moderate (predicted)	<i>Pdcd6ip</i>
miR-15b-5p	miRecords	Experimentally Observed	<i>Phkb</i>
miR-15b-5p	TarBase	Experimentally Observed	<i>Phldb2</i>
miR-15b-5p	TarBase,TargetScan Human	Experimentally Observed,Moderate (predicted)	<i>Pisd</i>
miR-15b-5p	TargetScan Human,miRecords	Experimentally Observed,High (predicted)	<i>Plag1</i>
miR-15b-5p	TarBase	Experimentally Observed	<i>Plk1</i>
miR-15b-5p	miRecords	Experimentally Observed	<i>Pms1</i>
miR-15b-5p	miRecords	Experimentally Observed	<i>Pnn</i>
miR-15b-5p	TarBase,TargetScan Human	Experimentally Observed,High (predicted)	<i>Pnp</i>
miR-15b-5p	TarBase,TargetScan Human	Experimentally Observed,Moderate (predicted)	<i>Ppif</i>
miR-15b-5p	TarBase,TargetScan Human	Experimentally Observed,Moderate (predicted)	<i>Ppp2r5c</i>
miR-15b-5p	miRecords	Experimentally Observed	<i>Prim1</i>
miR-15b-5p	miRecords	Experimentally Observed	<i>Primpol</i>
miR-15b-5p	TarBase,TargetScan Human	Experimentally Observed,Moderate (predicted)	<i>Psat1</i>
miR-15b-5p	TarBase	Experimentally Observed	<i>Ptgs2</i>
miR-15b-5p	Ingenuity Expert Findings,TarBase,TargetScan Human	Experimentally Observed,High (predicted)	<i>Pura</i>
miR-15b-5p	miRecords	Experimentally Observed	<i>Pwwp2a</i>



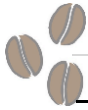
miR-15b-5p	miRecords	Experimentally Observed	<i>Rab21</i>
miR-15b-5p	TarBase,TargetScan Human	Experimentally Observed,High (predicted)	<i>Rab30</i>
miR-15b-5p	TargetScan Human,miRecords	Experimentally Observed,High (predicted)	<i>Rab9b</i>
miR-15b-5p	miRecords	Experimentally Observed	<i>Rad51c</i>
miR-15b-5p	Ingenuity Expert Findings,TargetScan Human	Experimentally Observed,Moderate (predicted)	<i>Raf1</i>
miR-15b-5p	TarBase	Experimentally Observed	<i>Rars</i>
miR-15b-5p	TargetScan Human,miRecords	Experimentally Observed,High (predicted)	<i>Reck</i>
miR-15b-5p	TarBase	Experimentally Observed	<i>Rf11</i>
miR-15b-5p	miRecords	Experimentally Observed	<i>Rhot1</i>
miR-15b-5p	miRecords	Experimentally Observed	<i>Rida</i>
miR-15b-5p	miRecords	Experimentally Observed	<i>Rnasel</i>
miR-15b-5p	TarBase,TargetScan Human	Experimentally Observed,Moderate (predicted)	<i>Rtn4</i>
miR-15b-5p	TarBase	Experimentally Observed	<i>Sec24a</i>
miR-15b-5p	TarBase	Experimentally Observed	<i>Serpine2</i>
miR-15b-5p	TarBase,TargetScan Human	Experimentally Observed,High (predicted)	<i>Shoc2</i>
miR-15b-5p	miRecords	Experimentally Observed	<i>Skap2</i>
miR-15b-5p	TarBase,TargetScan Human,miRecords	Experimentally Observed,Moderate (predicted)	<i>Slc12a2</i>
miR-15b-5p	TarBase	Experimentally Observed	<i>Slc16a3</i>
miR-15b-5p	TarBase,TargetScan Human	Experimentally Observed,Moderate (predicted)	<i>Slc25a22</i>
miR-15b-5p	miRecords	Experimentally Observed	<i>Slc35a1</i>
miR-15b-5p	miRecords	Experimentally Observed	<i>Slc35b3</i>
miR-15b-5p	TarBase	Experimentally Observed	<i>Slc38a1</i>
miR-15b-5p	TarBase	Experimentally Observed	<i>Slc38a5</i>
miR-15b-5p	TarBase,TargetScan Human	Experimentally Observed,Moderate (predicted)	<i>Slc7a1</i>
miR-15b-5p	Ingenuity Expert Findings	Experimentally Observed	<i>Spi1</i>
miR-15b-5p	TarBase,TargetScan Human	Experimentally Observed,Moderate (predicted)	<i>Sptlc1</i>



miR-15b-5p	TarBase	Experimentally Observed	<i>Sqstm1</i>
miR-15b-5p	TarBase,TargetScan Human	Experimentally Observed,High (predicted)	<i>Srpra</i>
miR-15b-5p	TarBase	Experimentally Observed	<i>Srprb</i>
miR-15b-5p	miRecords	Experimentally Observed	<i>Tia1</i>
miR-15b-5p	TarBase,TargetScan Human	Experimentally Observed,High (predicted)	<i>Tmem109</i>
miR-15b-5p	TarBase,TargetScan Human	Experimentally Observed,High (predicted)	<i>Tmem189-ube2v1</i>
miR-15b-5p	miRecords	Experimentally Observed	<i>Tmem251</i>
miR-15b-5p	TarBase,TargetScan Human	Experimentally Observed,Moderate (predicted)	<i>Tmem43</i>
miR-15b-5p	TarBase,TargetScan Human	Experimentally Observed,Moderate (predicted)	<i>Tnfsf9</i>
miR-15b-5p	TarBase,TargetScan Human	Experimentally Observed,Moderate (predicted)	<i>Tomm34</i>
miR-15b-5p	miRecords	Experimentally Observed	<i>Tpi1</i>
miR-15b-5p	TarBase,TargetScan Human	Experimentally Observed,High (predicted)	<i>Tpm3</i>
miR-15b-5p	TarBase,TargetScan Human,miRecords	Experimentally Observed,High (predicted)	<i>Tppp3</i>
miR-15b-5p	miRecords	Experimentally Observed	<i>Trmt13</i>
miR-15b-5p	TarBase,TargetScan Human	Experimentally Observed,Moderate (predicted)	<i>Txn2</i>
miR-15b-5p	TarBase	Experimentally Observed	<i>Ube2s</i>
miR-15b-5p	TarBase,TargetScan Human	Experimentally Observed,Moderate (predicted)	<i>Ube4a</i>
miR-15b-5p	Ingenuity Expert Findings,TargetScan Human	Experimentally Observed,Moderate (predicted)	<i>Ucp2</i>
miR-15b-5p	miRecords	Experimentally Observed	<i>Ugdh</i>
miR-15b-5p	miRecords	Experimentally Observed	<i>Ugp2</i>
miR-15b-5p	TarBase	Experimentally Observed	<i>Utp15</i>
miR-15b-5p	TargetScan Human,miRecords	Experimentally Observed,High (predicted)	<i>Vegfa</i>
miR-15b-5p	miRecords	Experimentally Observed	<i>Vps45</i>
miR-15b-5p	TarBase,TargetScan Human	Experimentally Observed,High (predicted)	<i>Vti1b</i>
miR-15b-5p	Ingenuity Expert Findings,TargetScan Human	Experimentally Observed,High (predicted)	<i>Wee1</i>
miR-15b-5p	miRecords	Experimentally Observed	<i>Wipf1</i>



miR-15b-5p	Ingenuity Expert Findings,TargetScan Human	Experimentally Observed,High (predicted)	<i>Wnt3a</i>
miR-15b-5p	miRecords	Experimentally Observed	<i>Wt1</i>
miR-15b-5p	TarBase,TargetScan Human	Experimentally Observed,Moderate (predicted)	<i>Yif1b</i>
miR-15b-5p	miRecords	Experimentally Observed	<i>Znf559</i>
miR-15b-5p	TarBase,TargetScan Human	Experimentally Observed,High (predicted)	<i>Znf622</i>
miR-15b-5p	Ingenuity Expert Findings,TargetScan Human	Experimentally Observed,Moderate (predicted)	<i>Zyx</i>
miR-199a-3p	Ingenuity Expert Findings,TargetScan Human	Experimentally Observed,Moderate (predicted)	<i>Calu</i>
miR-199a-3p	Ingenuity Expert Findings,TargetScan Human	Experimentally Observed,Moderate (predicted)	<i>Cd44</i>
miR-199a-3p	Ingenuity Expert Findings,TargetScan Human	Experimentally Observed,Moderate (predicted)	<i>Fn1</i>
miR-199a-3p	Ingenuity Expert Findings,TargetScan Human	Experimentally Observed,High (predicted)	<i>Fubp1</i>
miR-199a-3p	TarBase	Experimentally Observed	<i>Met</i>
miR-199a-3p	TargetScan Human,miRecords	Experimentally Observed,Moderate (predicted)	<i>Mtor</i>
miR-199a-3p	Ingenuity Expert Findings,TargetScan Human	Experimentally Observed,High (predicted)	<i>Pon2</i>
miR-199a-3p	Ingenuity Expert Findings	Experimentally Observed	<i>Prdx6</i>
miR-199a-3p	Ingenuity Expert Findings,miRecords	Experimentally Observed	<i>Ptgs2</i>
miR-199a-3p	Ingenuity Expert Findings,TargetScan Human	Experimentally Observed,Moderate (predicted)	<i>Runx1</i>
miR-199a-3p	miRecords	Experimentally Observed	<i>Smad1</i>
miR-199a-3p	Ingenuity Expert Findings	Experimentally Observed	<i>Suz12</i>
miR-199a-3p	Ingenuity Expert Findings	Experimentally Observed	<i>Vcan</i>
miR-199a-5p	miRecords	Experimentally Observed	<i>Alox5ap</i>
miR-199a-5p	Ingenuity Expert Findings,TargetScan Human	Experimentally Observed,Moderate (predicted)	<i>Dyrk1a</i>
miR-199a-5p	Ingenuity Expert Findings,TargetScan Human	Experimentally Observed,Moderate (predicted)	<i>Ets1</i>
miR-199a-5p	Ingenuity Expert Findings,TargetScan Human,miRecords	Experimentally Observed,Moderate (predicted)	<i>Hif1a</i>
miR-199a-5p	TarBase,miRecords	Experimentally Observed	<i>Lamc2</i>
miR-199a-5p	TargetScan Human,miRecords	Experimentally Observed,Moderate (predicted)	<i>Set</i>
miR-199a-5p	TargetScan Human,miRecords	Experimentally Observed,Moderate (predicted)	<i>Sirt1</i>



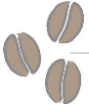
miR-342-3p	Ingenuity Expert Findings,TargetScan Human	Experimentally Observed,Moderate (predicted)	<i>Mtdh</i>
miR-335-5p	Ingenuity Expert Findings	Experimentally Observed	<i>Kit</i>
miR-335-5p	Ingenuity Expert Findings	Experimentally Observed	<i>Ptpn11</i>
miR-335-5p	Ingenuity Expert Findings,TargetScan Human	Experimentally Observed,Moderate (predicted)	<i>Pxn</i>
miR-335-5p	Ingenuity Expert Findings,TargetScan Human	Experimentally Observed,Moderate (predicted)	<i>Rasa1</i>
miR-335-5p	Ingenuity Expert Findings,TargetScan Human	Experimentally Observed,Moderate (predicted)	<i>Srf</i>
miR-376a-3p	MirTarBase	Experimentally Observed	<i>Pcna</i>

Supplementary Table 4. The main experimentally validated targets of differentially expressed miRNAs in CAF+TRI+CGA group.

Gene	EntrezID	Validated target of	PMID	Tissue/Cell type
<i>Bcl2</i>	12043	miR-15b-5p	26195352, 22374434, 19232449, 22487517, 26884837, 23142080	Liver, hepatic and pancreatic stellate cells, Hepatocellular carcinoma cells, CD4+ T cells
<i>Bcl2l2</i>	12050	miR-15b-5p	24070634	Mesenchymal stem cell
<i>Mcl1</i>	17210	miR-15b-5p	26195352, 23142080	Liver, CD4+ T cells
<i>Pcna</i>	18538	mmu-miR-376a-3p	24686458	Ovary
<i>Hif1a</i>	15251	miR-144-3p, miR-199a-5p	25083871, 19265035, 26344767, 25823824, 26783726, 23142080	Muscle, Cardiac myocytes, Brain, Liver cancer cells, Liver, CD4+ T cells
<i>Vegfa</i>	22339	miR-15b-5p	27070581, 22613985, 17205120	Joint, endothelial cells, nasopharyngeal carcinoma cell line
<i>Egfr</i>	13649	miR-144-3p	29072132	Liver

A decorative graphic consisting of three overlapping coffee rings in shades of brown and tan, with several small coffee droplets scattered around them. The rings are positioned in the lower half of the page, framing the text.

Conclusões



- Nossos achados sugerem que a **combinação dos compostos** mais comuns e biodisponíveis do café (assim como no café espresso e filtrado), ao invés da cafeína isoladamente, atenua a hepatocarcinogênese associada à fibrose quando administrados em doses semelhantes ao consumo humano de café. Tais efeitos benéficos são mecanisticamente mediados, em parte, pela **modulação da expressão de miRNAs** no fígado
- Assim, o **consumo de substâncias comuns e biodisponíveis do café, por meio da modulação de miRNAs supressores de tumor**, possui **efeito preventivo** durante a hepatocarcinogênese, e nossos achados devem ser confirmados por outras investigações translacionais utilizando de diferentes bioensaios. Considerando os dados epidemiológicos que serviram de justificativa para o estudo, nossos achados também indicam quais compostos e alguns dos mecanismos que podem **explicar os efeitos hepatoprotetores** do consumo de café ao nível populacional.



A seguir, segue a descrição das atividades acadêmicas realizadas pelo discente ao longo do doutorado (2016 a 2020). Sobretudo, é apresentado artigo publicado na revista PLOS One (fator de impacto 2,776, JCR 2018), referente à padronização do modelo quimicamente induzido de hepatocarcinogênese associada à fibrose que foi realizado como parte do doutorado do discente nos anos de 2016 e 2017.

Doutorado sanduíche no exterior:

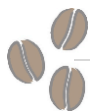
1. Università Degli Studi di Cagliari (Cagliari – Itália), supervisionado pelo Prof. Amedeo Columbano, no período de outubro de 2018 até abril de 2019. Beneficiário de bolsa do Programa de Doutorado Sanduíche no Exterior (PDSE) - Coordenação de Aperfeiçoamento de Pessoal de Nível Superior -Brasil (CAPES) (#88881.188786/2018-01).

Capítulos de livro publicados:

1. **Romualdo, Guilherme Ribeiro**; Da Silva, Flávia Regina Moraes; Zapaterini, Joyce Regina; Tablas; Mariana Baptista; **Barbisan, Luís Fernando**. Chapter 5: Zinc and Cancer Prevention. In: Nutrition and Cancer Prevention: From Molecular Mechanisms to Dietary Recommendations, Royal Society of Chemistry, 2019.
2. **Romualdo, Guilherme Ribeiro**; Vinken, Mathieu; **Cogliati, Bruno**. Chapter 7: Alcohol Intake and Cancer Risk. In: Nutrition and Cancer Prevention: From Molecular Mechanisms to Dietary Recommendations, Royal Society of Chemistry, 2019.

Artigos científicos publicados:

1. **Romualdo, Guilherme Ribeiro**; Silva, Elizangela Dos Anjos; Da Silva, Tereza C.; Aloia, Thiago P. A; Nogueira, Marina S. ; De Castro, Inar A. ; Vinken, Mathieu ; **Barbisan, Luis Fernando**; **Cogliati, Bruno**. Burdock (*Arctium lappa* L.) root attenuates preneoplastic lesion development in a diet and thioacetamide-induced model of steatohepatitis-associated hepatocarcinogenesis. Environmental Toxicology, 2019.
2. **Romualdo, Guilherme Ribeiro**; Rocha, Ariane Bartolomeu; Vinken, Mathieu; **Cogliati, Bruno**; Moreno, Fernando Salvador; Chaves, María Angel García; **Barbisan, Luis Fernando**. Drinking for protection? Epidemiological and experimental evidence on the beneficial effects of coffee or major coffee compounds against gastrointestinal and liver carcinogenesis. Food Research International, v. 123, p. 567-589, 2019.
3. Medeiros, Mariana; Ribeiro, Amanda Oliveira; Lupi, Luiz Antônio; **Romualdo, Guilherme Ribeiro**; Pinhal, Danillo; Chuffa, Luiz Gustavo De Almeida; Delella, Flávia Karina. Mimicking the tumor microenvironment: Fibroblasts reduce miR-29b expression and increase the motility of ovarian cancer cells in a co-culture model. Biochemical and Biophysical Research Communications, v. 516, p. 96-101, 2019.
4. **Romualdo, Guilherme Ribeiro**; Prata, Gabriel Bacil; Da Silva, Tereza Cristina; Fernandes, Ana Angélica Henrique; Moreno, Fernando Salvador; **Cogliati, Bruno**; **Barbisan, Luís Fernando**. Fibrosis-associated hepatocarcinogenesis



revisited: Establishing standard medium-term chemically-induced male and female models. PLoS One, v. 13, p. e0203879, 2018.

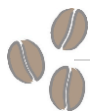
5. Crespo Yanguas, Sara; Da Silva, Tereza; Pereira, Isabel; Willebrords, Joost; Maes, Michaël; Sayuri Nogueira, Marina; Alves De Castro, Inar; Leclercq, Isabelle; **Romualdo, Guilherme Ribeiro**; **Barbisan, Luis Fernando**; Leybaert, Luc; **Cogliati, Bruno**; Vinken, Mathieu. TAT-Gap19 and Carbenoxolone Alleviate Liver Fibrosis in Mice. International Journal of Molecular Sciences, v. 19, p. 817, 2018.
6. Crespo Yanguas, Sara; Da Silva, Tereza C.; Pereira, Isabel V. A.; Maes, Michaël ; Willebrords, Joost; Shestopalov, Valery I. ; Goes, Bruna M. ; Sayuri Nogueira, Marina ; Alves De Castro, Inar ; **Romualdo, Guilherme Ribeiro**; **Barbisan, Luis Fernando**; Gijbels, Eva; Vinken, Mathieu; **Cogliati, Bruno**. Genetic ablation of pannexin1 counteracts liver fibrosis in a chemical, but not in a surgical mouse model. Archives of Toxicology, v. 92, p. 2607-2627, 2018.
7. Fragoso, Mariana F.; **Romualdo, Guilherme R.**; Vanderveer, Lisa A.; Franco-Barraza, Janusz; Cukierman, Edna; Clapper, Margie L.; Carvalho, Robson F.; **Barbisan, Luis F.** Lyophilized açai pulp (*Euterpe oleracea* Mart) attenuates colitis-associated colon carcinogenesis while its main anthocyanin has the potential to affect the motility of colon cancer cells. Food and Chemical Toxicology, v. 121, p. 237-245, 2018.
8. **Romualdo, Guilherme Ribeiro**; Goto, Renata L.; Fernandes, Ana A.H.; **Cogliati, Bruno**; **Barbisan, Luis Fernando**. Vitamin D₃ supplementation attenuates the early stage of mouse hepatocarcinogenesis promoted by hexachlorobenzene fungicide. Food and Chemical Toxicology, v. 107, p. 27-36, 2017.
9. **Romualdo, Guilherme Ribeiro**; Grassi, Tony Fernando; Goto, Renata Leme; Tablas, Mariana Baptista; Bidinotto, Lucas Tadeu; Fernandes, Ana Angélica Henrique; **Cogliati, Bruno**; **Barbisan, Luis Fernando**. An integrative analysis of chemically-induced cirrhosis-associated hepatocarcinogenesis: Histological, biochemical and molecular features. Toxicology Letters, v. 281, p. 84-94, 2017.
10. **Romualdo, Guilherme Ribeiro**; Goto, Renata Leme; Henrique Fernandes, Ana Angélica; **Cogliati, Bruno**; **Barbisan, Luis Fernando**. Dietary zinc deficiency predisposes mice to the development of preneoplastic lesions in chemically-induced hepatocarcinogenesis. Food and Chemical Toxicology, v. 96, p. 280-289, 2016.

Co-orientações:

1. Gabriel Bacil Prata. Aluno do curso de Ciências Biomédicas. Doença hepática gordurosa não alcoólica (DHGNA): variantes e modelos biológicos, 2019.

Experiência em docência:

1. Colaborador na disciplina “Carcinogênese Experimental” (responsável: Prof. Luis F. Barbisan) do curso de pós-graduação em Patologia (Faculdade de Medicina, UNESP - Botucatu), ministrando a aula “*Hepatocarcinogenesis: of mice and men*”, dos anos de 2016 a 2019.



2. Colaborador da disciplina “Técnicas Especiais Aplicadas à Pesquisa em Patologia” (responsável: Prof. Luis F. Barbisan), do curso de pós-graduação em Patologia (Faculdade de Medicina, UNESP - Botucatu), ministrando a aula de “Teste do Cometa”, no ano de 2017.
3. Colaborador da disciplina “Métodos de Estudo em Biologia Celular e Molecular” (responsável: Wellerson Rodrigo Scarano), do curso de pós-graduação em Biologia Geral e Aplicada (Instituto de Biociências, UNESP – Botucatu), ministrando a aula de “Teste do Cometa”, no ano de 2019.
4. Colaborador da disciplina “Hepatologia Experimental e Comparada” (responsável: Prof. Bruno Cogliati), do curso de pós-graduação em Patologia Experimental e Comparada (Faculdade de Medicina Veterinária e Zootecnia, USP – São Paulo), ministrando a aula “*Hepatocarcinogenesis: of mice and men*”, em 2016.
5. Colaborador da disciplina optativa “Práticas em Métodos de Estudos Clássicos em Morfologia” (responsável: Profª Claudia Helena Pellizzon), disciplina optativa dos cursos de graduação do Instituto de Biociências (UNESP – Botucatu), ministrando as aulas de “Teste do Cometa” (2016 a 2019), “Western blot” (2019) e “miRNômica” (2019).

Premiações:

1. Charles Capen Trainee Award 2018: Achievements in the field of toxicologic pathology. “The association of bioactive coffee compounds alleviates fibrosis-associated hepatocarcinogenesis *in vivo*”. International Academy of Toxicologic Pathology. https://www.iatpfellow.org/site_page.cfm?pk_association_webpage_menu=6694&pk_association_webpage=13986

Além disso, foram apresentados 14 resumos em congressos nacionais e internacionais, com destaque a participação do discente nas duas últimas edições do congresso “*American Association for Cancer Research (AACR) International Conference on Translational Cancer Medicine*”:

1. **Romualdo, Guilherme Ribeiro.** “*Drinking for the liver? Experimental evidence on the attenuation of fibrosis-associated hepatocarcinogenesis by the combination of bioactive coffee compounds*”. Second AACR International Conference on Translational Cancer Medicine, 2018, São Paulo – SP.
2. **Romualdo, Guilherme Ribeiro.** “*The association of caffeine, trigonelline and chlorogenic acid, active components from coffee, enhances caffeine-induced cytotoxicity in hepatocellular carcinoma cells.*” American Association for Cancer Research (AACR) International Conference on Translational Cancer Medicine, 2017, São Paulo – SP.

RESEARCH ARTICLE

Fibrosis-associated hepatocarcinogenesis revisited: Establishing standard medium-term chemically-induced male and female models

Guilherme Ribeiro Romualdo¹, Gabriel Bacil Prata², Tereza Cristina da Silva³, Ana Angélica Henrique Fernandes⁴, Fernando Salvador Moreno⁵, Bruno Cogliati³, Luís Fernando Barbisan^{2*}

1 Department of Pathology, Botucatu Medical School, São Paulo State University (UNESP), Botucatu, São Paulo, Brazil, **2** Department of Morphology, Biosciences Institute, São Paulo State University (UNESP), Botucatu, São Paulo, Brazil, **3** Department of Pathology, School of Veterinary Medicine and Animal Science, University of São Paulo (USP), São Paulo, São Paulo, Brazil, **4** Department of Chemistry and Biochemistry, Biosciences Institute, São Paulo State University (UNESP), Botucatu, São Paulo, Brazil, **5** Department of Food and Experimental Nutrition, Faculty of Pharmaceutical Sciences, University of São Paulo (USP), São Paulo, São Paulo, Brazil

* barbisan@ibb.unesp.br



OPEN ACCESS

Citation: Romualdo GR, Prata GB, da Silva TC, Fernandes AAH, Moreno FS, Cogliati B, et al. (2018) Fibrosis-associated hepatocarcinogenesis revisited: Establishing standard medium-term chemically-induced male and female models. PLoS ONE 13(9): e0203879. <https://doi.org/10.1371/journal.pone.0203879>

Editor: Jordi Gracia-Sancho, IDIBAPS Biomedical Research Institute, SPAIN

Received: April 3, 2018

Accepted: August 29, 2018

Published: September 13, 2018

Copyright: © 2018 Romualdo et al. This is an open access article distributed under the terms of the [Creative Commons Attribution License](https://creativecommons.org/licenses/by/4.0/), which permits unrestricted use, distribution, and reproduction in any medium, provided the original author and source are credited.

Data Availability Statement: All relevant data are within the paper and its Supporting Information files.

Funding: Guilherme R. Romualdo was recipient of a fellowship and grants from the National Council for Scientific and Technological Development (CNPq) (grant #140251/2016-2) and São Paulo Research Foundation (FAPESP) (grant #2016/12015-0). Luis F. Barbisan was recipient of support research from FAPESP (grant #2016/14420-0).

Abstract

Hepatocellular carcinoma causes ~10% of all cancer-related deaths worldwide, usually emerging in a background of liver fibrosis/cirrhosis (70%-90% of cases). Chemically-induced mouse models for fibrosis-associated hepatocarcinogenesis are widely-applied, resembling the corresponding human disease. Nonetheless, a long time is necessary for the development of preneoplastic/neoplastic lesions. Thus, we proposed an early fibrosis-associated hepatocarcinogenesis model for male and female mice separately, focusing on reducing the experimental time for preneoplastic/neoplastic lesions development and establishing standard models for both sexes. Then, two-week old susceptible C3H/HeJ male and female mice (n = 8 animals/sex/group) received a single dose of diethylnitrosamine (DEN, 10 or 50 mg/Kg). During 2 months, mice received 3 weekly doses of carbon tetrachloride (CCl₄, 10% corn oil solution, 0.25 to 1.50 μL/g b.wt.) and they were euthanized at week 17. DEN/CCl₄ protocols for males and females displayed clear liver fibrosis, featuring collagen accumulation and hepatic stellate cell activation (α-SMA). In addition, liver from males displayed increased CD68+ macrophage number, COX-2 protein expression and IL-6 levels. The DEN/CCl₄ models in both sexes impaired antioxidant defense as well as enhanced hepatocyte proliferation and apoptosis. Moreover, DEN/CCl₄-treated male and female developed multiple preneoplastic altered hepatocyte foci and hepatocellular adenomas. As expected, the models showed clear male bias. Therefore, we established standard and suitable fibrosis-associated hepatocarcinogenesis models for male and female mice, shortening the experimental time for the development of hepatocellular preneoplastic/neoplastic lesions in comparison to other classical models.

FAPESP—<http://www.fapesp.br/>, CNPq—<http://cnpq.br/>. The funders had no role in study design, data collection and analysis, decision to publish, or preparation of the manuscript.

Competing interests: The authors have declared that no competing interests exist.

Introduction

Hepatocellular carcinoma (HCC), the main type of primary liver cancer, is responsible for ~10% of all cancer-related deaths worldwide (~800,000 deaths/year, considering both genders) [1]. Although epidemiological data presents clear gender disparity, assuming that HCC is about three times more common in men (554,000 vs. 228,000 new cases/year), this malignant neoplasia displays increasing importance in women, being the ninth most common cancer and the sixth leading cause of cancer-related deaths in this gender [1].

HCC is considered a complex, multistep and multifactorial disease and it usually emerges in a background of liver fibrosis/cirrhosis (70% to 90% of all HCC cases), mainly caused by chronic hepatitis B and C virus infections, chronic ethanol abuse and nonalcoholic steatohepatitis (NASH) [2,3]. The pro-inflammatory and pro-fibrotic environment provided by these risk factors are the necessary background for the emerging of genetic and epigenetic alterations that can promote the development of dysplastic nodules and neoplastic lesions, mainly HCC [4].

The establishment of chemically-induced hepatocarcinogenesis models in rodents proved to be essential for both basic and translational research because of their remarkable similarities to the corresponding human disease [5,6]. Nonetheless, due to the great variability of chemically-induced protocols (*e.g.* different chemical compounds, doses, frequencies of administration, etc.) and mouse strains used (less or more susceptible), the literature lacks standard mice models for hepatocarcinogenesis in males and especially in females, neglected because the models reflect the HCC male bias in humans [7]. In addition, a long latency time is necessary for the development of hepatocellular preneoplastic and/or neoplastic lesions in these models [5]. Finally, most of chemically-induced hepatocarcinogenesis mice models do not feature liver fibrosis, calling into question whether these models can reliably recapitulate key events observed during human hepatocarcinogenesis and HCC progression.

In this context, this study aimed at proposing a medium-term fibrosis-associated hepatocarcinogenesis mouse model for male and female mice separately, allying chemically-induced protocol and a susceptible mouse strain in order to reduce the experimental time to the development of hepatocellular preneoplastic and neoplastic lesions associated to liver fibrosis. Thus, the establishment of standard medium-term mice models may favor the emerging diagnostic, preventive and therapeutic methods for fibrosis-associated hepatocarcinogenesis in humans.

Materials and methods

Experimental design

In order to reduce the experimental period, the C3H/HeJ mouse strain was selected due to its increased susceptibility to DEN-induced hepatocarcinogenesis compared to Balb/C and C57BL mouse strains [8,9]. C3H/HeJ male and female mice ($n = 8$ animals/sex/group), obtained from the Department of Pathology of School of Veterinary Medicine and Animal Science (University of São Paulo) and kept in Botucatu Medical School (São Paulo State University), were submitted to a classical infant hepatocarcinogenesis model [10] by receiving a single intraperitoneal (*i.p.*) injection of diethylnitrosamine [DEN, 10 or 50 mg/kg body weight (*b.wt.*) in 0.9% saline, Sigma-Aldrich, USA] at postnatal day (PND) 14 or just saline vehicle (Fig 1). Both single 10 and 50 mg/Kg DEN doses were based on previous studies [11,12]. Mice were weaned at PND 28 (week 4). From week 8 to 16, in order to promote DEN-induced hepatocellular preneoplastic and neoplastic lesions in a background of liver fibrosis, mice received 3 weekly *i.p.* doses of carbon tetrachloride (CCl_4 , 10% solution in corn oil, Sigma-Aldrich, USA) or just vehicle (Fig 1). The initial dose of CCl_4 was 0.25 $\mu\text{L/g}$ *b.wt.*, and there were

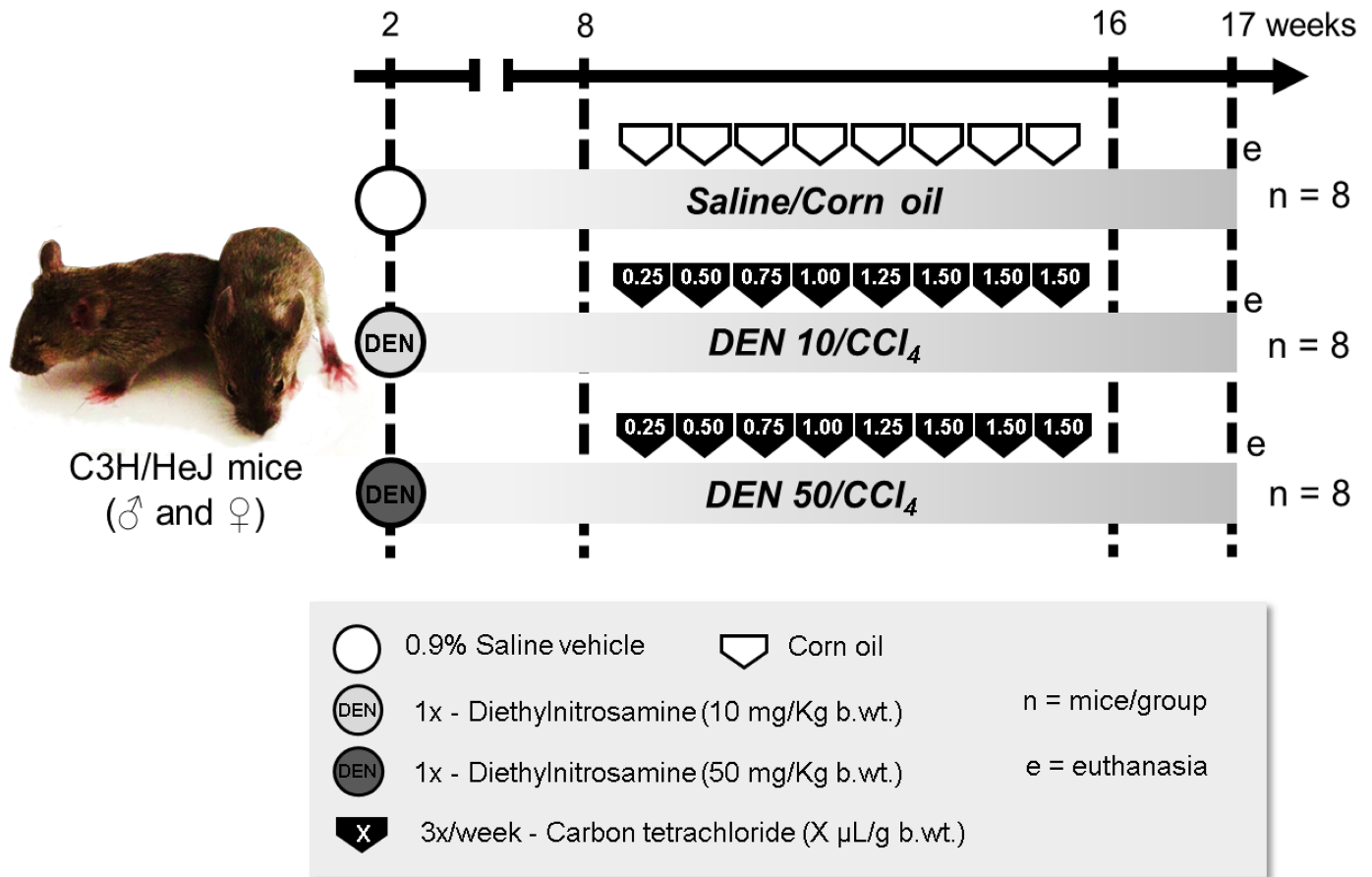


Fig 1. Experimental design. For details, see “Materials and methods” section.

<https://doi.org/10.1371/journal.pone.0203879.g001>

0.25 μL weekly increments to the utmost dose of 1.50 μL/g b.wt. [13]. All animals were euthanized by exsanguination under isoflurane inhalant anesthesia at week 17, a week after the last CCl₄ administration (Fig 1). Blood was collected from cava vein into heparinized syringes and centrifuged for 10 minutes at 1503xg, and samples were stored at -80°C for further analysis. Liver was sampled for histological analysis and additional samples were collected, snap-frozen in liquid nitrogen and stored at -80°C. All animals were kept in propylene cages with stainless steel cover and pine wood shavings bedding in a room with continuous ventilation (16–18 air changes/hour), relative humidity (45–65%), controlled temperature (20–24°C) and light/dark cycle 12:12 and were given drinking water and chow (Nuvital—Nuvilab, Brazil) *ad libitum*. Body weight and food consumption, as well as the health condition of the animals, were monitored and recorded one time *per week* during all the experimental period. The animal experiment was carried out under protocols approved by Botucatu Medical School/UNESP Ethics Committee on Use of Animals (CEUA) (Protocol number 1186/2016). All animals received humane care according to the criteria outlined in the “Guide for the Care and Use of Laboratory Animals” [14].

Macroscopy, histopathology and collagen morphometric evaluation

At necropsy, the liver was removed, weighed, washed in saline solution (0.9% NaCl) and grossly examined for the occurrence of liver nodules [15]. All macroscopically visible liver

nodules greater than 1 mm in diameter were registered. The incidence and multiplicity of the alterations were calculated for each group. Then, samples were collected from “normal-appearing” liver tissue (left lateral, right medial and caudate lobes) and from macroscopic gross lesions (for further histological diagnosis). The samples were fixed in 10% buffered formalin for 24 h at room temperature, stored in 70% ethanol and embedded in paraffin wax. Five-micron thick liver sections from paraffin-embedded blocks were obtained and stained with Hematoxylin and Eosin (HE) and Sirius Red.

Preneoplastic and neoplastic lesions were identified in HE-stained sections using previously well-established criteria [16] and their incidences were calculated for each group. For hepatocellular adenoma (HCA), it was also calculated the multiplicity (number of lesions/mice). For preneoplastic altered hepatocyte foci (AHF), it was calculated (1) *AHF number per liver area*, counting all AHF and dividing by the section liver area analyzed, (2) *AHF size*, by individually measuring all AHF, and (3) *AHF area*, dividing the sum of all AHF areas by the liver section area analyzed. The liver section area (cm^2) was measured by Stemi 2000 stereo zoom microscope (Zeiss, Germany) using a Dino Capture (ANMO Electronics Corporations, USA) image analysis system. The AHF size (mm^2) was measured by Olympus CellSens software (Olympus Corporation, Japan). The morphometric analysis of collagen in Sirius red-stained sections was performed according to previous studies [13] using Image-Pro Plus 4.5 software (Media Cybernetics, USA) in 10 randomly selected fields (20× objective) *per* section (left lobe), comprising portal areas [Collagen area (%) = Sirius red area / (total field area – vascular luminal area)].

Immunohistochemistry and semi-quantitative analysis

Immunoreactivity for α -smooth muscle actin (α -SMA, *i.e.* activated HSC marker), CD68 (*i.e.* macrophage/Kupffer cell marker), Ki-67 (*i.e.* cell proliferation marker), cleaved caspase-3 (*i.e.* apoptosis marker), transforming growth factor- α (TGF- α), cyclooxygenase-2 (COX-2) and β -catenin were detected using a one-step polymer-HRP system (EasyPath—Erviagas, Brazil). Briefly, deparaffinated 5- μm liver sections on silane-covered microscope slides were subjected to antigen retrieval in 0.01M citrate buffer (pH 6.0) at 120°C for 5 min in a Pascal Pressure Chamber (Dako Cytomation, Denmark). After endogenous peroxidase blockade with 1% H_2O_2 in phosphate-buffered saline (PBS) for 15 minutes, the slides were treated with low-fat milk for 60 min and incubated in a humidified chamber overnight at 4°C with anti- α -SMA (ab124964, 1:500 dilution, Abcam, UK), anti-CD68 (ab125212, 1:1000 dilution, Abcam, UK), anti-Ki-67 (ab16667, 1:100 dilution, Abcam, UK), anti-cleaved caspase-3 (5A1E, 1:50 dilution, Cell Signaling, USA), anti- β -catenin (ab32572, 1:400 dilution, Abcam, UK), anti-TGF- α (ab9585, 1:500 dilution, Abcam, UK) or anti-COX-2 (SP21, 72 kDa, 1:100 dilution, Biocare Medical, USA) primary antibodies. Then, the slides were incubated with a one-step polymer-HRP for 20 minutes. The reaction was visualized with 3′3-diaminobenzidine (DAB) chromogen (Sigma–Aldrich, USA) and counterstained with Harris hematoxylin.

For Ki-67, cleaved caspase-3 and CD68 semi-quantitative analysis in surrounding liver tissue (avoiding preneoplastic and neoplastic lesions), 10 random fields (40× objective) were assessed in left hepatic lobe sections. The Ki-67- and cleaved caspase-3-positive hepatocytes and CD68-positive macrophages were counted and divided by the liver area analyzed (mm^2). In AHF and HCAs, all Ki-67-positive hepatocytes were counted and divided by AHF or HCA area (mm^2). We also analyzed the TGF- α phenotype in AHF, calculating the incidence of TGF- α positive foci [17]. For β -catenin, the cellular location (membrane, cytoplasm or and/or nucleus) was evaluated in the hepatocytes of surrounding liver tissue, FHA and HCA [12]. These analyses were performed in Olympus CellSens software (Olympus Corporation, Japan).

The α -SMA semi-quantitative analysis was performed using Image-Pro Plus 4.5 software (Media Cybernetics, USA) in 10 randomly selected fields (20 \times objective) *per* section (left lobe), comprising portal areas [α -SMA area (%) = α -SMA positive area / (total field area – vascular luminal area)].

Western blot

Liver samples from the left lobe (~100 mg) were homogenized in lysis buffer (500 nM Tris-HCl, 0.2 M NaCl, 0.1% Triton X-100, 10 mM CaCl₂, and 10 μ L/mL protease inhibitor cocktail [Sigma-Aldrich, USA]) in the proportion of 30 mg of tissue/100 μ L of buffer (4°C, 2 h). After this procedure, the extracted material was centrifuged (1500 \times g, 4°C, 20 min) and the supernatant collected for protein quantification by Bradford method. Aliquots of liver homogenates containing 7 μ g of total protein were heated (95°C, 5 min) in Laemmli sample buffer (2.5 mM Tris, 2% SDS, 10% glycerol, 0.01% bromophenol blue, 5% 2-mercaptoethanol) and then electrophoretically separated in a 10% SDS-PAGE gel under reducing conditions and transferred to nitrocellulose membranes (Sigma Chemical, USA). Membranes were blocked with non-fat milk in TBS-T (1 M Tris, 5 M NaCl, pH 7.2, 500 μ L Tween-20) (1 h).

Membranes were subsequently incubated with rabbit polyclonal anti-NF κ B p65 (sc-372, 65 kDa, 1:1000 dilution, Santa Cruz Biotechnology, USA), rabbit monoclonal anti- β -catenin (ab32572, 92 kDa, 1:7000 dilution, Abcam, UK), anti-COX-2 (SP21, 72 kDa, 1:1000 dilution, Biocare Medical, USA) or goat polyclonal anti-actin (sc1815, 43 kDa, 1:1000 dilution, Santa Cruz Biotechnology, USA) primary antibodies in 5% BSA solution overnight. After 5 wash steps with TBS-T, membranes were incubated with specific horseradish conjugated secondary antibodies, according to the primary antibodies used (2 h). Finally, after 5 wash steps, the membranes were submitted to immunoreactive protein signals detected using an Amersham ECL Select Western Blotting Detection Reagent (GE Healthcare Life Sciences, UK). Signals were captured by a G:BOX Chemi system (Syngene, UK) controlled by an automatic software (GeneSys, Syngene, UK). Band intensities were quantified using densitometry analysis Image J software (National Institutes of Health, USA). Finally, NF κ B, COX-2 and β -catenin, protein expression were reported as fold change according to β -actin protein expression used as a normalizer. For each marker, we ran 2 samples of each group/gel, totalizing 3 gels and 6 samples/group.

Interleukin-6 (IL-6) analysis

Liver samples (~100 mg) were homogenized in phosphate buffer, centrifuged (10000 \times g, 4°C, 35 min) and IL-6 protein levels were evaluated by enzyme-linked immunosorbent assay (ELISA) in homogenate using Mouse IL-6 DuoSet ELISA (R&D Systems, USA). The assays were performed according to the manufacturer's instructions. The detection limit of IL-6 was found to be 2500–19.5 pg/mL.

Serum transaminases and liver biochemistry

Serum alanine (ALT) and aspartate (AST) aminotransferase levels were determined by a conventional kinetic assay according to the manufacturer's instructions (Liquiform Labtest Diagnóstica, Brazil). These determinations were performed in an automated spectrophotometric (Labmax 240 analyzer, Labtest Diagnóstica, Brazil).

For biochemical analysis, liver samples from the left lobe were homogenized in 50 mM phosphate buffer (pH 7.4) using a motor-driven Teflon glass Potter Elvehjem (100 \times g/min) and centrifuged (12000 \times g, -4°C, 15 min). The supernatant was used to determine catalase, superoxide dismutase (SOD), glutathione peroxidase (GSH-Px) activities and total glutathione,

reduced glutathione (GSH) and lipid hydroperoxide levels. Catalase activity was determined in sodium and potassium phosphate buffer containing 10 mM hydrogen peroxide [18]. GSH-Px activity was assayed by following the oxidation of 0.16 mM NADPH in the presence of glutathione reductase which catalyzed the reduction of oxidized glutathione (GSSG) formed by GSH-Px [19]. SOD activity was determined based on the ability of the enzyme to inhibit the reduction of nitro blue tetrazolium (NBT), which was generated by hydroxylamine in a medium containing phosphate buffer, 0.1 mM EDTA, 50 mM NTB, 78 mM NADH and 33 mM phenazine methosulfate [20]. GSH was measured in medium containing 2 mM 5,5'-dithiobis-(2-nitrobenzoic) acid (DTNB, Sigma-Aldrich, USA), 0.2 mM NADPH, and 2 U of glutathione reductase in phosphate buffer (100 mM, pH 7.4) 5 mM EDTA [21]. The total glutathione was assayed with 0.6 mM DTNB, and 1 U of glutathione reductase in buffer 0.1 M Tris-HCl, pH 8.0 containing 0.5 mM EDTA [21]. The lipid hydroperoxide levels were measured through hydroperoxide-mediated oxidation of Fe^{2+} , with 100 μL of sample and 900 μL of a reaction mixture containing 250 μM FeSO_4 , 25 mM H_2SO_4 , 100 μM xylenol orange and 4 mM butylated hydroxytoluene in 90% (v/v) methanol [22]. All determinations were performed using a microplate reader (25°C) (mQuant-Gen5 2.0 software, Bio-Tec Instruments, USA).

Statistical analysis

When compared Saline/Corn oil, DEN 10/ CCl_4 and DEN 50/ CCl_4 groups, data were analyzed by one-way ANOVA or Kruskal-Wallis test followed by *post hoc* Tukey test or Dunn's method, respectively. For DEN 10/ CCl_4 vs. DEN 50/ CCl_4 or male vs. female group comparisons, data were analyzed using Student t or Mann-Whitney tests. All data on incidence were analyzed by Fisher's exact test. Differences were considered significant when $p < 0.05$. Statistical analysis were performed using GraphPad Prism software (GraphPad, USA). All data were expressed as mean \pm standard deviation of the mean (S.D.) or median and interquartile (q1-q3) (box-plots).

Results

General findings

Male mice submitted to DEN 50/ CCl_4 protocol showed a reduction in body weight throughout the experimental period (S1 Fig), but mainly at weaning (week 3, after DEN administration) ($p < 0.001$), CCl_4 onset (week 8) ($p = 0.003$) and at the end of the experiment (week 17) ($p = 0.038$) compared to vehicles and/or DEN 10/ CCl_4 groups (Table 1). In addition, DEN 50/ CCl_4 -treated males presented a reduction in food intake when compared to the other groups ($p < 0.001$) (Table 1). As reported previously, reduced body weight and food consumption are common features of drug-induced liver toxicity in rodents [6]. However, animals did not show severe signs of illness and no mortality was observed.

DEN 50/ CCl_4 -treated females presented reduced body weight compared to vehicle-treated group only at weaning (week 3) ($p = 0.046$) (S1 Fig; Table 1). Although DEN 10/ CCl_4 -treated females showed increased food consumption ($p < 0.001$) (Table 1), all groups showed similar body weight evolution during the whole experiment (S1 Fig).

Serum transaminases and liver macroscopy

In males, both DEN/ CCl_4 protocols displayed enhanced hepatocellular damage, indicated by an increase in serum ALT and AST levels compared to vehicle-treated group ($p < 0.001$ and $p = 0.003$, respectively) (Table 1). The females submitted to DEN 10/ CCl_4 protocol only showed enhanced ALT levels ($p < 0.001$) (Table 1), while DEN 50/ CCl_4 protocol increased both ALT and AST serum levels ($p < 0.001$ and $p = 0.005$, respectively) (Table 1).

Table 1. Effects of different DEN/CCl₄ protocols on body and liver weights, food consumption and serum transaminases levels of male and female C3H/HeJ mice.

Parameters	Groups ¹		
	Saline/Corn oil	DEN 10/CCl ₄	DEN 50/CCl ₄
<i>Males</i>			
Body weight at week 3 (weaning) (g)	9.89 ± 2.00 ^a	9.12 ± 1.01 ^a	7.42 ± 1.24 ^b
Body weight at week 8 (CCl ₄ onset) (g)	23.27 ± 2.42 ^a	22.19 ± 1.65 ^{ab}	20.77 ± 1.08 ^b
Final body weight (g)	27.92 ± 2.64 ^a	27.15 ± 1.21 ^{ab}	26.09 ± 1.01 ^b
Food consumption (g/mouse/day)	4.34 ± 0.56 ^a	4.60 ± 0.57 ^a	3.76 ± 0.36 ^b
Absolute liver weight (g)	1.39 ± 0.18 ^b	1.80 ± 0.28 ^a	1.56 ± 0.17 ^b
Relative liver weight (%)	4.98 ± 0.49 ^b	6.62 ± 0.97 ^a	6.00 ± 0.57 ^a
ALT (U/L)	32.90 ± 7.30 ^b	63.40 ± 10.89 ^a	62.55 ± 17.75 ^a
AST (U/L)	47.20 ± 7.55 ^b	67.40 ± 11.92 ^a	59.46 ± 9.82 ^a
<i>Females</i>			
Body weight at week 3 (weaning) (g)	9.08 ± 2.22 ^a	7.69 ± 1.05 ^{ab}	7.26 ± 1.33 ^b
Body weight at week 8 (CCl ₄ onset) (g)	18.27 ± 2.31	18.06 ± 0.98	17.72 ± 1.42
Final body weight (g)	20.43 ± 2.56	21.46 ± 1.34	21.67 ± 1.31
Food consumption (g/mouse/day)	3.71 ± 0.31 ^b	4.44 ± 0.33 ^a	3.71 ± 0.26 ^b
Absolute liver weight (g)	0.99 ± 0.13 ^b	1.28 ± 0.18 ^a	1.33 ± 0.27 ^a
Relative liver weight (%)	4.88 ± 0.42 ^b	5.99 ± 0.70 ^a	6.13 ± 1.00 ^a
ALT (U/L)	27.40 ± 5.58 ^b	45.57 ± 11.85 ^a	40.90 ± 4.17 ^a
AST (U/L)	53.55 ± 6.87 ^b	62.20 ± 9.44 ^{ab}	64.60 ± 9.44 ^a

Values are mean ± S.D. n = 8 mice/sex/group.

¹DEN 10 or 50 = diethylnitrosamine 10 or 50 mg/kg b.wt. in 0.9% saline at week 2 and CCl₄ = carbon tetrachloride, i.p., 0.25 to 1.50 μL/g b.wt., in 10% corn oil solution for 8 weeks (see [Material and methods](#) section). Different letters correspond to statistical difference among groups by ANOVA and *post hoc* Tukey's test (p<0.05).

<https://doi.org/10.1371/journal.pone.0203879.t001>

At necropsy, in keeping with transaminases data, liver of male and female mice exposed to both DEN/CCl₄ protocols showed irregular macroscopic surfaces, typical of liver fibrosis, while the liver of vehicle-treated mice showed normal smooth macroscopic appearance ([Fig 2](#)). Besides the fibrotic aspect, all DEN/CCl₄-treated male mice developed multiple whitish macroscopic nodules (>1 mm in diameter) (p<0.001, for both), while vehicle-treated male mice did not ([Fig 2, Table 2](#)). Males from DEN 10/CCl₄ and DEN 50/CCl₄ groups demonstrated similar multiplicity of these gross alterations (5.87 ± 2.85 vs. 4.50 ± 2.20 nodules/mice, respectively, values are mean ± S.D.). The majority of females submitted to DEN 10/CCl₄ (p<0.001) and DEN 50/CCl₄ (p = 0.007) protocols developed these liver nodules as well ([Fig 2, Table 2](#)). The DEN 10/CCl₄ and DEN 50/CCl₄-treated females also showed similar multiplicity of these alterations [1.00 (1.00–1.50) vs. 1.00 (0.50–1.00) nodules/mice, respectively, values are median (q1–q3)]. All nodules were collected for further histopathological diagnosis.

Finally, considering the fibrotic aspect and the presence of nodules, male mice submitted to DEN 10/CCl₄ protocol displayed enhanced liver absolute and relative weights (p<0.001, for both) compared to vehicle group, whereas DEN 50/CCl₄-protocol just enhanced liver relative weight (p<0.001) ([Table 1](#)). In females, all DEN/CCl₄ protocols increased liver relative and absolute weights compared to vehicle-treated group (p<0.001, for both) ([Table 1](#)).

Histopathological evaluation

The histopathological evaluation of liver samples from males and females revealed the occurrence of preneoplastic AHF, sub-classified as basophilic, eosinophilic or clear cell foci, according to the predominant cell type ([Fig 3](#)). In both DEN/CCl₄ regimens applied in males and

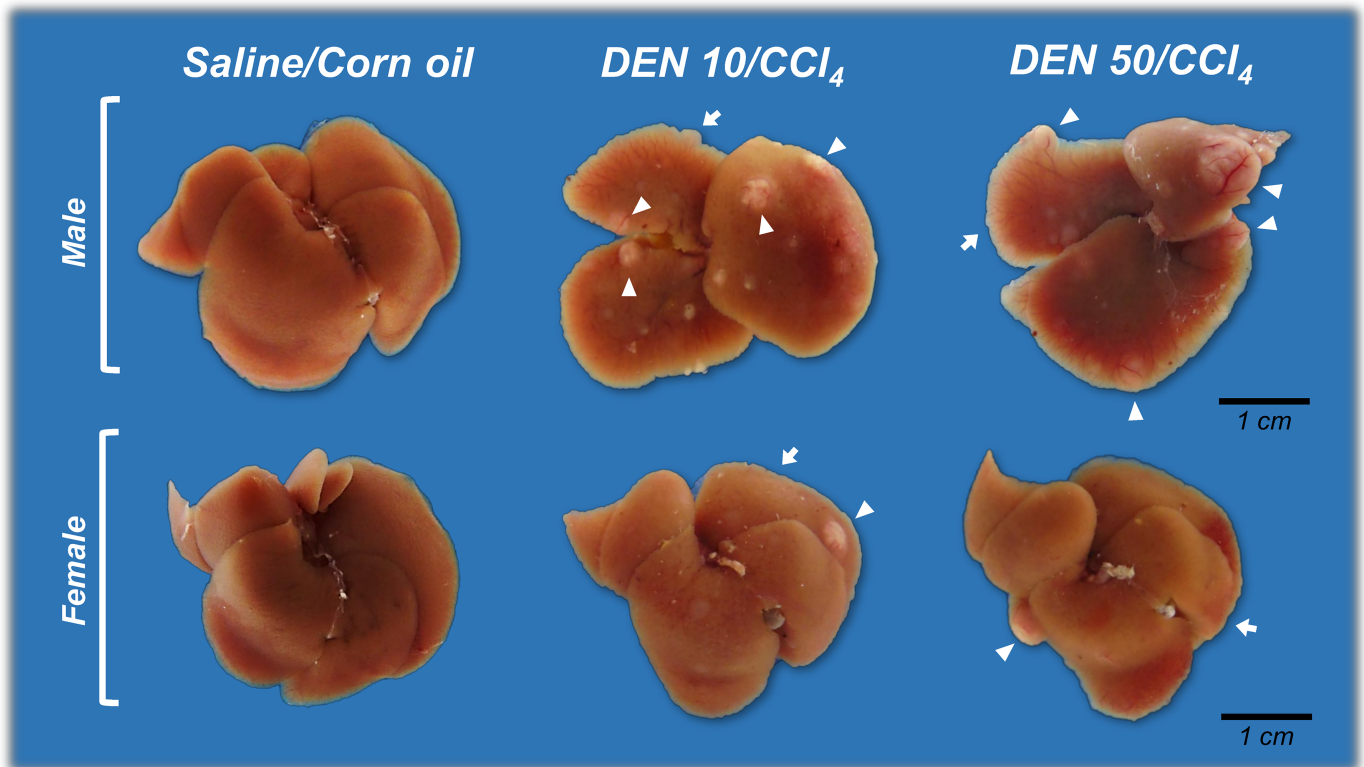


Fig 2. Representative macroscopic liver appearance of Saline/Corn oil and DEN/CCl₄-treated male and female C3H/HeJ mice. DEN/CCl₄-treated animals displayed typical “rough” fibrotic appearance (arrows) and developed whitish nodules (arrowheads). DEN 10 or 50 = diethylnitrosamine 10 or 50 mg/kg b.wt. in 0.9% saline at week 2, respectively and CCl₄ = carbon tetrachloride, i.p., 0.25 to 1.50 μL/g b.wt. in 10% corn oil solution for 8 weeks (see [Material and methods](#) section).

<https://doi.org/10.1371/journal.pone.0203879.g002>

females, all mice developed AHF, and these groups presented enhanced incidence of these pre-neoplastic lesions (considering all types) when compared to corresponding vehicle controls ($p < 0.001$, for all) ([Table 2](#)). Considering the different types of AHF, DEN 10/CCl₄ and DEN 50/CCl₄ protocols induced similar incidence of basophilic, eosinophilic and clear cell foci in both males and females ([Table 2](#)). In our models, at the chosen time-point (week 17), the occurrence of basophilic AHF displayed increased importance, since all males and the majority of females developed these specific lesions ([Table 2](#)). Also, male mice submitted to DEN 10/CCl₄ and DEN 50/CCl₄ protocols displayed similar number of AHF *per* liver area (cm²) ([Fig 4](#)). Interestingly, DEN 10/CCl₄ protocol displayed an increase in mean AHF size ($p < 0.001$) and total liver area occupied by all these lesions ($p = 0.022$) compared to DEN 50/CCl₄ group ([Fig 4](#)). In our female models, the all protocols did not differ in all parameters of AHF analysis ([Fig 4](#)).

In addition to preneoplastic lesions, the histopathological evaluation of liver nodules revealed the presence of neoplastic lesions, represented by HCA and HCC ([S2 Fig](#)). In male mice, we observed a significant increase in HCA incidence in both DEN 10/CCl₄ ($p < 0.001$) and DEN 50/CCl₄ ($p = 0.007$) protocols compared to vehicle-treated mice ([Table 2](#)). Yet similar in incidence ([Table 2](#)), the DEN 10/CCl₄ protocol resulted in an increase in HCA multiplicity in comparison to DEN 50/CCl₄-treated group ($p = 0.028$) ([Fig 4](#)). Lastly, although 12.5% of males in DEN 10/CCl₄ group developed HCC, our male models did not increase the incidence of this malignant lesion compared to vehicle group ([Table 2](#)). At the chosen time-point, female

Table 2. Effects of different DEN/CCl₄ protocols on the incidence of macroscopic nodules, preneoplastic and neoplastic lesions of male and female C3H/HeJ mice.

Parameters	Groups ¹		
	Saline/Corn oil	DEN 10/CCl ₄	DEN 50/CCl ₄
<i>Males</i>			
Macroscopic nodules	0/8 (0) ^b	8/8 (100%) ^a	8/8 (100%) ^a
All types of AHF	0/8 (0) ^b	8/8 (100%) ^a	8/8 (100%) ^a
Basophilic AHF	-	8/8 (100%)	8/8 (100%)
Eosinophilic AHF	-	3/8 (37.5%)	6/8 (75%)
Clear cell AHF	-	8/8 (100%)	4/8 (50%)
HCA	0/8 (0) ^b	8/8 (100%) ^a	6/8 (75%) ^a
HCC	0/8 (0)	1/8 (12.5%)	0/8 (0)
<i>Females</i>			
Macroscopic nodules	0/8 (0) ^b	7/8 (87.5%) ^a	6/8 (75%) ^a
All types of AHF	0/8 (0) ^b	8/8 (100%) ^a	8/8 (100%) ^a
Basophilic AHF	-	7/8 (87.5%)	8/8 (100%)
Eosinophilic AHF	-	4/8 (50%)	6/8 (75%)
Clear cell AHF	-	2/8 (25%)	3/8 (37.5%)
HCA	0/8 (0) ^b	5/8 (62.5%) ^a	2/8 (25%) ^{ab}

Values are the proportion of affected mice (percentage).

¹DEN 10 or 50 = diethylnitrosamine 10 or 50 mg/kg b.wt. in 0.9% saline at week 2 and CCl₄ = carbon tetrachloride, i. p., 0.25 to 1.50 μL/g b.wt. in 10% corn oil solution for 8 weeks (see [Material and methods](#) section).

AHF = altered hepatocyte foci; HCA = hepatocellular adenoma; HCC = hepatocellular carcinoma. Different letters correspond to statistical difference among groups by Fisher’s exact test (p<0.05).

<https://doi.org/10.1371/journal.pone.0203879.t002>

mice did not develop HCCs, only HCAs. However, only DEN 10/CCl₄ females significantly enhanced HCA incidence compared to vehicle-treated mice (p = 0.026) (Table 2). No significant changes were observed between DEN/CCl₄ female protocols in relation to HCA multiplicity (Fig 4).

Interestingly, the DEN 10/CCl₄ protocol in males and females displayed better results than DEN 50/CCl₄ protocol on inducing the development of AHF and/or HCA. Especially in DEN 10/CCl₄ models, the data on incidence and multiplicity indicate that these hepatocellular lesions can be applied as reliable end-point lesions.

Proliferation and apoptosis analysis

Sustained cell proliferation could favor the clonal expansion of DEN-initiated hepatocytes and predispose mice to the development of hepatocellular preneoplastic and neoplastic [23]. Furthermore, increased apoptosis after liver injury may also contribute to the initiation phase of HSCs activation and ultimately, to liver fibrosis [24]. In the proposed models, when analyzed the “normal-appearing” liver tissue (avoiding preneoplastic and neoplastic lesions), both DEN/CCl₄ protocols significantly increased hepatocyte proliferation (Ki-67) and apoptosis (cleaved caspase-3) labeling indexes in the liver from males (p<0.001, for both) and females (p = 0.002 and p = 0.0012, respectively) in comparison to corresponding vehicle-treated controls (Fig 5). DEN 50/CCl₄ regimens in males and females resulted in an increased hepatocyte proliferation in comparison DEN10/CCl₄ (Fig 5). No significant changes were observed between DEN/CCl₄ protocols in relation to hepatocyte apoptosis indexes (Fig 5).

Despite of presenting increased cell proliferation in “surrounding” liver tissue, DEN 50/CCl₄ regimen in males showed diminished hepatocyte proliferation into AHF in comparison

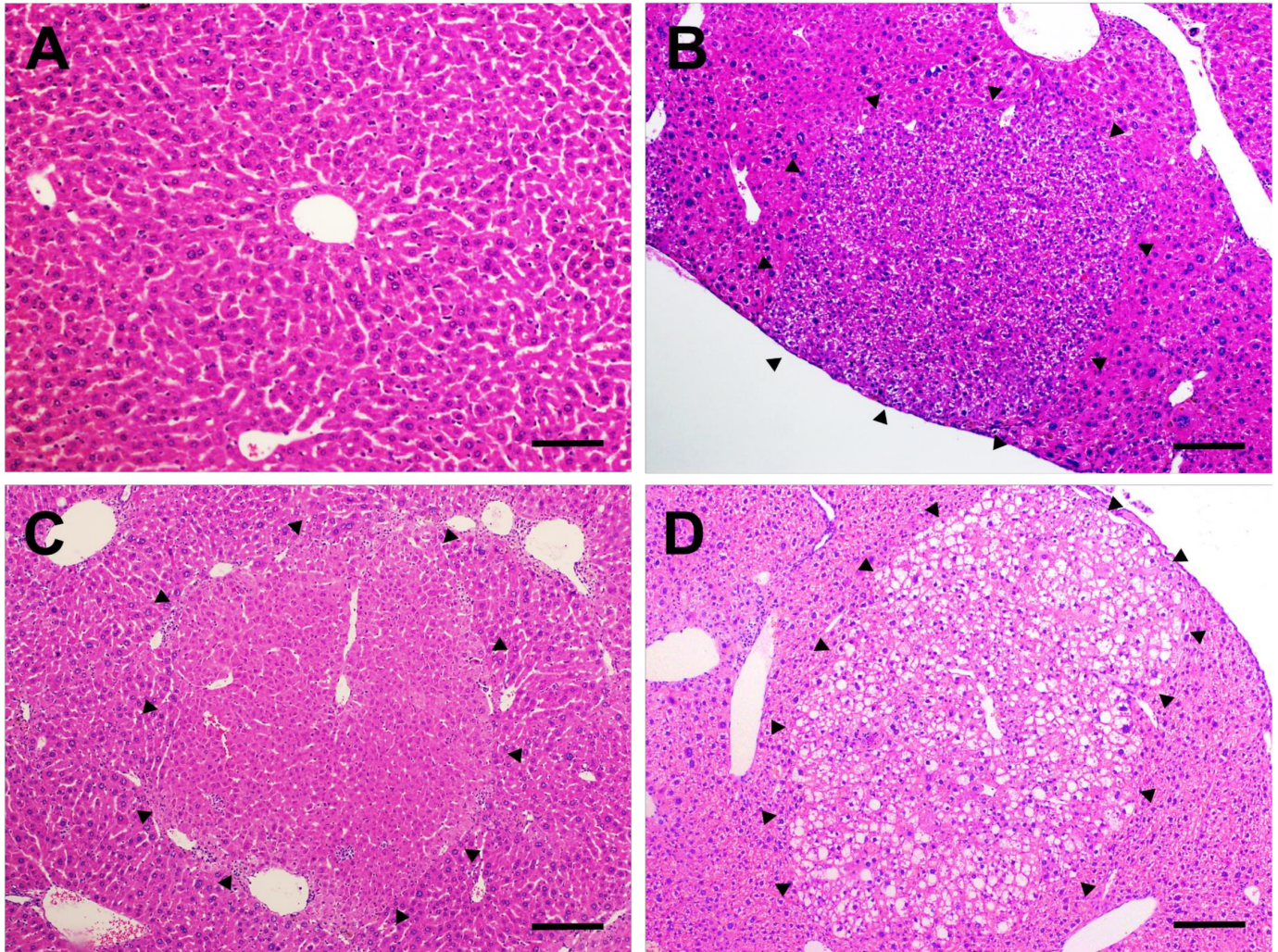


Fig 3. Preneoplastic altered hepatocyte foci. Representative photomicrographs of (A) normal liver of vehicle-treated groups (20× objective) (scale bar = 50 μm) and (B) basophilic, (C) eosinophilic and (D) clear cell preneoplastic foci found in the liver of DEN/CCL₄-treated mice (10× objective) (scale bar = 100 μm).

<https://doi.org/10.1371/journal.pone.0203879.g003>

to DEN 10/CCL₄ ($p = 0.025$) (Fig 6). This data corroborates with increased AHF size and area displayed by DEN 10/CCL₄ protocol (Fig 4). Hepatocyte proliferation into preneoplastic AHF favors the accumulation of molecular alterations that predispose these lesions to growth and progression to neoplastic lesions [23]. In females, no significant changes were observed between DEN/CCL₄ protocols in relation to cell proliferation into AHF (Fig 6A and 6C), in accordance to the AHF analysis in this sex (Fig 4).

DEN 10/CCL₄ and 50/CCL₄ male protocols were similar in HCA proliferation rates (520.36 ± 121.80 vs. 497.75 ± 55.68 Ki-67⁺ cells/mm², respectively. Values are mean \pm S.D.). Lastly, we did not characterize the cell proliferation rates in female HCA considering the non-significant incidence of these lesions in DEN 50/CCL₄ females (Table 2). Representative photomicrographs of Ki-67 immunostained sections of HCA and HCC are presented in S2 Fig.

β-catenin and TGF-α evaluation

The aberrant activation of Wnt/β-catenin signaling is frequently observed in human and mouse hepatocarcinogenesis [25], conferring to the hepatocytes the capacity of sustained cell

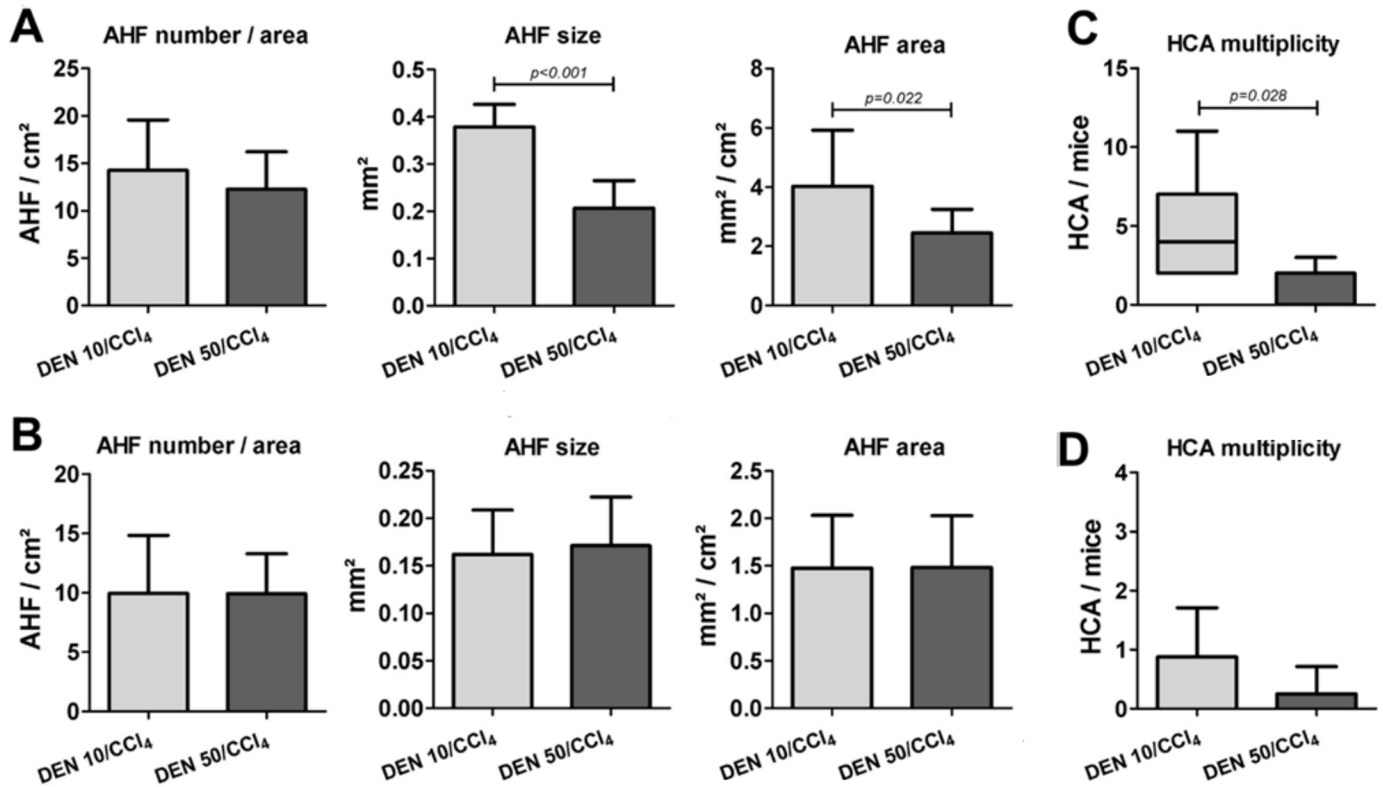


Fig 4. Effects of different DEN/CCl₄ protocols on AHF analysis (number/area, size and area) and HCA multiplicity of male and female C3H/HeJ mice. (A, C) male and (B, D) female. Values are mean + S.D or box and whiskers. n = 8 mice/sex/group. DEN 10 or 50 = diethylnitrosamine 10 or 50 mg/kg b.wt. in 0.9% saline at week 2, respectively and CCl₄ = carbon tetrachloride, i.p., 0.25 to 1.50 μL/g b.wt. in 10% corn oil solution for 8 weeks (see [Material and methods](#) section). AHF = altered hepatocyte foci; HCA = hepatocellular adenoma. Data were analyzed by Student t or Mann-Whitney test (p < 0.05).

<https://doi.org/10.1371/journal.pone.0203879.g004>

proliferation. Nonetheless, all animals of both female and male models presented typical membranous expression of β-catenin in surrounding liver tissue, altered hepatocyte foci (all types) and hepatocellular adenomas. As expected, western blot revealed similar hepatic β-catenin protein expression in both male and female models compared to their respective controls (S3 Fig). Consistently to our findings, a previous DEN/CCl₄-induced model in B6C3F1 mice also led to typical membranous β-catenin staining and did not display codon 2 mutations in *Ctnnb1* gene [26]. Indeed, at the analyzed time-point, cytoplasmic/nuclear and increased β-catenin expression did not show to be marked feature of our models.

The transforming growth factor-α (TGF-α), which binds to the epidermal growth factor receptor (EGFR), also act as a potent mitogenic signal to hepatocytes and it has been implicated in rat, mice and human hepatocarcinogenesis [17, 27, 28]. In all groups of male and female models, mice showed typical staining on endothelial and bile duct cells (S4 Fig) and only few DEN 10/CCl₄ [female: 25% (2/8); male: 12.5% (1/8)] and DEN 50/CCl₄ [female: 12.5% (1/8); male: 25% (2/8)] mice developed weakly stained TGF-α-positive foci (S4 Fig). Interestingly, in keeping with previous report [27], all TGF-α positive foci in these few animals displayed eosinophilic phenotype (S4 Fig). Basophilic, clear cell foci and adenomas (S4 Fig) did not present TGF-α immunoreactivity. Despite of being a marker of progression in DEN-initiated and DEN-initiated/PB-promoted mice models, [27], the TGF-α pathway was not significantly activated in our DEN-initiated/CCl₄-promoted bioassays after 17 weeks of experiment.

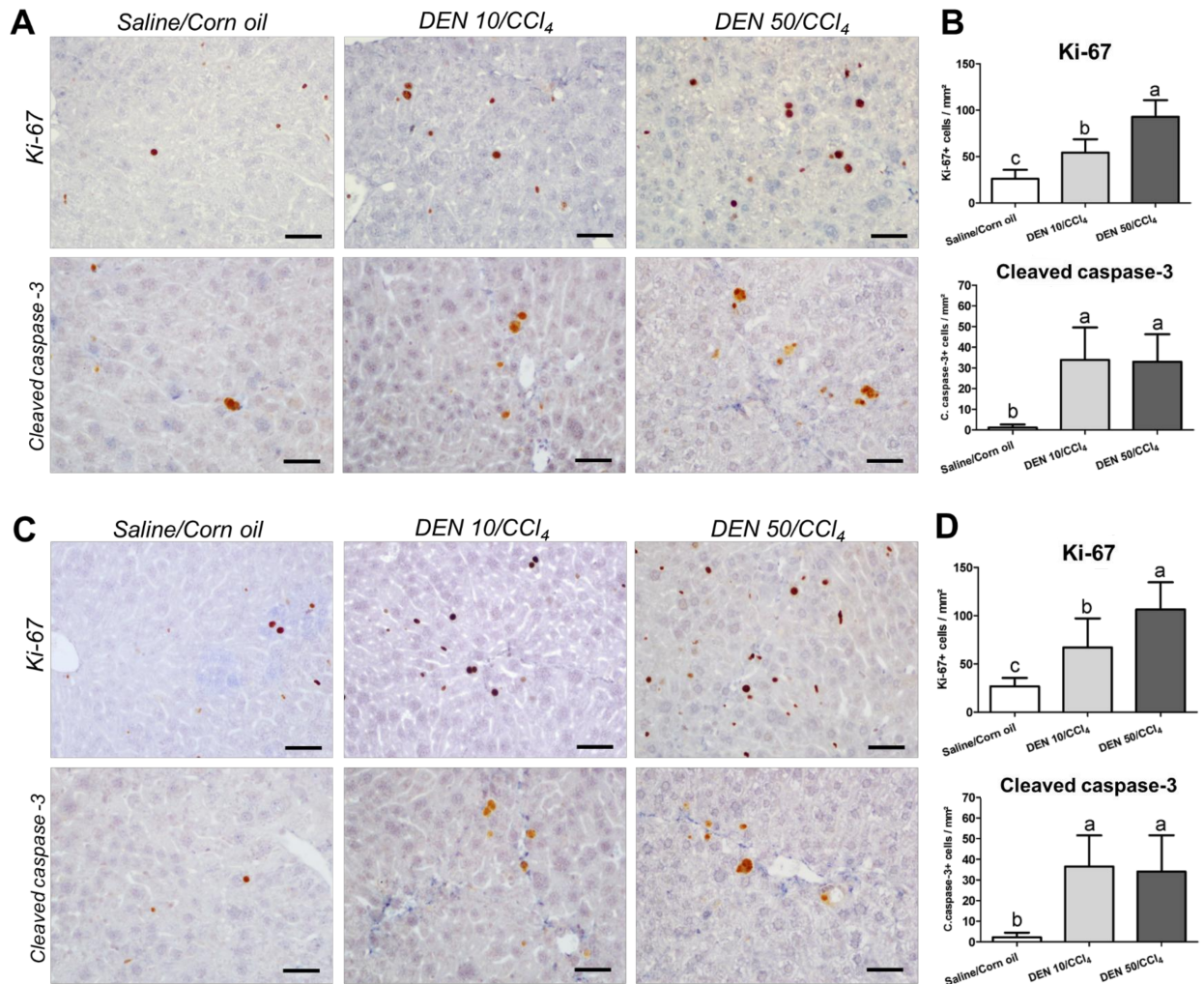


Fig 5. Effects of different DEN/CCl₄ protocols on Ki-67 (cell proliferation) and cleaved caspase-3 (apoptosis) immunostaining in surrounding liver tissue of male and female C3H/HeJ mice. (A, B) male and (C, D) female. (A, C) Representative photomicrographs (40× objective) (scale bar = 20 μm) and (B, D) semiquantitative analysis. Values are mean + S.D. n = 8 mice/sex/group. DEN 10 or 50 = diethylnitrosamine 10 or 50 mg/kg b.wt. in 0.9% saline at week 2, respectively and CCl₄ = carbon tetrachloride, i.p., 0.25 to 1.50 μL/g b.wt. in 10% corn oil solution for 8 weeks (see [Material and methods](#) section). Different letters correspond to statistical difference among groups by ANOVA and *post hoc* Tukey's test (p<0.05).

<https://doi.org/10.1371/journal.pone.0203879.g005>

Fibrosis analysis: Collagen, α-SMA and CD68

In keeping with the enhanced transaminases levels ([Table 1](#)) and irregular macroscopic appearance ([Fig 2](#)), Sirius red-stained liver sections of males from DEN/CCl₄-treated protocols revealed fibrous expansions in portal areas and marked bridging between portal areas and central veins, typical features of liver fibrosis ([Fig 7](#)). As expected, morphometric analysis demonstrated increased collagen deposition in the liver from DEN/CCl₄-treated groups compared to vehicle-treated group (p<0.001) ([Fig 7](#)). Moreover, these groups displayed marked activation of HSCs, considering the increased α-SMA immunostaining (p = 0.0036), in the same areas of fibrous expansion and bridging ([Fig 7](#)). In addition to HSCs, CD68⁺ liver macrophages already showed to play important roles on inducing pro-inflammatory and pro-fibrogenic responses in mice and humans [28]. Here, upon both DEN/CCl₄ regimens, we found a significant increase in the number of CD68⁺ cells in the liver (p = 0.0057). In fibrotic liver, these cells

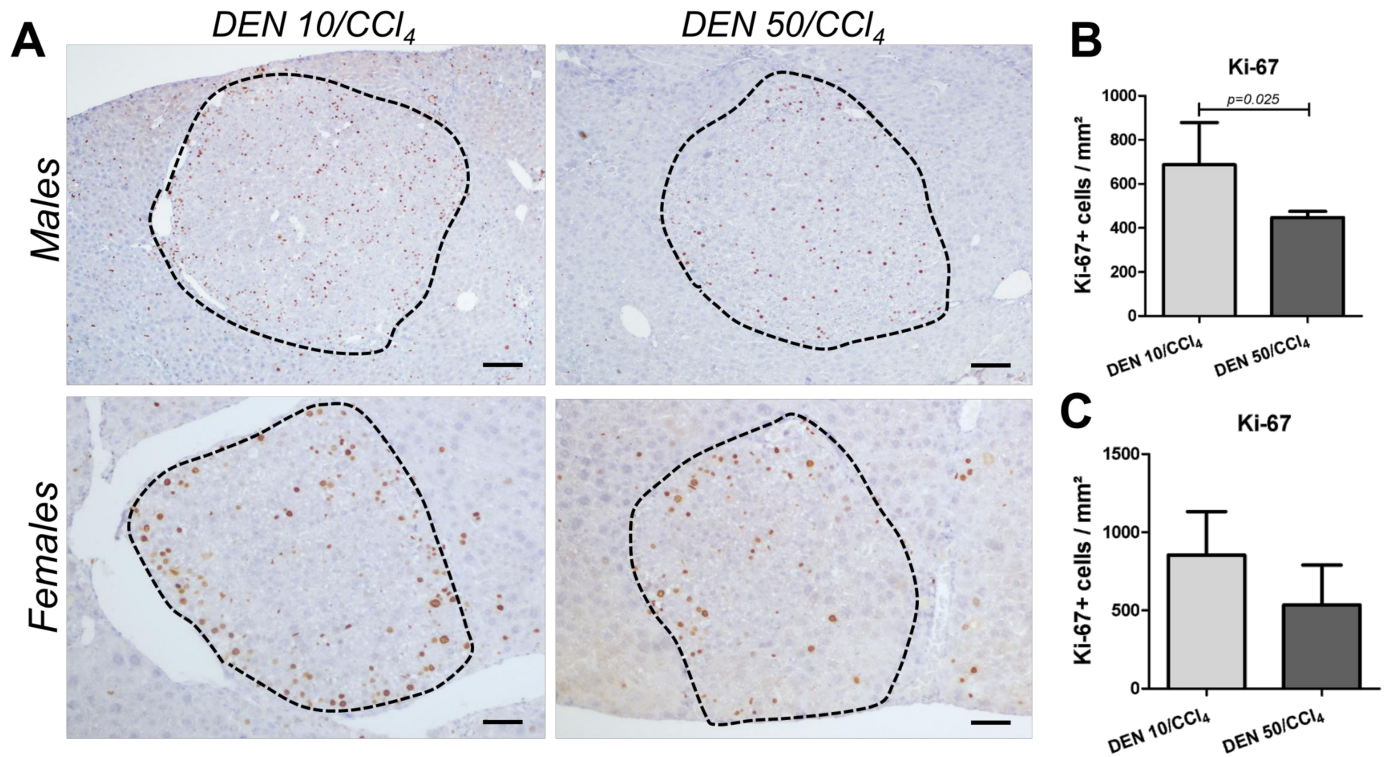


Fig 6. Effects of different DEN/CCl₄ protocols on Ki-67 (cell proliferation) immunostaining in preneoplastic AHF of male and female C3H/HeJ mice. (A, B) male and (A, C) female. (A) Representative photomicrographs (Males: 10× objective, scale bar = 100 μm) (Females: 20× objective, scale bar = 50 μm) and (B, D) semiquantitative analysis. Values are mean + S.D. n = 8 mice/sex/group. DEN 10 or 50 = diethylnitrosamine 10 or 50 mg/kg b.wt. in 0.9% saline at week 2, respectively and CCl₄ = carbon tetrachloride, i.p., 0.25 to 1.50 μL/g b.wt. in 10% corn oil solution for 8 weeks (see [Material and methods](#) section). AHF = altered hepatocyte foci. Data were analyzed by Student t test (p<0.05).

<https://doi.org/10.1371/journal.pone.0203879.g006>

were concentrated in areas surrounding the fibrous expansions, while in untreated mice, CD68⁺ macrophages were detected in the sinusoids (detail in [Fig 7](#)).

In females, fibrotic response to CCl₄ protocol was similar to males. The DEN 10/CCl₄ and DEN 50/CCl₄ groups also showed clear features of liver fibrosis, increased collagen deposition (p<0.0001) and enhanced α-SMA immunostaining (p = 0.0087) ([Fig 8](#)). Although CD68⁺ macrophages were also mainly found near the scar tissue, the number of these cells *per mm*² remained unchanged in fibrotic liver ([Fig 8](#)). Data indicate that the CCl₄ administrations were successful on establishing a similar fibrotic background in male and female C3H/HeJ mice. In addition, the different protocols of DEN-induced hepatocarcinogenesis (10 and 50 mg/Kg b. wt.) did not influence the collagen deposition and HSCs activation at the end of experimental period.

NF-κB, COX-2 and IL-6 analysis

Both IκB kinase β (IKKβ), part of NF-κB transcription factor, and cyclooxygenase-2 (COX-2), an enzyme that synthesizes prostaglandins, are related to the up regulation of interleukin-6 (IL-6) [[29](#), [30](#)]. Besides its role in acute inflammation, this multifunctional cytokine considered is a strong hepatomitogen involved in experimental liver carcinogenesis [[7](#)]. Indeed, in a DEN-induced neonatal mice model, IL-6 knockout attenuated hepatocarcinogenesis, reassuring the importance of IL-6 axis in this process even in the absence of liver fibrosis [[7](#)].

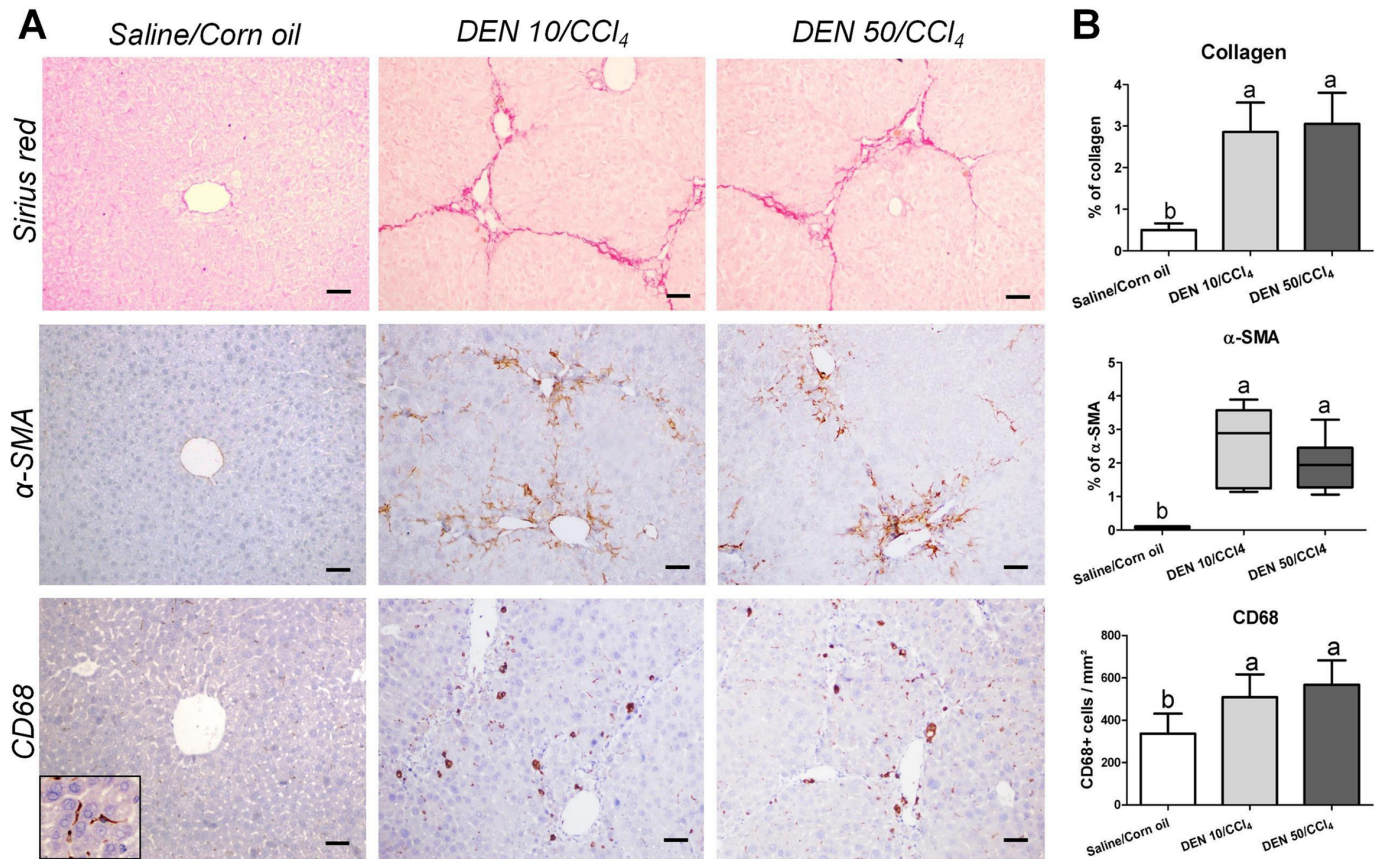


Fig 7. Effects of different DEN/CCl₄ protocols on collagen content (Sirius red), α -SMA and CD68 immunostaining in the liver of male C3H/HeJ mice. (A) Representative photomicrographs (20 \times objective; scale bar = 50 μ m) and (B) semiquantitative analysis. Values are mean + S.D or box and whiskers. n = 8 mice/group. DEN 10 or 50 = diethylnitrosamine 10 or 50 mg/kg b.wt. in 0.9% saline at week 2, respectively and CCl₄ = carbon tetrachloride, i.p., 0.25 to 1.50 μ L/g b.wt. in 10% corn oil solution for 8 weeks (see [Material and methods](#) section). Different letters correspond to statistical difference by ANOVA or Kruskal Wallis and *post hoc* Tukey test or Dunn's method, respectively (p<0.05).

<https://doi.org/10.1371/journal.pone.0203879.g007>

Despite of not altering p65 protein expression, both male models significantly enhanced COX-2 protein expression and IL-6 levels in the liver compared to their untreated counterpart (p = 0.0092 and p<0.0001, respectively) (Figs 9 and 10). These groups displayed many COX-2⁺ mononuclear inflammatory cells in the liver while untreated group, few COX-2⁺ in cells were found in the sinusoids (Fig 9). In chronic or acute thioacetamide- or CCl₄ induced liver damage, COX-2 mRNA expression is increased and restricted to mononuclear phagocytes [31]. In human cirrhosis, COX-2⁺ cells showed to be CD68⁺ as well [31]. Thus, the enhanced number of CD68⁺ macrophages in our male models corroborates with the increase in COX-2/IL-6 axis. Macrophages are responsible for IL-6 secretion and potential paracrine signaling on neighboring hepatocytes, contributing to preneoplastic and neoplastic lesion development [7]. In males, CD68/COX-2/IL-6 axis emerges as a molecular target for potential preventive or therapeutic strategies.

In contrast, female models showed no differences on IL-6 levels, COX-2 and NF- κ B protein expression and displayed similar immunolocalization of COX-2⁺ cells compared to Saline/Corn oil group (Figs 9 and 10). These data also endorse CD68 findings in female models. Although we characterized standard male and female models separately, we performed a sex comparison in order to confirm sex bias. Our models successfully recapitulated this feature of

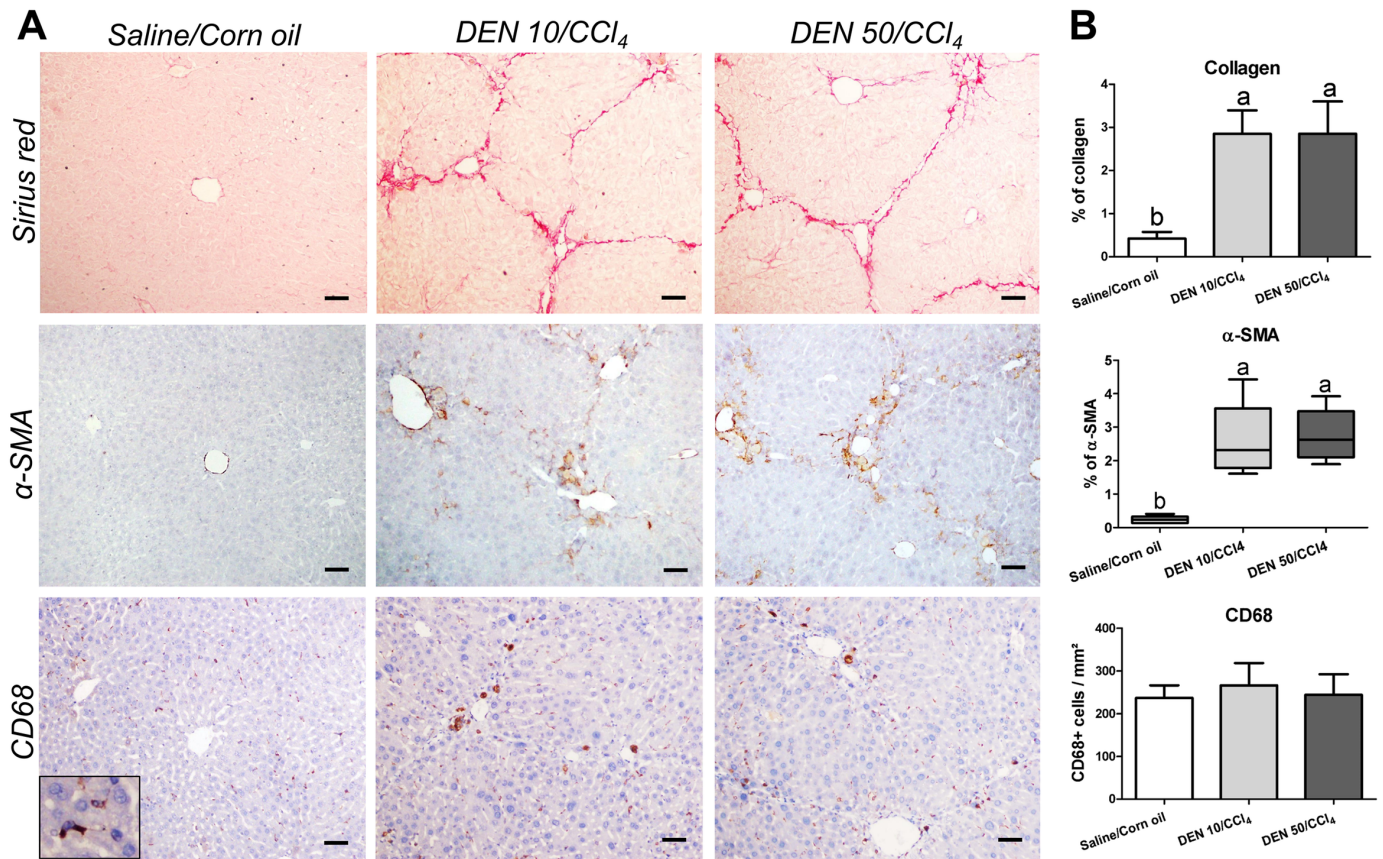


Fig 8. Effects of different DEN/CCl₄ protocols on collagen content (Sirius red), α-SMA and CD68 immunostaining in the liver of female C3H/HeJ mice. (A) Representative photomicrographs (20× objective; scale bar = 50 μm) and (B) semiquantitative analysis. Values are mean + S.D or box and whiskers. n = 8 mice/group. DEN 10 or 50 = diethylnitrosamine 10 or 50 mg/kg b.wt. in 0.9% saline at week 2, respectively and CCl₄ = carbon tetrachloride, i.p., 0.25 to 1.50 μL/g b.wt. in 10% corn oil solution for 8 weeks (see [Material and methods](#) section). Different letters correspond to statistical difference by ANOVA or Kruskal Wallis and *post hoc* Tukey test or Dunn's method, respectively (p<0.05).

<https://doi.org/10.1371/journal.pone.0203879.g008>

hepatocarcinogenesis, since male models displayed enhanced serum ALT levels [DEN 10/CCl₄ (p = 0.020); DEN 50/CCl₄ (p = 0.001)], preneoplastic AHF with increased size (only in DEN 10/CCl₄ model, p<0.001), area (p = 0.008, for both models) and enhanced HCA multiplicity [DEN 10/CCl₄ (p = 0.007); DEN 50/CCl₄ (p = 0.020)] compared to females ([S5 Fig](#)). Our data suggests clear sex difference, supporting previous studies showing that estrogen mediates a reduction in IL-6 signaling, leading to decreased hepatocarcinogenesis susceptibility in females [7].

Lipid peroxidation and antioxidant defense

The hepatic metabolism of CCl₄ results in trichloromethyl radicals, which are involved in lipid peroxidation and contribute to chronic liver damage and fibrosis [32,33]. Indeed, both protocols applied in male mice increased lipid hydroperoxide levels compared to vehicle-treated group (p = 0.013) ([Fig 11](#)) while those applied in females did not ([Fig 12](#)). Our male models also showed diminished activities of catalase and GSH-Px enzymes (p<0.001 and p = 0.014, respectively) and no effect on SOD, GSH and total glutathione ([Fig 11](#)), a week after the last CCl₄ administration. Females submitted to both DEN/CCl₄ regimens demonstrated decreased activity of catalase (p = 0.003), GSH-Px (p<0.001) and reduced levels of total glutathione

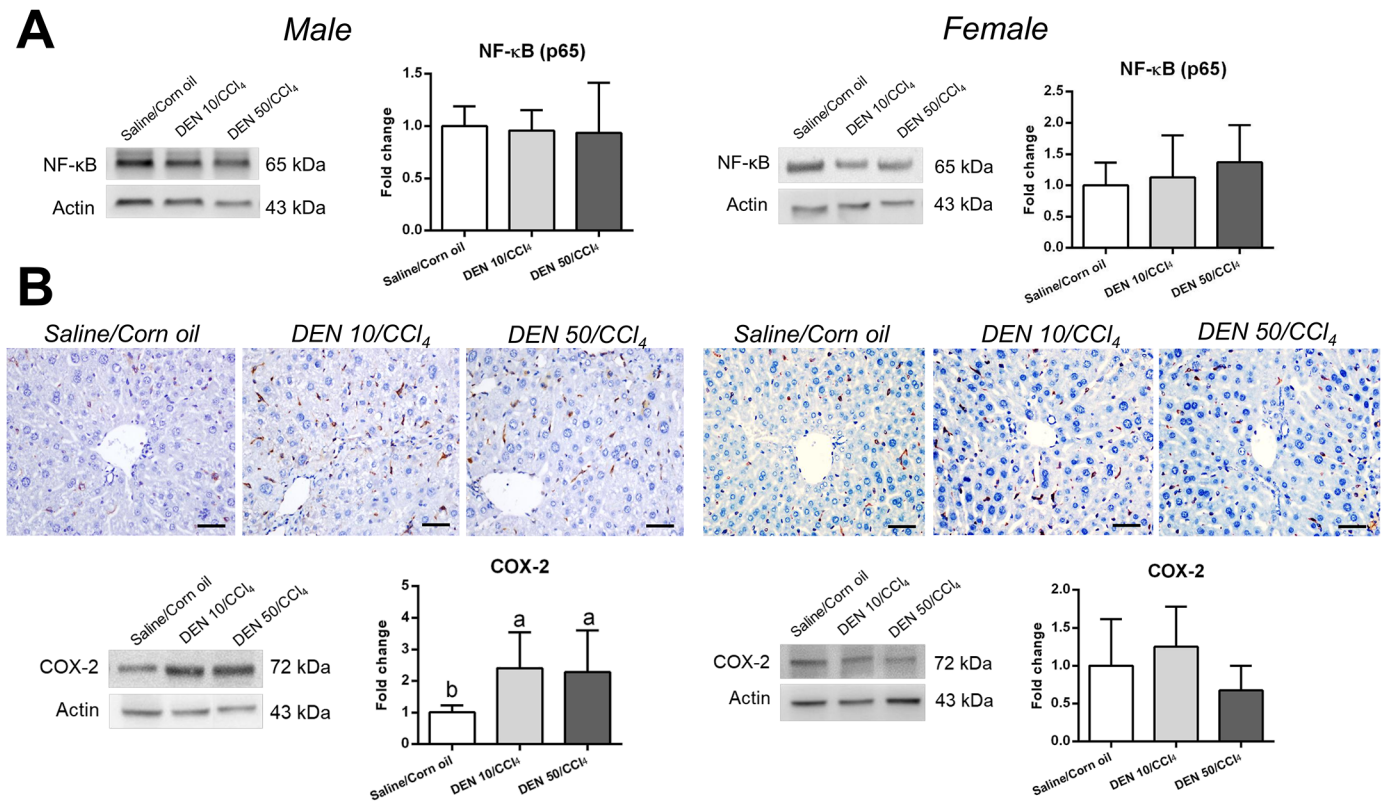


Fig 9. Effects of different DEN/CCl₄ protocols on (A) NF-κB (p65) protein expression and (B) COX-2 protein immunostaining and expression in the liver of male and female C3H/HeJ mice. Representative photomicrographs (40× objective; scale bar = 20 μm), western blot bands and semiquantitative analysis are presented. Values are mean + S.D. n = 6 mice/group. DEN 10 or 50 = diethylnitrosamine 10 or 50 mg/kg b.wt. in 0.9% saline at week 2, respectively and CCl₄ = carbon tetrachloride, i.p., 0.25 to 1.50 μL/g b.wt. in 10% corn oil solution for 8 weeks (see [Material and methods](#) section). Different letters correspond to statistical difference among groups by ANOVA and *post hoc* Tukey's test (p<0.05).

<https://doi.org/10.1371/journal.pone.0203879.g009>

(p<0.001) compared to the vehicle group (Fig 12). The DEN 50/CCl₄ protocol reduced GSH levels as well (p = 0.002) (Fig 12), but no difference was observed on SOD levels in both groups (Fig 12).

The catalase enzyme and the glutathione system (mainly GSH-Px and its non-enzymatic GSH substrate) can directly avoid the oxidative degradation of lipids by neutralizing reactive radicals [34]. Thus, the depletion or diminished activity of these antioxidant agents is a consequence of CCl₄ chronic administration. An impairment in antioxidant axis is a marked feature of both human and rodent hepatocarcinogenesis [6,12,35,36], predisposing mice to the development of preneoplastic and neoplastic lesions.

Discussion

In the current study, we proposed an early fibrosis-associated hepatocarcinogenesis model for male and female mice, focusing on establishing standard mice models and minimizing the required experimental time for the development of hepatocellular preneoplastic and neoplastic lesions in a fibrotic background. For this purpose, we applied DEN/CCl₄ regimen in a hepatocarcinogenesis-susceptible C3H/HeJ mice strain. After DEN administration in neonatal mice, this carcinogen is metabolized in the liver by CYP2E1, generating reactive oxygen species (ROS) and the nucleophilic ethyldiazonium ions, which lead to DNA damage and genomic instability, “initiating” hepatocytes for carcinogenesis [37,38]. In neonatal age, increased cell

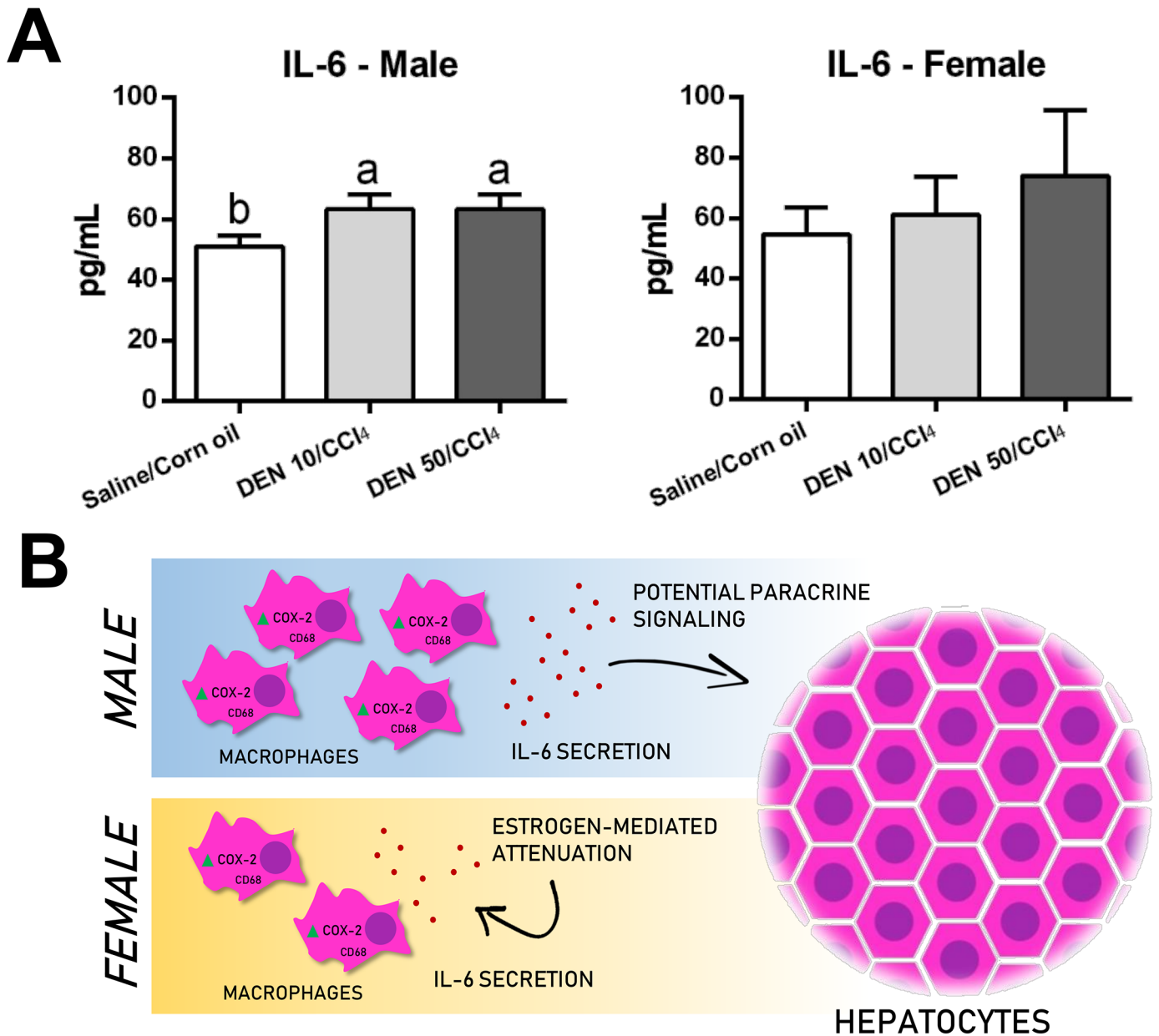


Fig 10. (A) Effects of different DEN/CCl₄ protocols on interleukin 6 (IL-6) levels in the liver of male and female C3H/HeJ mice. (B) Sex differences on CD68/COX-2/IL-6 axis in the proposed models. Values are mean + S.D. n = 6 mice/group. DEN 10 or 50 = diethylnitrosamine 10 or 50 mg/kg b.wt. in 0.9% saline at week 2, respectively and CCl₄ = carbon tetrachloride, i.p., 0.25 to 1.50 μL/g b.wt. in 10% corn oil solution for 8 weeks (see [Material and methods](#) section). Different letters correspond to statistical difference among groups by ANOVA and *post hoc* Tukey's test (p<0.05).

<https://doi.org/10.1371/journal.pone.0203879.g010>

proliferation rates in the developing liver facilitates the clonal expansion of DEN-initiated hepatocytes [10]. The main outcome of this feature is earlier occurrence of preneoplastic and neoplastic lesions compared to classical models that DEN initiation occurs in fully-developed liver of adult mice [39]. Besides, in order to promote DEN-induced liver lesions, we established a fibrotic microenvironment by administrating successive CCl₄ injections to mimic the chronic liver injury as in human liver disease. The CYP2E1 is also responsible for CCl₄ bio-transformation, which leads to the formation of trichloromethyl radical, involved in free

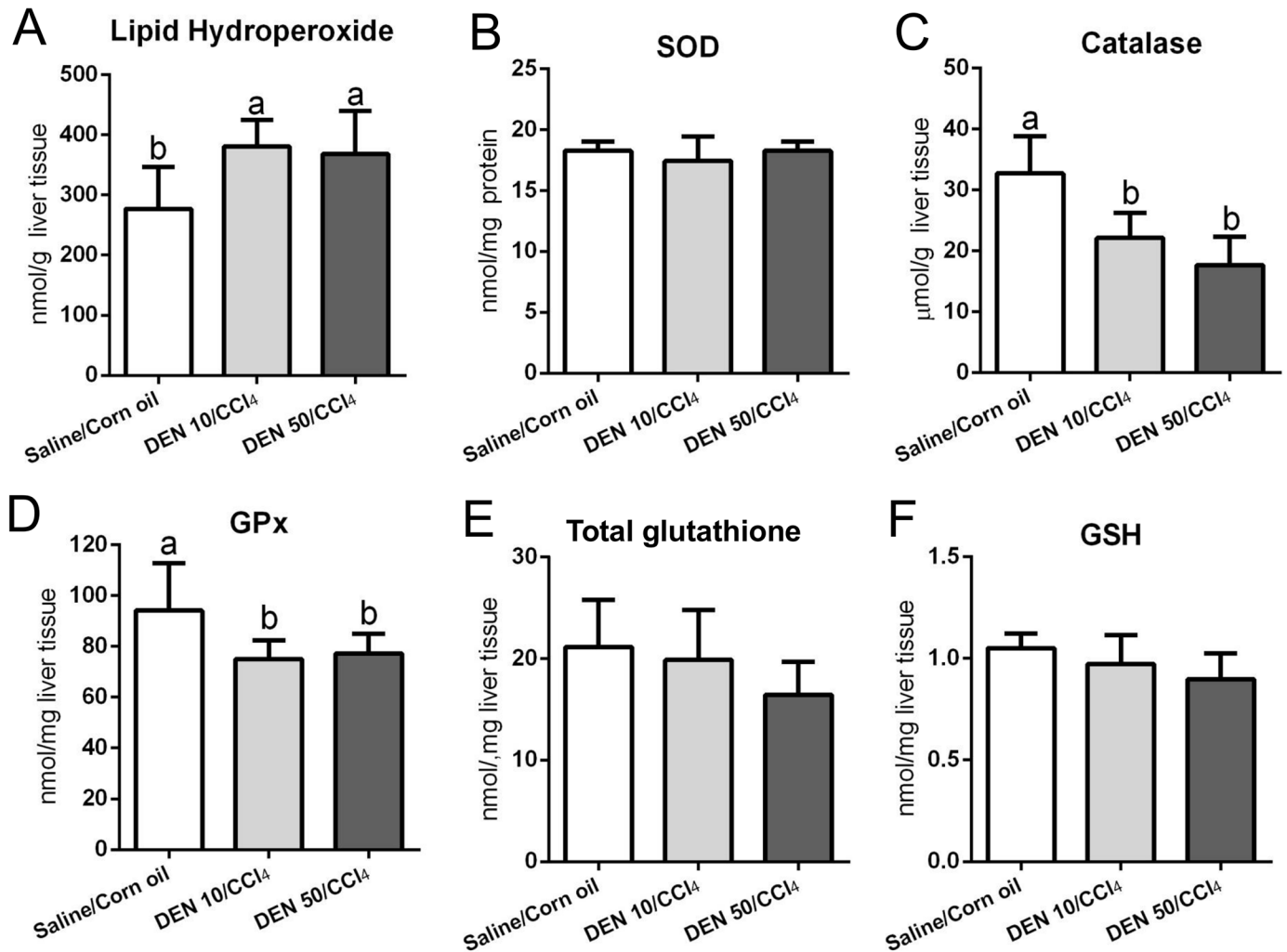


Fig 11. Effects of different DEN/CCL₄ protocols on (A) lipid hydroperoxide levels and (B-F) antioxidant defense in the liver of male C3H/HeJ mice. Values are mean + S.D. n = 8 mice/group. SOD = superoxide dismutase; GSH-Px = glutathione peroxidase; GSH = reduced glutathione; DEN 10 or 50 = diethylnitrosamine 10 or 50 mg/kg b.wt. in 0.9% saline at week 2, respectively and CCL₄ = carbon tetrachloride, i.p., 0.25 to 1.50 μL/g b.wt. in 10% corn oil solution for 8 weeks (see [Material and methods](#) section). Different letters correspond to statistical difference among groups by ANOVA and *post hoc* Tukey's test (p<0.05).

<https://doi.org/10.1371/journal.pone.0203879.g011>

radical and lipid peroxidation reactions [32,33]. The chronic CCL₄ administration contributes to the necrosis of centrilobular hepatocytes and the induction of a chronic inflammatory response, which promote HSCs activation and hence collagen deposition [40].

At the chosen time-point (week 17), we observed a clear liver fibrosis in both DEN doses in male mice (DEN10/CCL₄ and DEN50/CCL₄), characterized by increased collagen accumulation (Sirius red), HSCs activation (α-SMA), increased population of CD68⁺ macrophages and activation of COX-2/IL-6 axis. In addition, liver of males displayed increased oxidative stress (lipid hydroperoxide) and decreased activity of antioxidant enzymes (catalase and GSH-Px). Moreover, the two protocols resulted in increased cell proliferation (Ki-67) and apoptosis (cleaved caspase-3) in liver tissue surrounding the hepatocellular preneoplastic/neoplastic lesions. Regarding these lesions, all DEN10/CCL₄ and DEN50/CCL₄-treated male mice developed preneoplastic AHFs and HCAs whereas the vehicle group did not. Previous findings indicate that 10% to 15% of the DEN-induced AHFs in C3H/HeJ and B6C3F1 mice strains

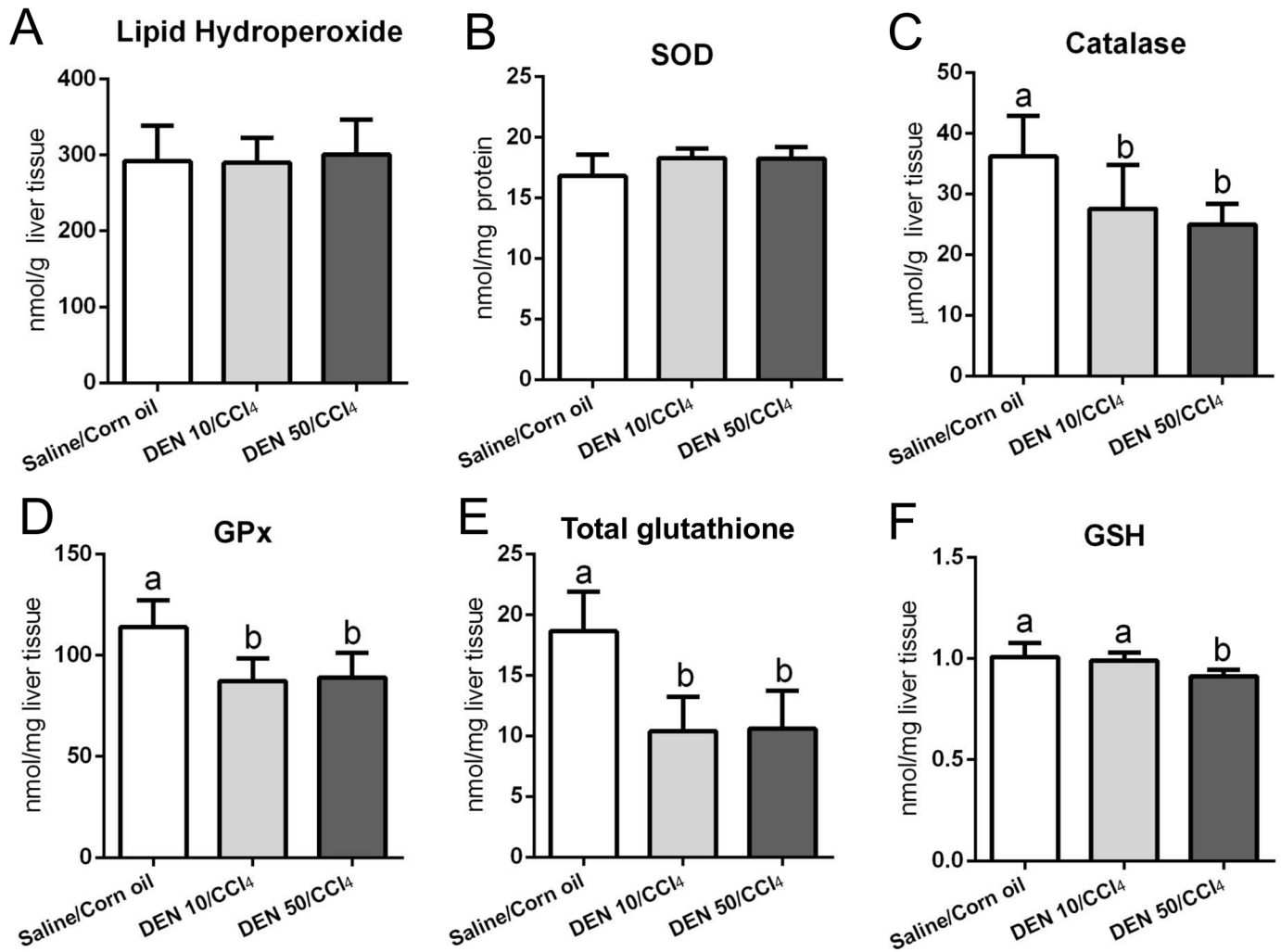


Fig 12. Effects of different DEN/CCL₄ protocols on (A) lipid hydroperoxide levels and (B-F) antioxidant defense in the liver of female C3H/HeJ mice. Values are mean + S.D. n = 8 mice/group. SOD = superoxide dismutase; GSH-Px = glutathione peroxidase; GSH = reduced glutathione; DEN 10 or 50 = diethylnitrosamine 10 or 50 mg/kg b.wt. in 0.9% saline at week 2, respectively and CCL₄ = carbon tetrachloride, i.p., 0.25 to 1.50 µL/g b.wt. in 10% corn oil solution for 8 weeks (see [Material and methods](#) section). Different letters correspond to statistical difference among groups by ANOVA and *post hoc* Tukey's test (p<0.05).

<https://doi.org/10.1371/journal.pone.0203879.g012>

presented mutations in proliferation-related *H-ras* gene [41,42]. Indeed, the enhanced expression of mutant *H-ras* alone is sufficient to induce hepatocyte proliferation and AHF growth [43]. Under growth stimuli, AHF can eventually accumulate other genetic and epigenetic alterations and progress from focal lesions to neoplastic lesions, as HCAs and HCCs [23]. For these reasons, AHF are considered putative hepatocellular preneoplastic lesions in mice [23]. Although HCAs are benign lesions and their progression to HCCs is not well documented in mice, HCAs display progressive atypia and ~50% also exhibit *H-ras* mutations in C3H/HeJ mice [42,44]. Besides, a recent study showed that both HCA and HCC cells in DEN/CCL₄-induced mice neoplasms are derived from the same genetic cell lineage [45], suggesting that HCAs can be precursor lesions for HCC. Therefore, in medium-term chemically-induced hepatocarcinogenesis bioassays proposed, both AHFs and HCAs can be considered suitable end-point lesions, permitting the screening of potential modifying factors (preventive or causative) of early hepatocarcinogenesis [23].

Table 3. Advantages of the proposed fibrosis-associated hepatocarcinogenesis models in males and females.

Models	Methods			Fibrosis	Incidence of end-point lesion	
	DEN	Promoter	Strain		AHF	HCA
Males						
Proposed models	Single 10 mg/Kg (week 2)	CCl ₄ (3x/week; 0.25 to 1.50 μL/g, for 8 weeks)	C3H/HeJ	Yes	100% (week 17)	100% (week 17)
	Single 50 mg/Kg (week 2)	CCl ₄ (3x/week; 0.25 to 1.50 μL/g, for 8 weeks)	C3H/HeJ	Yes	100% (week 17)	100% (week 17)
Chappell <i>et al.</i> (2014) [26]	Single 1 mg/Kg (week 2)	CCl ₄ (2x/week; 0.20 μL/g, for 14 weeks)	B6C3F1	Yes	31% (week 22)	100% (week 22)
Uehara <i>et al.</i> (2010) [47]	Single 1 mg/Kg (week 2)	CCl ₄ (2x/week; 0.20 μL/g, for 9 weeks)	B6C3F1	Yes	100% (week 17)	40% (week 17)
Goldsworthy & Fransson-Steen (2002) [46]	Single 1 mg/Kg (week 2)	Phenobarbital (500 ppm, for ~15–16 weeks)	C3H/HeJ	No	56% (week 22)	-
			B6C3F1	No	44% (week 22)	-
			C57BL	No	25% (week 22)	-
		None	C3H/HeJ	No	78% (week 22)	-
			B6C3F1	No	44% (week 22)	-
Weghorst <i>et al.</i> (1989)[9]	Single 5 mg/Kg (week 2)	Phenobarbital (500 ppm, for 24 weeks)	C3H/HeJ	No	-	100% (week 28)
			B6C3F1	No	-	100% (week 28)
			C57BL	No	-	50% (week 28)
		None	C3H/HeJ	No	-	100% (week 28)
			B6C3F1	No	-	100% (week 28)
			C57BL	No	-	90% (week 28)
Females						
Proposed models	Single 10 mg/Kg (week 2)	CCl ₄ (3x/week; 0.25 to 1.50 μL/g, for 8 weeks)	C3H/HeJ	Yes	100% (week 17)	62.5% (week 17)
	Single 50 mg/Kg (week 2)	CCl ₄ (3x/week; 0.25 to 1.50 μL/g, for 8 weeks)	C3H/HeJ	Yes	100% (week 17)	25% (week 17)
Romualdo <i>et al.</i> (2017) [12]	Single 50 mg/Kg (week 2)	Hexachlorobenzene (200 ppm, for 20 weeks)	Balb/C	No	100% (week 26)	-
Fukumasu <i>et al.</i> (2006) [53]	Single 10 mg/Kg (week 2)	None	Balb/C	No	100% (week 29)	-

DEN = diethylnitrosamine. “-” = data not available.

<https://doi.org/10.1371/journal.pone.0203879.t003>

In the present study, DEN-initiated and CCl₄-promoted protocols in males showed marked advantage to the classical DEN-initiated and non-promoted protocol, considering that only 33% to 78% mice submitted to the non-promoted method developed AHFs within 22 weeks, in a strain-dependent manner [46] (Table 3). Moreover, in the same model, a long time of experiment (28 weeks) was required for HCA development in 90% to 100% of male mice [9] in comparison to the present medium-term bioassay (Table 3). The current findings explicit the importance of fibrotic microenvironment induced by chronic CCl₄ regimen on the emerging of hepatocellular preneoplastic and neoplastic lesions.

The broadly-applied DEN-initiated and phenobarbital (PB)-promoted protocol also proved to be less effective for AHF and HCA development in comparison to our male mice models.

Under DEN/PB protocol, 25% to 56% of mice developed AHFs within 22 weeks and 50% to 100% displayed HCAs in 28 weeks, in a strain-dependent manner [9,46] (Table 3). In the light of the fact that PB is a non-fibrogenic promoter (Table 3) (*i.e.*, not resembling the fibrotic background of 70% to 90% human HCC cases), DEN-initiated and CCl₄-promoted protocols present clear advantage and thus, relevance to the study of the corresponding human disease.

Ultimately, our protocols for males increased in 60% the incidence of HCAs compared to other recent and similar fibrosis-associated hepatocarcinogenesis models in the intermediate-susceptible B6C3F1 strain [26,47] at the same time-point (100% *vs.* 40%) (Table 3). Its worthy of note that at week 17, these models showed non-significant incidence of HCC (20% of mice) as well as our DEN 10/CCl₄ assay (12.5% of mice). In these studies, 22 weeks of experiment were necessary for all mice to develop HCAs (Table 3). In addition, these assays only presented incidence data on preneoplastic and neoplastic lesions, lacking on other important and commonly applied histopathological parameters as number of foci/cm², size of foci, multiplicity of adenomas and others. All these parameters are presented and detailed in our models. Our results can be mostly attributed to the high-susceptible C3H/HeJ mice used herein. This specific strain displays genetic predisposition to hepatocarcinogenesis, developing HCC in senescence, independently of chemically-induced protocols [48]. Indeed, many studies have mapped multiple loci that can potentially confer hepatocarcinogenesis predisposition to this mouse strain [49,50].

In literature, chemically-induced models for hepatocarcinogenesis harbor a clear male predominance due to sex bias, reflecting the corresponding human disease [7]. In fact, experimental studies present solid evidence concerning the estrogen axis as a protective pathway for female hepatocarcinogenesis [7,51]. In accordance to previous sex bias data, our female models showed no IL-6 axis activation, decreased size and number of AHF and multiplicity of HCA compared to males, one week after the last CCl₄ insult. However, as a novelty of our work, we proposed standard medium-term fibrosis associated-hepatocarcinogenesis female models (Table 3). In the current bioassays (DEN10/CCl₄ and DEN50/CCl₄), it was observed marked liver fibrosis, featuring collagen accumulation (Sirius red) and HSCs activation (α -SMA). In addition, females clearly showed diminished activity of antioxidant agents (catalase and glutathione system). As well as males, females presented enhanced apoptosis and cell proliferation in surrounding liver tissue. At the same time-point as males (week 17), both female protocols increased the incidence of preneoplastic AHFs and only DEN10/CCl₄ significantly enhanced HCA incidence compared to vehicle group. Due to increased experimental time for neoplastic lesion development in females, most of bioassays present preneoplastic AHFs as end-point lesions [12,52]. In comparison to a classical DEN-initiated model in Balb/C mice, in the absence of a promoter stimulus, the models presented here diminished in twelve weeks the required experimental time for AHF development in all mice [52] (Table 3). Similar reduction can be observed when models are compared to DEN-initiated and hexachlorobenzene (HCB)-promoted model in Balb/C female mice [12] (Table 3) In addition to the long experimental time, the referred models lack liver fibrosis and do not apply HCAs as end-point lesions.

Although we presented optimized male and female fibrosis-associated hepatocarcinogenesis models, results indicate a threshold in the proposed DEN doses, not presenting a dose-response relationship for preneoplastic and neoplastic lesion development as in other mice models [53,54]. DEN 50/CCl₄ protocol in males resulted in a lower HCA multiplicity, decreased AHF size, occupied area and proliferation whereas females presented non-significant incidence of HCAs in comparison to respective DEN10/CCl₄ regimens. Besides, DEN 50-treated males exhibited marked features of toxicity including diminished food consumption and body weight from DEN initiation (week 2) until the end of the experiment (week 17). In adult rat, DEN-initiation exhibited a plateau as increased doses of DEN (>160 mg/Kg) did

not necessarily lead to an increased number of liver GST-P⁺ AHF [55]. DEN initiation at high doses could have led to hepatocyte death instead of initiating these cells to hepatocarcinogenesis and, ultimately, resulting in decreased number of preneoplastic lesions [55]. In fact, we observed high liver damage in both male and female submitted to DEN 50 when compared to DEN 10, twenty-four hours after a single DEN administration (S6 and S7 Figs).

In order to evaluate the effect of DEN-initiation in the models, the authors performed a short-term study: male and female C3H/HeJ mice (n = 5 mice/sex/group) received single injections of diethylnitrosamine or saline vehicle (as described in item 2.1) at PND 14 and were euthanized a day after DEN-administration. HE-stained liver sections revealed that DEN at 50 mg/Kg increased the incidence of early bridging centrilobular necrosis compared to vehicle and DEN 10 mg-treated mice in both male (DEN 50: 100% vs. DEN 10 and Saline: 0%, p = 0.018, for both) and female (DEN 50: 100% vs. DEN 10: 20% and Saline: 0%, p = 0.048 and p = 0.018, respectively) (S6 and S7 Figs). Indeed, the occurrence of bridging necrosis in DEN 50 mg/Kg-treated mice, as observed in our short-term study, could have impaired preneoplastic and/or neoplastic lesion development in our male and female DEN 50/CCl₄ models. However, the effect of intermediate doses (20, 30, 40 mg/Kg, for example) on preneoplastic and neoplastic lesion development should be evaluated in neonatal C3H/HeJ mice model in further studies.

In summary, we proposed standard fibrosis-associated early hepatocarcinogenesis models for male and female C3H/HeJ mice, applying a chemically-induced protocol in a high-susceptible mouse strain. As expected, these models showed clear sex bias and for DEN 10/CCl₄ protocols in males and females, we reduced the required experimental time for the development of multiple preneoplastic (AHF) and neoplastic (HCAs) lesions in comparison to other classical mice models.

Supporting information

S1 File. NC3Rs ARRIVE guidelines checklist.

(PDF)

S1 Fig. Effects of different DEN/CCl₄ protocols on body weight evolution of male and female C3H/HeJ mice. Dots are mean ± S.D. n = 8 mice/sex/group. DEN 10 or 50 = diethylnitrosamine 10 or 50 mg/kg b.wt. in 0.9% saline at week 2, respectively and CCl₄ = carbon tetrachloride, i.p., 0.25 to 1.50 μL/g b.wt. in 10% corn oil solution for 8 weeks (see [Material and methods](#) section). *Statistical difference among groups by ANOVA and *post hoc* Tukey's test (p<0.05).

(TIFF)

S2 Fig. Representative photomicrographs of H&E-stained and immunostained (Ki-67) sections of hepatocellular adenoma (HCA) and hepatocellular carcinoma (HCC) found in the liver of DEN/CCl₄-treated mice. (A, B, C) HCAs displayed typical loss of normal lobular architecture, enlarged cells, and vacuoles. (D, E, F) HCCs were composed of well-differentiated hepatocytes arranged in trabeculae of multiple cell layers and acinar structures, (A, D: 4× objective; scale bar = 200 μm) (B, C, E, F: 40× objective; scale bar = 20 μm).

(TIF)

S3 Fig. Effects of different DEN/CCl₄ protocols on β-catenin protein expression in male and female C3H/HeJ mice. (A) Representative photomicrographs β-catenin immunostained sections of surrounding liver tissue (40× objective; scale bar = 20 μm) and (B) preneoplastic and neoplastic lesions (10× objective, scale bar = 100 μm). Representative western blot bands and semiquantitative analysis of (C) male and (F) female mice. Values are mean + S.D. n = 6

mice/group. DEN 10 or 50 = diethylnitrosamine 10 or 50 mg/kg b.wt. in 0.9% saline at week 2, respectively and CCl₄ = carbon tetrachloride, i.p., 0.25 to 1.50 μ L/g b.wt. in 10% corn oil solution for 8 weeks (see [Material and methods](#) section).

(TIFF)

S4 Fig. TGF- α expression in DEN/CCl₄ models. (A) Representative photomicrographs of TGF- α immunostained sections of surrounding liver tissue (40 \times objective; scale bar = 20 μ m) and (B) H&E-stained and respective TGF- α immunostained sections of basophilic foci and hepatocellular adenoma (20 \times objective; scale bar = 50 μ m). DEN 10 or 50 = diethylnitrosamine 10 or 50 mg/kg b.wt. in 0.9% saline at week 2, respectively and CCl₄ = carbon tetrachloride, i.p., 0.25 to 1.50 μ L/g b.wt. in 10% corn oil solution for 8 weeks (see [Material and methods](#) section). (TIFF)

S5 Fig. Sex comparison of (A) transaminases data and (B) preneoplastic and neoplastic lesions in DEN 10 and DEN 50/CCl₄-induced fibrosis-associated hepatocarcinogenesis models. Values are mean + S.D or box and whiskers. n = 8 mice/sex/group. DEN 10 or 50 = diethylnitrosamine 10 or 50 mg/kg b.wt. in 0.9% saline at week 2, respectively and CCl₄ = carbon tetrachloride, i.p., 0.25 to 1.50 μ L/g b.wt. in 10% corn oil solution for 8 weeks (see [Material and methods](#) section). ALT = alanine aminotransferase; AST = aspartate aminotransferase; AHF = altered hepatocyte foci; HCA = hepatocellular adenoma. Data were analyzed by Student t test ($p < 0.05$).

(TIFF)

S6 Fig. Representative photomicrographs of the liver of vehicle, DEN 10 and DEN 50-treated neonatal C3H/HeJ male mice. Above: scale bar = 100 μ m, below: scale bar = 50 μ m. In special, DEN 50-treated mice displayed early bridging centrilobular necrosis, with swelling and diffuse inflammatory cell infiltrate. DEN 10 or 50 = diethylnitrosamine 10 or 50 mg/kg b.wt. in 0.9% saline at week 2. Mice were euthanized 24h after DEN injection. (TIF)

S7 Fig. Representative photomicrographs of the liver of vehicle, DEN 10 and DEN 50-treated neonatal C3H/HeJ female mice. Above: scale bar = 100 μ m, below: scale bar = 50 μ m. In special, DEN 50-treated mice displayed early bridging centrilobular necrosis, with swelling and diffuse inflammatory cell infiltrate. DEN 10 or 50 = diethylnitrosamine 10 or 50 mg/kg b.wt. in 0.9% saline at week 2. Mice were euthanized 24h after DEN injection. (TIF)

Acknowledgments

The authors thank Professor Alexandrina Sartori and Thais F. C. Fraga da Silva for the technical support during ELISA and Sarah V. Mattioli, Isadora P. de Souza and Lucas V. de Souza for immunohistochemistry and biochemical analysis.

Author Contributions

Conceptualization: Guilherme Ribeiro Romualdo, Ana Angélica Henrique Fernandes, Fernando Salvador Moreno, Bruno Cogliati, Luís Fernando Barbisan.

Data curation: Guilherme Ribeiro Romualdo, Gabriel Bacil Prata, Tereza Cristina da Silva, Ana Angélica Henrique Fernandes.

Formal analysis: Gabriel Bacil Prata, Fernando Salvador Moreno.

Funding acquisition: Luís Fernando Barbisan.

Investigation: Guilherme Ribeiro Romualdo, Gabriel Bacil Prata, Tereza Cristina da Silva, Fernando Salvador Moreno, Luís Fernando Barbisan.

Methodology: Guilherme Ribeiro Romualdo, Gabriel Bacil Prata, Tereza Cristina da Silva, Ana Angélica Henrique Fernandes.

Project administration: Tereza Cristina da Silva, Bruno Cogliati.

Supervision: Fernando Salvador Moreno, Bruno Cogliati, Luís Fernando Barbisan.

Validation: Guilherme Ribeiro Romualdo, Tereza Cristina da Silva, Ana Angélica Henrique Fernandes.

Visualization: Guilherme Ribeiro Romualdo, Tereza Cristina da Silva, Ana Angélica Henrique Fernandes.

Writing – original draft: Guilherme Ribeiro Romualdo, Fernando Salvador Moreno, Bruno Cogliati, Luís Fernando Barbisan.

Writing – review & editing: Guilherme Ribeiro Romualdo, Gabriel Bacil Prata, Ana Angélica Henrique Fernandes, Fernando Salvador Moreno, Bruno Cogliati, Luís Fernando Barbisan.

References

1. GLOBOCAN, 2012. GLOBOCAN 2012: Estimated cancer Incidence, Mortality and Prevalence Worldwide in 2012. <http://globocan.iarc.fr/Default.aspx> (accessed 31.10.17)
2. Sanyal AJ, Yoon SK, Lencioni R. The Etiology of Hepatocellular Carcinoma and Consequences for Treatment. *Oncologist*. 2010; 15: 14–22. <https://doi.org/10.1634/theoncologist.2010-S4-14> PMID: 21115577
3. Yang JD, Kim WR, Coelho R, Mettler TA, Benson JT, Sanderson SO, et al. Cirrhosis Is Present in Most Patients With Hepatitis B and Hepatocellular Carcinoma. *Clin Gastroenterol Hepatol*. 2011; 9: 64–70. <https://doi.org/10.1016/j.cgh.2010.08.019> PMID: 20831903
4. Liu M, Jiang L, Guan X-Y. The genetic and epigenetic alterations in human hepatocellular carcinoma: a recent update. *Protein Cell*. 2014; 5: 673–91. <https://doi.org/10.1007/s13238-014-0065-9> PMID: 24916440
5. Bakiri L, Wagner EF. Mouse models for liver cancer. *Mol Oncol*. 2013; 7: 206–223. <https://doi.org/10.1016/j.molonc.2013.01.005> PMID: 23428636
6. Romualdo GR, Grassi TF, Goto RL, Tablas MB, Bidinotto LT, Fernandes AAH, et al. An integrative analysis of chemically-induced cirrhosis-associated hepatocarcinogenesis: Histological, biochemical and molecular features. *Toxicol Lett*. 2017; 281: 84–94. <https://doi.org/10.1016/j.toxlet.2017.09.015> PMID: 28943392
7. Naugler WE, Sakurai T, Kim S, Maeda S, Kim K, Elsharkawy AM, et al. Gender disparity in liver cancer due to sex differences in MyD88-dependent IL-6 production. *Science*. 2007; 317: 121–4. <https://doi.org/10.1126/science.1140485> PMID: 17615358
8. Lee GH, Nomura K, Kitagawa T. Comparative study of diethylnitrosamine-initiated two-stage hepatocarcinogenesis in C3H, C57BL and BALB mice promoted by various hepatopromoters. *Carcinogenesis*. 1989; 10: 2227–2230. <https://doi.org/10.1093/carcin/10.12.2227> PMID: 2591012
9. Weghorst CM, Pereira MA, Klaunig E. Strain differences in hepatic tumor promotion by phenobarbital in diethylnitrosamine- and dimethylnitrosamine-initiated infant male mice. *Carcinogenesis*. 1989; 10: 1409–1412. <https://doi.org/10.1093/carcin/10.8.1409> PMID: 2752514
10. Vesselinovitch SD. Certain aspects of hepatocarcinogenesis in the infant mouse model. *Toxicol Pathol*. 1987; 15: 221–228. <https://doi.org/10.1177/019262338701500216> PMID: 3616406
11. Hara A, Yoshimi N, Yamada Y, Matsunaga K, Kawabata K, Sugie S, et al. Effects of Fas-mediated liver cell apoptosis on diethylnitrosamine-induced hepatocarcinogenesis in mice. *Br J Cancer*. 2000; 82: 467–71. <https://doi.org/10.1054/bjoc.1999.0944> PMID: 10646906
12. Romualdo GR, Goto RL, Fernandes AAH, Cogliati B, Barbisan LF. Vitamin D₃ supplementation attenuates the early stage of mouse hepatocarcinogenesis promoted by hexachlorobenzene fungicide. *Food Chem Toxicol*. 2017; 107: 27–36. <https://doi.org/10.1016/j.fct.2017.06.030> PMID: 28634113

13. Cogliati B, Da silva TC, Aloia TPA, Chaible LM, Real-Lima MA, Sanches DS, et al. Morphological and molecular pathology of CCL4-induced hepatic fibrosis in connexin43-deficient mice. *Microsc Res Tech*. 2011; 74: 421–429. <https://doi.org/10.1002/jemt.20926> PMID: 20830702
14. National Research Council (US) Committee for the Update of the Guide for the Care and Use of Laboratory Animals. *Guide for the Care and Use of Laboratory Animals*. 8th ed. Washington (DC): National Academies Press; 2011.
15. Da Silva TC, Da Silva AP, Akisue G, Avanzo JL, Nagamine MK, Fukumasu H, et al. Inhibitory effects of *Paffia paniculata* (Brazilian ginseng) on preneoplastic and neoplastic lesions in a mouse hepatocarcinogenesis model. *Cancer Lett*. 2005; 226: 107–113. <https://doi.org/10.1016/j.canlet.2004.12.004> PMID: 16039950
16. Thoolen B, Maronpot RR, Harada T, Nyska A, Rousseaux C, Nolte T, et al. Proliferative and nonproliferative lesions of the rat and mouse hepatobiliary system. *Toxicol Pathol*. 2010; 38: 5S–81S. <https://doi.org/10.1177/0192623310386499> PMID: 21191096
17. Pires PW, Furtado KS, Justullin LA Jr, Aparecida M, Rodrigues M, et al. Chronic ethanol intake promotes double glutathione S-transferase/transforming growth factor- α -positive hepatocellular lesions in male Wistar rats. *Cancer Sci*. 2008; 99: 221–228. <https://doi.org/10.1111/j.1349-7006.2007.00677.x> PMID: 18271918
18. Bergmeyer HU. *Methods of Enzymatic Analysis*, 2nd ed. New York: Academic Press; 1974.
19. Nakamura W, Hojoda S, Hayashi K. Purification and properties of rat liver glutathione peroxidase. *Biochim Biophys Acta*. 1974; 358: 251–261.
20. Ewing JF, Janero DR. Microplate superoxide dismutase assay employing a nonenzymatic superoxide generator. *Anal Biochem*. 1995; 232: 243–8. <https://doi.org/10.1006/abio.1995.0014> PMID: 8747482
21. Tietze F. Enzymic method for quantitative determination of nanogram amounts of total and oxidized glutathione: Applications to mammalian blood and other tissues. *Anal Biochem*. 1969; 27: 502–22. PMID: 4388022
22. Jiang ZY, Woollard A, Wolff S. Lipid hydroperoxide measurement by oxidation of Fe³⁺ in the presence of xylenol orange. *Lipids*. 1991; 26: 853–6.
23. Klaunig JE, Kamendulis LM. Mechanisms of cancer chemoprevention in hepatic carcinogenesis: modulation of focal lesion growth in mice. *Toxicol Sci*. 1999; 52: 101–6.
24. Tsuchida T, Friedman SL. Mechanisms of hepatic stellate cell activation. *Nat Rev Gastroenterol Hepatol*. 2017; 14: 397–411. <https://doi.org/10.1038/nrgastro.2017.38> PMID: 28487545
25. de La Coste A, Romagnolo B, Billuart P, Renard CA, Buendia MA, Soubrane O, et al. Somatic mutations of the beta-catenin gene are frequent in mouse and human hepatocellular carcinomas. *Proc Natl Acad Sci U S A*. 1998; 95: 8847–51. <https://doi.org/10.1073/pnas.95.15.8847> PMID: 9671767
26. Chappell G, Kutanzi K, Uehara T, Tryndyak V, Hong HH, Hoenerhoff M, et al. Genetic and epigenetic changes in fibrosis-associated hepatocarcinogenesis in mice. *Int J Cancer*. 2014; 134: 2778–2788. <https://doi.org/10.1002/ijc.28610> PMID: 24242335
27. Moser GJ, Wolf DC, Goldsworthy TL. Quantitative Relationship Between Transforming Growth Factor-Alpha and Hepatic Focal Phenotype and Progression in Female Mouse Liver. *Toxicol Pathol*. 1997; 25: 275–283. <https://doi.org/10.1177/019262339702500305> PMID: 9210259
28. Beljaars L, Schippers M, Reker-Smit C, Martinez FO, Helming L, Poelstra K, et al. Hepatic localization of macrophage phenotypes during fibrogenesis and resolution of fibrosis in mice and humans. *Front Immunol*. 2014; 5: 13–15.
29. Maeda S, Kamata H, Luo J, Leffert H, Karin M. IKK β Couples Hepatocyte Death to Cytokine-Driven Compensatory Proliferation that Promotes Chemical Hepatocarcinogenesis. *Cell*. 2005; 121: 977–990. <https://doi.org/10.1016/j.cell.2005.04.014> PMID: 15989949
30. Hinson RM, Williamst JA, Shacter E. Elevated interleukin 6 is induced by prostaglandin E2 in a murine model of inflammation: Possible role of cyclooxygenase-2. *PNAS*. 1996; 93: 4885–4890. PMID: 8643498
31. Wójcik M, Ramadori P, Blaschke M, Sultan S, Khan S, Malik IA, et al. Immunodetection of cyclooxygenase-2 (COX-2) is restricted to tissue macrophages in normal rat liver and to recruited mononuclear phagocytes in liver injury and cholangiocarcinoma. *Histochem Cell Biol*. 2012; 2: 217–233. <https://doi.org/10.1007/s00418-011-0889-9> PMID: 22131058
32. Basu S. Carbon tetrachloride-induced lipid peroxidation: Eicosanoid formation and their regulation by antioxidant nutrients. *Toxicology*. 2003; 189: 113–127. [https://doi.org/10.1016/S0300-483X\(03\)00157-4](https://doi.org/10.1016/S0300-483X(03)00157-4) PMID: 12821287
33. Weber LWD, Boll M, Stampfl A. Hepatotoxicity and Mechanism of Action of Haloalkanes: Carbon Tetrachloride as a Toxicological Model. *Crit Rev Toxicol*. 2003; 33: 105–136. <https://doi.org/10.1080/713611034> PMID: 12708612

34. Birben E, Sahiner UM, Sackesen C, Erzurum S, Kalayci O. Oxidative Stress and Antioxidant Defense. *WAO J.* 2012; 5: 9–19. <https://doi.org/10.1097/WOX.0b013e3182439613> PMID: 23268465
35. Czczot H, Scibior D, Skrzycki M, Podsiad M. Glutathione and GSH-dependent enzymes in patients with liver cirrhosis and hepatocellular carcinoma. *Acta Biochim Pol.* 2006; 53: 237–242. PMID: 16404476
36. Czuczejko J, Zachara BA, Staubach-topczewska E. Selenium, glutathione and glutathione peroxidases in blood of patients with chronic liver diseases. *Acta Biochim Pol.* 2003; 50: 85–92. PMID: 12035004
37. Vesselinovitch SD, Mihailovich N. Kinetics of diethylnitrosamine hepatocarcinogenesis in the infant mouse. *Cancer Res.* 1983; 43: 4253–4259. PMID: 6871863
38. Jin SK, Wanibuchi H, Morimura K, Gonzalez FJ, Fukushima S. Role of CYP2E1 in diethylnitrosamine-induced hepatocarcinogenesis in vivo. *Cancer Res.* 2007; 67: 11141–11146. <https://doi.org/10.1158/0008-5472.CAN-07-1369> PMID: 18056438
39. Vesselinovitch SD, Koka M, Mihailovich N, Rao KV. Carcinogenicity of diethylnitrosamine in newborn, infant, and adult mice. *J Cancer Res Clin Oncol.* 1984; 108: 6–5. PMID: 6746718
40. Iwaisako K, Jiang C, Zhang M, Cong M, Moore-Morris TJ, Park TJ, et al. Origin of myofibroblasts in the fibrotic liver in mice. *Proc Natl Acad Sci U S A.* 2014; 111: E3297–305. <https://doi.org/10.1073/pnas.1400062111> PMID: 25074909
41. Buchmann A, Mahr J, Bauer-Hofmann R, Schwarz M. Mutations at Codon 61 of the Hras Proto-Oncogene in Precancerous Liver Lesions of the B6C3F1 Mouse. *Mol Carcinog.* 1989; 125: 121–125.
42. Bauer-Hofmann R, Klimek F, Buchmann A, Müller O, Bannasch P, Schwarz M. Role of mutations at codon 61 of the c-Ha-ras gene during diethylnitrosamine-induced hepatocarcinogenesis in C3H/He mice. *Mol Carcinog.* 1992; 6: 60–67. <https://doi.org/10.1002/mc.2940060110> PMID: 1323970
43. Stein TJ, Bowden M, Sandgren EP. Minimal cooperation between mutant *Hras* and *c-myc* or *TGF α* in the regulation of mouse hepatocyte growth or transformation *in vivo*. *Liver Int.* 2011; 31: 1298–1305. <https://doi.org/10.1111/j.1478-3231.2011.02596.x> PMID: 22093452
44. Jang J-J, Weghorst CM, Henneman JR, Devor DE, Ward JM. Progressive atypia in spontaneous and N-nitrosodiethylamine-induced hepatocellular adenomas of c3h/hencr mice. *Carcinogenesis.* 1992; 13: 1541–1547. PMID: 1394837
45. Shin S, Wangenstein KJ, Teta-Bissett M, Wang YJ, Mosleh-Shirazi E, Buza EL, et al. Genetic lineage tracing analysis of the cell of origin of hepatotoxin-induced liver tumors in mice. *Hepatology.* 2016; 64: 1163–1177. <https://doi.org/10.1002/hep.28602> PMID: 27099001
46. Goldsworthy TL, Fransson-Steen R. Quantitation of the Cancer Process in C57BL/6J, B6C3F1 and C3H/HeJ Mice. *Toxicol Pathol.* 2002; 30: 97–105. <https://doi.org/10.1080/01926230252824770> PMID: 11890483
47. Uehara T, Ainslie GR, Kutanzi K, Pogribny IP, Muskhelishvili L, Izawa T, et al. Molecular mechanisms of fibrosis-associated promotion of liver carcinogenesis. *Toxicol Sci.* 2013; 132: 53–63. <https://doi.org/10.1093/toxsci/kfs342> PMID: 23288052
48. Li D, Chen S, Becker FF, Chen S. Specific reduction of i-compound levels in dna from spontaneous hepatomas of 22–24 month old male c3h mice. *Carcinogenesis.* 1991; 12: 2389–2391. <https://doi.org/10.1093/carcin/12.12.2389> PMID: 1747944
49. Gariboldi M, Manenti G, Canzian F, Falvella FS, Pierotti MA, Della Porta G, et al. Advances in Brief Chromosome Mapping of Murine Susceptibility Loci to Liver Carcinogenesis 1. *Cancer Res.* 1993; 209–211.
50. Bilger A, Bennett LM, Carabeo RA., Chiaverotti TA., Dvorak C, Liss KM, et al. A potent modifier of liver cancer risk on distal mouse chromosome 1: Linkage analysis and characterization of congenic lines. *Genetics.* 2004; 167: 859–866. <https://doi.org/10.1534/genetics.103.024521> PMID: 15238534
51. Hong E, Levasseur M, Dufour CR, Perry M, Giguère V. Loss of estrogen-related receptor α promotes hepatocarcinogenesis development via metabolic and inflammatory disturbances. 2013; 110: 17975–17980. <https://doi.org/10.1073/pnas.1315319110> PMID: 24127579
52. Fukumasu H, Da Silva TC, Avanzo JL, De Lima CE, MacKowiak II, Atroch A, et al. Chemopreventive effects of *Paullinia cupana* Mart var. *sorbilis*, the guaraná, on mouse hepatocarcinogenesis. *Cancer Lett.* 2006; 233: 158–164. <https://doi.org/10.1016/j.canlet.2005.03.007> PMID: 15885883
53. Klaunig JE, Pereira MA., Ruch RJ, Weghorst CM. Dose-Response Relationship of Diethylnitrosamine-Initiated Tumors in Neonatal Balb/c Mice: Effect of Phenobarbital Promotion. *Toxicol Pathol.* 1988; 16: 381–385. <https://doi.org/10.1177/019262338801600310> PMID: 3194660
54. Kushida M, Kamendulis LM, Peat TJ, Klaunig JE. Dose-related induction of hepatic preneoplastic lesions by diethylnitrosamine in C57BL/6 mice. *Toxicol Pathol.* 2011; 39: 776–86. <https://doi.org/10.1177/0192623311409596> PMID: 21628716
55. Satoh K, Hatayama I, Tateoka N, Tamai K, Shimizu T, Tatematsu M, et al. Transient induction of single GST-P positive hepatocytes by DEN. *Carcinogenesis.* 1989; 10: 2107–11. PMID: 2805231